THE ELASTIC-PLASTIC BEHAVIOUR OF SOME AXISYMMETRIC PRESSURE VESSEL HEADS AND NOZZLES

BY

JOHN CHEUNG SHING TAI B.Sc.(Eng.),D.I.C.,G.I.Mech.E.

A thesis submitted for the degree of Doctor of Philosophy of the Faculty of Engineering, University of London.

November,1969. Department of Mechanical Engineering,
Imperial College of Science and Technology,
LONDON,S.W.7.

ABSTRACT

This investigation sets out to test the accuracy of a numerical method of stress analysis by Marcal for the elastic-plastic behaviour of axisymmetric thin-walled pressure vessels, with special reference to the possible application of the method to achieve more accurate vessel designs. Some torispherical heads and axisymmetric flush nozzles are selected for study. An extensive literature review is made on researches into the behaviour and design of pressure vessels, helping to set the course of this work.

The Marcal method, already coded into general purpose computer systems, is initially extensively tested with elastic problems, and is found to give good accuracy, within the limitations of the assumptions. However, exaggerated stress concentrations are noted among many elastic flush nozzle results, when the nozzle geometry is approximated by the usual shells intersection procedure. A new procedure is tried giving a smooth transition from nozzle to shell, and found to give good improvement of accuracy for flush nozzles with rounded fillets and corners based on the ASME Nuclear Vessel Code. Further improvement is obtained with this procedure after the program is modified, such that the basic equations give better approximation for thick curved shell elements which occur at the junctions.

A number of strain gauged vessel tests are made to obtain detailed comparison with the elastic-plastic analysis. They include axial loading tests on two mild steel nozzles attached to shallow spherical caps. They form the

preliminary to a hydraulic pressure test on a specially built stainless steel vessel, closed by two nominally identical heads where one has a central symmetric nozzle. Calculations are also tried, based on two published elastic-plastic tests on vessel heads. The comparisons reveal some sources of inaccuracy of the programs, and some factors, e.g. material strain-handening and change of vessel geometry, affecting the vessel's elastic-plastic behaviour. A reliable method is found as a basis for defining plastic collapse of vessel components. The programs as shown by these results should give good accuracy for some possible design application based on plastic collapse, shakedown or low-cycle fatigue.

ACKNOWLEDGEMENTS

The author is grateful for the financial support for three years of the Berkeley Nuclear Laboratories, Central Electricity Generating Board through a research contract. Part of this work is also supported by a Science Research Council contract.

Sincere acknowledgement is due to Dr. C.E.Turner, Reader in Mechanical Engineering, Imperial College, for supervising this research and giving the much needed advice and guidance, to Mr. C.H.A.Townley of the B.N.L. for his continued interest, and to Dr. P.V.Marcal for co-supervising part of this work.

Thanks are due to the library and technical staffs of the Mechanical Engineering Department, especially the Librarian Miss E.M.Archer, who have helped in the course of this work.

Finally the author wishes to thank Miss W.L.Wong and others who helped in the preparation of this thesis.

J.S.T.Cheung

C O N T E N T S

		ABSTRACT	1
		ACKNOWLEDGEMENTS	3
		CONTENTS	4
1.		INTRODUCTION	7
2.		HISTORIC REVIEW	11
	2.1	General	11
	2.2	Pressure Vessel Heads	13
	2.3	Pressure Vessel Openings	15
	2.4	New Techniques and Interests	18
3.		RECENT LITERATURES: THEORETICAL INVESTIGATIONS	21
		Notations	21
	3.1	Shell Theories	21
	3.2	Numerical Solution	27
	3.3	Pressure Vessel Nozzles	31
4.		RECENT LITERATURES: EXPERIMENTAL INVESTIGATIONS	36
	4.1	Experimental Techniques	36
	4.2	Pressure Vessel Heads	39
	4.3	Pressure Vessel Nozzles	40
5.		RECENT LITERATURES: FAILURE BEHAVIOUR	43
	5.1	Modes of Failure	43
	5.2	Static Loading	45
	5.3	Repeated Loading	48
6.		AVAILABLE COMPUTER PROGRAMS FOR VESSEL ANALYSIS	53
		Notations	53
	6.1	Elastic Program: Capabilities	55
	6.2	Elastic Program: Numerical Procedure	57
	6.3	Elastic-Plastic Program	65
7.		ACCURACY TESTS FOR ELASTIC PROGRAM	74
		Notation	74
	7.1	Size of Problem for Converging Solution	74

7.2	Cylinders Under Internal Pressure	77
7.3	Comparison With Published Results	80
7.4	Comparison With Other Pressure Vessel Programs	84
7.5	Conclusions	89
8.	ACCURACY TESTS FOR ELASTIC-PLASTIC PROGRAM	91
8.1	Previous Comparisons	91
8.2	Use of Elastic-Plastic Results	93
8.3	Further Comparisons	96
8.4	Tests by Stoddart	98
8.5	Tests by Kemper et.al.	101
9.	AXIAL LOADING TESTS OF FLUSH NOZZLES	106
9.1	Nozzle Configuration	106
9.2	Strain Gauge Techniques	109
9.3	Material Properties	113
9.4	Test Arangements and Preparations	117
9.5	Test Procedure and Results	123
10.	THEORETICAL SOLUTIONS TO COMPARE AXIAL TEST RESULTS	129
10.1	Approximations to the Nozzle Junction Configuration	129
10.2	Modifications to the Computer Program	133
10.3	Comparison of Results	137
10.4	Conclusions	150
11.	PRESSURE TEST OF VESSEL:PREPARATION	153
11.1	Introduction	153
11.2	Vessel Design	154
11.3	Measurements	156
11.4	Strain and Deflection Gauging	157
11.5	Oil Circuit	161
12.	PRESSURE TEST OF VESSEL:TEST AND COMPARISON	163
12.1	Elastic Test	163
12.2	Elastic Calculations	163
12.3	Elastic-Plastic Test	166

12.4	Elastic-Plastic Calculations	170
12.5	Discussions on Strain and Displacement	172
12.6	Discussions on Collapse Load	175
12.7	Conclusions	178
13.	OTHER GENERAL DISCUSSIONS	181
13.1	Pressure Vessel Programs	181
13.2	Vessel Behaviour	186
13.3	Design Interest	189
14.	CONCLUSIONS	195
	REFERENCES	201
	APPEDNICES	219
	LIST OF ILLUSTRATIONS	253
	FIGURES	255
	PLATES	310

1. INTRODUCTION

In the general sense, a pressure vessel is a container which holds a fluid at a different pressure from its environment. As such a device is often required in many industrial processes, it is often used in industry, and can be found in many shapes and forms. The steam boiler-plant industries have been a big user of pressure vessels since the advent of steam, so have the chemical and petroleum industries. They are also used in nuclear reactor plants, aircraft, and rockets as well as the humble but numerous gas containers.

The characteristic of a pressure vessel is the pressure it can hold. This however makes the vessel a possible source of danger if it breaks, causing uncontrolled release of the pressure. Study of the failure and of the general behaviour of pressure vessels has been of great value in preventing failures. This also leads of course to better design, which is not only safer, but also more economical. The areas of study cover a wide field. In the early steam and chemical vessels, rivet joints were the weakest link and were the subject of much investigation. The development of the welding process and its adoption switched attention to other areas, one of which was the improvement made possible by better shapes and reinforcements for the vessel.

Most vessels are built as cylinders for ease of fabrication. Their actual configuration may vary according to purpose. Great attention is generally given during design to vessel heads enclosing the ends of the vessels, and to nozzle openings where branch pipes

are attached. These two components are selected for special study in this thesis.

Most vessel heads are slightly domed outwards and of a shape called a torisphere, consisting geometrically of a shallow spherical centre and a curved-in edge of a much smaller torus radius, Fig.1-1. A circumferential weld joins the head to the cylindrical vessel shell. The simplest pressure vessel nozzle consists of a circular, or appropriately shaped, opening, in either the vessel head or the shell, onto and covering which (i.e. the opening) is welded a cylindrical tube or pipe. There are many variations of nozzle arrangements, most of which can be classified under methods of reinforcement, although nozzles are also classified according to the alignment between the vessel and nozzle.

Studies of the behaviour and the failure of vessel components- in many cases the latter is very much connected with the former - lead not only to stronger shapes and better arrangements for these components, but also to better design procedures. It has, for example, been recognised that different criteria are needed for application in low temperature and in sustained high temperature environments, or for loading of a constant and of a frequently repeated nature. Some of this knowledge has been gained from studying the properties of the materials used, under fatigue, under creep, and for low temperature brittle fracture. Study has also been made on local effect of weld, and of crack or notch.

Outside these fields of study, the investigation of overall behaviour of vessel components has also recently

been drawn towards their non-elastic behaviour, especially in cases where parts of the component have begun yielding. The yielded regions are in an elastic-plastic stress state when the elastic strain component cannot be neglected in comparison with the plastic strain component. Elasticity theory is not sufficient for studying this behaviour. It has, however, been known for some time that many vessels do yield locally at the working load, and some can safely withstand loads which cause initially a substantial yielding. Also some vessels, designed against fatigue within a finite number of cycles of repeated loading, may have stress concentration factors giving stresses higher than the material yield stress. Designers are faced with the problem of whether or not more accurate design based on elasticity considerations alone is adequate, or whether further investigation into non-elastic behaviour would only modify the present considerations, or if radically different criteria are needed. All these factors account for the interest in elastic-plastic behaviour of pressure vessels.

Much of the stimulus to this interest comes from the successful analysis, by numerical solution on the electronic computer, of the thin-walled shell equations, leading to the general solution of many elastic pressure vessel problems, and subsequently from the development of methods extending this to elastic-plastic stress analysis. This latter development is recent, and its implications, and applications in design are not fully exploited.

In parallel with this development of numerical methods

of elastic-plastic analysis, there is current theoretical work on the limit analysis of thin shells, leading to solutions of the collapse failure of pressure vessel by general and local yielding. This is an extension of the work on plastic analysis of frame and truss structures, and determines the final collapse of thin shells through the formation of plastic hinges at locations of high bending stresses. There is also current theoretical and material testing research on the behaviour of pressure vessels under repeated loadings of high magnitude, causing a certain amount of local plasticity at each cycle, and leading to fatigue failure at a relatively small number of cycles. This is commonly called low-cycle fatigue, or high-strain fatigue. These researches should be able to complement each other in leading to a better understanding of the behaviour of, and better design of, pressure vessels.

2. HISTORIC REVIEW

2.1 General

The invention of the steam engine in the 18th Century and its subsequent extensive use, brought about the need of steam boiler vessels that is large enough to generate the required amount of steam, and at the same time strong enough to support the weight of water inside and resist the steam pressure. An example of a well designed vessel at that time was an horizental egg-ended boiler built by Richard Trevithick in 1800 (see Ref.(2-1)). The vessel was 3 to 4 ft. diameter, 40 ft. long and was made of wrought iron plates. The ends were deep and egg-shaped, and the two openings at the side of the vessel were oval in shape. This vessel was used under a pressure of 80 lb/in^2.

The two weakest arrangements of the early vessel were the riveted joints of the vessel plates and the many tube connections necessary for both fire-tube and water-tube boilers. In many of the smaller vessels, the design of these two arrangements governs the plate thickness. However the plate thickness has also to be checked against the stength of the whole vessel under pressure. The stresses in a complete spherical shell or a cylindrical shell under pressure were well known, and the simple formulas to obtain them had served designer for many years.

Until 1920, the working pressure of water-tube boilers rarely exceeded 225 lb/in^2, and the safety design of vessels had not changed very much. It was after this period that a great stimulus for further studies came

from the chemical and petroleum industries. Unlike the steam boiler industry, where the working pressures for steam engines were not excessive and increased only slowly through the years, the chemical and petroleum industries required vessels for a large variety of application, size, temperature and pressure. The intense development of the thermal cracking of petroleum in the 1920's and 1930's at the United States demanded better design. Leakage at high pressure was a constant source of trouble. Oxy-acetylene welding was first tried for thin-walled vessels, and forging or hammer welding of vessels was also introduced from Germany for thicker ones. The electric-arc welding process had initially the disadvantage of leaving welds which were brittle and prone to cracking, although the subsequent development of flux-coated electrodes soon overcame the trouble.

The above practices were gradually introduced and tried by the steam-boiler makers, who were then stimulated further by higher efficiencies obtained from the possible higher working pressure, and by the successful development of the steam turbine for power generation.

By the beginning of the Second World War, forge-welded drums were still unacceptable to the boiler makers in England(2-2), although the use of X-ray for non-destructive examination of welds had increased the confidence of the insurers in the complete fusion-welded steam boilers (2-1).

Follow-up investigations and tests after boiler explosions often created interests in the general behaviour of pressure vessels and components. In 1903,

C,Bach published the results of two destructive tests on specially built vessels after an explosion occurring from a fracture originated at the edge of an unreinforced manhold opening. One of the findings was that elliptical openings would be stronger if the major axes were perpendicular to the vessel axis.

Many other tests to destruction were made during the trial and first introduction of the forge-weld method and the fusion-weld method to pressure vessel construction. These tests were necessary because, at the early stages of the development of these methods, reliability of the welds were low and vessels occassionally failed at unexpectedly low pressures. They also brought to light many other weaknesses not considered important in the past, when attention was focused on riveted joints and on expanded tube connections. Some examples of things noticed and discussed include, excessive deformations at some conventionally shaped heads, the advantage of contoured and extruded outlets at manholes, and of putting in reinforcements there, the recommended practice of avoiding pipe-connections and manholes at the knuckle and the edge of heads. Stress-lines among the mill-scales or rust at the knuckle of heads revealed the occurrance of yielding there before other parts of the vessels. These investigations were mostly done at the Europe Continuent where the two noval welding methods were first introduced.

2.2 Pressure Vessel Heads

Many of the earlier investigations on the behaviour of pressure vessel head were from Germany and Switzerland.

C.Bach of Germany published his studies as early as 1899 (2-3), and continued to be associated with many tests on dished ends and elliptical heads at the same period, E.Hoehn, chief engineer of the Swiss Association of Steam-Boiler Owners was also associated with many tests for a number of years starting in 1914, He was assisted from time to time by Dr. A.Huggenberger. Many of his analyses and recommendations were lasting contributions to the knowledge and the design of pressure vessels. One emperical approach of his to the design of torispherical heads, based on the then known tests of such heads, formed the basis of a number of design codes. The formula was published in his paper 'On the strength of dished heads and cylindrical shells' (2-4) which was subsequently abstracted into English by Engineering in 1929 (2-5).

Theoretical analyses of shells were made possible by the pioneering work on the mathematical theories of shells and elasticity by A.E.H.Love in England. His principal work 'Treatise on the Mathematical Theory of Elasticity' appeared in 1892-93. The book, in its second edition in 1906, was translated into German. Since then, the development of the theory was transferred to the Europe Continuent, where H.Reissner extended the theory into cylinders and spheres, and E.Meissner started the breakthrough into other shapes (2-6) by successfully reducing Love's equations into two linear differential equations, one first order and another of fourth order, although the latter could not then be solved in general. Four of Meissner's students extended his work to cover the specific shells of the shapes of a sphere, a cone,

and a cone with linearly varying thickness.

It was due to these pioneering works that the theoretical studies of pressure vessels could proceed concurrently with the many experimental studies. J.W.Geckeler proposed in 1926 simplifying approximations to Love's thin-shell theory, and reduced the complications for getting a solution. W.M.Coates' paper in 1930 (2-7) was one of the important papers in English. There he emphasised why and where the discontinuity stresses cannot be neglected, and showed how Geckeler's general method could be applied in a step-by-step procedure to approximate to the correct solution. The now well-known beam-on-elastic-foundation method is the same in principle to one of Geckeler's approximations, although the former has the attribute of being easier to apply and be comprehend by engineers.

The Pressure Vessel Research Committee (PVRC) of the United States published in 1953(2-8) a report containing a very comprehensive historical review of investigations into pressure vessel heads. The review covered many of the studies in the United States as well as in the Continent until the 1930's. After this period, it turned its attention to the development, and the related works, leading to the drafting of the section on pressure vessel head in the Unfired Pressure Vessel Code of the American Petroleum Institute and ASME.

2.3 Pressure Vessel Openings

Nozzles and other openings did not receive as much early interest as pressure vessel heads, since opening are more local in nature than heads, and since it is possible

to put in reinforcements to compensate for the weakening to the vessels. Bach's tests in the 1900's contained vessels with openings, and so did tests by Siebel & Koerber in the 1920's,(2-9). It had already been noticed at that time,that circular openings were more efficient at vessel heads,that rolled-in openings were bad design especially at regions of high stresses,and that extruded or drawn-out shapes following the natural contour of a membrane under internal pressure were the best shapes for good stress distribution. These recommendations are now well known,although not many of them were immediately accepted in those days. The last mentioned recommendation has frequently been followed in branch connections to main-folds and headers.

A very early series of tests specially planned for pressure vessel nozzles was made by Taylor and Waters in the 1930's (2-10). Thirty-six tests were made,using three cylindrical test vessels and a variety of conventional nozzles used at that time. It is interesting to note that, the state of pressure vessel design then was such that twelve of the attachments were riveted and only seven welded. Surveys of strains were made with 2 in. gauge-length mechanical strain-gauges. It was concluded that for good design,reinforcements should be as closed as possible to the edge of the opening,that over-reinforcement should be avoided,as this would shift the stress concentration from the edge of the opening to regions further away. Siebel further reported,in 1940, on the work at Stuttgart on reinforced openings. The advantage of a balanced reinforcement was clearly demonstrated in his tests,which were all on balanced reinforcement nozzles.

Branched pipes were of great interest in the pipe-line industry and in the construction of boiler headers. A series of tests were reported by Everett and McCutchan in 1938 (2-11) on equal diameter branch-pipes to determine the efficency of collar reinforcements. Huggenberger Tensometers were used at as many as 50 stations at each configuration. Lateral load and internal pressure were applied. Internal strain measurements were of course impossible, and it was clearly admitted that, because of this, the stress picture was incomplete. An attempt was however made to separate the membrane and bending stesses by assuming a hole-in-an-infinite-plate solution as the membrane values.

Very little theoretical work had in those early days been possible with the problem of vessel openings, other than the two-dimensional solution of an infinite plate with a central hole. The solution for a uni-directional load is attributed to Kirsch who published it in 1898. It was known that this two-dimensional solution was inaccurate except for small ratios of opening-diameter to vessel-diameter. Kirsch's stress concentration factor of 3 for uni-directional load becomes $2\frac{1}{2}$ for the stress condition of a cylindrical vessel under internal pressure. Research workers in general agreed that this factor would increase with the diameter ratio, but the precise amount it would increase was not known.

The analysis of holes with raised reinforcements was discussed by Timoshenko in 1924, but it was Beskin's publications in 1944 (2-12) that attracted people's attention. Further discussions of his work are given

in the next Section. Elliptical holes has been a pet problem of many applied mathematicians from an early date, and one of the early exposition in English was that by Inglis in 1913.

2.4 New Techniques and Interests

After the 1930's two experimental techniques were introduced which gave great contribution to the analysis of pressure vessel behaviour. The first is the use of the electrical resistance strain gauge which was conceived in the late 1930's and have since replaced the cumbersome mechanical gauges. Subsequently the technique of water proofing the gauges was developed and this made possible the first convenient measurement of stresses inside an enclosed vessel. Early reference of the application of this technique can be found in Ref.(2-14), and in the reports in this period of the British Welding Research Association (BWRA)(2-15). The other technique was that of stress analysis by photoelasticity. This has of course been known for many years and has been applied to engineering problems ever since the 1900's. The stress analyst had however to wait many years, until better synthetic resins had been developed and until the invention of the polaroid, before the photoelastic bench could be made available to many universities and industrial research establishments. In the 1940's, the stress-freezing technique for photoelasticity made three-dimensional analysis possible (2-16), and opened the way in the 1950's for the analysis of thick-walled pressure vessel problems, and, very recently, to thin-walled vessel problem as well.

The civil use of nuclear power came into existence more

than ten years ago. Many novel and unsual problems were, and have since been,posed to pressure vessel designers connected with the constuction of nuclear power plants. One particular problem that had initiated many investigations was the design of the steel containment vessel for the large graphite reactor. Both the size and the thickness were of a different order of magnitude to that of the usual boiler and chemical vessels or gas containers. Accurate analysis was necessary,as little experience could be drawn upon. During this period many new investigations into such pressure vessel problems were made,backed by nuclear-vessel manufacturers or encouraged by nuclear-vessel code-making bodies. This is reflected in the increase in the published literatures on such subjects,two special examples of which are the collections of papers at the 1960 Glasgow Symposium on nuclear structures and containment (2-16), and the 1962 Inst. Mech. Engr. Symposium on pressure vessel research (2-17). The United States and Britain both published new codes on the design of nuclear pressure vessels.

This period of activity coincides with the advent of the automatic digital-computer which made possible the use of many methods of theoretical analysis which are otherwise impossible, especially those for the solution of shells of complex shapes and shells under unusual loadings. The computer has been used initally as an extension of the mechanical calculating-machine,helping to obtain the final solution from analytical procedures,like compiling tables or computing the series solution for asymptotic methods. It is subsequently also used with

the technique of numerical analysis which is, in many cases, more flexible, and it is soon possible to remove the restrictions of fixed geometical shapes and simple modes of loading to many shell calculations.

3. RECENT LITERATURES: THEORETICAL INVESTIGATIONS

NOTATIONS

E	Young's modulus of elasticity.
G	Shear modulus
ν	Poisson's ratio
σ	Stress, or direct stress
τ	Shear stress
e	Strain, or direct strain
γ	Shear strain
θ	Angle around circumference
U	Product, merid. radius of curvature and transverse shearing force.
V	Rotation of targent to shell meridian
$\bar{x}$	X- coordinate, or independent vainable
$\bar{y}$	Y- coordinate, or function of $\bar{x}$

3. 1. Shell Theories

First Order Theories

The basic equations for thin elastic shells first derived by Love, and another version of these equations by E. Reissner in 1941 (3-6), contain a number of fundamental assumptions. They are that

1. The shell is thin,
2. The shell deflections are small,
3. The transverse normal-stress is negigible, and
4. Normal to the reference surface of the shell remain normal and undergo no change in length during deformation.

These are commonly referred to as Love's first approximations for thin shells.

The first assumption forms the basis of the theory. With this assumption, the ratio t/R_m (shell thickness/ radius of curvature of the mid-wall reference-surface) can be neglected, compared with unity, in the derivations of the equations. With the second assumption, the original geometry of the shell can be used in the calculations. The fourth assumption is a direct extension of the Bernoulli-Euler hypothesis of beam theories, that plane cross-section of the beam remains plane under deformation. All strain components in the direction of the normal n to the mid-wall surface would thus vanish, i.e.

$$e_{nn} = \gamma_{1n} = \gamma_{2n} = 0 .$$

The third assumption states that in the derivation of other stresses, the normal stress to the mid-wall surface is zero, i.e.

$$\sigma_{nn} = 0$$

With the third and fourth assumptions, we can write the direct stresses σ_{11} and σ_{22}, and the direct strains e_{11} and e_{22}, all in the plane of the mid-wall surface, simply as σ_1 and σ_2 , e_1 and e_2 respectively. The stress strain relations for a Hookean, isotropic material are thus reduced to the form

$$e_1 = \frac{1}{E} (\sigma_1 - \nu \sigma_2)$$

$$e_2 = \frac{1}{E} (\sigma_2 - \nu \sigma_1)$$

$$\gamma_{12} = \frac{1}{G} \tau_{12}$$

where E, G, ν are the Young's modulus, the shear modulus

and the Poisson's ratio respectively.

A shell of revolution with axisymmetric loadings has a complete symmetry with respect to the circumferential angle θ . Three equations of equilibrium can be written for a small shell element, two equations are for forces and one for moment, all taken in the radial plane through the axis of rotation. They are in the form of three differential equations in three unknown quantities. It has been mentioned that H.Reissner and E.Meissner first made the solution of these equations possible,(the process involved has been well documented in books on shell theories.*) They successfully reduced the equations into two, using two special variables, one being the angle of rotation V of a tangent to the meridian, and the other U being the product of the meridional radius of curvature and the transverse shearing force. Two second-order simultaneous differential equations were obtained. The two unknowns were then separated leaving a fourth-order linear differential equations of one or the other unknown. Thus the process of obtaining a solution for individual problems consists of finding the complementary and the particular solutions of these problems,represented by

$$U = U^c + U^p$$

or $$V = V^c + V^p$$

The particular solution accounts for the external loadings, and the complementary solution satisfies the

---

* See chapter 16 of (3-7) or Chapter 5 of (3-8).

boundary conditions to the shell. For many years the history for the solution of many practical shell problems has been one of finding solutions to these fourth order equations.

Exact analytical solution to the above equation was generally not possible, unless it could be split into two convenient second order equations, and this can be done only for cases where the shells are of constant thickness and constant or zero meridional radius of curvature. A knowledge of a number of mathemetical and physical functions is required to obtain the analytical solutions; but the method does open the way for solving many problems involving cylindrical shells, conical shells, and spherical shells, as well as a combination of such shapes forming a number of practically shaped pressure vessel components. All these meant that engineers and applied mathematicians had to be armed with such functions, or their tabulated values. There are many examples of the use this analytic solution of shells, (3-9) to (3-13).

Many other shell problems do not fall into the above category. Toroidal shells and ellipsoidal shells are two commonly used shells of revolution where the fourth order equation cannot be separated into two convenient second order ones. Instances may also arise when problems involving shells that can be analysed exactly cannot however be solved because tables of the required mathematical functions are not readily available. A number of methods giving approximate solutions have been developed for many of such cases. One method is due to

Geckeler (3-14), and consists of a number of alternative approximations made to the normal procedure for solving the equations. The approximations give varying degree of convenience and of accuracy to the solution, depending on the problem. One other method that has been found useful is a general mathematical procedure called asymptotic integration. One variant of this method was systemmatically applied to shells of revolution by Naghdi and DeSilva, first discussed in 1954, and then successfully applied to ellipsoidal shells (3-15) and to paraboloidal shells (3-16). Leckie and Penny applied it to shells of revolution under arbitrary loadings (3-17) and (3-18).

Higher Order Theories

The above works have all been on linear first-approximation theories of thin shells. Work has also been done on other kinds of theory, many of them ~~were~~ are sophisticated ones developed initially by applied mathematicians and later found to be of use to engineers or to give important observations of interest to them. Shell theories that suspend one or more of Love's assumptions, except the one on small deflections, are still linear in nature and are called 'higher order' thin shell theories. Those that do not follow completely the assumption of small deflections are non-linear.

One group of higher order theories delays the application of the first thin-shell assumption in the devivation of the equations. If y is the normal distance of a shell fibre from the mid-surface, and R is the radius of curvature at that location in one of the two principal

directions, the term y/R can be neglected compared with unity under the strict application of the thin shell assumption. Theories as developed by Flügge (3-19) and Lur'e (3-20) do not neglect this term in the initial derivations of the shell equations and expressions. The terms comes into the equations through expressing the relations between the mid-surface displacements and the general fibre strain, and this term is passed on to the stress-strain relations. When the normal forces and the bending moments are derived in terms of the displacements, integration of the fibre stresses has to be made through the wall thickness, and here Flügge and Lur'e retained the terms y/R compared with unity, but dropped $(y/R)^2$ and higher order terms.

Another group of higher order theories drops the third assumption, that the transverse normal stress is zero, and the fourth one, that the normal to the mid-surface remains normal and unchanged in length. Such theories were proposed and developed by many, including E.Reissner (3-21) and Naghdi (3-22).

It is not often that these higher order theories are applied to solve actual problems. There is thus great interest to see how they compare. Klosner and Levin (3-23) compared for one particular problem the results from a elasticity theory solution and from two shell-theory solutions. One of these shell theories was based on Love's postulates, and the other one was a higher order theory based on the above Reissner-Naghdi theory which basically incorporated the effect of transverse shear and normal stress. The problem is that of a long circular

cylindrical-shell loaded under periodically spaced pressure bands. Two cylinders of different thicknesses were compared, one falling outside the normally regarded accuracy range of the thin-shell theory, and the other within it, the outside-diameter to thickness ratio d/t being 6.7 and 28.5 respectively. The stress magnitudes and distributions across the cylinder thickness were obtained and compared, with the elasticity solution regarded as the exact one. The conclusion drawn was that the R-N theory did not necessarily lead to a better prediction of the stresses than a first approximation theory. A further comparsion of the transverse displacement showed that here the R-N theory gave a better estimation.

3.2 Numerical Solution

The digital computer has opened up many possibilities to the solution of shell problems. The first use of the computer by engineers and applied mathematician has been on existing procedures of analysis and whenever tedious calculations were necessary, such as solution of linear equations or integration of differential equations not in a suitable form for direct analysis. In the late 50's and early 60's, Galletly solved many of his shell problems by numerical integration, and tabulated influence-coefficients with the aid of the computer for a variety of shell geometries, most of which had defied attempts at analytical solution in the past. As the potential of the computer was better and more widely known, it was gradually realised that its usefulness in the solution of pressure vessel problems

could be very wide and general, and that without much additional efforts, computer programs could be made into general-purpose tools avoiding much duplication of efforts.

Three Numerical Methods

There are three methods of numerical analysis that has been found useful in shell problems. The first is the method of finite-difference which is well known in the numerical analysis of differential equations. If y is the unknown function of x , the first and second derivative of y, at a general point x_i of a equally divided mesh along x , are approximated by the finite-difference formulas

$$\left(\frac{dy}{dx}\right)_i = \frac{y_{i+1} - y_{i-1}}{2}$$

$$\left(\frac{d^2y}{dx^2}\right)_i = \frac{y_{i+1} - 2y_i + y_{i-1}}{2}$$

where $y_i = y(x_i)$

and $x_{i+1} - x_i = x_i - x_{i-1}$

Differential equations of y are thus converted into algebraic equations of the unknown values y_i and then solved algebraically. This procedure can also be applied to differential equations with more than one dependent variables. Here we note that the original Reissner-Meissner form of the equations for shells of revolution are simultanious second-order equations with two dependent variables V and U. For this reason the finite-difference method can be directly applied to obtain numerical solutions with no necessity for using the combined fourth-order

equations which, as mentioned, cannot always be obtained. This procedure has been successfully applied by many workers (3-24 to 3-26), and there have also been extensions to arbitrary loadings (3-27).

Ordinary differential equations can also be solved by the method of stepwise integration, also referred to as numerical integration. This has also been used on shell problems. The shell equations are integrated in a step-by-step manner, through given intervals, and starting from prescribed values at the initial point. The required solution must also satisfy the conditions at the end points, and, for this, additional manipulation is needed to find out what are the correct initial values. Two integration procedures are commonly used, the fourth-order Runge-Kutta procedure (3-13, 3-28, 3-29) and the Adams' procedure (3-30 to 3-32), which is a particular type of the 'predictor-corrector' method.* The integration is performed on first-order equations. For the basic problem of shells of revolution with axisymmetric loads, four simultaneous first-order equations are used. They are obtained either from breaking up the two Reissner-Meissner equations or from the more fundamental equilibrium and strain-displacement equations.

The third numerical method for solving these shell problems, the finite-element method, is also commonly used for other structual and continuum stress-analysis problems. Here the body to be analysed is physically sub-divided in the analysis into small units, called finite-elements, of sufficiently small size. The equations defining the inter-

* See Chapter 9, (3-33), or Chapter 3, (3-34).

action between the adjacent shell elements are written down and solved using the procedures of matrix manipulation and invertion that can be done very conveniently on the computer. Because of symmetry, thin shells of revolution can conveniently be approximated by using truncated cones as the finite-element (3-35), although curve-sided elements have also been used (3-36).

Study by Kraus

Kraus made a study of these numerical procedures and compared a number of these computer programs (3-37). One particular shell problem, that of a cylindrical shell with hemispherical head under internal pressure, was analysed with four programs and the results compared. The vessel and head have the same uniform thickness and have a mean-diameter to thickness ratio of 41:1. Two of the programs, by Radkowski et.al.(3-26) and by Penny (3-24) and (3-38) are based on the finite-difference method, while the third one, by Kalnins(3-31), uses the predictor-corrector method of stepwise integration. The equations they use are from the first-approximation thin-shell theory. The fourth program, by Friedrich (3-36), is a finite-element program, and, in addition, it is based on a higher order theory which incorporates the effect of transverse shear and normal stress similar to the Reissner-Naghdi Theory. A first-approximation thin-shell analysis of the geometry has been made by Watts and Lang (3-11), and was regarded by Kraus as the exact thin-shell solution and used as a basis for comparison of stresses. Kraus found that the results of the first three programs agreed nearly exactly with each other with regard to both stresses and displacements.

They also agree nearly exactly with the values where stress results from Watts and Lang are available. The Friedrich program ,because it is not based on the same theory, gives slightly different results from the others. This comparison shows the general agreement of the programs but no conclusion can be drawn from the slight differences between the two theories or their relative accuracies.

3.3 Pressure Vessel Nozzles

Theoretical studies of pressure vessel derive direct benefit from the above mentioned works on shell theories and their solution, and many of the solutions tried were actually on heads of one shape or another. Pressure vessel nozzles however can have a variety of shapes and arrangements. Extra efforts have to be made in addition to a straight forward solution of the shell theory to make the mathematical idealisation suit the local geometry.

The effect of reinforcement has attracted attention for some time. The paper by Beskin in 1944 (2-12) is a well known example of this study. He represented the reinforcement by a pair of pads on both sides of the vessel wall, or a rim at the edge of the hole, or a combination of both. The vessel wall was however considered as an infinite flat-plate and the results are thus strictly applicable only to small openings.

With larger opening-diameter to vessel-diameter ratio, the effect of curvature increases the stress concentration. Among the very first investigators who considered the full effect of curvature, treating the vessel as a

spherical shell, is Galletly,who in 1956 (3-29) solved the problem of a hemispherical shell with a central hole. It is also in this same report that he used three variations of the Geckeler approximations and discussed their accuracy. Rose and Thompson (3-40) also used the same procedure to plot stress concentration factors and stress distributions,both for flush nozzles and for semi-infinite protruding nozzles.

Local Junction Stress

These solutions are already good improvements over the Beskin and similar formulas,but,when detailed comparisons were made with experiments,it was found that the high predicted stresses at the junction were sometimes much greater than that observed. Agreement may be good along the nozzle and the vessel wall, but the theoretical meridional bending-stress at the junction does not represent adequately the actual local stress at the junction and are, in many cases,much too high when the nozzle is of the protruding type or when the nozzle is finished with no sharp stress-raiser. This disagreement caused confusion to those designers who tried to use the theoretical junction stress to design against fatigue or to distinguish a good design from another.

The inaccuracy is in short due to the limitations of the thin-shell theory which represents the shell as being located at its mid-wall position, and thus cannot picture accurately the local stresses at a shell discontinuity unless additional correction is made there to a direct application of the thin-shell theory. One remedy taken by Leckie and Penny (3-41) was to neglect the maximum

stress value at the nozzle and use that found at the vessel shell. The reason they put forward, was that the actual maximum stress was found from many experiments to occur at the vessel side of the junction. Another approach was to spread the interacting forces between the two intersecting shells such that, instead of acting at one circumferential line at the end of the shell they act, for each shell, on a circumferential band equal in width to the projected width of the thickness of the other shell. An example of this, applied to protruding nozzles, can be found in O'Connell and Chubb,(3-42).

Non-linear Analysis

Analyses into the non-linear or non-elastic behaviour of shells tend either to get more involved or to use very different approaches. The limit analysis of shells is also an important method for the understanding of pressure vessel behaviour. This method of limit analysis, sometimesknown in the theory of structures as plastic analysis, has been applied for many years to the problems of framed and other building structures, and in a different form to metal-working problems. Symmetrically loaded cylindrical shells without axial force was first studied by Drucker in 1953(3-43) and the problem of general shells of revolution was treated by Onat and Prager in 1954 (3-44),other problems studied include spherical caps (3-45) and flat plates (3-46,3-47). The theory and the results of a number of works on symmetrical plates and shells was summarised by Hodge in 1963 (3-48). Further works, specifically applied to pressure vessel components,are mentioned in a later section 3.3 in connection with vessel failure behaviour.

Elastic-plastic stress analysis aims to determine the behaviour at different stages after yielding of the material. It can thus give a more complete picture than a limit analysis. The yielding behaviour of the commonly used metals are approximated mathematically by a yield criterion. The subsequent stressing behaviour is then approximated by plasticity flow-rules. The relations are much more complex than that for elastic stress-strain behaviour, and their general solution has not been possible until the introduction of the digital computer to engineering analysis. Marcal (3-49) has successfully analysed the elastic-plastic behaviour of some shells of revolution on the digital computer. The structures were analysed in small steps of load increment and, within each increment, the problem is considered linear with the stress-strain law given by the plasticity flow-rules. Spera(3-50) has also analysed such problems using a different technique.

Non-symmetrical Nozzles

Theoretical solutions of non-symmetric shells are more difficult than shells of revolution. A problem of great interest is that of a cylindrical nozzle attached to the side of a cylindrical vessel since this is a common arrangement in many pressure vessels. It has been possible to analyse the problem of circular cylindrical shells under arbitrary loads with the aid of Fourier expansion around the circumference of the cylinder. This procedure was extended by Bijlaard to analyse the local radial load and local moment on cylindrical pressure vessels (3-51),(3-52). The work has since been published in a form more convenient to designers (3-53).

Circular openings in a cylindrical shell was first

analysed by Lur'e (3-54), although certain errors has since been found. Withum (3-55) used a perturbation scheme to consider the torsion problem. A more accurate analysis of the nozzle problem is to treat it as the intersection of two cylindrical shells. Reidelbach investigated the special case of equal-diameter cylinders intersecting at right angles (3-56). Eringen, Naghdi and Thiel investigated the state of stress of circular holes under different loading conditions at the edge of the hole and at the ends of the cylinder (3-57). Using these results, solutions were then presented (3-58) for the problem of intersecting cylindrical shells with the restriction of small diameter ratios. The finite-element method of shell analysis has recently been successfully applied to the bending solutions of general shell elements. Using a simple element, Clough & Johnson (3-59) took the cylindrical-nozzle problem as a test example and obtained a solution agreeing well with experimental results by photoelasticity.

4. RECENT LITERATURES: EXPERIMENTAL INVESTIGATIONS

4.1 Experimental Techniques

Electrical Strain Gauge

The most common tool for stress analysis of prototype vessels or metallic model vessel is the bonded electrical-resistance strain-gauge, or called simply the electrical strain gauge. The gauge is laid on and usually adhered on to the surface of the vessel. Any straining of the surface in the direction of the gauge causes a small change in the electrical resistance of the gauge wire, which is detected and quantitatively measured by a sensitive amplifying instrument. Mechanical strain gauges were of course once used, but except for special reasons, for example in (4-1), the electrical gauge is at present exclusively used because of its many advantages.

The electrical strain gauge has made it possible to make internal strain measurements of enclosed vessels, even those under liquid pressure. The technique for such measurement has taken some time to develop because of two difficulties. The first one is to get the lead wires of the gauges out of the vessel without leakage and loss of pressure. Kooistra and Blaser (2-14) were among the first to describe the successful application of techniques to overcome this. Similar uses of the technique, but differing in details, were described by Swanson and Ford (4-2), and Mantle and Proctor (4-3). The basic idea is to provided a satisfactory seal to the individual wires, or wires grouped as a cable, out of the hole provided in the vessel or its flange cover. With a commonly used method, liquid expoxy resin is poured around

the wires or the cable and allowed to set in situ. Another method requires pulling the wires or the cable through a prepared softplastic sleeve which is held in place and squeezed by a tightening nut. Both the resin plug or the plastic sleeve are tapered in shape with the larger end facing the pressure to give it a self-sealing action.

The other difficulty is the protection of the gauges. This is of course not necessary if air is used as the pressurizing medium, but there is in this case a great danger of explosion if the vessel fails, which is why air is not often used, with very few exceptions (for example, (4-4)). Water is commonly used, (4-5)-(4-10). Here complete protection in the form of water-proofing is necessary. The electrical strain gauges give very small changes in resistance under strain, and the conductivity of water can cause a sufficient shunting of the resistance to change the strain readings. Although water-proofing is widely described, and even disscussed in textbooks (see Ch.8 (4-11)), it is still a troublesome process, especially when a large number of gauges are used or when they are used inside a confined space. Pressurizing liquids with very high insulating properties reduce this trouble, and investigations have been reported where transfomer oil, hydraulic oil, or liquid paraffin (4-2) are used. When fatigue tests are performed, investigators may prefer to use water in order to provide a similar environment to that of boiler water on vessels. Kooistra and Lemco (4-7) stated this as the raason, and it is probable that Lane and Rose (4-16) and other workers at BWRA used water for the same reason.

Geometrical accuracy is an interesting consideration in the stress analyses of vessels. Most of the tests on metallic vessels using strain gauges are either on actual vessels in service or on special experimental vessels fabricated in a similar way to normal manufacturing practices. They would thus give an indication of actual behaviour of vessels in service, but they suffer from the disadvantage that the error due to imperfect fabrication would also appear in the results. Many of these results have been compared with theoretical stress analyses and there has always been the problem of finding the cause when discrepancies occur. Morgan and Bizon, of the NASA Lewis Research Centre, carried out carefully executed tests (4-17) on two thin toriconical heads made to the same shape, the only difference being the accuracy of the fabrication method. One head was spun and welded to a cylindrical vessel. The other was contour machined from a complete billet. The strain gauge results were compared with that from a linear thin-shell theory and good agreements were obtained for both test results. There is however a definite superiority of the machined-head results, where differences to the theoretical results average at 3.8% , whereas the corresponding average of the spun head was 9.2% .

Photolastic Analysis

The other commonly used method for analysing stresses at a pressure vessel is photoelastic analysis. Stress freezing inevitably has to be used because of the three-dimensional nature of the geometry. Vessel components forming shells of revolution simplify the analysis and

reduce the work because of symmetry, but stress freezing is still required. The first investigations were all on thick vessels,(4-18) to (4-20), but recently thin vessels have also been analysed, notably by Fessler and Stanley (4-21) and by a few investigators in the U.S. (4-22). The one great advantage of stress-freezing photoelastic-analysis over strain-gauge analysis is that stress changes through the shell wall can also be measured. A complete picture can thus be made of the stresses if required. This is especially useful for thick-walled vessels; thin walled vessels are known to have a linear distribution of stresses through the thickness.

There is always an unknown in the use of photoelastic results, this being the effect to the stress values caused by differences in the Poisson's ratio ν . Steel and other common pressure vessel materials have a value ν of about 0.3 while photoelastic plastics undergoing stress freezing have a value of 0.5. Studies on the nature of this effect have been made, for example, (4-23) and (4-24), Unfortunately the observations were found to apply only to specific problems and could not be generalised; even extensions of observations to other similar geometries and loadings have to be treated with care.

4.2 Pressure Vessel Heads

The great interest on pressure vessel heads also attracted a large number of experimental investigations. Photoelastic tests are normally on accurately machined components. It was mentioned previously that many

strain-gauge tests were however on actual vessel or normal shop-floor fabricated models and suffered from an unknown amount of inaccuracies caused by manufacturing tolerances. There were none the less a few accurately conducted strain-gauge tests. Tests results on the common shape of torispherical ends have been collected and intepreted by Fessler and Stanley (4-25), who also refer to their series of photoelastic tests on such heads reported in 1965, (4-21). A number of the investigators quoted in Ref.(4-25) also did tests on ellipsoidal heads. Conical heads were the objects of a series of tests at Purdue University sponsored by the Pressure Vessel Research Committee (PVRC) of the United State, and a report in 1953 (2-8) by the Design Division of PVRC gave a summary and complete bibliography of these tests. Flat heads are normally used in thick-walled vessels. Photoelastic tests of integral flat-heads were made by Fessler and Rose (4-18) and by MacLaughlin (4-26) who also presented results of a Russian reference (4-27).

4.3 Pressure Vessel Nozzles

Experimental stress analysis of pressure vessel nozzles is complicated by the fact that, unless analysis of a specific nozzle or a specific nozzle arrangement is required, the problem can be divided into many types depending on the overall arrangement, the local detail, and the kind of loading. The arrangement can be such that the geometry is completely symmetrical, or that the nozzle rests radially on a cylindrical vessel, or that the nozzle is oblique. Whilst pressure is the fundamental loading on a pressure vessel, external forces and moments have to be considered for a nozzle. Local

details are important at a nozzle, because the stresses depend as much on this as on whether the nozzle is flush located or protruding, reinforced or unreinforced, and on the method of reinforcement.

The PVRC did an impressive series of tests on nozzles spreading over a number of years. Their main attention was on flush contoured nozzles mostly analysed by three-dimensional photoelasticity. Both symmetrical nozzles on spherical vessels and side-nozzles on cylindrical vessels were tested. There was also a certain number of metallic models analysed with strain gauges. Summaries and intepretations of these test results, as well as a good bibliography of these and other American works, can be found both in the earlier report by Mershon (4-28) and in the later one edited by Langer (4-29).

In the United Kingdom, the British Welding Research Association (BWRA) did a number of fatigue tests on pressure vessels. In connection with this work, static stress concentration factors of many nozzles were obtained (4-6),(4-9). Their nozzles are mostly welded with partial penetration, some pad-reinforced and none of them contoured.

One method of reinforcing nozzles is to use forged rings at the intersections. A number of these nozzles were stress analysed by Kitching and his colleague (4-8),(4-30), (4-31). Different types of loadings were used.

Kaufman and Spera (4-32) did an experimental analysis of nozzle opening in a spherical vessel testing into

the elastic-plastic range. They also tried to correlate the results with a theoretical elastic-plastic analysis, the first known attempt for pressure vessels. The opening had unfortunately a rectangular cross-section reinforcement which is not a suitable shape for their theoretical analysis. For this reason, the comparison of the local stress is not exact.

5. RECENT LITERATURES: FAILURE BEHAVIOUR

5.1 Modes of Failure

The investigations mentioned above in Ch.3 and 4 are on the study of the behaviour and the stresses at vessel and vessel components. The hope is that they will lead to better design, through, for example, better layout of the vessel, better geometry of the component, or better positioning of the reinforcements. One of the final aim of a vessel design is its safety, and it is necessary that a vessel and its components are safe enough to withstand normal service loadings and other possible loading without failure. We can thus find a number of other investigations, some very much connected with the mentioned investigations, looking into the problem of vessel failure - the manners, cause, and mechanism of failures, and the methods of predicting them.

Early interests on failure have often been on the phenomena of excessive yielding, bursting, brittle fracture, collapse and buckling, and many experiments have been performed to reprodude them.* Theoretical analysis of failure have however been lagging behind in many cases. Recently, emphasis has also been on the study of repeated plastic loading. The failure connected with this type of loading is not as catastropic as the others mentioned above, and occurrs often initially in the form of fatigue cracks. But in the power-plant, chemical or petroleum industries, this type of repeated loading does occur

*See Maker, F.L. and Burrows, W.R. History of the design of heads for pressure vessel. Appendix 1 to Ref. (2-8)

frequently, through, for example, the starting-up and shutting-down of plants. This, coupled with the lack of understanding and knowledge of this type of failure, is also one of the major problems facing the designers.* A brief summary of the different types of failure of pressure vessels is laid out below.

For the case of static loading (usually mechanical like pressure, dead weight and thrust from attachments or nozzles, but this can also be thermal loading) failure can be due to:

1. Excessive deformation { Elastic / Elastic-plastic
2. Instability { Elastic - Buckling / Elastic-plastic { collapse / Bursting
3. Brittle fracture

Under repeated loading (again both mechanical or thermal) failure can be due to:

1. Elastic fatigue,
2. Elastic-plastic stressing { Plastic fatigue (or Alternating plasticity) / Incremental collpase

Failure at high temperature can, in addition to the above, be due to:

1. Large creep deformation,
2. Creep rupture

The study of failure can also be about aspects of corrosion which is one of the influening factors of failure, and about the theoretical phenomenon of shake-down, which is when a vessel does not tend to fail by

*See Hessler, H. and Stanley, P. (Eds.) Current pressure vessel problems. London, Inst. Mech. Engr, 1968.

plastic fatigue nor incremental collapse.

In the following review, not all the above mentioned modes of failure are discussed, but more attention is focused on those modes of failure subsequent to elastic-plastic behaviour, since this is the interest of this thesis.

5.2 Static Loading

Excessive Deformation

In the design of some pressure vessels, for example, the housing of some close-fitting pumps or the top cap of graphite-moderated nuclear reactor vessel, excessive deformation is considered as a mode of failure, or strictly speaking, a criterion of design. The deformation can be kept within limits by previous experience or by prototype testing. It can also be estimated in some cases by theoretical calculation, and here it is important to distinguish between elastic deformation and elastic-plastic deformation, which of course makes the calculation much more difficult.

The study of excessive deformation is, in general, closely connected to the general study of pressure vessel behaviour. For example, during many strain gauge testing of prototype or model vessel components, deformation are often recorded. A number of numerical and analytical methods for solution of vessel stresses and strains also yield the displacements, i.e. deformations. No study of deformation is thus specially mentioned here as they have been reviewed in Ch.3 and 4.

Closely associated with this study is the detection of gross yielding over a large area, during proof testing of

vessels or components whose design is beyong the scope of the Codes. The vessels are either strain-gauged, or coated with brittle lacquer, and pressurized until yielding at the external surface is clearly detectable. The maximum allowable working pressure is then defined as a certain fraction of this pressure.

Plastic Bending Instability-'Collapse'

This is commonly called collapse failure. It occurs when the applied load attains such a magnitude as to cause certain areas of the vessel to yield to such a degree that the amount of constraint of the elastic areas is not sufficient. The vessel then proceeds to a mode of unrestrained deformation. This deformation is caused by bending around yield hinges. In many cases, there is a definite limit to the load-holding power of the structure. This failure is quite similar to the commonly called 'bursting' instability of vessel, where a similar unrestrained deformation is caused by the elastic areas failing to restrain the plastic areas that yield, in this case, under direct stressing rather than bending.

The theoretical analysis of such an instability is centred around the bending action of the shell. The original idea came from the plastic structural analysis or limit analysis of beams and frames, which was well developed at around the 1950's (see Refs. (5-1) and (5-2)). The application of this limit analysis was extended to continuum mechanics, and next to plates and shells of simple shapes. For plates and shells, the solution can become very involved, since the yield surface enveloping the safe-load vector is found to be quite complicated. Various simplifying approximations have to be made for some

problems. Drucker and Shield (5-3) suggested an approximation neglecting the contribution of the hoop moment in a symmetrically loaded thin shell of revolution, and proceeded to obtain solutions for toroidal knuckles and for torispherical pressure vessel heads (5-4). The solution for a whole range of torispherical pressure vessel heads was later published in graphical from, making it available to a wide group of investigator and designers (5-5).

Gill made further use of the Drucker and Shield procedure and obtained approximate solutions for flush cylindrical-nozzles on spherical vessels (5-6),(5-7). A similar but less extensive investigation was made by Cloud at the same time (5-8).

This theoretical limit analysis of axi-symmetrical shells assumes that the shells fail under bending moment around yield hinges formed around the circumference of the shells. Assumption and limitation made to the method are very similar to the plastic analysis of frame-structures. Unless modifications are made to the solution, the usual assumption are,that the material stress-strain property is perfectly-plastic,and that the effect of goemetry change is negligible until collapse.

Early tests on collapse failure have been found usefull for determining specifically the strength of vessels and for helping in selecting a good geometry from others. No general quantitative relations can be determined from these tests because of the large number of parameters involved. Theoretrical analysis has however been able to provide this quantitative picture,establishing the

influence of the different parameters and their relative importance. With theoretical solutions being available, the emphases of many tests were then changed to checking these theoretical solutions where they are available, and of filling up the gaps of knowledge where they are not. Both Gill (4-10) and Cloud (5-8) made a number of tests on symmetrical nozzles in parallel with their theoretical works. They have in general found reasonable agreements.

The above mentioned limit theory of shells is on symmetrical problems only. Cottam and Gill tested to collapse a large number of nozzles attached to the side of cylindrical shells (5-9). There was, at the time, no appropriate theory for such a case, although subsequently an approximate analysis of this problem was reported (5-10).

Stoddart (5-11) reported tests on a single mild-steel torispherical head to collapse, and found again reasonable agreement with the Drucker and Shield solution. Kemper et.al. tested two identical vessels made of different stainless steels to find their pressure-holding strength (5-12). The high degree of ductility and of strain-hardening of the steels caused the vessels to remain intact even after a large amount of deformation.

5.3 Repeated Loading

General Introduction

The behaviour under repeated loading of many civil engineering structures, especially frames, has been much studied in order to establish a more general plastic design procedure of structures. Detailed discussions

of the different modes of behaviour and their methods of solution can be found in the books by Hodge (5-2) and Neal (5-1).

In an example taken from Ref.(5-2),Ch.5, a pin-supported portal frame is loaded by two time-dependent repeating load systems,a horzonital one F_1 at the top of the frame, and a vertical one F_2 on the top bar. To establish the theory,the same assumptions as the limit theory of frames aretaken, that the material is elastic perfectly-plastic. Thus, under bending, perfect yield-hinges are assumed at the beam. It was shown that, under varying modes of cycling of the two loads F_1 and F_2, various resulting behaviour of the frame can be observed. Under sufficiently small loads, the frame may of course remain elastic throughout; but as the loading is increased,there is also a case where initially the frame yields at certain region, but the strains are gradually relaxed and the frame 'shakedown' to a elastic condition again. The frame may, in some cases,deform plastically during each cycle, but return to the same condition after each complete cycle,i.e.a condition of cyclic collapse, or alternating plasticity. Thirdly, the frame may also deform plastically during each cycle,but at the same time suffer a steady and uni-directional deformation after each cycle,i.e.a state of incremental collapse.

These three modes of behaviour would each cause failure after a sufficient number of cycles,although the degree of severity varies greatly. Incremental collapse is not an immediate collapse as that predicted by the limit theory. Failure occurs through the total deformation

increasing at every cycle. Alternating plasticity is also undesirable since fatigue failure will occur at the areas of the yield hinges. Elastic shakedown behaviour is,relatively, a much safer one than the others, and failure occurs only through the common elastic-fatigue caused by the repeated nature of the loading.

With pressure vessels under repeated loading a similar situation to the above for frames may occur. In this case the fundamental element is a plate or a shell element under bending, with shear and direct forces as the subsidiary loads. (In the above frame example, the fundamental element is a beam or column under bending plus direct and shear forces.) The two-dimensional nature of a plate or shell element makes the problem more complex. Nevertheless attempts have been made, giving steady progress.

Shakedown

A structure under repeated loading is in a shakedown condition when, after possible initial yielding of part of the structure, this yielding is gradually relaxed giving a final condition of complete elastic behaviour. The structure would undergo no alternating plasticity nor incremental collapse. The shakedown load can be determined for simple structures by trial and error calculations,following the load history of the structure under cycles of load. This is the method used by Neal and Symonds (5-13) for portal frames.

Bounds for shakedown load as defined by mathematical theorems has been proposed and justified for elastic-perfectly-plastic materials. A lower bound theorem

was proposed and applied to structures by Symonds and Prager (5-14) and others.* A complementary upper-bound theorem was proved by Koiter (5-15). This is less useful practically, and further application of it has not been noticed.

Symonds (5-16) successfully expressed the lower-bound theorem as applied to a continuous medium, opening the field to structures and bodies other than frames. In general terms, it states that, if any set of residual stresses can be found such that the addition of an elastic stress state, calculated for all possible load combination, results in stresses which do not violate the yield conditions, then the structure eventually will shakedown.

Leckie in 1965 (5-17) successfully determine lower bounds for symmetrical nozzle under internal pressure following this lower bound theorem. Elastic solutions of nozzles were used to determine probable residual stress systems. Any internal pressure load that can be superpositioned on these residual stress systems without causing yielding at any part of the shell is a lower bound to the highest shakedown load. Further results for other loadings have been reported (5-18).

Alternating Plasticity

A structure that is under a higher load cycle than the highest shakedown load cycle either proceeds to behave under alternating plasticity or under incremental collapse. The state of alternating plasticity is one where, after

---

*See section 8.3, Shake-down theorems, of Ref.(5-1).

each cycle of loading, the same state of stress and deformation is obtained, but at each cycle the behaviour is not elastic throughout the structure.

The damage to the structure is accumulative, as energy consumed in plastic straining is not reversible. Fatigue cracks and subsequent failure occur after more and more plastic energy is consummed. ~~Greater detail of this as a failure mode is treated under Fatigue below.~~

Incremental Collapse

Incremental collapse as a mode of failure was first recognised for civil engineering structures in connection with the other investigations on repeated loading. It was the aircraft structure investigators who later showed their interest (5-19). In this case, the loading may be a combination of mechanical and thermal ones. Edmunds and Beers (5-20) demonstrated its occurance in loading systems similar to those in pressure vessels, the example being that of plates under simulataneous bending and direct load.

6. AVAILABLE COMPUTER PROGRAMS FOR VESSEL ANALYSIS

Notations

General

E	Young's Modulus
G	Shear Modulus
ν	Poisson's Ratio
p	internal pressure
h	half of shell thickness
ℓ	distance or length along shell meridian, the independent variable of shell differential equations
$\delta\ell$	meridional length of a shell element
r	radius vector of a point in the shell
θ	angle of inclination of outward normal to shell from normal to shell axis.

Shell Equations

u	radial displacement of mid-shell-wall
v	axial displacement of mid-shell-wall
ϕ	rotation of shell meridian
ϕ'	$\frac{d\phi}{d\ell}$.
F	radial force per unit circumference
$X_1\ X_2\ X_3\ X_4$	the independent variable u, ϕ, ϕ', F in the shell differential equations.
$\Delta\ell$	interval length in integration

Boundary Control Process

$G_{1m}\ G_{2m}$	linear functions of the X_i s, denoting boundary conditions at branch m
C_{ijm}	constant coefficients in functions G_{im}
M	number of shell branches radiating from junction
ζ	accuracy in boundary control procedure.

Stress-Strain Relations

σ stress, or direct stress

τ shear stress

e strain, or direct strain

γ shear strain

$\bar{\sigma}$, $\bar{e}$ equivalent stress and strain

σ', e' deviatoric stress and strain

e_p plastic strain component

H' $\frac{d\bar{\sigma}}{d\bar{e}_p}$

$d\lambda$ constant in Prandtl-Reuss equations, see equation 6.15.

Y yield stress

α ratio, elastic strain increment / total strain increment at a transition point

Yield Stress Expression

k_i i th constant in algebraic poly nomial for yield stress, see equation 6.26

Special Subscripts

S-1, S, S+1, interval points for integration

m branch number, m = 1, M.

e elastic component.

p plastic component.

Special Superscripts

(o),(1) zero and first estimate

A at starting point of shell branch, ie. at junction.

B at end point of shell branch

' derivative, except when used on σ and e.

f fititions value, see eq.(6.26a).

In parallel with the author's works, two computer programs were being developed at the Imperial

College, London, by P.V. Marcal, who was assisted by W.R.Pilgrim at the Computing Branch of the Central Electricity Generating Board (C.E.G.B.), London. The programs are both for stress analysis of pressure vesels where the loading and geometry can be altered to suit each individual problem. The earlier program, called PVA1 is for the linear elastic analysis of thin shells of revolution. The other program exists in a number of versions, but are all generally referred to here as PLINTH. This is an extension of PVA1 to take progressively increasing load beyong the first yield of the vessel, so that an elastic-plastic stress analysis of the vessel is obtained.

The theoretical part of the author's present work is connected with both the development and the testing of the two programs. Although the programs have now been documented (3-32),(6-1),(3-49), a short description of them is given here in order that the present work may be followed. The parts the author contributed to the development of these programs shall be described in greater detail.

6-1 Elastic Program: Capability

PVA1 is a general purpose stress analysis program for the axisymmetric loading of thin shells of revolution. It is general purpose in the sense that the same program can analyse a large variety of problems. The program requires only the supply of a relatively small amount of data drawn up according to each individual calculation. A wide range of geometrical shape and loading can be accepted although the loading has to be static. Solutions can be obtained for the stresses,

strains, displacements, shear forces and bending moments at points along the shell.

The program is written in Fortran IV for the IBM 7090 and 7094 computers with 32,000 words of 36 bits in the core store. No magnetic tape or other subsidiary stores are required. For normal use, no access and correction to the program instructions are necessary. All the informations are to be supplied in a concise manner in data cards drawn up by the user for each specific problem. Very detailed instructions for using the program are given in the user's manual published by the C.E.G.B.(6-1).

The author has written a set of flow-diagrams, given in appendix A, to complement the above report, giving the flow within the important subroutines and the interconnections between them. The flow-diagrams are necessary and very useful if any corrections and alterations are to be made to the contents of the program.

The shape of a shell of revolution can be defined completely by that of a cross-section on a plane through the shell axis. The cross-section is called here as a branch, with the defining parameters of length, curvature and thickness. The program can analysis shells consisting of up to four branches joined together at a common junction. A well known example of such a junction forming a four-branched shell is that between a spherical nuclear-reactor vessel and its through-thickness cylindrical support-skirt. A specific length must be supplied for each branch. However, apart from a

physical end to the branch, the vessel can 'close on' itself at the axis and this becomes the end of that branch, or the vessel can have a region where the condition is known to be in a membrane state of stress and the branch in this case terminates at any position in this region with an end-condition of membrance stresses. The branch may, in general, vary in shape and thickness along the length. To represent this, each branch can consist of a large number of shorter elements, each with a linearly varying (or uniform) thickness, and each can be in one of five basic shapes-flat disc, cylinder, cone, sphere and torus.

A large selection and combination of loading is permitted. The program can accept body forces at the whole vessel, internal pressure in combination with axial thrust at each branch, and/or distributed forces at each element. At the ends of the branches, boundary conditions have to be supplied for the integration of the governing differential equations, and through these boundary conditions it is possible to supply external bending moments, edge forces, or specific values of radial displacement, or the ends can be left at either a free condition, fixed condition or give a membrane state of stress. The program does not deal with internal thermal stressing although external constraint or movement due to thermal expansion can be simulated.

6-2 Elastic Program: Numerical Procedure

Shell Equations

The shell equations used in the program are according to Turner (6-2), (6-3), written for the linear behaviour

of thin-walled shells of revolution under axisymmetric loads. The basic assumptions are the same as that of the first-approximation theory of Love and Reissner discussed above in Section 3.1. The equations are mathematically speaking linear ordinary-differential-equations. A step-wise integration method is used to solve for the solution, and for this, first-order differential equations are required consisting in this case of the basic equilibrium equations, the strain-displacement compatibility relations and the stress-strain relations. There are four of these first order equations. For this program, the four dependent variables are:

u Radial displacement;

ϕ rotation of meridian line;

ϕ' rate of change of this rotation along the shell meridian; $\frac{d\phi}{d\ell}$, and;

F radial force per unit circumference.

The independent variable is l, the length along the shell meridian. Fig.6.1. shows these parameters on a typical shell element of length $\delta\ell$, according to the notations of Turner.

Rewriting the above four variables as X_1 ,X_2 ,X_3 ,X_4 respectively, the four first-order equations are in the general form

$$\frac{dX_i}{d\ell} = f_i \left(X_1, X_2, X_3, X_4, \ell \right) \quad i = 1 \ldots 4 \qquad (6.1)$$

f_i are linear functions since the govering equations are linear.

Integration Process

A predictor-corrector process is used for the integration. The Runge Kutta process is probably better known, but the reason it is not used is because in the next elastic-

plastic program, this process is found to be unsuitable. Normally the predictor-corrector process suffers a disadvantage that it is not self-starting, which means that a different initiating procedure has to be adopted for the first integration step from l=0. In this program the first-order Adams procedure is used, this being one of a few special cases where a different initiating procedure is not required because the procedure is first order. The procedure can be explained below.

The integration proceeds in step from one point to the next one down the line. At a point l_s , the next point is l_{s+1} with $l_{s+1} - l_s = \Delta l_s$ The first prediction $X^{(0)}$ of $X(l_{s+1})$ is

$$X^{(0)} = X(l_s) + \tfrac{1}{2} \cdot \Delta l_s \cdot X'(l_s) \qquad -(6.2)$$

From this we get the first estimate

$X'^{(0)}$ of $X'(l_{s+1})$

making use of the supplied equations (6.1)

$$X'^{(0)} = f(X^{(0)}, l_{s+1}) \qquad -(6.3)$$

The next estimate $X^{(1)}$ of $X(l_{s+1})$ uses the more accurate corrector formula

$$X^{(1)} = X(l_s) + \tfrac{1}{2} \Delta l_s (X'(l_s) + X'^{(0)}) \qquad -(6.4)$$

Followed again by

$$X'^{(1)} = f(X^{(1)}, l_{s+1}) \qquad -(6.5)$$

Formulas (6.4) and (6.5) are then repeated as often as necessary until the derivative $X'^{(n)}$ converges to a stable value.

We notice here equations (6.4) and (6.5) do not require the values at and before the previous point l_s -1. They can thus be applied even when s is at l = 0,

making the procedure self-starting.

Adaptation to Boundary- Value Problems

The stepwise integration procedure for differential equations is an initial-value procedure and requires specific values of the variables at the initial point before the solution can be obtained. It can however be adapted to two-point boundary-value problems provided that sufficient number of boundary conditions are known. For a fourth-order problem, specified values of four linear-functions of the end variables are required. The adaptation of stepwise integration procedure to two-point boundary value problems is well known, and reference can be made to it in books on numerical analysis of differential equations, or specifically to the book by Fox, ref. (6-4).

A slight variation of the standard method is used in the program. Here a junction is provided with a maximum of four, and a minimum of two, radiating branches. Boundary conditions are supplied at the ends of the branches. The variation from the standard procedure is described below.

Assuming that there are M branches, where $2 \leqslant M \leqslant 4$, integration proceeds from the junction A along a branch, one at a time, to the end point B of the branch. The variables X_i have the values

$$X_{im}^{A} \quad \text{and} \quad X_{im}^{B} \quad , \quad i = 1, 4,$$

at the initial and end point respectively of branch m. It is allowed to specify boundary conditions consisting of two linear functions G_{1m} and G_{2m} of the end values X_{im}^{B} of each branch m. They must be such that

$$G_{1m}(X_{1m}^{B}, X_{2m}^{B}, X_{3m}^{B}, X_{4m}^{B}) = 0 \qquad -(6.6)$$

$$G_{2m}\,(X^B_{1m}, X^B_{2m}, X^B_{3m}, X^B_{4m}) = 0, m=1,M$$

We are required to convert this problem with the 2M known end-functions into determining the 4M initial values X^A_{im} at the junction point A making it an initial-value problem.

Noticing the linear nature of the whole problem, we gather that each X^B must be a linear function of the four X^A of the same branch. Together with equation (6.6), we conclude that the functions G must also be a linear function of the four X^A of the same branch, i.e.

$$G_{jm} = \sum_{i=1}^{4} c_{jim}\, X^A_{im} = 0 \qquad \begin{matrix} j = 1,2 \\ m = 1,M \end{matrix} \qquad -(6.7)$$

There are no constant coefficients outside $\sum$, because if three of the variables X^A at a branch are zero, the fourth one must also be zero. The unknown but constant coefficients c_{jim} are obtained by integrating along all the branches and the way of doing this is described later in more details. It is sufficient to say here that, after a certain number of integration along the branches, we obtain the values of these coefficients. There is however only 2M equations in (6.7) and not sufficient to determine the 4M unknown values of X^A.

The other 2M relations are obtained from the inter-relations between the X^A's. They are parameters belonging to different branches at the same junction point A and by the conditions of compatibility and of equilibrium further relations can be obtained.

X_1, X_2, X_3, X_4 are the alternate terms ~~from~~ for u, ϕ, ϕ' and F

By the condition of compatibility that u is common at all branches, we have $X^A_{11} = X^A_{12} = \cdots\cdots = X^A_{1M}$ $\quad -(6.8)$

ϕ is also common at all branches, i.e.

$$X^A_{21} = X^A_{22} = \ldots = X^A_{2m} \qquad -(6.9)$$

The third variable is ϕ'. This is related to the meridional bending moment M by the relations

$$M_\theta = \frac{2Eh^3}{3(1-\nu^2)} \left(\phi' + \sin\theta/\phi \right) \qquad -(6.10)$$

For equilibrium of the point A, the sum of this moment for all branches, plus the ~~in~~ternal moment M^E, if any exists, must be zero

$$\sum_{m=1}^{M} (M^A_\theta)_m + M^E = 0 \qquad -(6.11)$$

with due account taken for the sign of ϕ, ϕ' and M.

The equilibrium of forces at a gives

$$\sum_{m=1}^{M} F^A_m + F^E = 0 \qquad -(6.12)$$

taking again account of the sign of F.

Equations (6.8), (6.9), (6.11) and (6.12) constitute a total of $2(M \neq 1) + 2 = 2M$ independent linear-equations of the variables X^A.

There is thus a total of 4M independent linear-equations, which is sufficient to obtain a solution for the 4M unknown variables X^A_{im}. With these initial values known, the boundary-value problem has been successfully transformed into an initial-value problem. A further integration along each of the branches will complete the solutions for u , ϕ , ϕ' and F.

Accuracy during Computation

The above description gives, without detailing the equations, the theoretical basis for the numerical procedure for solution. The manner of execution is however influenced by other factors. Two procedures used in the program, and described below, are adopted because of the nature of numerical calculation on digital

computers.

The first special procedure is on the application of the predictor-corrector process which consists here of the repeated application of the two formulas, (6.4) and (6.5), making the r^{th} estimates for both $X^{(r)}$ and $X'^{(r)}$ more and more accurate. This iteration is the most basic step in the solution of the shell problem and its accuracy is of vital importance. The iteration cycle is thus repeated until the four derivatives $X'^{(r)}$ have all converged to within a tolerance according to the formula, $|X'^{(r)} - X'^{(r-1)}| / |X'^{(r-1)}| \leq \epsilon$ -(6.13) The value of ϵ is specified along with the supplied data and can be varied for different calculations. However the computing time increases in proportion to the number of iteration cycle. If the convergency is slow at a certain step and failed to satisfy eq.(6.13) at a specified upper limit to the number of cycles, a warning message is printed on the computer output and the integration proceeds to the next interval point.

The other procedure is the determination of the coefficients in eq.(6.7), which provides for the conversion of the fixed boundary-values to known initial-values, a process called here as boundary control. It was mentioned that the problem is a linear one. Basing on this assumption, one straight forward method of solving for the coefficients c_{jim} in (6.7) is to give, at each branch m, unit value to one particular X^A_{im} leaving the other X^A in the same branch zero. An integration along this branch M gives the solutions X^B_{im} (i = 1,4) at B, and from these values G_{1m} and G_{2m} are calculated from the known re-

lations (6.6). These values of G_{1m} and G_{2m} would then be the coefficients c_{1im} and c_{2im} ,according to their definition in (6.7). This procedure is then repeated with unit value given in turn to the other initial values X^A_{im}, resulting in the complete set of c_{1im} and c_{2im} ,(i = 1, 4,m = 1, M).

The actual execution of such a process in the computer may not yield accurate results because of possible errors in the numerical procedure. There are two possible sources of such errors, the first is during the numerical integration, and the second is during the subtraction of nearly equal large numbers which in the computer have finite lengths.* The boundary control process is thus programmed as if the problem is slightly non-linear. A set of non-zero initial guess values of X^A_{im} is first assumed, and an integration is performed using these values. This gives a corresponding set of values of G_{jm} . Each X^A_{im} is then altered in turn by a certain small proportional amount, ΔX^A_{im} , and further integrations are performed each time. The resulting changes ΔG_{jm} from the previous value G_{jm} are divided by ΔX^A_{im} to give the current solution c_{jim},i.e.

$$c_{jim} = \frac{\Delta G_{jm}}{\Delta X^A_{im}} \qquad -(6.14)$$

(This is another way of expressing eq.(6.7).)

We can thus return to the solution of the set of linear

* On the IBM 7090 and 7094, numbers are stored as 32 binary digits giving an accuracy of seven to eight significant figures.

equations given by (6.7),(6.8),(6.9),(6.11) and (6.12) to give the current solution for the initial values X^A . If both the problem and the solution are completely linear, these X^A , on a further integration, will give zero values for all G_{jm} according to eq. (6.6). This is not necessarily so, because of different kinds of numerical errors and a test is made to see if all the 2M values of G are less than a specified accuracy $\leq$. If this is so, the current X^A and their results are taken as the correct solution. In general this is not so, and these current values of X^A are taken as the next estimate values of the next cycle of iteration and the boundary control process is repeated.

6-3 Elastic-Plastic Program

Introduction

The elastic-plastic program is an extension of the elastic program PVA1. It analyses the state of stress and the behaviour of a pressure vessel at and beyond the first yielding of the vessel according to supplied material properties, the most important of which is an equivalent yield-stress against equivalent strain curve. The elastic strain is not neglected compared with the plastic strain and the Prandtl-Reuss equations for incremental plastic-flow is used to represent the post-yield behaviour. Yielding is governed by the von Mises yield criterion. Work-hardening material can be considered.

The organisation of the program and its basic integration procedure are the same as that of the elastic program.

A full description of these two aspects as well as the other procedures adopted for the elastic-plastic analysis have now been published by Marcal and Pilgrim,ref.(3-49).

The program has the name PLINTH and is also written in Fortran IV for the IBM 7094 and 7090 computers. Because of the additional facilities required by the program, the maximum number of interval points is less than that of PVA1, and three magnetic tapes are required during execution although only as working (or scratch) tapes to be used as subsidiary stores. A user's manual giving detailed instruction for using the program has been written as a report for the C.E.G.B.

The fundamental difference in the theory behind the elastic-plastic calculation compared with the elastic calculation is firstly that the elastic-plastic cal - culation is repeated many times, each one being for a small increment of loading. Secondly, at each small load increment the stress-strain relations is different, being in this case according to the Prandtl-Reuss flow-rule for stress and strain increments.

The Elastic-Plastic Stress-Strain Relations

The elastic stress-strain relations for different states of stress are easily available in text books, the same cannot be said,however for the elastic-plastic relations. In the following, the basic expression for the elastic-plastic flow-rule is developed into stress-strain re - lations for the state of stress at a thin-walled shell and written in a suitable form for use in the program . After this explanation is giving for a few procedures that have been altered to suit an elastic-plastic

calculation. Both the stress-strain relations and these procedures are explained in ref.(3-49),they are however repeated here,being described differently and in a more detailed manner. All other procedures that remain the same or similar to that for the elastic program shall not be described here.

In the elastic program,the problem is expressed mathematically by relating the stress equilibrium conditions and the strain compatibility requirements by the elastic stress-strain relations. These relations are generally called Hookean relations, and according to them the principal stresses can be expressed explicitly in terms of the principal strains, and alternatively the same can be done for the principal strains in termsoof the principal stresses.

In the elastic-plastic state, the incremental stresses are related to the incremental strains through the Prandtl-Reuss equations. It is found that if the increments are small, the relations are linear, and this fact is made use of in the solution.

In the general form, the Prandtl-Reuss equations are written as expressions for the deviatoric strain - increments de'_{ij} in the form

$$de'_{ij} = \sigma'_{ij}\, d\lambda + d\sigma'_{ij}/2G \qquad -(6.15)$$

with $$d\lambda = \frac{3}{2}\frac{d\bar{e}_p}{\bar{\sigma}} = \frac{3}{2}\frac{d\bar{\sigma}}{\bar{\sigma} H'}$$

The notations are according to that of many English and American text books on plasticity, for example, ref. (6-5). The superscript ' refers to deviatoric values, - to equivalent values. H' is the slope of the equivalent

stress against plastic equivalent-strain curve, i.e. $\frac{d\bar{\sigma}}{d\bar{e}_p}$

Because of the simplified stress system at a shell of revolution, a reduced set of equations can be formed. A shell element with a complete symmetry of geometry and loading will have the system of forces shown in Fig.6-2a. Taking a smaller element at a certain distance from the shell mid-wall, the general system of stresses is reduced to Fig.6-2b, with the other stresses zero. According to the mathematical model of yielding, this element will yield when the equivalent stress $\bar{\sigma}$ reaches a certain value Y.

A further simplification is made by neglecting the contribution of σ_3 and τ_{12} to yielding. σ_3 has always been neglected in all developments of the basic thin-walled shell theory. τ_{12} exists because of the bending of the shell element and varies parabolically across the wall thickness with zero values at the shell wall surfaces and maximum values at mid-wall. In first-order thin-walled shell theories, τ_{12} is assumed to have no contribution to the deformation. Its contribution to yielding is also neglected here in the elastic-plastic program.

There are thus only the two direct stresses σ_1 and σ_2 that are also the principal stresses. The corresponding principal strains are e_1, e_2 and e_3 in the three fixed directions.

Expanding eq.(6.15) for such a state of stress and strain, this results in

$$de_1 = \frac{3}{2}\frac{d\bar{e}_p}{\bar{\sigma}}\sigma_1' + \frac{d\sigma_1}{E} - \nu\frac{d\sigma_2}{E}$$
$$de_2 = \frac{3}{2}\frac{d\bar{e}_p}{\bar{\sigma}}\sigma_2' + \frac{d\sigma_2}{E} - \nu\frac{d\sigma_1}{E} \qquad -(6.16)$$

The von Mises yield-criterion gives the expression for the equivalent stress for a three-dimensional stress-state as

$$\bar{\sigma} = \frac{1}{\sqrt{2}}\left\{(\sigma_1-\sigma_2)^2+(\sigma_2-\sigma_3)^2+(\sigma_3-\sigma_1)^2\right\}^{\frac{1}{2}} \qquad -(6.17)$$

This for the case here of $\sigma_3 = 0$, becomes

$$\bar{\sigma} = (\sigma_1^2 + \sigma_1\sigma_2 + \sigma_2^2)^{\frac{1}{2}} \qquad -(6.18)$$

Equation (6.15)gives an explicit expression giving the strain increments de_1 and de_2 in terms of the stress increments and the present state of stress. In the elastic-plastic calculation the opposite relations ~~is~~ are also required giving the stress increments $d\sigma_1$, and $d\sigma_2$ in terms of the strain increments. Ref.(3-49) shows that this is done by inverting the coefficient matrix formed by both equations (6.16) and anadditional equation, this being the von Mises yield criterion in the form of an implicit differential

$$3\sigma_1' d\sigma_1 + 3\sigma_2' d\sigma_2 = 2\bar{\sigma}\,d\bar{\sigma} = 2\bar{\sigma}H' d\bar{e}_p \qquad -(6.19)$$

The resulting matrix equations is

$$\begin{bmatrix} \frac{1}{E} & -\frac{\nu}{E} & \frac{3}{2}\frac{\sigma_1'}{\bar{\sigma}} \\ -\frac{\nu}{E} & \frac{1}{E} & \frac{3}{2}\frac{\sigma_2'}{\bar{\sigma}} \\ \frac{3}{2}\frac{\sigma_1'}{\bar{\sigma}} & \frac{3}{2}\frac{\sigma_2'}{\bar{\sigma}} & -H' \end{bmatrix}\begin{bmatrix} d\sigma_1 \\ d\sigma_2 \\ d\bar{e}_p \end{bmatrix} = \begin{bmatrix} de_1 \\ de_2 \\ 0 \end{bmatrix} \qquad -(6.20)$$

Inversion of this coefficient matrix is done at the computer resulting in coefficients referred to by Marcal as 'partial stiffness-coefficients' for plastic straining

$$\left(\frac{\partial\sigma_1}{\partial e_1}\right)_p ,\ \left(\frac{\partial\sigma_1}{\partial e_2}\right)_p ,\ \left(\frac{\partial\sigma_2}{\partial e_1}\right)_p ,\ \left(\frac{\partial\sigma_2}{\partial e_2}\right)_p ,\ \left(\frac{\partial\bar{e}_p}{\partial e_1}\right)_p ,\ \left(\frac{\partial\bar{e}_p}{\partial e_2}\right)_p$$

Similar coefficients for points which are completely

elastic can be formed directly, being,

$$\left(\frac{\partial \sigma_1}{\partial e_1}\right)_e = \left(\frac{\partial \sigma_2}{\partial e_2}\right)_e = \frac{E}{1-\nu^2}$$

$$\left(\frac{\partial \sigma_1}{\partial e_2}\right)_e = \left(\frac{\partial \sigma_2}{\partial e_1}\right)_e = \frac{\nu E}{1-\nu^2} \qquad -(6.21)$$

It is of interest to note that recently Yamada et.al.(6-6) have derived the values of these elastic-plastic coefficients directly, i.e. without inversion on the computer, both for the general three-dimensional stress-state and for the above plane stress state.

Transition Point

A solution of the states of stress and strain is obtained at each increments of load. In the process of integration, each mesh point in each shell element is tested to see whether the point is elastic or has yielded at the previous load. If the point has already yielded, elastic-plastic coefficients as defined above are used to obtain the stress increments from the strain increments. If the point is elastic, it is further tested if it remains so after the load increment, in which case the elastic coefficients are used. If it is otherwise, these points that yield during the load increment, called transition points, are to be treated specially. The process for this is mentioned below.

The feature of a transition point is that at a certain portion of the load increment the point remains elastic, while at the remaining portion of the increment, the point behaves elastic-plastically. Since this ratio cannot be determined directly, but by iterations of the the solution of the complete shell, the elastic-plastic calculation has to be planned accordingly.

Consider one such point where, at a certain increment, the strain changes from $\bar{e}$ to $\bar{e} + \delta\bar{e}$. If the portion of the strain increment $\delta\bar{e}$ that is elastic is $\alpha\delta\bar{e}$, where $\alpha \leq 1$, then the elastic-plastic part is $(1-\alpha)\delta\bar{e}$. Marcal assumes that for small load-increments, the first approximation can be made that the ratio α_1 for the strain increments δe_1 has the same value as α_2 for δe_2 and thus both of them are the same as the ratio α for $\delta\bar{e}$.

Using the elastic and the plastic partial-stiffness-coefficients, the stress increments are

$$\delta\sigma_i = \alpha \left(\frac{\partial\sigma_i}{\partial e_j}\right)_e \delta e_j + (1-\alpha)\left(\frac{\partial\sigma_i}{\partial e_j}\right)_p \delta e_j$$

$$i = 1, 2 \quad \text{and} \quad j = 1, 2 \qquad -(6.22)$$

An overall coefficient can thus be defined, being

$$\frac{\partial\sigma_i}{\partial e_j} = \alpha \left(\frac{\partial\sigma_i}{\partial e_j}\right)_e + (1-\alpha)\left(\frac{\partial\sigma_i}{\partial e_j}\right)_p \qquad -(6.23)$$

We now proceed to explain how α is determined. Let the transition point have a current condition of σ_1, σ_2, e_1, e_2, they being elastic have the relations

$$F(\sigma_1, \sigma_2) = (\sigma_1^2 - \sigma_1\sigma_2 + \sigma_2^2)^{\frac{1}{2}} < Y$$

and

$$\sigma_1 = \frac{E}{1-\nu^2}(e_1 + \nu e_2)$$

$$\sigma_2 = \frac{E}{1-\nu^2}(e_2 + \nu e_1)$$

In the next load increment, we make certain guess for the values of the strain increments δe_1, and δe_2, and assume first that they are the correct values. The elastic portion of these increment are thus $\alpha\delta e_1$, and $\alpha\delta e_2$, with the corresponding elastic stress increment, for direction 1, as

$$\delta\sigma_1)_e = \frac{E}{1-\nu^2}[e_1 + \alpha\delta e_1 + \nu(e_2 + \alpha\delta e_2)] - \frac{E}{1-\nu^2}(e_1 + \nu e_2)$$

$$= \alpha\frac{E}{1-\nu^2}(\delta e_1 + \nu\delta e_2) \qquad -(6.24a)$$

$$= \alpha\delta\sigma_1^f$$

If we call for convenience, $\frac{E}{1-\nu^2}(\delta e_1 + \nu \delta e_2)$ as $\delta \sigma_1^f$ This is a fictitious value, being the stress increment if δe_1, and δe_2 are elastic which they are not.

Similarly for direction 2,

$$\delta \sigma_2)_e = \alpha \frac{E}{1-\nu^2}(\delta e_2 + \nu \delta e_1) = \alpha \delta \sigma_2^f \qquad -(6.24b)$$

By definition of yielding,

$$Y = F\{\sigma_1 + \delta\sigma_1)_e, \sigma_2 + \delta\sigma_2)_e\}$$
$$= F\{\sigma_1 + \alpha\delta\sigma_1^f, \sigma_2 + \alpha\delta\sigma_2^f\}$$

and $Y^2 = (\sigma_1 + \alpha\delta\sigma_1^f)^2 - (\sigma_1 + \alpha\delta\sigma_1^f)(\sigma_2 + \alpha\delta\sigma_2^f) + (\sigma_2 + \alpha\delta\sigma_2^f)^2$

This gives $a\alpha^2 + b\alpha + c = 0 \qquad -(6.25)$

with $a = \delta\sigma_1^{f2} + \delta\sigma_1^f \delta\sigma_2^f + \delta\sigma_2^{f2}$

$b = \sigma_1(2\delta\sigma_1^f - \delta\sigma_2^f) + \sigma_2(2\delta\sigma_2^f - \delta\sigma_1^f)$

$c = \sigma_1^2 - \sigma_1\sigma_2 + \sigma_2^2 - Y^2$

The roots for the quadratic equation (6.25) are

$$\frac{-b \pm (b^2 - 4ac)^{\frac{1}{2}}}{2a}$$

They are as mentioned above, based on the estimated values of δe_1, and δe_2. If these values are sufficiently close to the correct values, there should be only one root which lies between 0 and 1, and this is taken as the estimated value for α from which the overall partial-stiffness-coefficient of (6.23) can be calculated.

Knowing the partial-stiffness-coefficients of the elastic points, plastic points and transition points, the complete relations between all incremental stresses and incremental strains can be obtained. The normal integration can thus be made to obtain the solution throughout the shell. Any such solution is necessarily based on the current estimated values of δe_1, and δe_2 at a number of transition points. An iteration process

is thus necessary here when, after each solution, a better one can be obtained by using at each transition point the previously calculated value of α to get a better estimate of δe_1, and δe_2. The first of these iterations started off with $\alpha = 1.0$ for all transition points.

Yield Stress

Mention should also be given here of the derivation of the yield-stress value Y. In the program, Y is not necessarily a constant, but can vary at each point in the shell according to the amount of plastic strain $\bar{e}_p$. It thus means that the material need not be perfectly plastic. The form of the relation between Y and $\bar{e}_p$ used in the program is

$$Y = \sum_{i=0}^{n} k_i \bar{e}_p^{\,i} \qquad -(6.26)$$

A perfectly-plastic material, for example, would thus have the form

$$Y = k_o \quad ,$$

while a linearly strain-hardening material is expressed by

$$Y = k_o + k_1 \bar{e}_p$$

Other Useful Informations

Detailed flow-charts have again been drawn for the first two subroutines of the program, one being the main routine and the other being the main flow and control subroutine called MASTER. They are given in Appendix A.

A list of the errata and other nessary corrections to ref.(3-49) by Marcal and Pilgrim describing the program has been drawn up, and is given in the same appendix.

7. ACCURACY TESTS FOR ELASTIC PROGRAM

Notations

This list is in addition to that in Ch.6.

r radius vector of a point in shell

a radius of revolution for toroidal shell, cylinder radius for cylindrical shell.

b radius of torus cross-section for toroidal shell, sphere radius for spherical shell.

k integration constant for cylinder equations, $4k^4 = 3(1 - \nu^2) / a^2 h^2$

η integration constant for sphere equations, $\eta = \sqrt{2} \left\{\frac{3}{4}(1-\nu^2)\right\}^{\frac{1}{4}} \frac{\lambda}{\sqrt{bh}}$

ξ accuracy in integration procedure.

ζ accuracy in boundary control procedure.

M_ℓ, M_ψ meridional, circumferential bending moments per unit length

The following accuracy tests on the elastic program PVA1 were performed by the author in parallel with the development, coding and error detection of the program.

7.1 Size of Problem For Converging Solution

The first test consists of a determination of the size of the problem that can be accurately analysed by the program. The term size is taken here in the context of the numerical-analysis procedure, and not on the physical size of the shell to be analysed. This size is also not related to the storage size in the computer since the program uses fixed storage location for the matrices necessary in the computation. The 32,000-word core store of the IBM 7090 or 7094 computer allows the shell problem to have a maximum of 4 branches, each branch with a maximum of 10 elements and 300 interval

points. These limitations are larger than are necessary for most problems that have to be solved.

It was found on using the program for shell analysis that there was a limitation to the length of the branch of a specific shell geometry, beyond which the boundary-control procedure lose its accuracy and converged very slowly or not at all. Similar observation has since been reported by Kalnins (3-31). This loss of accuracy is not due to cumulative errors in the integration process. It is basically due to the subtraction of very large, almost equal numbers in the solution of the unknown initial variables X^A during the boundary-control process.

In an analytic solution to shell problems, it is very often noticed that the complementary solution can be expressed in terms of two types of functions. Of these, one type of functions decays exponentially while the other type of function grows exponentially with the meridianal length l of the shell. Thus the coefficients Cjim, defined by the relations between the initial and end values of a branch, equation (6.7),

$$G_{jm} = \sum_{im=1}^{M4} c_{jim} X^A_{im} = 0$$

increase as the length of the shell branch increases. The final solution of the unknown initial values X^A requires inverting a matrix with the values Cjim as coefficients. During this inversion, the coefficients are multiplied and subtracted from each other. If the values Cjim are exceedingly large, such that the significant figures are lost during subtraction, the invertion would either loose its accuracy or break down

completely in some cases.

To test this phenomenon and to check its accuracy, a large number of ' numerical experiments ' are performed on the computer varying the length, diameter and thickness of a cylindrical shell with built-in ends under internal pressure. Analytical solution to the cylindrical problem (see for example, Chapter 4 of Ref. (6-3)) reveals that the exponentially increasing function is the term $e^{kl}(A_1 \cos kl + A_2 \sin kl)$ which is always smaller in value than $(A_1 + A_2)\, e^{kl}$. k in this problem has the relations $4k^4 = 3(1-\nu^2)/a^2 \cdot h^2$, with a = radius and h= semi-thickness of the cylinder. A_1 and A_2 are constants of integration. Thus we have

$$kl = \left\{\frac{3}{4}(1-\nu^2)\right\}^{\frac{1}{4}} \frac{l}{\sqrt{ah}}$$

which is approximately $0.91\, l/\sqrt{ah}$ for $\nu = 0.3$. The range of integration in the program is a branch of the shell. Thus the length of a branch rather than the length of a complete shell is the parameter that has to be limited. From these experiments on the cylindrical shell, it was observed that, on the IBM 7090 or 7094 when $l^* = \frac{l}{\sqrt{ah}}$ of a cylindrical shell branch is greater than 15, the boundary-control process cannot make the boundary functions converge to the desired zero values. This factor represent a magnification ratio of the order of $e^{0.91 \times 15} \doteq 10^6$.

This limiting value of 15 for $\frac{l}{\sqrt{ah}}$ should be dependent only on the cylindrical geometry of the shell and not on the loading and the boundary arrangements. Further tests have been made on this using the problem of an open-ended cylindrical shell under internal pressure,

with one half of it at a different thickness from the other. Each half is thus considered as a branch with the junction point at the discontinuity. Discontinuity stresses occur at and near the junction, and die away towards the open end. Because of the difference in thickness t, the length l to give the same value to the parameter $\frac{l}{\sqrt{ah}}$ is different. From a number of calculations with different lengths supplied to each branch, it was found that slow or break down of convergency occurred at approximately the same value of 15.

Shells of other geometries are expected to have other limiting criterion. The case of a shallow spherical-shell was next investigated. Again the complementary solution to the governing equations consists of a rapidly increasing function and a rapidly decreasing one. The former is not an exponential function, but consists of Kelvin Functions (see, for example, Chapter 4 of Ref. 6-3). It is of the form $A_1\, ber'\eta + A_2\, bei'\eta$ where $\eta = \sqrt{2} \times \left[\frac{3}{4}(1-\nu^2)\right]^{\frac{1}{4}} \times \frac{l}{\sqrt{bh}}$, l = meridional length, b = radius of curvature, h = semi-thickness

For $\nu = 0.3$, $\eta = \sqrt{2} \times 0.91 \times \frac{l}{\sqrt{bh}}$

Again the influencing parameter is $\frac{l}{\sqrt{bh}}$. There would be a different critical value for this parameter. In the case of the shallow spherical shell with a central hole, it is found that this value varies with the diameter of the hole making it impossible to draw up a convenient rule to determine the critical value.

7.2 Cylinders Under Internal Pressure

The same problem as in section 7.1 above, of a circular cylindrical-shell with built-in ends and under internal

pressure, was solved varying different parameters, and the results were compared. The junction of the shell in the computation is taken as the mid-point. One comparison is on the symmetry of the resulting solution.

The dimension of the shell are:

half-thickness, $h = 0.09$ in.

cylinder radius, $a = 1$ in.

Young's Modulus, $E = 14{,}000$ ton/in^2

Poisson's ratio, $\nu = 0.30$

Internal pressure, $p = 1$ ton/in^2

Four values of branch length ℓ were tried,

$\ell = 0.5$ in, 1.25 in, 2.5 in, 5.0 in

with $\ell^* = \ell/\sqrt{ah}$ = 1.58, 3.96, 7.91, 15.82 respectively.

Using integration tolerance ξ = 0.0001,

boundary-control tolerance ς = 0.0001,

the resulting behaviour is shown below:-

Run No.	Length		Symmetry error (difference between maximum values)	Speed of convergency (No. of boundary-control iterations)
	ℓ	ℓ^*		
1	0.5in	1.50	M_ℓ 0.3% ϕ 0.07%	1
2	1.25 in	3.96	M_ℓ < 0.01% ϕ < 0.01%	2
3	2.5in	7.91	M_ℓ 0.44% ϕ 1.2%	2
4	5.0in	15.82	M_ℓ 0.78% ϕ 9.6%	4

Run No.1 and 2, for ℓ^* = 1.58 and 3.96 respectively, give nearly exact symmetry. Run No.3, with ℓ^* = 7.91, is reasonably accurate, and Run No.4 with ℓ^* = 15.82 looses its symmetry for the ϕ solution.

Decreasing next the tolerance for the case of ℓ^* =7.91, to ξ =0.00001, ζ =0.0001, give the following improved behaviour,

Run	Symmetry Error	Speed of Convergency
3a	0.14% 0.07%	2

For the case ξ =0.0001, ζ =0.00001, the result is

Run	Symmetry Error	Speed of Convergency
3b	0.03% 0.01%	2

Complete analytical solution to this problem can be obtained from solving the governing differential equation $\frac{d^4F}{d\ell^4} + 4k^2 F = 0$, F = radial shear force per unit circumference, k = a parameter, where $4k^4 = \frac{3(1-\nu^2)}{a^2h^2}$ The expressions for the solution are directly evaluated on the computer and considered as the exact solution. The above numerical-analysis results are compared against it.

Run	ℓ^*		Error(%)	
			Branch 1	Branch 2
1	1.58	Max M_ℓ	+ 1.13	+ 0.88
		Max ϕ	+ 2.04	+ 1.98
3	7.91	Max M_ℓ	+ 0.48	+ 0.02
		Max ϕ	- 0.49	+ 0.72
4	15.82	Max M_ℓ	+ 0.77	- 0.02
		Max ϕ	+ 6.57	- 3.71

It is seen that except for the case ℓ^* =15.82, both the cases with ℓ^* =1.58 and 7.91 give results that agree to within 2% of the exact solution.

7.3 Comparison With Published Results

The program PVA1 was tested over a wide range of shell shapes and parameters, and comparisons were made with a selected number of published results. The range of problems covers those encountered in pressure vessel analysis. The results are shown in Fig. 7-1 to 7-5. In all cases the dimensions of the shell structure are shown in the figures.

Cylinders with Abrupt Thickness Change

A number of thin-walled cylinders with an abrupt change in wall thickness and loaded under internal pressure have been carefully machined and analysed experimentally by Morgan and Bizon(4-5). In all cases the results were compared with theoretical analysis based on the analytical methods of Johns and Orange (7-1), where the equations are also first-approximation ones according to Timoshenko and Woinowsky-Krieger (3-7). The same theory is thus used as in the present computer program although the source of the equations is different.

Program PVA1 was used to analyse one of the above cylinders with the two parts of thicknesses 0.082 in and 0.205 in and having the same mid-wall diameter of 5.785 in. Fig.7-1 shows the stress distributions. The two theoretical solutions coincide at all location on this plot of the distribution and are shown as the same lines.

Toriconical Heads Under Internal Pressure

Morgan and Bizon did a further series of experimental analyses on toriconical heads (4-17). The same care have been taken on these tests as on those above. Two heads of the same shape were tested. The larger one was spun from an aluminium sheet, while the smaller one was more accurately contour-machined from an aluminium billet and found to have a very accurate geometry, the contour being within 0.002 in of the true shape out of a 12 in diameter vessel. Again they compared the results with theoretical results based on the same analytical methods; for the solution of the conical portion, tables of Bessel-Kelvin functions were used.

The results of the contour-machined head were compared with the solution using PVAl. In this case the vessel is quite thin,making the shell meridianal-length parameter ℓ^* too large for accurate analysis by the program. Fortunately the regions of discontinuity at the cone-sphere and at the sphere-cylinder intersections are sufficiently remote that there is a region in between where the stress falls to a near membrane condition. The problem is thus solved by two computations - one for a cone-on-sphere geometry and one for a sphere-on-cylinder geometry. The results again nearly coincide with the published theoretical results. They are both plotted as the same lines in Fig.7-2.

Expansions Bellows Under Axial Thrust

Turner and Ford reported in 1957 (7-2) experimental studies of the stress and deflecion of a number of pipeline expansion-bellows under axial loading.

Theoretical analysis was also presented based on an approximate theory using a series solution for the minimum strain-energy. A torus geometry, given by the expression

$$r = a \pm b \cos\theta$$

was used for the convolution, with

a = radius of revolution

b = radius of the torus cross-section.

In the analysis it was assumed that $a \gg b$ so that terms of the form

$$\frac{r}{a} = \frac{a \pm b\cos\theta}{a}$$

were approximated to unity.

In a subsequent paper in 1959 (6-2), Turner reduced the governing shell-equations for a toroidal geometry to two second-order differential equations each of which was a special case of the Mathieu equation. The same approximation that $a \gg b$ was used. The solutions were obtained through influence coefficients by tabulating the Mathieu functions. Using the theory, detailed comparisons were made in Ref.(7-3) of the stress and deflection of a few selected bellows units tested in Ref.7-2.

Two typical shapes of expansion bellows have been analysed with the program PVA1. The first is a flat-plate bellows unit shown in Fig. 7-3a . Extensive strain ganging was made during the original test and from it stress results were obtained at different positions. Two calculations were made to give a full analysis, one analysing the convolution attached to the end of the bellows, and the other analysing the middle

root convolution. Different end-conditions were simulated in the computation. For the other end of the end-convolution, an extension pipe estimated to be of similar stiffness to the actual arrangement was assumed. Otherwise an assumption of a condition of symmetry of $\emptyset = 0$, and $F=0$, can be made.

Figures 7-3a and b show the stresses from computation compared with both the strain gauge test results and the theoretical solution of Turner in 1959. The two theoretical results were in good agreement with each other. Moderate agreement was found between the theories and the experiment. The experimental stress values have, according to Ref.7.2, an accuracy of $\pm$ 10%

The other bellows unit is called bellows C, shown in Fig.7-4. There are six quarter-convolutions, forming one middle crest and two adjacent roots both of which are each carried further by a quarter-convolution to end at a thick end-plate. Both the strain and the deflection values were studied with the computer program. For the prediction of the axial deflection, exact idealisation must be used in the computation. For this purpose, one half of the bellows is analysed with one end of the shell terminating with a fixed-end condition of $u = 0$, and $\emptyset = 0$, and the other end, being the middle crest, terminating with a symmetry condition of $\emptyset = 0$, $F = 0$. The circumferential strain distribution between the root and the middle crest is presented in Fig.7-4, and is shown together with the strain gauge test points, and the theoretical results of Turner in 1959 which only give the midwall value (for a thin shell, the midwall

value should be the average of the external surface and internal surface values). The agreement between these results are good.

The axial deflection from computation is shown below with the other two results.

Deflection between roots, per ton load:

Measured	0.0071 in.
Calculated, Turner 1959	0.0071 in.
Present program	0.00718 in.

Again very good agreement is obtained.

7.4 Comparison With Other Pressure Vessel Programs

In Ref.3-37, H. Kraus made a review and evaluation of pressure vessel programs, and critically compare the results obtained from four of them using three complex shell problems, all of them shells of revolution under axisymmetric loading.

Four Other Pressure Vessel Programs

The first program originated from R.K. Penny (3-24, 3-38) who was with the Central Electricity Generating Board. It solves the axisymmetric problem using the Love-Meissner equations and by the method of finite-difference. The next program, by A.Kalnins (3-31) who was with the Yale University, can analysis symmetric and non-symmetric loads. The equations are reduced to a system of first-order differential equations, and solved by the Adams-Bashforth stepwise integration method along each shell segment, of which, a maximum of ten is allowed. Continuity conditions are then applied to the variables at the end-points of the segments, to give a simultaneous

system of equations which is solved by Gaussian elimination to complete the solution. The third program originated from Radkowski and others (3-26) at the AVCO corporation. It solves the standard axisymmetric problem allowing of temperature and material properties varying through the shell wall. Multi-branch junctions of up to three shells can be analysed. The differential equations derived by E. Reissner for shells of revolution are solved by the finite-difference method. These three programs, although differing in their generality and in methods of solution, use basically the same class of first-approximation thin-walled shell theory for shells of revolution.

The fourth program, by Friedrich (3-36) of the Westinghouse Bettis Atomic Power Laboratories, solves the standard axisymmetric problem with additional consideration of thick-shell effects. The method of solution is the finite-element method. This approximates the generating curves of the shell of revolution by ellipsoidal finite-elements of shell where middle surface shifts between the elements are allowed. Instead of proceeding from the governing differential-equation of shells, a stiffness matrix is calculated from the strain energy by the principal of virtual work. The thick-shell effect is introduced by determing the contribution to the strain energy from both the normal stress and the shear deflection, both of these are neglected in Love's first approximation theory.

Two of three problems used by Kraus for comparing the above programs are solved with the present program.

Test Problem 1 - Spherical Cap

The first one is a 60^{o} semi-angle spherical cap with 20 in means-radius and 1 in thickness, simply supported at the edge. At the support a condition of zero radial-displacement and zero meridianal-moment is assumed. The top of the shell is closed. Most computer programs have difficulty in analysing this closed condition since the shell differential-equations are singular at the closed apex, this is unless special facilities are added. The first three programs by Kalnins, Radkowski et.al. and Penny have such a facility. The fourth program by Friedrich cannot analyse a closed end, and Kraus left a small hole at the apex of the shell. Kraus observed that this was a valid procedure since the disturbance caused by the hole was very localized. Program PVA1 can analyse a closed vessel, although no output is shown for the very last point, and depending on the particular problem and the accuracy specified, a loss of accuracy in the results may be found at the last one or few points. Kraus presented the results of stresses and displacements for only certain key locations in the vessel considered.

Using 120 steps for the integration, the elastic program PVA1 gave the following results, for 1 lb/in^2 internal pressure:

Running time on IBM 7094,min	less than 0.12
Outside stress at apex, lb/in^2	9.864
Inside stress at apex, lb/in^2	10.035
Normal displacement at apex, 10^{-6} in	5.224
Outside axial stress at support, lb/in^2	9.636
Inside axial stress at support, lb/in^2	9.636

Outside circ.stress at support, lb/in^2	3.5032
Inside circ.stress at support, lb/in^2	2.2786
Rotation at support, 10^{-6} radian	14.140
Peak stress (axial outside), lb/in^2	14.431
Location of peak stress, degress from support	8.5

This table is so constructed that a direct value by value comparison can be made with the results from other programs listed in Ref.(3-37). There is very good agreement with the results from the other first-order programs, on the stresses as well as the deflection and rotation values. In general, the results from PVA1 are closer to that of both the Penny and the Kalnins programs, agreement being to the third and fourth significant figures. The results from the higher-order Friedrich program are slightly different from all others.

Test Problem 2- Hemispherical Vessel Head

The other vessel was a closed hemispherical pressure-vessel head under internal pressure. The mean diameter was 20in , and the thickness for both the head and the vessel body was 1 in. The cylinder part of the vessel had a length of 40in which is sufficiently long for the discountinuity stress at the vessel head to die away to a very small value.

The problem was solved with both PVA1 and the elastic-plastic program PLINTH. The same E and ν were used and the pressure was again 1 lb/in^2

	PVA1	PLINTH
Number of separate output points	144	124
Outside stress at apex, lb/in^2	9.990	9.956
Inside stress at apex, lb/in^2	10.010	10.050

Normal displacement at apex.lb/in^2	9.711	9.732
Outside axial stress at junction,lb/in^2	10.007	10.007
Inside axial stress at junction,lb/in^2	9.993	9.993
Outside circ.stress at junction,lb/in^2	14.996	14.996
Inside circ.stress at junction,lb/in^2	14.992	14.992
Normal displacement at junction,10^{-6}in	7.996	7.996
Rotation at junction,10^{-7}rad.	9.600	9.600
Outside axial stress at end,lb/in^2	10.026	9.988
Inside axial stress at end,lb/in^2	9.974	10.012
Outside circ.stress at end,lb/in^2	20.007	20.040
Inside circ.stress at end,lb/in^2	19.992	20.048
Normal displacement at end,10^{-6}in	11.330	11.363
Peak stress in cyl.(circ.outside)lb/in^2	20.638	20.641
Location,in.from junction	6.5	6.67

The axial displacement values are relative to the end of the vessel.

In addition to the results from the four programs presented in Ref.(3-37). Kraus subsequatly presented in Chapter 10 of Ref.(3-8)*, analytical results for this problem based on Watts and Lang,1953 (3-11).

Comparing these altogether seven sets of results, it can be seen that again the results of the Friedrich program are slightly different from all others because it is based on a different class of theory. The present results from PVA1 and PLINTH agree closely with the remaining four, the largest difference being only of the order of 0.5%. The closest set of results to the present results

---

* Fig.10.12 of Ref(3-8) shows the vessel with an inner diameter of 20.0" rather than a mean diameter of that same value which was used in the calculations in Ref. (3-37). The author believes that it is this diagram that is in error, and that the calculations were all on identical vessels.

are those of the Kalnins program which happen to use also the predictor-corrector step-by-step integration procedure.

7.5 Conclusions

The comparisons above show that there is nearly exact agreement between the results of the program PVA1 and other theoretical results. The heimspherical-head results and toriconical-head results using the Johns and Orange analysis procedure, are all stress results. These analyses do not give the displacement and rotation values. The computer program of Penny and Kalnins using numerical procedures of finite-difference and prediter-correcter integration do give them, and in these cases it is found that there is again nearly exact agreement between these numerical results. All these suggest that the present computer program PVA1 does not give error in the process of transcribing Love's thin-walled first-approximation theory into the analysis of general pressure vessel.

The particular problems studied above are governed by the availability of published results of sufficient detail and accuracy. They are however selected such that they cover the range of problem encountered in most pressure vessel analysis. They have included the toroidal element, the bellows convolution, and the closed-apex problem, ~~and the problem of cylindrical-nozzles on sphere.~~ Both internal pressure loading and axial thrust loading have been studied.

Greater discrepencies were, as expected, found between the theoretical results of PVA1 and the experimental

results. This is because there are at least two additional sources of discrepency. Inaccuracy can occur at the experiment, this includes deviations in the shell from the ideal geometry and possible errors in the measuring techniques. The theories can also be in error if the assumptions behind them are not precise enough, for example, the most well-known assumption that cannot always be followed is that the shell wall ~~is not~~ must be sufficiently thin.

If we consider inaccuracies during the experiment, accuracy of the measuring techniques can in many cases be estimated by calibration. In the bellows tests of Turner, the actual measured dimensions, found to be different from the nominal ones, were used in the calculations. Smaller inaccuracy caused by geometry would be expected for this. The two tests of Morgan and Bizon were conducted with special care to reduce errors caused by deviation in the shell geometry. The test vessels were machined to the prescribed geometry. During the tests on toriconical heads, Morgan and Bizon confirmed that this geometrical inaccuracy can greatly affect the final accuracy of results. It thus pays to put in extra effort to get accurate geometry if exact comparison of results is desired.

8 ACCURACY TESTS FOR ELASTIC-PLASTIC PROGRAM

8- 1 Previous Comparisons

A number of tests on this elastic-plastic program PLINTH have already been conducted and published. They are all compared against the published experiments of vessels or vessel components. A brief summary of these tests is presented below.

Marcal and Pilgrim,1966

In the same paper (3-49) that Marcal and Pilgrim presented the elastic-plastic program,they also presented two calculations,one on a toroidal bellows labelled S tested by Marcal and Turner (8-5), the other on a torispherical pressure-vessel head tested by Stoddart (8-10). Both are of mild steel and the mechanical proporties as reported with the tests were used in the calculations.

The bellows unit was loaded axially, Strain and deflection readings were obtained beyond its limit of elastic behaviour. Only two appropriate curves from the calculation were shown compared with the experiment. The first is the curve of load $\sim$ maximum surface-strain. The agreement on this is very good. The other is the curve of load $\sim$ axial-deflection. Here the calculated deflection results were higher at low loads by about one fifth. The collapse load from the calculation was taken as the load when the convergency of the numerical process become very slow.

The torispherical head was tested under pressure,beyond yield, and until the head nearly collapsed. The elastic stresses from the calculation were compared in detail with the test results and good agreement was found in

nearly all positions. For the elastic-plastic behaviour, the curve of pressure ~ stress for one maximum stress location of the head was compared. The agreement here is less than that of the bellows test. There was during the test a sudden increase in stress at the external gauges (although, surprisingly, the internal gauges which were at the same location did not show any sudden change of behaviour at the same pressure), and this behaviour was not shown on the calculated curves. There was no explanation of how the collapse pressure from the calculation was arrived at.

Marcal and Turner

Marcal and Turner (8-13) presented a modified procedure to the solution of the thin-walled shell theory to predict more realistically the local behaviour of flush nozzles in spherical pressure vessels. This modified procedure was incorporated into the program PLINTH and a few calculations were again made to compare with a few published tests.

The first tests that were compared, were by Cloud(5-8), who tested three nozzles with no fillet-weld nor reinforcement. The nozzles were loaded under pressure until collapse. The second tests were by Dinno and Gill (4-10), who in a similar manner tested two nozzles with fillet-weld. Calculations were made using the normal thin-walled shell theory and the modified theory. Comparisons were made on the deflection behaviour and the behaviour of the maximum meridianal-strain. On the Cloud nozzles, the modification did not affect the deflection values but there was little agreement between the

calculation and the experiment. The calculated strain results of the same nozzles were greatly affected by the theory used. Because of these two reasons it was not possible to judge whether the elastic-plastic program gave good results or not. On the two nozzles with weld tested by ~~of~~ Dinno and Gill, the two theories gave different values of elastic deflection, with that of the modified theory closer to the experimental deflection. After initial yielding, the modified theory gave deflection values which started to increase rapidly from a lower load than experiment, and further gave, after that, a load which, for the same deflection, is 10 to 25% lower than the measured load. No comparison can be made of the behaviour of load against strain, since the experimental results were not shown.

These comparison of results for the nozzles were complicated by the presence of local effects at the nozzle junction which is also the location of maximum stress. The modified theory is thus necessary to take this into account. However, this means that the above elastic-plastic comparisons are not straight-forward tests of the accuracy of the program. No conclusion can thus be drawn in this case on this latter point.

8.2 Use of Elastic-Plastic Results

Both the literatures and Ch.7 show that the accuracy of prediction of stresses by elastic thin-shall theory is fairly well established for many shapes of shells of interest to pressure vessel designers. It is probable that carefully machined vessel and accurately conducted tests can even reveal the accuracy or otherwise of the assumptions behind the theories. The prediction of

elastic-plastic stresses and strains is still in its infancy. We have seen in Sec.8.1 that many more factors influence the accuracy of such predictions than is the case for elastic calculations. It was thus difficult to compare the results in detail.

Two methods can be adopted to tackle this problem. The first is to eliminate, as far as possible, those subsidiary factors that may affect the experimental results (by subsidiary factors is meant those that cannot be included in elastic-plastic calculations as limited by the theory). ~~This~~ case includes, for example, trying to remove any residual stresses and any difference in hardness of the material, ~~accuracy measurement of~~ measuring accurately the vessel geometry as tested, and using the actual geometry in the calculations. Details of this are given in Ch.11 which gives the preparations to the author's vessel test. The second method is to find out, to what uses these calculations may be put ~~into~~ to help with design, and discuss the accuracy or otherwise of the results in the context of these probable uses. For this purpose, the vessel research and vessel design interests of these elastic-plastic calculations are reviewed below, followed by a discussion of the kind of results that may be required.

In the design against excessive deformation and collapse, elastic-plastic calculations can (8-1) fill the gaps left by limit analysis, where at present approximate solutions to only torispherical heads(5-4) and symmetrical nozzles (see Ref.8Q2), are possible. Study can also be extended to the solution of shells with various strain-hardening material properties. In the design of

components under reversed loadings, such as expansion bellows and pipe bends, the design can be made more economical by allowing alternating plasticity rather than limiting the working load to one giving no yielding. Here design to some low cycle fatigue life N requires the plastic strain e_p (8-3). One commonly used relation (8-4) is $e_p N^{\frac{1}{2}}$ = constant. Other relations with the total strain e_t have been proposed for small plastic strain. To predict the maximum value of e_p or e_t on such vessel components, elastic-plastic computation is required (8-5),(8-6) using a 'cyclic' rather than the oridinary 'monotonic' stress-strain curve of the material. Loading direction does not reverse with components loaded only under pressure , but in most cases there is a sufficient number of loading and unloading cycles in general service to justify the consideration of shakedown under repeated load(8-7),(8-8) in addition to collapse. While one procedure to obtain shakedown load, applicable to symmetric nozzles, requires only elastic analysis (5-17), (5-18), the elastic-plastic solution up to not greater than twice the first yield load is required in another procedure applicable to the general shell(8-1),(8-8),(8-9).

From this brief review, it appears that interest is on the prediction of collapse load, of shakedown load, and of fatigue life.

Where low cycle fatigue is of interest, Ref.(8-5) and (8-6) pointed out that elastic-plastic calculations using the value of settled cyclic yield-stress for non-work-hardening material, or settled cyclic yield-curve for workhardening material were used instead of the ordinary

'monotonic' stress-strain curve. The strain range of interest should be less than 2.5 times the maximum elastic range except for very short fatigue-life.

Where elastic-plastic calculation is used (8-1) to predict shakedown pressures, stresses at less than twice the first-yield pressure are required, the strains these being ~~about~~ less than 2.5 or 3.0 times the first yield ~~stresses~~ strains.

In the prediction of collapse, this can be observed either through the strain results or the deflection results. The component may be judged to be in a state of collapse when there is a sudden change in slope of the load-strain or load-deflection curve, or when the strain or deflection has reached a certain large value. The final interest is on the load value at this condition and no consideration of repeated load behaviour is necessary.

Closely allied to the prediction of collapse is the prediction of excessive deformation. This is important in applications where close fitting of the vessel component is necessary, as in the case of standpipes for fuel rods in nuclear reactor vessels and of high pressure turbine, compressor and pump casings. Again the value of the load is required.

8.3 Further Comparisons

Since the present research was planned, the author noticed two pieces of experimental work that could serve as basis for a further detailed comparison of the results of the elastic-plastic program. Both of them involved testing pressure vessels beyong yield to a state of collapse, while strain measurements were made with electrical strain

gauges. As mentioned in Sec.5.3, Stoddart (8-10) carried out, at the now University of Newcastle-upon-Tyne, elastic and plastic tests on two identical torispherical pressure-vessel heads, made of mild steel $\frac{1}{4}$in thick, and of 24in mean diameter. Extensive gauging of both the inside and the outside surfaces was made. Kemper et.al.(5-12) of the APV Ltd. and of the Firth-Vickers Stainless Steel Ltd. tested two pressure vessels of identical geometry, but made of stainless steels differently heat-treated. Only nine strain gauges at the outside of each vessel were used, since the purpose of their test was to show the advantage of one of the steels that had been warm - worked to a higher proof-strength, and thus gauges were used only to record the general vessel behaviour until collapse. The vessels had mean diameter of $41\frac{1}{8}$ in. and thicknesses of $\frac{1}{4}$in at the body and 5/16in at the head.

The heads of the Kemper vessels are slightly less than twice the size of that of the other vessels, but both have similar height/diameter and knuckle-radius/diameter ratios. They can be classified as medium-thick pressure-vessel heads. The following Table 8-1 gives detail of their geometry and some other useful information. (Also shown on this table are the geometry and information of the author's vessel to be described later in Ch.11 and 12.)

Table 8-1 Details of Test Vessel Heads

	Author's tests Head A	Head B	Stoddart Ref.(8-10)	Kemper Ref.(5-12)
Head dimension(in.)				
Shell diameter D	23.678	23.848	24.000	41.125
Crown radius R	20.474	19.444	24.125	41.844
Knuckle radius r	3.839	4.344	2.000	3.156
Head thickness t	0.322	0.312	0.250	0.310
Shell thickness T	0.322	0.312	0.250	0.250
Head height h (see note below)	5.890	6.384	4.387	7.295
h/D	0.249	0.268	0.183	0.177
t/D	1/73.5	1/76.3	1/96.0	1/132
r/D	16.21%	18.22%	8.33%	7.67%
Strain gauging, Gauge lengths	2mm, 5mm, 10mm		$\frac{1}{4}$ in.	3mm, 5mm
Gauge location	Inside and out - side surface		Inside & outside surface	Outside surface
Material	Stainless Steel		Mild Steel	Stainless steel
Heat treatment	After fabrica - tion, 900°C		After fabrica- tion	None

Note: D, R, r and h are mid-wall values. No significance is implied in the number of figures as these are the values used in the calculations.

8.4 Tests by Stoddart

Stoddart's vessel was analysed with the elastic-plastic program using values, as quoted in Ref.(8-10), of Young's Modulus of 30.354×10^6 lb/in^2 and Poisson's ratio of 0.31. An elastic perfectly-plastic stress-strain behaviour was assumed with a yield stress of 40,197 lb/in^2 this value being obtained from a tensile test specimen from the same plate as used for the vessel head and subjected to the same heat treatment. The calculation

gave a theoretical first-yield at 213 lb/in^2*. Four peak strain values at three strain-gauge locations were plotted alongside the corresponding experimental curves and are shown in Fig.8-1. The inside meridional strain at the 45^o station was maximum for the whole vessel. The curves for this strain value show that the elastic values agree very well while the theoretical plastic-strains increase more rapidly with pressure than the experimental values. The agreement is different with the other pairs of curves. Here, while all the experimental curves bend down sharply at around 375 lb/in^2, the theoretical ones show a more gradual change of slope making it difficult to intepret a corresponding pressure at which the vessel starts to deform rapidly. A quantitative comparison of the collapse pressure is however very useful, and two methods are proposed here to intepret this value.

Definition of Collapse

In the first method a tangent is drawn to the plastic part of the load-strain or load-deflection curve, and its intersection point with the elastic line is used as a criterion of the start of collapse. (In what follows, the tangent is drawn at a point on the curve where the actual strain, or deflection is three times the value expected for that load had the response remained elastic). This stems from the observation (8-11) that simple structures of linear-hardening material behave such that

---

* The complete elastic-plastic computation took 20 minutes on the IBM 7094 computer, this includes calculation at every load increment, each at 0.2 of the yield pressure, until a pressure of 468 lb/in^2.

a tangent to the nearly straight part of the load-deflection curve intersects the elastic line at the same point as that for a perfectly-plastic material. For these structures, this point both marks physically the start of rapid deformation and coincides with the results from a limit analysis.

The second definition tries to indicate the load where signs of physical collapse, in the form of excessive straining, actually occur. It is chosen as the pressure giving a maximum total strain of 0.5% at the vessel outside surface.

Comparison

Table 8-2 below compares the collapse pressures thus obtained from the test curves and from the calculation. The tangent method for collapse was applied to the experimental curve for the maximum meridional strain. The value from the test results is 380 lb/in^2 and happens to agree with the value where the strain readings increased suddenly. The collapse values from calculation is higher, at 410 lb/in^2. A limit analysis, assuming also perfectly-plastic material and according to Shield and Drucker (5-4), gives upper bound pressure of 465 lb/in^2 and lower bound of 375 lb/in^2.

The tangent method gives collapse loads within the bounds of the limit analysis, while the 0.5% strain criterion gives as expected, a higher collapse, although the difference is not large (21% for the test curve and 13% for the calculated curve),

Table 8-2 First yield and collapse pressure for Mild steel pressure vessel head, Stoddart (8-10).

	Test results Ref.(8-10)	Elastic-plastic calculation
First yield	250 lb/in^2	213 lb/in^2
Collapse		
Method 1 (tangent)	380	410
Method 2 (.5% strain)	470	about 490

8.5 Test by Kemper Et.Al.

Stress-strain Curve

Material properties were also give in the report on the tests by Kemper et.al., (5-12). They were obtained from tests in general on the two types of steels used, but not specifically on the individual plates used to fabricate the vessels. This is unfortunate, since, as is shown in Fig.3,Ref.(5-12), the proof stress can vary over a wide range even for the same type of steel. Two representative stress-strain curves, one for the high-proof steel and one for the normally used low-proof steel,are given in the Fig.1 and 2 of Ref.(5-12). The curves were used in the present calculations as data for the elastic-plastic pressure-vessel program PLINTH. There is a high degree of strain-hardening,and a perfectly-plastic calculation would not be accurate. In the program PLINTH strain-hardening in the stress-strain curve is defined through the coefficients of an algebraic polynomial. In this way, the measured curve, with any amount of strain-hardening,can be approximated and used in the calculation. For this purpose, a least-square curve-fitting program

was written, based on Ref.(8-12), for fitting an algebraic polynomial of specified order to a set of unequally spaced data points. The supplied curve for the low-proof material, within the range 0 to 2% plastic strain, was converted to a second-order polynomial. The elastic-plastic calculation for this problem took a total of 20 minutes on the IBM 7094, the pressure increment, after the initial yielding at 95.7 lb/in^2, was 0.4 of this value until a pressure of 287 lb/in^2 was obtained. Fig.8-2 shows the elastic strain distribution. The maximum straining occurs near mid-knuckle, on the internal surface, giving a strain-concentration factor of about 4.0 over the vessel-body circumferential strain.

Sources of Possible Error

Before comparing the theoretical and test results, it should be noted that the former had assumed a uniform material property throughout the vessel as given by the assumed Young's Modulus, Poisson's Ratio and the approximated stress-strain curve. The test vessels had however not been heat-treated after fabrication as in the Stoddart test. The vessel plates would certainly suffer a certain amount of work-hardening during fabrication. The most severe hardening would occur at the knuckle region of the heads where 5/16 in. thick plate was rolled into 3 in. knuckle radii.

The two test vessels were nominally indentical, and the measured elastic strain from both are expected to be the same or similar. They are however found to disagree in nearly all cases and to disagree also with the corresponding

calculated values. The following Table 8-3 compares the strain values at five gauge locations, the measured values were obtained from the slope of the elastic part of the curves plotted on the appropriate figures of Ref.(5-12).

Table 8-3 Elastic Strains

10^{-6} per 100 lb/in^2 pressure

Position	Gauge No.	Measured Strain Ref.(5-12)			Corresponding Calculated Strains
		Low-proof	High-proof		
		Fig.9	Fig10	Fig.11	
Crown centre	9	22	13	17	16
Mid-knuckle					
Circ.	8	-43	-60		-55
Merid.	5	-8	-28		-29
Vessel body					
Circ.	2	18	-	24	24
Merid.	3	5	8		6

This disagreement in elastic strains makes it impossible to get a meaningful comparison of the elastic-plastic strain values. Only the theoretical strains are thus shown in Fig.8-3 where the peak strain values labelled A to D in Fig.8-2 were plotted against pressure. A few of these readings are internal ones whose behaviour could not be observed during the experiment. The axial deflection of the crown centre relative to mid-vessel was also plotted and is shown as curve δ.

Comparison

The theoretical first-yield using the properties of the low-proof steel is at 95.7 lb/in^2, and at 150 lb/in^2 all the peak strain curves get progressively non-linear.

Fig.9 of Ref.(5-12) gives the strain behaviour of the low-proof vessel during the test. This figure is repeated here as Fig.8-4 for convenience of comparison. Of the nine strain gauges in the test, two, No.6 and 7, were on the junction of the nozzles and were not plotted. The other gauges plotted were on the vessel head or the vessel body. The plastic behaviour of these other seven gauges showed a progressively non-linear response after 300 lb/in^2, expecially for gauges No.4,8 and 2, the former two located at the mid-knuckle and the last at the vessel body. After 500 lb/in^2, a rapid increase at No.2 and 1, both of which were at the vessel body. At this pressure, the other mid-knuckle gauges, showed only a steady increase, which is a continuation of their previous behaviour.

Table 8-4 below compares the elastic-plastic behaviour as observed from the external strain gauges and as predicted by calculation.

Table 8-4 Stainless Steel Vessels, Kemper Et.Al.

	Test Ref.5-12	Elastic-plastic calculation
Low-proof vessel		
First-yield pressure	200 lb/in^2	115 lb/in^2
Collapse pressure		
Method 1 (tangent)	270	190 190
Method 2 (.5% strain)	530	240
High-proof vessel		
First-yield pressure	300	200
Collapse pressure		
Method 1 (tangent)	690	340 340
Method 2 (.5% strain)	590	420

Since only external strain gauges were used in the tests, and in order to give a fair comparison, only external strain results are used to give the calculated values

of the first-yield pressures and the collapse pressures by the tangant method. Two values for each vessel are listed against the collapse pressure by the tangent method, they are obtained from the maximum external meridional-strain and the maximum external circumferential-strain curves respectively. In this calculation the values agree with each other.

Only seven strain gauge results are available for each test vessel, and of these only two were positioned near the location of maximum straining of the vessel head, at the centre of the knuckle radius surface. The yield and collapse pressures from these test results are thus expected to be higher than what would actually happened. The table shows that first yield and collapse as predicted from the calculation do occur at a lower pressure than that from the test. Two other factors, ~~un~~ NON-uniform degrees of yield and work-hardening, and disagreement of the elastic results, have already been mentioned above that would throw doubt to an elastic-plastic comparison. It is thus not possible to judge the value of this comparison.

9 AXIAL LOADING TESTS OF FLUSH NOZZLES

9-1 Nozzle Configuration

Nozzles can be attached to pressure vessels in different manners, and different methods of reinforcement can be used to reduce the weakness of having openings in vessels. From operating experience, and from special researches into nozzles and openings, good design configurations have gradually replaced the bad ones. Design codes can prevent both extreme over- and under-reinforcements, and according to these practices certain bad methods of arrangement of welds have been eliminated from important types of pressure vessels. Reinforcing pads and partial-penetration welds are at present commonly used because of their convenience during manufacturing. Specially machined reinforcements and through-penetration welds are however the better practice, both as regards to better distribution of stresses and for easier analysis by photoelasticity or by theoretical prediction.

Junction Arrangements

Many pressure vessel nozzles are fabricated leaving fillet welds at the junctions. Experimental analyses of such nozzles with strain gauges are possible only as far as the edge of the welds. The unknown stress-concentration due to the weld arrangement would be added to the peak stress at the junction, and thus no exact estimate of the local condition can be made. This is of course not a disadvantage in the many cases where only the load-holding strength of the nozzle is important. The stresses are very local in nature and the ductility of the pressure vessel material is usually adequate for taking up such stresses.

As safety and economy are both of importance in the design of pressure vessels, increasing number of design considerations will be brought in,and stricter designs will be imposed. Better knowledge of the local but high stresses at the nozzle junction will be necessary for the design of nozzles. Already this is a requirement for the design of many nuclear vessels. The ASME Boiler Code, Section III, for nuclear vessels (9-1), specifies that nozzle welds should not be left as welded, but the corner and fillet are to be ground and machined to specific radii. A few recommended shapes are given in the Code, according to which the designs can be based, In such cases, definite stress indices can be used in the design of such nozzles against fatigue failure. Nozzles not according to these recommended shapes must be designed with stress indices obtained from specially conducted experimental stress analysis.

It was mentioned in Section 14.3 that the Pressure Vessel Research Committee launched a major program of experimental study of pressure vessel nozzles and their reinforcements (9-2),(9-3). All the nozzle configurations that were analysed were of these smoothened types. It was felt that they would be the only configurations used in advanced nozzle design of the future, and that such a big research effort should be directed towards these configurations and not to any less-advanced shapes. For the very same reasons, the author's present test is on the smooth nozzles.

A complete vessel is not necessary for conducting axial load tests on nozzles. The bending stresses and strains

are local in nature and an enclosed container is not necessary, as would be required in a pressure test. Two mild-steel spherical caps with flat bases were used. Branch pipes of sufficient length were welded on top to simulate the condition of a nozzle on a spherical vessel, or on the centre of a torispherical vessel. The nominal dimensions of the two test components are shown in Fig. 9-1. These two test components will be referred to as the Thick Cap and the Thin Cap.

The base plates of both Caps are 24 in. in diameter and the base circles of the spheres are approximately 22 in. diameter. Both nozzles are of the same diameter and thickness, being machined out of a 4 in. outside diameter, $\frac{1}{4}$ in. thick, mild-steel tube.*

This diameter of nozzle was selected so that the nozzle was not too small for sticking and manipulating strain-gauges inside the nozzle bore, but not too large as to cause interference between the bending stresses originating both from the nozzle junction and from the base plate. The weld preparation and the final machining of the nozzle are shown in Fig. 9-2+. This weld preparation is in accordance with that recommended for Flush Set-through Nozzles in the three British Standards for Carbon-Steel Pressure Vessels, (9-4) to (9-6). It was selected because the weld zone, being situated on the vessel side, is slightly away from the fillet and corner regions, and

---

*Hot finish seamless steel tubing, according to BS 3601, steel 22.

+Dried, low hydrogen FORTEX 30 (i.e. 30 ton/in^2 UTS) electrodes, kindly supplied by MUREX Welding Processes Ltd. was used.

because it has been found by observing other experimental results that the maximum stress may occur nearer the nozzle end of the above regions. The nominal radius at the fillet, this being the same for both caps, was selected to be the same as the nozzle nominal thickness of $\frac{1}{8}$ in. Any smaller value for this radius would cause great difficulties in the satisfactory strain measurement of this region by strain gauges. The corner radii, on the other hand, have different nominal values for the two caps. In each case it was selected to equal the sum of the values, cap thickness and nominal fillet radius. This is not the normal practice, but the reason, for doing it is that it will result in a shape similar to that used in the theoretical analysis which will be explained later in Ch.10.

9.2 Strain Gauge Techniques

It was noticed, from previous experience of other colleagues at Imperial College, that the strain-range required of the gauges, for elastic-plastic tests of pressure vessel components until or near collapse, is in the range of a few percent. Ordinary gauge and adhesive combination may break or become gradually non-linear within this strain range. Specially manufactured post-yield wire gauges called TML* has been found by other colleagues to be suitable for such high strains. Two types of gauges of this make were used in the tests here, a linear post-yield gauges of 5mm gauge-length for the high strain regions, and a 5 mm, 90° overlapping

---

* By Tokyo Sokki Kenkyujo Co.Ltd. Tokyo.

rosette-gauge for the other regions. Apart from having the distinction of being designed for high and low strains, the former type of gauge has a backing which is more flexible and can follow a surface contour reasonably well, unless the contour is a doubly-curved one. The latter type of gauge can only be applied to a flat surface or a slightly curved one.

After some initial trial, it was found later that gauges of even smaller gauge-length and size were necessary at the fillet position. Most stress analysis experiments on nozzles that uses strain gauges neglect any measurement at the fillet position, because, with a sharp fillet or a fillet weld at that position, it is extremely difficult, if not impossible, to find accurately the strains there with strain gauges. The author however considers that a knowledge of the fillet strain is very important, for the very reason that, in most cases, the maximum strain resides there. The present fillet has, as mentioned, a smooth surface of radius about $\frac{1}{8}$ in. The 5 mm gauge, 5 mm being about 0.20 in, is too large and was found difficult to fit around this small radius. No gauge of smaller size was available in this range of TML post-yield gauges, and a KYOWA foil gauge * with 2mm gauge-length was selected. In addition to being available in this small size, the KYOWA foil gauges were supplied with lead-wires already attached, a very useful arrangement in the present circumstances.

A rapid setting adhesive was used on all gauges, called cyanoacrylate (with the trade name of Eastman 910). No

* By Kyowa Electionies Instruments Co.Ltd., Tokyo.

mixing nor heating is required for its use. The gauge to be positioned has only to be held down by finger pressure, since the setting time is only from one to a few minutes. A certain amount of skill is however needed, since any wrong positioning, or any uneven pressure in the first few instants of contact between the gauge and the prepared surface, cannot be remedied without much trouble, removing the gauge and replacing by a new one. This adhesive was however very necessary for this job because many gauges were, of necessity, close to each other, and some had to be positioned at awkward locations or unflat surfaces.

All the different types of gauges used were checked for their gauge factors and the linearity at different strain ranges. The strain values at breaking point were also observed. The same adhesive, the same surface preparation procedure, and the same strain recording arrangement were used as in the actual tests. Further details of these techniques are given in Section 9.4 below.

The gauge factors at small strain values were measured using a four-point beam-bending rig designed for such calibrating purposes. Within the range of 0.1% strain, which is the range possible for this calibrating arrangement, the response of the gauges were all linear and the gauge factors were very close to the manufacturer's value and within the accuracy expected from the test.

For calibrating at higher strains, a $\frac{3}{4}$ in. by $\frac{1}{4}$ in. stainless-steel bar pulled in tension was used. The gauges were all positioned on the same side of the bar

to prevent errors caused by bending of the bar under off-centre loadings. The strain values were checked by taking accurate measurements with a travelling-microscope of the length between two transversely scribed lines, on the same side of the bar as the gauges. With this travelling-microscope arrangement there was no limit to the strain range that could be measured. Two gauges of each type were tested. The two rosette-gauges failed both at about 1.7% strain by a complete slipping of the adhesive bond. The two linear post-yield gauges failed by a gradual peeling-off of the backing from the metal surface, and the response became non-linear after strains of 6% and 7.5% . The two 2mm foil-gauges both failed by an excessive stretching of the foils near the weld tags until the foils necked and broke. Their failure strains were around 2.3% .

The gauge readings were all plotted against the strain calculated by the microscope measurement, to determine the gauge factors and to observe the linearity. A small amount of scatter existed at small strains below about 0.3%, because the microscope arrangement is not suitable for such small strains. A similar pattern of behaviour was observed on all gauges, in that the plots showed a very slight deviation from a straight line at around the range of 0.5 to 0.7% , but settled to another straight line with a different gauge factor all the way afterwards. In view of the slight scatter below 0.3% , it is hard to obtain accurately the gauge factor at low strains, but lines according to the manufacturer's value do fit very closely the points below 0.5 to 0.7% strain. At higher strains, all the wire gauges have a lower gauge

factor with between 6 to 8% difference, while the foil gauges have a higher gauge factor with a 13% difference.

9.3 Material Properties

A knowledge of the material properties is necessary for elastic-plastic calculation. The static stress-strain curve of the material beyong yield was needed as data for the computation. The strain range of interest was within 4 per cent. It was also useful to know the ultimate tensile-stress.

Test Specimens

The nozzles of the two components were made from the same piece of pipe, but the spherical caps may have different properties. The arrangement of the nozzle weld was such that the actual junction, especially the zone where most of the yielding occurs, consists completely of the pipe material. It was thus decided to prepare test specimens and to conduct measurements on the material properties on only the pipe materials. A spare piece of pipe material was taken and heat-treated together with the two completed nozzle and cap components, the procedure being described in Section 9.4 below.

From theoretical analysis of the elastic strains, done beforehand, it had been found that the maximum strain of the whole test component would occur as a compression in the meridional direction, which would be very nearly the axial direction of the nozzle. The maximum value for tensile strains also occurred in the same direction. The pipe was $\frac{1}{4}$ in. thick, 4 in. outside diameter. Tensile-test specimens were machined from this in the

axial direction. Two types of plane strain compression specimens, designed for test with the platen in the axial and the hoop directions were also made.

Tensile Tests

The tensile test was easy to conduct. The tensile specimens were designed to fit between the shackles of the Hounsfield Tensometer, but were actually loaded at a slow and constant strain-rate in a Instron Universal Testing Machine. The stress-strain curve from tensile tests on mild steel, with its upper and lower yield point, is very sensitive to the loading and the measuring arrangements and to the strain rate (9-7). The Instron machine has a long and free linkage behind the shackles thus reducing any non-axiality in the test set-up. It would be preferable to be able to measure the extension of the uniform portion of the specimens. Unfortunately the space between the ends of the two shackles, when locked around a specimen, is very small, with a clear gap of only about $\frac{1}{2}$ in. Attempts had been made to insert and take measurements with some home-made " clip-gauges", bent strips of spring steel with the change of curvature detected and measured by resistance strain gauges. This however was not successful. It was thus decided to record the cross-head movement as an indication of the plastic straining of the specimens. The calculated elastic straining of a specimen, which could be quite small compared with the plastic one, was then added to find the total strain. The Instron machine's own autographic plotter was used, the extension being plotted against the load value recorded by a load cell. Two tensile specimens were tested.

Table 9-1 Tensile Test Results

	Initial Dimensions (in)		Load Values (lb)			Stress Values(lb/in^2)		
	Average Diam. d	Eff. gauge length L	Upper yield load U.Y.L.	Lower yield load L.Y.L.	Ult. tensile load U.T.L.	U.Y.S.	L.Y.S.	U.T.S.
1	0.1255	0.90	592	568	779	47,900	45,900	62,900
2	0.1255	0.92	590	550	775	47,500	44,500	62,500
Average						47,800	45,200	62,800

Table 9-1 gives the test results of the two specimens. The ratio of yield/ ultimate stress is about 75%. The load-extension curves near the yield points are show in Fig. 9-3 a and b.

Compression Tests

The technique of the plane-strain compression test (9-8),(9-9) as originally developed by Watts and Ford (9-10) and commonly used on relatively thin strips and sheets, is normally suitable for finding the compression stress-strain behaviour at high strains, from 5% to 80% reduction or even higher. With the usual procedure, the test strip is compressed between two narrow tool-steel plates, and after a certain increment of load, it is removed and the resulting strip thickness is read by a micrometer. The strain range of interest in our case is however only 4%. At small strain ranges, the reduction in thickness is small and scatter of the results can occur.

An alternate procedure finally adopted is to dispense with the micrometer for thickness measurement, and to measure the movement of the platens during loading. A home-made Clip Gauge, mentioned above, was used, with the ends of the gauge inserted between the shoulders of the platens. The loading on the strip can thus be made continuously and, unless the clip gauge is disturbed in-between readings, one continuous run is sufficient for one set of readings, corresponding to one stress-strain curve.

It was mentioned that the maximum compressive strain at the nozzle would be in the axial direction. These plane-strain compression tests result in a maximum strain in the through-thickness direction, and may not be representative of the desired axial-direction properties. They can however serve as a rough check on the uniformity of material properties in the two important

hoop and axial-directions. The load-deflection curves of the three tests performed with the platen perpendicular to the hoop direction, and the two tests with the platen perpendicular to the axial direction, are presented in Fig.9-4 to 9-6. It can be seen that the value of the yield stress at each group of test is fairly consistent; the slope of the plastic lines are however not so. The reason for the latter may be caused by the different amounts of friction between the strips and the platen.

9.4 Test Arrangements and Preparations

Residual stresses would be left at and around the nozzle junction after the welding fabrication. While this may not affect the strain gauge readings in the elastic ranges of the shell, the yielding load and yielding pattern may be altered as a result. For this reason, the two shells were both given a stress-relieving heat-treatment after welding at a temperature of 650° C (see Ref.(9-11)). As mentioned in Section 9.3, the spare piece of pipe needed for preparing test specimens was heat treated at the same time.

An important aim of these tests is to obtain accurate measurements of the strain distribution of the shells, especially around the nozzle junctions. Strain gauges were applied on both surfaces of the shell. The geometry and loading should be symmetrical, and the principal strain directions were known at the axial and meridional directions of the shell. Gauge locations were chosen along a particular cross-sectional plane of the shell. At each location, two linear gauges or one right-angled

rosette gauge were positioned in the two principal-strain directions. Two further planes were selected, one diametrically opposite and one at right angles to the measurement plane. One these latter two planes, strain gauges were positioned at a selected few of the locations to check on the symmetry of the arrangement.

It is important to measure accurately the straining at the fillet and corner radii surfaces. Three pairs of 5 mm post-yield wire gauges were positioned on each surface, one pair at the centre of the curve and two pairs at the ends. From theoretical prediction, the meridional strains nearer the nozzle-end of the fillet were found to have the highest values and, furthermore, found to have a sharp gradient. Three 2mm foil-gauges were positioned there, all in the meridional direction. Two of them were placed at the corresponding locations of the 5mm gauges,i.e. at the centre and at the nozzle-end of the fillet radius curve, and the third one was placed in-between.

The normal surface-preparation procedure was used. The surfaces of the spherical caps were rough and slightly pitted, probably as a result of the hot-pressing process generally used for making such caps and dished-ends. The 650° heat-treatment applied to the shells further left the caps and nozzles with coatings of oxide. Thus, at and around the strain gauge loactions, they were given machine-sanding with a sanding-drum attached to a portable electric-drill. At rough places on the caps, a light carbide-wheel grinding had to be used.

Cementing of gauges was mostly done on the surfaces as

was left after machine sanding, because it was felt that extra polishing by hand was not necessary. Cleaning and degreasing of the metal surfaces and the back of the gauges was done using carbon tetrachloride. Acetone was also tried, but was finally not used for this purpose because the cement cyanocarylate was found to be slightly soluble in it. Acetone was however useful for cleaning the metal surfaces from spare cement left by neighbouring gauges, or by a previous gauge that had been found defective and been removed.

The strains were recorder using a mult-channel automatic strain-recorder made by Solatron Ltd, Plate 9-1, designed for measuring static strain. The basic bridge-circuit of each channle is shown in Fig.9-7. It is a direct-current, Wheatstone bridge circuit with the electric potential drwan from a constant voltage electronic power-pack. A digital voltmeter reads the out-of-balance voltage. Fifty bridges are provided in the recorder unit, each with its own balancing unit, thus giving 50 available channels. A commutator unit selects the channels, either repeatedly or in turn, and the voltage reading is displayed each time on the digital voltmeter and printed on to paper tape through a fast printer for permanent record.

The maximum selection speed of the unit is 10 channels per second. It is thus possible for a set of 50 readings to be recorded within 5 seconds from the moment of trigger. The loading during experiment could however be held relatively constant for a reasonable period of time. A slower speed of 5 channels per second was used

throughout this series of tests.

Since a d.c. bridge circuit is used in the recorder, the considerations of accuracy of readings are very much simplified. The normal precautions as necessary for any resistance strain-gauge measurements using d.c. bridge circuits were taken here. These include the balancing of lead wires, temperature compensation with the same type of dummy gauges on the same metal surfaces, testing that sufficient insulating resistance to earth exists at each gauge,etc. There were more than 50 gauges on each shell. Two terminal boxes were thus connected to each shell. One box was connected to the gauges around the nozzle junction, and the other to the gauges necessary for checking the axisymmetry of the arrangement during loading. Since the bridges in the recorder are separated from each other, each active gauge must be provided with a corresponding dummy gauge. This would normally add to the financial expense of any test that involve many gauges. Fortunately two shells were being tested here with all the gauges on one duplicated on the other. It was thus arranged that while one shell was being tested the gauges of the other were used as dummies.

Two of the channels of the strain recorder were used for special purposes. One channel was connected to a thermo-couple,arranged to detect the temperature difference between the two shells. Two distinct thermocouple junctions were made, each attached on to the surface of a cap and connected through the commutator unit to the digital voltmeter,by-passing the bridge. Any difference in the temperature of the shells would be detected as

thermo-e.m.f.difference at the voltmeter, and be recorded together with the set of strain readings. The same voltage range at the voltmeter could be used for both purposes.

Connected to the other channel was a separate pair of gauges with the active one kept under constant strain throughout the test. The same four-point beam-loading rig as used for the gauge-factor calibration (Section 9.2) was used here to supply the constant strain. This served as a check against any drift of the whole gauge-bridge-recorder system. This precaution was taken because the whole series of loading and reading of each shell, with all the necessary interruptions, took between half to a whole working day.

The value of the excitation voltage was fixed at 2.00 volts to give a direct reading at the digital voltmeter and printer.* The last digit of the voltmeter and printer has a value of 10 μV and 0.02 V $\pm$ 20 μV respectively. Comparing with the uniaxial yield-strain of the shell material of about 1500 μstrain (i.e.1500μV), the resolution and the accuracy are sufficiently small, except probably for measurements much below yield.

The loading was performed on an Olsen Universal Testing Machine. Vertical load could be transmitted to the crosshead through four screws located at the four corners

*This direct reading is strictly correct only if all the gauge factors are 2.00. The quoted gauge factors of the manufacturers have values of 1.94 to 2.08, according to the different batches of gauges. This variation has however been neglected, because the purposes of the test were more to survey the strain distribution and to observe their variation under plastic loading, and not as much to obtain precise strain readings.

of the horizontal load sensing table,leaving a wide and clear table-space for positioning the shell. The arrangement during test is shown in Plate 9-2. Compression loading was applied. The shell under test was supported on three blocks and lightly clamped on to the table. The loading force acted from the cross-head,through a conical anvil and a hardened steel ball, which, in turn, sat on a central hole drilled in the end-flange of the nozzle, Fig.9-1.

At two diametrically opposite positions at the junction, displacement dial-gauges fixed with right-angled attachments were used to measure the axial deflection of the nozzle junction relative to the base of the cap.

The test loading,during which the final measurements of the test were to be made,must be the first one to cause any yielding after the post-weld stress-relieving. This was a necessary measure to prevent the unknown effects of residual stresses and to get a true comparison with the predictions of the elastic-plastic shell program. Before the test loading, a number of elastic loadings were however made to the shells for the purpose of checking for the correct connection of all the hundred and odd gauge-circuits, for the linearity of response of the gauges, and for the symmetry of the shell loading-arrangements. These loading were all kept within the range of elastic response of the shells.

Gauges that were found to be defective were removed and replaced. In addition to being checked for the correct alignment and location,they were visually inspected with the aid of a strong light and magnifying glass,for

any air bubbles or voids under the gauge wires or gauge foils. Such air bubbles could give fictitious strain readings to the gauges. The final check for this defect required an elastic loading, and all bad gauges that gave non-linear responses were replaced.

The symmetry of the shell and the arrangements was checked using the three sets of gauges positioned around each shell for this purpose. In both shells the readings from the three sets were in agreement.

9.5 Test Procedure and Results

The Thin Cap

The Thin Cap was the first one to be loaded beyong yield to obtain the plastic and the collapse behaviours. Initally, readings were taken at every 1000 lb.interval. During each interval the load was held steady for about one minute and the readings were taken, this consisting of triggering the scanner of the strain recorder and reading the two dial gauges. At a load of about 5000 lbs, the highest strain reading showed signs of deviating from a linear relation with load. Subsequently and until 9000 lbs the load increment was decreased to 500 lbs. At about 14,000 lbs, the rate of straining had to be increased because the corresponding rate of increase of load had slowed down. The load reached a maximum at 14,210 lbs, when the load started to drop even for a further increase of the rate of straining of the loading machine. Straining was thus finally stopped and the load relaxed, this occured at about a deflection of 0.1 inch at the nozzle junction. During the unloading, the recording of the readings was continued at larger intervals.

All the strain readings were individually plotted against the load and the gradient of the initial, linear part of the graphs were measured and taken as the elastic strain value. The elastic strain distribution around the nozzle junction,could thus be obtained. The meridional and the circumferential strain distributions are given in Fig.9-8 and 9-9 respectively.* The readings of the foil gauges,with their smaller gauge-length of 2mm, are shown differently, the circular symbol having an additional cross. The highest strain is a meridional one at the external fillet radius of the nozzle junction. It can be seen that this high strain is very local in nature and the strain changes very rapidly across this region. It is also interesting to note that the circumferential strains at the nozzle have the same value on both shell surfaces, indicating that no circumferential bending strains existed there.

A selected few strain readings were taken and plotted in Fig.9-10 against load, to show the initial plastic behaviour. The curves are numbered according to the channel number of the gauges at the recorder. These numbers are also shown in Fig.9-8 and 9-9. No.2 is the gauge giving the highest strain reading. This gauge recorded a deviation from a linear relation with load at about 5500 lbs. This is a foil gauge. No.7, a wire gauge next to it, has the next highest strain reading. Its curve deviates from a straight line at a slightly higher load, and this is as expected. This

* In these figures, and all other figures giving experimental results of the nozzles, the strains are given the same sign as the load, and thus compressive strains are shown positive.

similarity of their behaviours confirms that this non-linearity is a true indication of the yielding of the shell, and not due to any misbehaviour of the gauge readings. Gauges No.28 and 6 give the peak meridional strains at the corner radius and the peak circumferential strain at the fillet radius respectively. They happen to have the same elastic reading and their curves remain straight until about 7500 lbs although their subsequent plastic readings are different. Gauges No.40 and 48 are plotted to represent the behaviour of the part of the shell away from the nozzle junction. No.48 at the nozzle wall, gives a very straight plot, while the curve of No.40 at the shell wall is nearly so. It is interesting to note the behaviour of gauge No.19 which lies on the nozzle side quite near to the region of high plastic straining; the strain there actually decreased after a load of about 6500 lbs.

The complete collapse behaviour of the Thin Cap is represented in Fig.9-11 using the few representative strain readings and the axial deflection of the nozzle junction indicated by the curve δ . The bend in the No.2 curve is quite sharp at first yeild, but subsequently settles to a near-straight line at about 1/12th of the elastic slope. The axial-deflection curve does not deviate much from a straight line, and at 13,000 lb load has a value of 36.5 thousandth inch, which is only about 40 percent more than the extrapolated elastic value.

After recording the set of readings obtained at 13,000 lb load, the next two sets of readings at 14,000 lbs and 14,120 lbs were unfortunately lost, in the sense that they

are unusable. This explains the trucation of the curves before reaching the maximum load of 14,120 lbs. It was found after the test that the last two sets of strain readings were shifted by large but varying amounts, even the readings of the constant-strain channel.* The unfortunate outcome of this is that the strain variations at final collapse of the shell cannot now be seen.

The Thick Cap

The Thick Cap was next tested. As mentioned in Section 9-4, the gauges of the Thin Cap were used as dummies. A few gauges of the latter had been broken under the excessive straining they had suffered. They were replaced by ordinary resistors with the same resistance of 120 ohms; because of this there was for these channels no temperature-compensation property inherent in the circuit. As a precaution, a longer warming-up time was allowed for the whole electrical circuit, so that the circuit, especially the gauges and resistors, could stabilize to a constant temperature under the balancing influence of I^2R heating and of natural cooling. Very little additional precaution could be taken against a change of the surrounding air temperature, but the laboratory in which the tests were conducted has no windows and very little natural draught.

* The reason for this very probably lie with the strain recorder, and may be connected with the necking failure of foil gauges 1 and 2 observed after the test. Such failure caused an open-circuit to the active bridge arm and resulted in a large reading equal to the bridge excitation-voltage. On the strain recorder, any such extraordinarily large readings on a data channel usually causes confusion to the readings of the following channels.

Load was increased in steps of 500 lbs with the same holding time of about one minute. After about 8000 lb loading, the gauges No.1 and 2 with the highest readings began to behave non-linearly with the load. After 24,000 lbs, readings were taken at every 1000 lb interval. Here the maximum strain reading,gauge No.2,increased nearly linearly with load, but at a smaller slope of about one fifth of the elastic slope. After 30,000 lbs this strain increased even faster with load. Loading was stopped at 34,000 lbs when the peak strain exceeded 4 per cent.

The different strain readings were plotted against load, and similarly the gradients of the initial linear part of the curves were used to get the elastic strain values. Figs.9-12 and 9-13 show their distribution. Gauges 1 and 2 are the 2mm foil gauges. The general pattern is similar to that of the Thin Cap, with the highest strain at the fillet radius and in the meridional direction. This peak strain is,as expected,lower than that of the Thin Cap owing to theextra thickness and the larger curvature radius of the Thick Cap.

The initial plastic behaviour of the shell is given in Fig. 9-14,and again the behaviour is similar to that of the Thin Cap. This shell also showed a decrease in strain at the region next to the peak strain region at the fillet radius. This is seen in the behaviour of gauge No.9. The complete behaviour of the shell up to the maximum load is given in Fig.9-15. No.2 gauge is the maximum for the whole shell. No.42 is the other peak strain at the corner radius in the meridional direction. No.18 is the circumferential strain at the fillet radius. No.48 represents the behaviour of the nozzle away,from the

junction region, and this remained linear as expected. The positions of these gauges can also be seen in Figs. 9-12 and 9-13.

After 30,000 lbs, both the No.18 and No.42 lines curve down sharply showing a non-linear response of the whole junction in addition to the very local region around No.2 gauge. This is a clear sign that the shell was beginning to collapse, and is confirmed by the similar behaviour of the axial deflection curve labelled δ .

Fig.9-15 shows also the behaviour of gauges No.2 and 42 during unloading of the shell. The first part of the unloading curve is,as expected, linear and has a very similar slope to the elastic part of the loading curve. After unloading through half the load range, the behaviour however became slightly non-linear with the strain relaxing at a faster rate than the first part of the curve.

Cycling

A few more reloading cycles were applied to both shells. It was observed in both shells that the previous maximum load could not be attained again. The probable reason for this comes from the geometrical change suffered by the spherical shell, which under compressive loadings always results in a weaker shape than before. The change in geometry of the Thin Cap was especially pronounced with the top (or centre) part of the cap becoming noticeably flattened.

No visible cracks appeared at or around the two nozzle junctions during and after the loading.

10. THEORETICAL SOLUTIONS TO COMPARE AXIAL TEST RESULTS

10.1 Approximations to the Nozzle Junction Configuration

Theoretical methods of stress analysis at nozzles in pressure vessels have, in the past, used the approximation of unreinforced circular openings in flat plates (10-1) and, later on, of circular openings in hemispherical shells (10-2). Various loadings are applied to the edge of the openings to simulate the different kinds of loadings,usually pressure or external loads on the nozzles. Small-diametered or thick-walled nozzles can be treated as solid cylinders for analysing the stresses from external loadings(10-3),(10-4).

Large diameter and/or thin-walled nozzle can only be accurately approximated by considering the nozzle also to be a shell. Leckie and Penny (10-5) have analysed the problem as the intersection of a cylindrical shell and a spherical shell with its appropriate hole. The thin-walled shell theory was solved with the aid of the digital computer, and the equilibrium of forces and the compatibility of displacements and rotations at the shell intersection were allowed for. The results obtained clearly showed the influence of the strength of the nozzle on the stress concentration on the vessel. The present computer program PVA1 and PLINTH can conveniently analyse such shell intersection problems, since it was designed as a general purpose shell program treating the shell structure as a combination of a number of shell elements of varying shapes.

A certain amount of experimental results have been published giving the stresses and/or strains of pressure

vessel nozzles (10-6),(10-8). The author has made rough comparisons using the above shell-intersection analyses to check their accuracy and for any errors in the above programs. In general the stress and strain distributions have been satisfactory on both the nozzle and the spherical vessel. There are however discrepancies on the local peak stresses at the nozzle junction. These stresses are local and secondary in nature, and in normal cases accuracy cannot be expected from both the experimental analysis and the thin-walled shell theoretical analysis. Unfortunately, in this case of pressure vessel nozzles, the accuracy of these local stresses are most important since the stress concentration factors for the nozzle components are calculated from them.

Further comparisons were made with other published experimental results that included stresses at the local junction region. Most of the theoretical results were found to give a high stress concentration, although a few were satisfactory. To quote two specific examples, the two shells tested here were theoretically analysed using the mentioned shell-intersection procedure and the results plotted as curves No.III, labelled as "Simple" in Figs.9-8 and 9-9, and Fig.9-12 and 9-13. The circumferential strains give reasonable agreement. The higher strains are meridional ones, and here it is noticed that, whereas the distributions in general are satisfactory, the peak values are very much higher than the strain gauge results. A fuller discussion of this is given in Section 10.3, in connection with the comparison of all the theoretical results.

One possible explanation of this high prediction is the phenomenon of discontinuity stresses at changes in shell thicknesses. At any sudden change of thickness in a shell, local stress concentrations are often found which decay rapidly away from the discontinuity. The magnitude of these concentrations depend on how abrupt and how much the thickness is altered. The less sudden the change, the smaller is the local concentration. In our theoretical model, the two intersecting shells have in general different thicknesses, and a sudden change is assumed. In actual nozzles, the rate of transition depends on the junction detail and its fabrication arrangements.

It is believed that the ultimate theoretical tool for analysing the many possible shapes and sizes of the junction configuration, especially the many possible arrangements for local reinforcements, is the numerical method of finite-elements (10-9) . However this method, at present, is not well developed for analysing thin shells of revolution of varying shapes and thicknesses. The author thus decided instead to apply the existing thin-walled shell, computer program to this nozzle problem in the best possible way.

The present program can, as mentioned, calculate with shell elements of the shape of a toroidal surface. Such an element with a very tight radius is positioned in between the cylindrical shell representing the nozzle and the spherical shell representing the vessel. The complete shell thus consists of three elements instead of two. The torus is given a uniform taper of the

correct amount so that the thicknesses at its two ends agree with that of the nozzle and of the vessel. Under this method of representation, there is no abrupt change of thickness nor change of direction of shell wall in passing from the vessel to the nozzle.

One parameter of this torus element can be varied at will. This is its meridional radius of curvature r_m, which is defined in the program as that of its mid-surface. In the procedure adopted here, a value for r_m is chosen such that the smallest radius of curvature of the element's concave surface (corresponding to the fillet surface) agrees with the actual fillet radius, see Fig.10-1. A smaller curvature would be left at the convex surface corresponding to the corner. This procedure is adopted in all the following calculations and is called the Smooth Representation of the nozzle.*

At the subsequent comparison, improvements are noticed in the theoretical results of all the nozzles compared. The Simple Representation gives very bad prediction for the few nozzles where the nozzle thickness near the junction is very different from that of the vessel. At such nozzles the improvement is especially noticeable. More details of these comparisons with published photo-elastic results are given in Appendix B, where the difference in accuracy between the Simple Representation and the Smooth Representation can be seen,

* There is also an alternative procedure whereby the volume of material at the junction is kept the same as that of the actual junction; but here a lot of trial and error adjustments are necessary in the process of approximation, and is not used here.

10.2 Modification to the Computer Program

The torus element used in the Smooth Representation has, in most cases, a small radius comparable in magnitude to its thickness, and falls outside the range within which the thin-shell theory can be accurately applied. It is highly probable that further improvements in the theoretical results can be obtained if some kind of thick-walled-shell modification is made.

Various thick-shell theories or methods have been proposed in the past, mostly based on the thin-walled shell theory. Either fundamental alterations were made to the equations, or the results were modified according to empirical relations or from physical intuition. The former method should be more reliable if the theory is well based, but here there is at present no clear consensus of opinion on what equations are the best ones to be used.

One of these theories has been written into a pressure vessel program for axisymmetrical shells. This is due to the work of Friedrich at the Bettis Atomic Power Laboratory, Pittsburgh (10-10). Thick curved shell elements are linked up and solved by a finite-element procedure. Among the problems analysed to check the program was a reinforced nozzle with rounded fillet and corner, on which carefully executed photoelastic analysis had been made. Five such curved elements of changing thicknesses were used in the calculation to fit the junction shape. The results gave very good agreement. The highest and the second highest peak streeses gave differences of -6.9% and 1.7% respectively, and these differences are of similar order of magnitude to the

possible errors in the photoelastic analyses.

The author has applied the present thin-shell program PVA1 to this problem using a single torus element in the Smooth Representation. This gave differences of 7.3% and 21% to the same mentioned peak stresses, which is a reasonable result. It is thus seen that if a thick-shell modification is made to this program, the results should be further improved and could be used for reasonable prediction of nozzle stresses.

Thin shell or thin beam theories assume that the stresses are distributed linearly across the thickness. This is however not true for thick and curved shells or beams. In the case of pure bending, the stresses at the concave side are higher and that at the convex side are lower than predicted from thin shell or thin beam theories. This non-linear distribution can be observed in photo-elastic tests by taking slices at different layers across the thickness, and this has actually been observed and reported in connection with photoelastic tests of nozzles. A complete elasticity solution of the problems should also predict this phenomenon.

A quite accurate solution to the thick-curved-beam problem can be obtained by relaxing the requirement that the strains and stresses vary linearly, but keeping the assumption that plane sections across the beam thickness remain plane after bending.* The procedure for this method is

---

* See for example Chapter 16 of "Advanced Mechanics of Materials" by Hugh Ford, Longmans,Green & Co.,Ltd.1963.

usually attributed to E.Winkler. A beam, originally of curvature radius b_o at the middle axis and being bent to a new radius b, would have a bending strain distribution at the fibre distant z from the middle axis, of

$$e = \frac{b_o \; z}{b_o - z} \left(\frac{1}{b_o} - \frac{1}{b} \right)$$

If $z/b_o \to 0$, the strain would vary linearly with z, i.e. linearly across the thickness. In the simple beam theory this is assumed from the start of the derivation, and thus giving

$$e = \left(\frac{1}{b_o} - \frac{1}{b} \right) z$$

Assuming no stress in the lateral direction, the stress in the same longitudinal direction is thus

$$\sigma = E \; e = E \left(\frac{1}{b_o} - \frac{1}{b} \right) z$$

Shell elements have, in general, curvatures in two principal directions. A similar modification as the above could be made to thick-curved-shell elements. Plane sections of the elements normal to the two principal directions are assumed to remain plane under loading. Again no linearity is assummed for the stresses and strains. Tangential displacements of the fibre along the principal directions would vary linearly with the perpendicular distance z from the shell mid-surface. Rotations of this fibre perpendicular to the sectional planes would thus be constant across the thickness. In deriving strain values from such displacements and rotations, the thickness and z can not now be assumed small compared with the two radii of curvature b_1 and b_2 .

A modification of this nature has been made to the elastic-plastic version PLINTH of the thin-walled shell program. Details of the modifications involved in the equations are given in Appendix C. The program integrates four first-order differential equations along the generator of the shell of revolution to obtain the solution. These equations are obtained directly and without many changes from the equilibrium equations. The other stress-strain relations and strain-displacement relations are also used in the program without many changes to obtain the different working parameters, or to calculate one parameter from the others. The modification here involves, at the basic level, the alteration of the strain-displacement relations to included terms that contain the ratio y/R. At junction of nozzles, only the meridional curvature is severe; the circumferential curvature has the same order of magnitude as the thickness, as in other thin shell problems. Thus bearing in mind only nozzle problems, only the terms z/b_1 (b_1 being the meridional radius of curvature) is added. Any other expressions and equations that require the use of the above strain-displacement relations would also be appropriately modified, and because of this, many additional coefficients and terms in the program that were previously zero have to be specifically defined.

The modified program is called the C program, C standing for the Curved-element. No fundamental change is required, but additional terms have been added to many equation and expressions used in the original program. To check the program, three problems were used. Two of the problems contain no toroidal or spherical elements and the results were checked against that using the unmodified program

PLINTH. The third problem has a thick toroidal element with meridional curvature radius very small compared with the circumferential radius. The result for this can be compared with a Winkler Solution for a thick curved cylindrical element. Details of the comparison are given in the Appendix D . For the first two problems, the elastic and the elastic-plastic solutions agree exactly confirming the basic accuracy of the C program after modification. For the third problem, the results of the modified program are very close(to the second figure) although not in exact agreement with the analytical Winkler Solution for cylindrical ring. The results for this problem using the original program are however out by a large amount, indicating the vast improvement with the C program.

10.3 Comparison of Results

Accurate measurements of the dimensions of the two shells are required to give correct geometrical data in the computer program. The thicknesses of the cap and the nozzle shells were measured with hand micrometers before the shells were welded together, and uniform thickness was assumed in the calculation at each of the shell walls. The curvatures of the spherical caps were measured with drawing-office radius templates. The Thick Cap was found to have fairly constant meridional curvatures from the top to the base, and a single spherical shell element was used for the cap in the calculation. The centre portion of the Thin Cap was found to have a smaller meridional radius than the rest of the cap, and to be flatter there than a true spherical shape. As these shells are usually formed by hot-pressing over spherical dies, it is

probable that the centre portion had suffered some deformation prior to its use in this experiment. The data in the calculation for this shell were thus adjusted to be according to its actual shape. This results in a toroidal shell element with a near-spherical shape being used near the centre, and this element is joined at its outer edge to a spherical shell element of a larger radius of curvature. The fillet and corner radii of the two nozzle junctions were accurately measured with workshop radius gauge, and these values were used to calculate the mid-wall radii of curvature of the toroidal shell elements needed in the Smooth Representation.

Using the terminology used to describe the data for the computer program as described in Ch.6 and more fully in the program's manual 10-11, the nozzle shell was taken in the calculation as one branch of the complete shell, and the cap shell as the other. Boundary conditions in the form of displacements or forces were required at the end of each branch. A membrane state of stress was taken at the end of the nozzle branch, with

$$\emptyset = 0$$

and $$\emptyset' = \frac{d\ \emptyset}{d\ l} = 0$$

This signifies that no rotation exists at the edge of the shell nor change of rotation with respect to the shell meridian. The length of this nozzle branch was taken sufficiently long to ensure that the resulting stresses and strains would actually die away asymptotically to this membrane condition. The cap branch was given its actual meridional length, and terminated with a fixed-end condition of

$$u = 0 ,$$

$$\phi = 0$$

u being the radial displacement. The base ring and the weld between it and the shell were considered sufficiently rigid.

10.3.1 Elastic Results

The elastic behaviour of the shells was first compared before comparisons were made to their plastic behaviour. Altogether three methods of representing the junctions were tried with this pressure vessel program. The predicted strain distributions were plotted on the same figures as the experimental strain gauge results, these being on Fig.9-8,9-9,9-12 and 9-13.

Around the Junction Region

The Simple Representation of the nozzle junction is where the normal shell-theory procedure for shell intersections is used. Its results are show as the set of curves labelled No.III. In both shells the circumferential strains give good agreement with experiment whether at the junction or away from it. A very high meridional strain value is however predicted at the nozzle side of the junction, the discrepancy being very large for the Thin Cap.

Due to Marcal (8-13), the program has also an additional facility to overcome, for this nozzle problem, this high predicted strain from a Simple Representation. This procedure, also referred to in Section 8-1, assumes in the calculation that the force transmitted between the intersecting shells is spread over a circumferential band of finite width, rather than over the mid-shell-

wall line. The resulting strain distribution using this facility, called here the 'Band Representation', is plotted as curves No.IV in the same figures. A reduction is found in the value of the high meridional strain at the nozzle. The peak strain value for the Thick Cap is now lower than the experimental value , but that for the Thin Cap is still very high.

In the Smooth Representation both the results using the original version of the pressure vessel program PLINTH, and that using the modified C program are presented. They are plotted as the curves II and curves I respectively; in many areas the two curves coincide. The circumferential strains shown in Figs.9-9 and 9-13 again show good agreement with experiment, and actually improve on the slight over-prediction of the other representations at the shell-end of the junction. The meridional strains at the external surface of the Thin Cap, in Fig.9-8, show very good agreement even at the peak strain region at the fillet, this being the maximum strain for the whole shell. The C Program gives better agreement for this peak strain value. On the internal surface, the two programs give the same result and reduce the previous predicted peak strain value by nearly a half and a third. This predicted peak strain is none the less still 2.4 times the highest strain gauge reading at that vicinity, that of gauge No.28. This difference can partly be accounted for by the probable chance that this gauge might not necessarily lie at the narrow peak strain region, since the gauges there were not as close together as those at the fillet region of the external surface. It is also probable that the theoretical

approximation or the geometrical representation is not sufficiently refined, or thirdly that the gauge No.28 might be at fault. Fig.9-12 shows the meridional strain distribution for the Thick Cap. Here the prediction of the highest junction strain, also at the external fillet, is not as good as that for the Thin Cap. This strain value is 21% lower for the C Program and 32% lower for PLINTH. On the other hand agreement is very good for the internal surface strain values including the peak one.

Away from the Junction Region

We now turn to a comparison of the strain distributions at the other parts of the shells not at the junction regions. The strains are thus not local strains. The geometry of the Caps are such that the stresses are expected to fall, as we move away from the junction, to the membrane states of stress of a cylinder or of a sphere. Thus the parts of the shells near the junctions are still regions of interest. The stresses there would not be influenced by the detail shape of the fillet or corner, but are stresses caused by discontinuity of the shell junction.*

At the nozzle the calculated strains are found in general to lie quite close to the measured ones. The strains vary rapidly along the shell because the shell wall there is thin, but all the calculated strains follow this variation quite well. The single exception to this is

* Although stress is mentioned here, the same also applies to strain which is what was measured and what has been compared.

in the Simple Representation calculation on the Thick Cap, where the bending strain component seems to be less than that of the others. At the spherical shell, the strain vary less rapidly. The agreement here in general is reasonable but not as good as that at the nozzle. On the Thin Cap, the Smooth Representation calculation gives very close predictions. The Simple and the Band Representation calculations on the same shell give curves that are parallel to but slightly displaced from the measured ones. At the cap shell of the Thick Cap the comparison is similar in most respects.

The better strain predictions at the nozzle shell than at the cap shell is very probably because the nozzle is machined and thus has a true circular cylindrical shape and a uniform thickness at all points. If this is the case, this shows the sensitivity of the strains to the variation in the shell geometries. The slight superiority of the Smooth Representation results, even away from the junction region, deserves some comments as well. This shows that, even disregarding the local stresses, the stresses obtained by the normal shell-intersection procedure, i.e., the Simple Represenation, can be improved upon by a better representation of the actual junction. The probable reason is that the Simple Representation does not give the correct stiffness to the junction region. The Smooth Representation, because it approximates closer to the actual shape of the junction, give a better prediction of not only the local stresses, but also the elastic stiffness of the region.

Equivalent Stress

A comparison is also made of the equivalent stress intensity which governs the yielding of the shell material. The same von Mises Criterion as uaed in the calculations is used,

$$\bar{\sigma} = \left(\sigma_1^2 - \sigma_1\sigma_2 + \sigma_2^2\right)^{\frac{1}{2}}$$

where σ_1 and σ_2 are the principal stresses on the shell surfaces. The third through-thickness stress σ_3 is zero under the assumptions of the thin shell theory. The stress distributions on the two Caps are plotted in the same way as previously, and shown in Figs.10-2 and 10-3. To compare this, the calculated equivalent stress from the C Program is also plotted. The location of the maximum stress should be where the shell first starts to yield. This is found to be the same in both shells, at the nozzle end of the external fillet radius. It can be seen that the predicted peak stress of the Thin Cap agrees quite closely with the measured one, but that at the Thick Cap is 17% too low.

A plot of the equivalent stress is useful not only because the engineer is more accustomed to thinking in terms of stresses, but also because it can show where the first yielding of the shell occurs, and thirdly because it combines the results of two curves into one making the comparison of results an easier task.

Deflection

Next to be studied is the shell deflection. The computer program can also give solutions for the axial and radial deflections at every interval-points of each shell branch. This information has been asked for in each of the above

calculations, in order that a comparison can be made with the measured vertical,i.e.axial,deflection of the nozzle junction. The two dial gauges used to measure the latter were fixed on to the loading table. They were located at diametrically opposite positions of the nozzle, and were found to give nearly the same readings on each of the two series of loadings of each Cap, signifying the absence of any tilting deflections of the nozzles. The delfection readings were plotted against load, and the slope of the straight portion of each graph is measured to give the elastic deflection of the nozzle junctions. The measured and calculated deflections are listed in the table below; in thousandth inch per 1000 lb load.

	Thick Cap	Thin Cap
Measured	1.7	2.0
Calculated		
Smooth,C Program	0.8	2.5
Simple	1.1	3.0
Band	1.1	3.2

The results of the different calculations are consistent among themselves, in the sense that the Smooth Representation gives the stiffest junction,while the calculations with the Simple and Band Representations give a slightly less stiff junction. There are differences of 36% and of 26% in deflection between the stiffest and the weakest junction.

The measured and calculated deflections,show,in both shells,a great discrepancy. The geometries of the caps were however a bad one for getting a good deflection prediction. The deflection was found to be very sensitive

to the amount of restraint at the base of the cap shell, as well as to the latter's height and curvature. This was observed from a further number of calculations where these factors were changed. For example, rather than having a fixed-end condition at the base of the cap shell giving it a high degree of rigidity, the end condition can be assumed to be a freely supported one with zero meridional bending moment and zero meridional force at the edge, i.e. $M_\theta = 0$, and $F = 0$. Here the support offers no restraint to the cap shell. The actual support must therefore be at a condition in between these two. The free-end condition increases the calculated deflection to 1.51 thousandth inch for the Thick Cap, and 2.86 thousandth inch for the Thin Cap.*

A further numerical experiment has also been tried changing the shape of the Thin Cap. Based on measurements, the shape of the cap shell has been assumed in the calculations to have a spherical radius of 16.1 inches with the top part assumed to be flattened to a torus of radius 12.1 inches. The exact height of the shell has unfortunately not been measured before the test and there is thus no way of confirming whether this assumed shape is exact or not. If instead of the above shape, the extreme shape of a single spherical shell of 12.1 inches radius is assumed in the calculation, the axial deflection is found to be drastically reduced to a value of 0.78 thousandth inch instead of 2.51 thousandth inch.

---

* This change of support gives only a slight alteration to the strain distribution at and around the junction region, and the conclusions drawn above from the comparison of strains would not be affected.

10.3.2 Elastic-Plastic and Collapse Results

The Thin Cap

For the purpose of comparing the elastic-plastic behaviour, only the results of the C program calculations are used. Fig.9-11 gives the variation against load of the meridional and calculated peak strain values and the deflection values for the Thin Cap. The highest experimental strain is that of gauge No.2, which starts to deviate from a linear relation with load at 5000 lb, and this deviation starts to become noticeable at 6000 lb. The corresponding curve for the calculation is labelled EM on the same figure, and this has a first-yield load of 4550 lb. Their elastic-values are similar, and it is seen that their elastic-plastic behaviour compares very well, with the calculated value being slightly lower. The peak meridional strain at the internal corner has a calculated value of nearly twice the experimental value. The corresponding calculated elastic-plastic curve, labelled IM, is much more non-linear than the curve of the strain gauge No.28, the former bending down noticeably after 7000 lb while the latter only becoming so after 11,000 lb. The calculated circumferential strain has the same elastic peak value both on the internal and on the external surfaces and has also the same elastic-plastic behaviour on these two surfaces. They are shown together as the curve labelled C. The corresponding experimental curve is that of gauge No.6. Here the elastic calculated and measured value are nearly the same and their elastic-plastic behaviours are also found to be similar. The calculation gives an elastic axial deflection about 25% higher than

the experiment, and if this difference is taken into account their elastic-plastic behaviours are found to be similar.

The Thin Cap collapsed during test at a loading of 14,120 lbs. Since, during the test, no readings could be obtained near this collapse load, their values cannot be plotted on the graph, but it is known that all the peak strains near the junction and the axial deflection did increased very rapidly with load. No similar collapse behaviour could however be seen in the calculation, which was carried on until a load of 18,200 lb and stopped when the computing has taken a full 45 minutes on the IBM 7090 computer.

The Thick Cap.

The Thick Cap, as expected, proved to be stronger than the Thin Cap. Fig.9-15 shows that the first sign of non-linearity during test was at 8000 lbs; this occurred at strain gauge No.2 which gave the highest reading. The calculation predicted a first yield at 8710 lbs, which is higher, although it should be pointed out that the calculation predicted a smaller elastic peak strain. Presumably because of the difference of elastic strain values, the corresponding elastic-plastic strain values, shown as the curves labelled No.2 and EM, differ more and more as the loading is increased. The peak meridional strains at the internal surface have nearly the same elastic values from the experiment and from the calculation. Their elastic-plastic behaviour, shown by the curves labelled No.42 and IM, are similar in shape, ignoring for the moment

the region above 30,000 lbs. The calculated elastic-plastic strain has a slightly higher value, by about 25% at a load of 18,000 lbs. The circumferential peak strain curves are labelled C and No.18, and here both the elastic and plastic values coincide until the beginning of collapse. The deflections are difficult to compare; the elastic values differ by a large amount and become more so at larger loads.

On this test of the Thick Cap, readings have been obtained all the way until the maximum load of 34,200 lbs. The curves from these readings clearly show a large increase as the load approaches this maximum. Again no such collapse behaviour can be seen in the calculation which is carried on until 40,000 lbs.

Discussions on Collapse

Collapse of shells of the type where circumferential plastic hinges are formed have been predicted in the past using this elastic-plastic shell program, and, although more comparisons are still needed, the prediction of this collapse value has been reasonable successful. The failure here in this respect for both shells, tempts one to believe that there may be other influencing factors that do not exist elsewhere.

It is noticed that the loading used here was a compressive one which tended to inwardly deform the spherical load-supporting shell. The stiffness of such a flatter deformed shell gets less, and so does its load holding resistance. Internal pressure loading, on the other hand would push the shell around the nozzle outwards. During the test on the Thin Cap, there was an axial

deflection of 85 thousandth inch, about 3/32 inch, before the deformation started to get increasingly non-linear and finally collapsed, in the sense that no load increase could be withstood. The corresponding deflection for the Thick Cap was about 60 thousandth inch, about 1/16th inch. These deformations were sufficient to decrease the radii of curvature of the shells near the nozzle junctions, to decrease the shells' resistance against such loading, and to contribute to an earlier collapse than would be expected from an ideal rigid shell that would not change its shape according to load.

It is possible to test directly this drop in load-holding capacity of the shell. For this purpose the Thin Cap was loaded a second time. This shell had already suffered a permanent axial-deflection of 62 thousandth inch after the first loading with a 14,120 lb maximum. The reloading was, as expected, reasonably linear until about 12,500 lbs when the deformation became increasingly non-linear. A maximum load of only 13,000 lbs was attained; this is a drop of 8 per cent. In a third loading, the straining rate of the loading machine cross-head was kept constant, thus giving a constant cross-head velocity. A continuous record of the load and the deflection was kept. Straining and recording was maintained even after the maximum load was reached. The variation of load against time, and of deflection against time, are shown in Fig.10-4. The deflection-time curve is nearly linear, as expected. A maximum load 12,900 lbs was attained at a deflection of about 40 thousandth inch, after which the load dropped. At 80 thousandth inch, the load was about 12,000 lbs; and at 160

thousandth inch, 11,000 lbs.

10.4 Conclusions

These tests were performed in order that the elastic-plastic pressure vessel program might be compared and checked. They also have the role of helping to develop and try out testing techniques in preparation for a further more detailed pressure test of a specially built model vessel described later in Ch.11 and 12. The tests are found to be successful on the latter purpose, but the conclusion is mixed as to the first.

The post-yield strain gauges and the miniature foil gauge both stood up well to the purposes for which they were being used. In common with other small strain gauges, a certain amount of skill is necessary for their satisfactory operation and the casualty rate dropped rapidly with increasing experience. The use of the fast-action cyanoacrylate cement, and of the automatic strain-gauge recorder, enables many more gauges to be used than would otherwise be possible for the same man-hours. This made it possible to have more detailed survey of the strain distribution and a clearer picture of the local stress variation through the nozzle junction region.

Accurate measurement of the material's stress-strain curve was important, as the calculation could only be as accurate as the material properties with which the program was supplied. Elastic-plastic calculations are especially sensitive to the value of the yield stress. Tensile tests on small specimens were found to be the only method suitable for thin-walled materials, and

they seemed to give satisfactory results.

It was known that the normal shell-intersection procedure would not give accurate local stress results at the shell joints. The Band Representation procedure mentioned in Marcal and Turner(8-13) was expected and was found to improve on the calculated local strain or stress at the nozzle junction. The suggested Smooth Representation, gave even better improvement for the two nozzles tested, both of them have had the corners and the fillets ground smooth. When these methods of representation were compared with each other, there emerged the important finding that the different methods allotted different contributions of the local region to the overall shell stiffness. This was noticed by the fact that they gave different calculated strains away from the junction region, and gave different shell deflections. The best local representation was found to give the better prediction for the general strain values.

The Smooth Representation still cannot predict reliably the value of the highest strain, although this strain is very local in nature. In a modification to the program PLINTH, the assumption of a linear stress variation across the shell thickness at sharp curvature regions was removed. This gave improvement to the predicted value of the highest strain, but still did not seem to provide the full answer. Whether this double improvement is considered sufficient will depend ultimately on the requirements of the designer, since it is this that governs how important is the absolute value of this very local stress.

The accuracy of the elastic-plastic strain prediction was found to depend on that of the elastic strain prediction. It is encouraging to note that in most of the cases where the elastic peak strains agree between calculation and measurement, the elastic-plastic strains also agree or have very similar behaviour. This result will increase the confidence in any futher use of such an elastic-plastic strain calculation.

The calculations failed to predict two things, the collapse behaviour and the deflection value of the shell. It is likely that the unsuitable arrangement of the loading can account for the former and the proximity of the base of the cap shell can account for the latter. Whether they can account for the whole discrepancy cannot of course be known until further tests giving affirmative conclusions are available.

11. PRESSURE TEST OF VESSEL: PREPARATION

11.1 Introduction

Elastic analysis of torispherical pressure-vessel heads is in general possible and is increasingly becoming familiar to designers. The reason for this is the advance in the development and solution of thin-walled shell theories, and the introduction of the digital computer. These vessel heads have also been successfully analysed with the method of limit analysis making it possible to find the plastic collapse pressure, assuming the heads fail under severe plastic bending. Elastic-plastic analysis can, however, give an understanding of how the heads behave in the intermediate stages. It can also serve other useful purposes.

It, can, for example, provide a complete picture of the stresses and deflections, which the limit analysis cannot. The numerical method can also be programmed on the computer to accept work-hardening stress-strain properties not possible with limit analysis; this is important for materials like stainless steel and aluminium. The usefulness of this analysis actually extends beyong the design against vessel failures under steady loading, for example, during hydrostatic test. The important future application of this analysis lies in the design against repeated loading that has very often been ignored in the past.

A torispherical head has a shape that is easier to be accurately stress analysed by a shell analysis program, than a vessel with a cylindrical nozzle. This is because the former does not have local geometrical details that

are at the same time stress raisers. The stress concentrations that exist on a head are due to overall change in shape from one part of the head to another. Good accuracy has already been shown possible for the elastic stress analysis of such heads by computer programs using thin-walled shell theory, the analysis and the expected accuracy must of course be within the limitations of the theory and the numerical process. The torispherical head is thus a better shell component to be used for checking the accuracy of an elastic-plastic analysis. There should, in this case, be less uncertainty about the cause of any inaccuracy, than in the case of symmetrical nozzles.

To get an elastic-plastic calculation, a knowledge of the material's stress-strain curve beyong yield is required. Mild steel, the commonpressure vessel material which was also used in the nozzle tests in Ch.9 and 10, has during a tensile test, unfortunately, an unstable region after the first yielding. This behaviour cannot be approximated in detail in the calculation and has thus been neglected in the nozzle calculation. A material without this instability would be more suitable. For this reason, stainless steel is used in the present vessel test.

11.2 Vessel Design

Torispherical heads can be tested and stress analysed in the laboratory in two arrangements. One can either use a single head which is closed by a thick flange (as used, for example, in Ref. ~~11-1~~ 8-10 and ~~11-2~~ 4-17), or use two heads forming a complete vessel with possibly a side

opening for access (as used in Ref. ~~11-3~~ 5-12). The latter arrangement was used in this test.

A 24 in. diameter stainless steel vessel, Fig.11-1, was built under normal manufacturing standards to a design pressure of 360 lb/in^2 * and according to BS 1500,class 1. Two torispherical dished ends with the same nominal dimensions were used as heads, one of which had a centrally attached unreinforced nozzle 3.642 in. bore and $\frac{1}{8}$ in. thick, for stress analysis purposes. For access to the vessel interior, a 10 in. nominal bore, pad reinforced opening was made at the side. The former test nozzle, Fig.11-2, had the same thickness and junction arrangement as the mild-steel nozzles that were tested. For identification, the dished end without nozzle is called A, and the other dished end called B.

The steel was austentic 18/8 chromium-nickel steel stabilised by the addition of titanium. The plates making up the body and heads, made according to ICI specifications MI53H class 'A' (1958) (18/8/Ti), had the following chemical composition:-

Carbon	0.15% max.
Chromium	17.5% min.
Nickel	7.5% min.
Titanium	C x 4 min. and 1% max.
Silicon	1.2% max.
Manganese	2% max.
Sulphur	0.05% max.
Phosphorus	0.05% max.

---

* All pressure readings in connection with these vessel tests are gauge pressures.

These plates were supplied in the fully annealed condition, being cooled or quenched from a temperature of 950/1150° C,

During vessel fabrication a certain amount of work-hardening was expected because of the forming and welding operations. This change of properties might vary at different parts of the vessel. The mathematical assumption of uniform material property, including the stress-strain curve, would thus be inexact. The vessel was thus given an annealing stress-relief at a temperature of 900° C, this being after an hydraulic test to only the design pressure of 360 lb/in^2.

11.3 Measurements

The stress-strain curves of the vessel steels were also determined by obtaining the instantaneous tensile load-deflection curve on the Instron universal testing machine. The test pieces were machined from three test plates, one being a piece from the same pipe making up the end nozzle, the second being from the same plate making up the vessel body, and the third being from this same plate but which has, in addition, been roll-formed to a cylindrical shape of the same diameter as the vessel. No plane-strain compression tests were made.

The vessel dimensions were measured after being received from the manufacturer. The diameter, of the vessel body was measured with a pair of hand-held calipers for fabrication tolerances. Only the vertical and the horizontal diameters were taken. The average outside diameter was found to be 23.84 in. with the maximum and minimum readings being + 0.75% and - 0.8% respectively

of this value. The maximum difference for any one cross-section was 1.4%. Since according to BS 1500, the maximum out-of-roundness for any one cross-section for a 24 in.vessel must not be greater than 1.0%, it can be seen that the vessel shell was not an accurately fabricated cylinder.

The shell thickness is an important data for the calculation, but it could not be known for sure that the dished ends,after the hot-pressing and edge-rolling operations, would keep to the nominal thickness accurately. For this reason,a survey was taken of the thickness with ultrasonics. An ultrasonic flaw-detector,which could double as a measuring instrument for the thickness of metallic plates,was used. The closed dished end A was found to have an average thickness of 0.322 in.with maximum difrences of + 3.4% and - 2.2%. The other dished end B with the nozzle, had corresponding values of 0.323 in, + 2.5% and - 4.3%. The vessel body had an average thickness of 0.331 in. and better tolerance. The nominal thickness for all three is 5/16 in.(0.313 in.)

The shape of the dished ends governs their stress distributions and it was important that they should be measured accurately. A precision plate camera was used to obtain, at distances between six and eight feet, silhouette photographs of the two ends. The images were enlarged to full sixe. Best fit torispherical shapes were then constructed following these profiles, and used as geometrical data for calculations.

11.4 Strain And Deflection Gauging

Strain Gauging

The same strain gauge technique was used. With a few exceptions, 5mm, post-yield strain gauges of the wire type with epoxy backing were used for the high strain regions, and 5mm, 90° overlapping rosette gauges were used in other regions. Three 10mm gauges were used to measure the circumferential strains around the vessel body.

The junction of the test nozzle had smooth radii left at both the fillet and the corner, and the strain there was also measured by 2mm foil gauges.

The rapid setting adhesive, cyanoacrylate, was used on all gauges.

The gauges inside the vessel did not require careful water-proofing since the pressurising liquid was to be hydraulic oil with sufficiently good insulating properties. Preliminary tests had also shown that, over a reasonable period of time, the gauge and the adhesive were not damaged nor attacked by the oil. Nevertheless, a coating of epoxy resin was applied over these gauges and around the end of the lead wires where they joined the gauges. These lead wires were led through the cover flange of the 10 in. side-opening with the help of two sealing glands, specially made by the Conax Corp.* for such purposes.

The same arrangement for recording the strain readings was used. The Solatron multi-channel automatic strain-recorder was used to scan, display and record the strain

*Conax Corporation, 2300 Walden Ave., Buffalo, New York.

at each gauge. This recorder had, since the nozzle tests, been enlarged to take 100 channels; it was otherwise the same. No special set of gauges was prepared as dummy, but instead the gauges already on one of the mild-steel shells tested above were used for this purpose. Mild steel may have different temperature coefficient of expansion to stainless steel. The readings many thus be prone to slight drifting when the temperature changes. Additional precautions were thus necessary during test, firstly to have a long warm-up period before every test, and secondly to ensure that the room temperature remined constant. The first was kept during the tests and the second was found to be true as mentioned later. Nearly all the strain gauges were positioned on the same vessel meridian, which was on the horizontal plane at right angles to the plane containing the centre of the side opening. Their locations are given in Fig.11-3. Four gauges are not shown in this figure, they are at meridians 90° and 180° away in order to check the symmetry of the arrangement.

Gauges were placed nearer together at three main areas of interest. One of these was the junction of the test nozzle, and the other two were the knuckles of the two dished ends. Otherwise, the dual restrictions of finance and of number of gauge channels, required that an economy of gauges had to be made to obtain the stress picture of the whole vessel. The selection of gauge locations was based on theoretical elastic analysis, presumed correct, and judgement was made such that the important strain peaks would be recorded, and that the strain distributions at the areas of interest would be observed

in detail.

Deflection Gauging

Fig.11-4 shows the twelve displacement dial gauges positioned around the vessel to detect the vessel wall deflection. The easiest way to observe the collapse, if any, of a vessel is through its deformation. These dial gauges were in the same horizontal plane as that of the strain gauges,and were attached to a rigid frame built around the vessel and supported independently of it. Their readings should also serve to check the theoretical deflection results.

Preliminary Tests

After the usual visual and physical inspection of the strain gauges and balancing of all the Wheatstone bridge circuits, the vessel was first subjected to a pneumatic test under low pressure from the shop-air supply. The plan was to check the linearity of the strain-gauge response under elastic straining of the vessel. Unfortunately this was not successful, and because of this, the internal gauges and their bond could not be strain checked prior to their being immersed under oil, after which no replacements would be possible.

The vessel was then filled with oil, bled as far as possible of all air bubbles, and then pressurised. Pressure of less than 160 lb/in^2 was kept throughout these preliminary tests. Both the internal and the external gauges were checked for their linearity of response. Three of the external gauges were found to be unsatisfactory. They were subsequently replaced, checked,and found to be satisfactory. Five of the

sixteen internal gauges were fouhd to be sufficiently non-linear to have to be rejected, and from then on, only the remaining eleven internal gauges were used for measurements.

11.5 Oil Circuit

A common hydraulic oil was used for the test. The oil pressure was measured with pressure gauges of the Bourdon-tube type. Two gauges were used, according to the pressure in use, one with a face 12 inch diameter measuring up to 1000 lb/in^2 gauge in 10 lb/in^2 divisions, the other with a face 6 inch diameter measuring up to 1500 lb/in^2 in 50 lb/in^2 divisions. Both gauges had been dead-weight calibrated before putting in use.

A diagram of the complete oil circuit is shown in Fig. 11-5. The pump consists of two Madan airhydro pumps in series, capable of working to a pressure of 2400 lb/in^2 and of maintaining reasonably constant pressure within the range 60 lb/in^2 to 2400 lb/in^2. Normal shop-air supply could be and was used for working the pumps. A plunger in the pumps acts both as a pressure intensifier and as the pumping piston. Since the air pressure can be regulated and kept constant within fine limits by a regulating value, the oil pressure can be maintained constant for long periods, even with slow leakage from the pressure circuit. No circulating of oil is involved in this process. Rotary pumps, on the other hand, normally circulates the liquid continuously during periods of constant pressure, and may thus raise the liquid temperature, making this a grave disadvantage in the present application where the strain gauge measurements

demand both a long holding time and a constant oil temperature.

The volume of oil required for raising the pressure can be measured on a 6 ft. long measuring tube, 3 inch bore. This actually measured the volume of oil supplied to the pump. However, with all the air inside the pressure part of the oil circuit removed as far as possible, the volume of oil required for elastic deformation of the vessel was found to be sufficiently small so that the elastic-plastic vessel-deformation should be detected easily on the pressure-volume curve. This measuring arrangement can only measure the pumping volume. During unloading of the vessel, the oil was slowly released from the shut-off value at the exit, and no oil measurement of this could be made.

12. PRESSURE TEST OF VESSEL - TEST AND COMPARISON

12.1 Elastic Test

During the initial setting up, calibration,and trial of the strain gauges and circuit, the pressure in the vessel had been kept not higher than 160 lb/in^2 so that no plastic straining of the test regions might occur. Elastic strain values were obtained by taking the vessel to 160 lb/in^2 and back to zero, and recording the strain reading at each 20 lb/in^2. The readings from each individual gauge were plotted against pressure, and the slope of the straight line portion of each plot was interpreted as the elastic strain. 46 gauges were considered satisfactory and used at the subsequent elastic-plastic tests.

Figs.12-1 to 12-4 show the strain distribution with the strain values plotted against the meridional distance along the vessel wall. The highest strain concentration occurred at the nozzle junction where the gradient of the local strain was very high. The highest strain value was at the meridional gauge No.7 at the middle of the external fillet radius. Another strain concentration occurred, as expected, at the knuckle of the torispherical heads. The highest strain here was the meridional one on the inside surface, where the pressure load caused a high tensile strain. Gauges Nos.12,13,14 and Nos.23, 24,25 were grouped each at the same meridional location but were on different circumferential positions from the others in the group. The results showed that there was reasonable symmetry of the vessel.

12.2 Elastic Calculations

The heads were then each analysed elastically using the pressure vessel programs. Young's Modulus was taken as 30×10^6 lb/in^2 and Poisson's ratio 0.3. The shape of the heads were measured from the profiles obtained by photographic technique mentioned in Section 11.3. The nearest torispherical shapes were used in the calculation. Following the procedure used for the axial load tests, the nozzle junction was represented in the calculation by a small toroidal element to fit the actual machined radii. For the same reason that the curvature there was not large compared with the wall thickness, the modified version of PLINTH, Program C, was used, which took into account the non-linear nature of the stress across the shell wall at such regions.

The closed end A of the vessel was analysed with the normal version PLINTH since the problem of small curvature radius did not arise here. The resulting distribution of strain are plotted in the same Figs. 12-1 and 12-2 as the measured strain values. The calculated peak strains are in general higher than the few measured strain values near these locations. The one exception is at the centre of the crown where the two measured strain values, both at the outside surface, are higher.* In general, however, there is reasonable agreement between the results, con-

* There is an inherent fault with the programs thtthey may loose accuracy when the shell closed in on itself, which means that the shell meridians meet at the axis of rotation. This is believed to be because the numerical process used cannot give accurate solution at very small values of r - the radius vector from the shell axis, because the differential equations become singular. Fortunately it was noticed, from experience with the programs, that this loss of accuracy would affect only the results at a narrow region near the shell axis, and the overall results were not affected. In plotting the calculated strains, this narrow region was thus neglected.

sidering that both the location of the strain gauges and the shape of the head cannot be measured with sufficient accuracy.

The vessel head B with the test nozzle was analysed with Program C and shown also on Figs.12-1 to 12-4. There are two regions of stress concentration, the knuckle and the nozzle junction. At and around the knuckle, the picture is a similar one to the other knuckle mentioned above, with the calculated strain values also larger than the measured ones, although the agreement here is relatively better. At and around the nozzle junction, there is good agreement in general, with perhaps one exception, and an important one, which is at the highest measured strain reading at gauge No.7 which measured the meridional strain at the external fillet radius. Here the calculated strain is lower, being only 60 per cent of the measured value. It should now be recollected that at the axial test comparison, the Winkler modification to the program was made in order to improve the correlation of this particular strain value at the external fillet radius, and an improvement was found, although not aufficiently to give a good agreement. It is seen here that again good agreement cannot be obtained in the present pressure test.

Stress concentration factors of the knuckle and the nozzle junction are calculated taking the theoretical membrane stress at the vessel body as unity. The factors are expressed either as ratios of the direct stresses or of the equivalent stresses, the equivalent stresses being based on the von Mises yield criterion. They are listed below,

	Knuckle	Nozzle junction
Direct stress concentration factor		
Measured	1.56	3.80
Calculated	1.72	3.11
Equivalent stress concentration factor		
Measured	2.02	4.15
Calculated	2.26	3.52

The maximum stress at the knuckle was a meridional one at the internal surface near the centre of the knuckle. These factors at the knuckle are based on the results of the closed end of the vessel. At the nozzle junction, the maximum stress was also meridional but near the centre of the external fillet radius.

12.3 Elastic-Plastic Test

To 400 lb/in^2

The first post-elastic loading of the vessel was to a pressure of 400 lb/in^2, which is slightly above the design pressure of 360 lb/in^2. Loading was increased at 50 lb/in^2 intervals, and during each interval, readings were taken in the following order:-

1. Automatic scan of the strain gauge readings.
2. Reading of the 12 dial gauges.
3. Reading of the oil level in the volume tube.
4. Second scan of the strain gauges.

Normally, the time necessary for raising the pressure and taking the readings was 5 to 10 minutes. Temperature readings of the surrounding air was also recorded using a mercury thermometer at every other pressure increment. In general the temperature was found to remain substantially constant during each half-day period of testing, varying by less than one or two degree C.

The pressure was then reduced in steps back to zero, by a gradual release of the oil. No volume measurements were possible during such pressure reduction, although the other readings were still taken. At zero pressure most of the strain and deflection readings returned to zero.

To 870 lb/in^2

The next and subsequent reloading were made without readjusting the dial gauges or rebalancing the strain-gauge bridges. Pressure was raised, again in 50 lb/in^2 increments, to 700 lb/in^2. At this pressure, the highest strain reading, at gauge No.7, was 0.6%. This reading and a number of other high strain readings had already shown a high degree of non-linearity with load. Thereafter, smaller pressure increments were made until loading stopped at 870 lb/in^2.

Throughout this loading, the pressure had always been kept steady or increasing. Only once did the pressure drop, at 800 lb/in^2, when, due to flange leakage at the side opening, the pressure dropped back to 750 lb/in^2 before the leakage was remedied by tightening of the holding bolts. Figs.12-5 and 12-6 show two typical readings, at the nozzle junction, one deflection and one strain reading, plotted against pressure, It can be seen that the load reduction causes little, if any, deviation to the normal trend of the curves.

At 870 lb/in^2 the pressure was then reduced in steps to zero as before. This is followed by reloading to only 870 lb/in^2, with readings being taken all the time at selected intervals. This cycle of unloading and loading

to 870 lb/in^2 was made altogether seven times. The effect of this is also shown on Figs.12-5 and 12-6. The strain and deformation increased progressively by small amounts during each cycle, but the amount of increment decreased steadily, and at the seventh cycle became very small and fell within the accuracy of measurement. Typical values of deflection and maximum strain, after each cycle, at zero pressure, are shown in Table 12-1a.

In each case, the increment between the 6th and 7th cycles was about, or less than, 1 per cent of the actual value. Since the nozzle and the dished-end knuckle had the most severe deformation in the vessel, it is expected that other parts of the vessel suffer less incremental deformation. During each cycle a narrow loop can be observed on the load-strain or load-deflection curves, similar in shape to the hysteresis loop of a stress-strain curve of a metal. The loops did not in general narrow down and disappear when the incremental deformation was gradually reduced to zero. Table 12-1a also shows the loop width of representative strain.

To 1070 lb/in^2

The next increase of maximum pressure was to 1070 lb/in^2. During this increase, slow leaking occurred again at the gasket of the side opening, and was remedied in the same way. The further increase in volume of the vessel can be seen in Fig.12-7 where the volume of oil added to the vessel is plotted against pressure.

Another seven cycles of the pressure were made between zero and this maximum pressure of 1070 lb/in^2. The

Table 12 - 1a. Change in Strain and Deflection Readings at Zero Pressure after Pressure Cycling.
Cycles of 0-870 lb/in^2

Cycle No.	1	2	3	4	5	6	7
Guage 38, head A max. strain (%)	0.214	0.232	0.241	0.248	0.252	0.255	0.257
(hysteresis loop width/range) (%)		8.3	5.9	5.3	NA*	NA	NA
Guage 44, head B max. strain (%)	0.234	0.248	0.257	0.263	0.267	0.268	0.270
Head A deflection (thou.)	46	48	50	51	52	52	53
Head B deflection at opening (thou.)	156	164	168	172	173	174	175

Table 12 - 1b. Cycles of 0-1,070 lb/in^2

Cycle No.	1	2	3	4	5	6	7
Guage 38 (%)	0.648	0.688	0.709	0.724	0.733	0.743	0.752
Guage 44 (%)	0.645	0.677	0.695	0.708	0.714	0.722	0.728
Head A deflection (thou.)	100	107	109	111	111	112	114
Head B deflection at opening (thou.)	350	368	375	382	386	389	394

*Not available

increment of the same strains and deformations can be seen from Table 12-16.

The increments dropped to 1-2 per cent of the actual values.

Final Increase to 1165 lb/in^2

The next and last load increment brought the pressure to 1165 lb/in^2 which is 3.2 times the design pressure of 360 lb/in^2. At this maximum pressure the total axial movement of the test nozzle was more than 1/2 inch relative to mid-vessel, and a region of the nozzle within 1/2 inch of the junction had clearly bulged outwards such that this region was no longer cylindrical but conical in shape. The experiment was thus stopped, since it had not been the intention to fail the vessel but only to observe its elastic-plastic behaviour until collapse.

Final Results

Typical variations of strain and deflection with pressure over the total range, 0 to 1165 lb/in^2, are shown on Figs.12-8 to 12-15. Detailed explanation and discussion of these curves are given later in connection with comparisons with the calculated results.

The experimental readings of two representatives strain gauges No.28 and No.24, are plotted in greater details than the others in Figs.12-8 and 12-16 respectively, one shows the behaviour of the dished-end and the other that of the vessel body. On each graph the three loading curves were drawn separately, and gaps exist where the strain values were increased under load cycling. Both of them show that the unloading and the cycling appear

to make no difference to the overall plastic behaviour of these strain values. This behaviour was found to be the same for the other strain and deflection readings plotted in these and other figures. For this reason, only the envelope to the curves were plotted for all the other readings. Also, in the subsequent discussions, the vessel will be treated as being loaded under a monotonically increasing pressure, with the unloading parts neglected.

These plastic load - strain curves are identified by labelling them with strain gauge numbers which are shown both in Fig.11-3, which gives the physical location of these gauges, and in Figs.12-1 to 12-4, which give the elastic strain distribution. Readings for strain gauges No.7 and 6 came adrift before the end of the test due to peeling off of the gauge backings. In general, each curve, of either strain or deflection reading, shows first a deviation from linearity, followed at higher pressures by an increasing change of slope, which then slows down giving a more or less constant slope. The pressures where these changes occur vary for different gauges, and probably also vary according to the elastic values.

12.4 Elastic-Plastic Calculations

The comparison of these experimental results with the elastic-plastic calculations is one of the main interest of this study. To do these calculations the stress-strain curves of the shell material are required as data. Similar to the procedure used in the calculation of the stainless steel APV vessel, two second-order algebraic

polynomials were approximated to the measured stress-strain curves, one belonging to that of the 5/16 in. steel plate used for the vessel heads and the body, and the other to that of the steel pipe used for the end nozzle. The former curve is shown on Fig.12-16, where the polynomial equation is

$$\bar{\sigma} = 3.34996 \times 10^4 + 1.33691 \times 10^6 \bar{\varepsilon p} - 1.81592 \times 10^7 \bar{\varepsilon p}^{\,2} \text{ lb/in}^2$$

The latter curve is shown on Fig.12-17, where the polynomial equation is,

$$\bar{\sigma} = 3.92603 \times 10^4 + 1.23774 \times 10^6 \bar{\varepsilon p} - 1.63857 \times 10^7 \bar{\varepsilon p}^{\,2} \text{ lb/in}^2$$

These curves are great improvements over the approximation of perfect plasticity. Their proof stresses can be compared below.

		0.2% proof	1% proof
Vessel Steel	Measured	39,170 lb/in^2	47,100 lb/in^2
	Equation	37,000 lb/in^2	45,000 lb/in^2
Nozzel Steel	Measured	45,000 lb/in^2	51,800 lb/in^2
	Equation	41,700 lb/in^2	50,000 lb/in^2

The same Young's Modulus of 30×10^6 lb/in^2, and Poisson's ratio of 0.3, were used as in the elastic calculations.

The calculation of the closed dished-end A predicted a first (local) yield at 464 lb/in^2, occurring at the inner surface of the knuckle near its centre. Thereafter the calculation was repeated at load increments of 100 lb/in^2 and subsequently at 50 lb/in^2 increment. The final calculation was at 964 lb/in^2 when the deformation became very large. The total computing time was 30 minutes on the IBM 7094.

The calculation on the nozzle-end B of the vessel, using

the modified version of the program and the appropriate stress-strain curves for the two parts of the shell, predicted a first yield at 368 lb/in^2 at the external surface on the fillet radius of the nozzle. Thereafter loading was increased at 0.2 of this yield pressure until 809 lb/in^2. This computing also took 30 minutes.

The calculated results were plotted against pressure on the same graphs as the experimental results in Figs. 12-8 to 12-16. Each calculated curve is paired with the measured curve obtained from a strain gauge or a dial gauge, the former curve being the curve of the corresponding values at the location of the gauges.

12.5 Discussion on Strain and Displacement

For the stress concentration area near the knuckles, there is generally good agreement between calculated and measured strain values. Fig.12-8 and 12-9 show the strains around the knuckle of the closed dished-end A. The calculated strains at all gauge locations agree very well at the initial elastic-plastic stage until about 800 lb/in^2, which is 1.7 times the theoretical first yield. This is true even for gauges 38 and 33 where the elastic agreement is not close. After 800 lb/in^2 the theory predicted a higher strain. When expressed as strain difference, this is appreciable; but because of the flatness of most of the curves, the pressure difference for the same strain appears less formidable, say 15 per cent difference at 1 per cent strain for the point of maximum strain (gauge 38). It is difficult to interpret the meaning of this difference because firstly, at such large straining the stiffening of the

actual vessel due to geometry change would become noticable, and secondly, the difference in the elastic values (for all peak strains in Fig.12-8 and 12-9, the theory gives higher values) is magnified increasingly at large plastic strains. Both these effects tend to make the calculation over-estimate the strain values, but the contribution of each cannot be conveniently determined.

The strains at the knuckle of the other dished-end B are shown in Fig.12-10 and 12-11. The elastic agreement is not as good as the above dished-end, and neither is the agreement of the elastic-plastic strain.

The strains at the nozzle junction of this dished-end are given in Fig.12-12 and 12-13. At gauge locations 6,42 and 43, good elastic agreement is found. The corresponding elastic-plastic strains agree closely until about 560 lb/in^2 (1.5 times first yield), after which the predicted strains become larger than that measured.

The strains at lower stress regions of the vessel - the barrel, and the centre of the closed end - did not agree as closely with the predicted values as those already described at the knuckle regions. At the centre of the dished-end A, Fig.12-15, gauges 35 and 36 showed some non-linearity as low as 400 lb/in^2, and by 700 lb/in^2 non-linearity was very well developed, whereas the predicted strains were linear until 950 lb/in^2. A similar discrepancy was shown by the circumferential strain at the barrel (Fig.12-15) where the measured strain showed

non-linearity from 500 lb/in^2 upwards*, while the calculated strain remained linear until a much higher pressure of 950 lb/in^2. These discrepancies can be partly accounted for by the stress-strain approximation which has a 30 per cent higher proportional limit. This difference of proportional limit would not by itself affect noticeably the solution at a bending region of shell, but tend to show up in the above regions which have little bending component of stresses.

The predicted displacements of the heads relative to mid-vessel (Fig.12-14) shows quite good agreement, although they also go non-linear at a higher pressure than that observed.

In order to observe the effect of different stress-strain behaviour, and for another reason connected with collapse load described below, a calculation was repeated for head A but with a non-hardening material. A yield stress of 34,900 lb/in^2 was used, obtained from the experimental curves by the same 'tangent' method to find the collapse load mentioned both below and in Section 8.4 above. This value also happens to be approximately the 0.1 per cent proof-stress. The solution for any other yield stress values should vary proportionately. The resulting behaviour is also plotted in Figs.12-8,12-9 and 12-14 with first yield occurring at 482 lb/in^2. The top parts of the curves are flatter

*This is actually shown on two of the three circumferential strain gauges. The third one remained linear throughout the test because it happened to rest on weld material which presumably has a much higher yield point.

as expected, and the transitions from the elastic lines are slighly sharper.

12.6 Discussion On Collapse Load

The vessel steel has a high degree of strain hardening and it can be seen from the vessel behaviour that collapse cannot be clearly defined. Two different methods were used previously in Section 8.4 to define collapse, the first being the intersection point of the elastic line and a tangent to the strain or deformation curve and the second being the load where a maximum strain of 0.5 per cent occurs at the outside surface of the vessel head or nozzle.

Table 12-2 compares the collapse pressure thus obtained from the two vessel heads and from the end nozzle. The first yield pressure is also cited for reference. The tangent method for collapse gives different values according to the curves used. As far as possible, three curves are used, namely that for the maximum meridional and the maximum circumferential strains, and that for the axial deformation. The limit pressure, also quoted at the bottom, assumes perfectly-plastic materials. The results are according to the theory by Shield and Drucker for the head A and according to the theory by Gill for the nozzle. In the latter case, only the lower bound is available and the two values quoted for this, at the bottom of the last column are based on the first yield stresses of the theoretical approximation to the two stress-strain curves, one for the vessel steel and the other for the end-nozzle steel.

Comparisons Of Collapse Pressure (lb/in^2) As Measured And As Predicted By Different Methods

	Vessel Head A		Vessel head B (with nozzle opening)	End Nozzle
Test Results				
First (local) yield pressure	360		320	340
Collapse pressure by				
Method 1 (tangent) (a)	810		725	610
Method 1 (tangent) (b)	850		780	610
Method 1 (tangent) (c)	820		640	640
Method 2 (0.5% strain)	about 1210		920	660
Elastic-plastic Calculation	(d)	(e)	(d)	(f)
First yield pressure	464	482	515	368
Collapse pressure by				
Method 1 (tangent) (a)	810	816	NA	560
Method 1 (tangent) (b)	840	865	NA	590
Method 1 (tangent) (c)	880	890	660	640
Method 2 (0.5% strain)	about 980	920	NA	660
Limit Analysis				
Upper Bound		(e) 865	NA	(f) NA
Lower Bound		765	NA	613-718

... Continued from Table 4

Note: NA - Not available

(a) - From max.merid.strain curve

(b) - From max.circ.strain curve

(c) - From head deflection curve

(d) - Based on fitted (0.2%) stress-strain curve

(e) - Based on non-hardening yield stress of 34,900 lb/in^2

(f) - Based on non-hardening yield stress of 40,200 lb/in^2

The heads of the present vessel are nominally identical and as shown above give similar elastic strains at the knuckles. Table 12-2 shows, however, that their plastic collapse behaviours are different, the weaker head being head B with the opening. It is noted here that the nozzle is not reinforced.

The vessel head A, with no opening, gives good agreement for collapse loads derived by the tangent method as between the test results and the calculation, using the fitted stress-strain curve (column (d), Table 12-2). Similar agreement is also found for the calculation using a perfectly-plastic stress-strain curve based on a yield of 34,900 lb/in^2 (column (e), Table 12-2). In both cases the collapse load based on the calculated deflection curve is higher than that observed. The limit load using a yield of 34,900 lb/in^2 agrees well with the above collapse loads.

At 0.5 per cent maximum outside strain, a large amount of work-hardening has already occurred, and calculation (e) based on a perfectly-plastic property is expected

to give a low prediction. This is found to be true. It is found that calculation (d) also predicts a lower load of about 980 lb/in^2, compared with the load of about 1,210 lb/in^2 observed from the test where the change of shape of the vessel head may strengthen it substantially.

The presence of an end-nozzle on vessel head B made it fail by collapse at lower loads. The collapse based on the calculated deflection compares well with observation. No other comparison is possible because the calculation did not go to a high enough load for this purpose. No limit load can be obtained because the theory cannot conveniently account for weakening caused by an end nozzle.

The collapse loads of the end nozzle obtained by the same procedures give fair agreement betweem calculation and observation. Worth noticing is the agreement of the 0.5 per cent strain collapse values. At this low pressure the change of geometry is small and its effect is probably negligible.

12.7 Conclusions

In the last few chapters, we have seen how the pressure vessel programs were checked in various ways for their accuracy. The elastic program was found to be free from basic errors and its solution could give accuracy to three or four significant figures from the thin-walled shell theory. The two preliminary comparisons with the published plastic tests by Stoddart and by Kemper of pressure vessel heads gave, first and foremost, more understanding of the different behaviours of mild steel

heads and stainless steel heads. The large amount of strain-hardening of stainless steels allow such vessels to withstand higher pressure after an initial yielding. The actual comparisons gave mixed results.

Great care was taken in the preparation and conduction of the present stainless-steel vessel test. The care taken appeared to be well rewarded. The strain gauging of the vessel interior went without much trouble despite the few rejected gauges. The use of hydraulic oil for applying the pressure, airhydro pump for maintaining constant pressure, and the specially made Conax sealing gland for the strain gauge lead wires, made the preparation and testing an easier task.

During the test, the vessel was unloaded and given repeated loading cycles, both action being common in the life of pressure vessels including those in boiler, chemical and nuclear reactor plants. These actions were found to interrupt, but not to affect, the general trend of the increasing elastic-plastic strains or deflections of the vessel. It can be seen more clearly here that the large amount of strain-hardening of the steel caused the vessel to show a slow transition into rapid straining, thus giving slightly more warning than other vessels of the on-coming collapse. Even after this transition, there was a reserve of strength since the increasing hardening of the material caused the load resistance to increase with increasing straining.

The calculated elastic results compared well with experiment. At the dished ends the calculated peak strains were in general slightly higher. At the nozzle

junction,where there was a severe stress concentration, there was good agreement,except unfortunately the largest measured strain value where the corresponding calculated value was very much lower. With small amount of plastic straining, it is seen that the calculation predicted the behaviour with fair accuracy. Agreement is less satisfactory at larger strain, where geometry change from large deformation undoubtedly influences the behaviour,although this gives lower predicted loads and thus conservative estimates for vessel heads and nozzles under internal pressure.

There is no sharply defined collapse load for this vessel, both because of the high degree of strain-handening and because of the relatively large kunckle radius (16% for dished-end A and 18% for dished-end B). The previously suggested procedure to define the start of collapse by drawing tangents to the load-strain or load-deflection curves is found to work well with good agreement,although in most applications the method may not be convenient to use.

13. OTHER GENERAL DISCUSSIONS

13.1 Pressure Vessel Programs

Theoretical Basis of Programs

The shell equations used in the programs are from small deformation, thin-walled shell theory. This gives a limitation to the possible accuracy from the programs. However there is a wide range of medium thick vessels, say, of thickness to diameter ratio from 1:10 to 1:100, depending on the vessel geometry and on the application, where the elastic-plastic program is of great use. The programs can of course analyse thinner vessels than the above, although the change of actual geometry under load may in this case give noticeable change to the stress distribution, throwing doubts on the results at large amount of deformation. On even thinner vessels, the interest would be on buckling where completely different theories would have to be used.

Another limitation arising from the theory used is on the accuracy of the local stress and strain at shell discontinuities. Shell discontinuities are normally assumed in calculations on pressure vessel nozzles, and in many cases they give inaccurate results at the junction of the nozzle and vessel shells. To reduce this inaccuracy, the shell discontinuity was in the present investigation removed and the nozzle shell was joined to the vessel shell using a small toroidal shell element. This is the method of Smooth Representation. The improvement as a result can be seen in Appendix B. A further attempt to improve this was made in modifying the thin-walled shell assumption resulting in the C Program. These efforts were however found to be in-

sufficient. The comparison of the nozzle junction stress calculations with the three nozzle test results showed that the accuracy achieved was less than that at other parts of the shells. Possibly more accurate solutions can be obtained with finite-element stress-analyses programs capable of analysing solids of revolution, but this would be an academic exercise until more study is made of the meaning of these very high but local stress at nozzle junctions, and of the design use to which the stress results are to be put. Designers in the past did not have to face this problem since substantial reinforcement was placed at the nozzle junctions using the area replacement rule. Present methods proposed to design to limit (or collapse) load, or to shakedown load do not require the knowledge of the local stress intensity. Designing against ordinary and low-cycle fatigue will however require the value of the stress intensity, and here one may find it profitable to investigate in detail the local stress intensity at nozzle junctions.

The method of obtaining elastic-plastic solution was developed by Marcal. This is the tangent modulus method, as it is now commonly called. With this method,problems of extreme non-linearity can be analysed and the solution for large amount of plastic stressing can be obtained. There is another method by Mendelson that has also been applied to elastic-plastic analyses of plates and shells. This method is very efficient in computing time, but it is not able to solve very non-linear problems, and is thus not suitable for calculating the collapse behaviour or that at large amount of stress and strains. One

cause of the relative inefficiency of the Marcal procedure is the large number of iterations necessary at transition points. At points which have already yielded, it was noticed that the calculation procedure can determine reasonable estimates of the stress and strain from the tangent, $H' = \frac{d\bar{\sigma}}{d\bar{\varepsilon}}$, of the stress-strain curve, and reasonable rate of convergency can be obtained. At transition points, however, good estimates of the strain increment cannot in general be made and this slows down the rate of iteration convergency during each load increment.

At and near the shell axis the computer program is found to give slow integration convergency or inaccurate result. This is a property of the method of numerical analysis of the shell equations when the distance from the shell axis approaches zero. This phenomenon has also been noticed by originators of some other pressure vessel programs, because in some of them, special facilities were written into the program to remedy this, for example, by using special shallow spherical shell equations at the region near the shell axis. In the present programs, a provision is also made to remedy this slow convergency, but it has been found that in some problems this may not give a sufficiently accurate solution near the apex. Indeed the misbehaviour was very noticable during the calculation on the closed pressure vessel head A, where the calculated results at the apex, i.e. the region very near the shell axis, has to be neglected. It is also seen in Fig. 12-15A that the elastic-plastic results for this region seem to behave differently from what would be expected.

Usage of the Programs

The computer programs are found to be very flexible, and capable of analysing a large range and variety of shell geometry and loadings. One of the few drawbacks is that it cannot analyse directly ellipsoidal shell elements and thus cannot conveniently analyse, for example, ellipsoidal pressure vessel heads. The other disadvantage is the limitation on the length of shell branches. The Spera toriconical head compared in Ch.7 has to be analysed as two problems, one consisting of a cone on a sphere and other of a sphere on a cylinder. The Thin Cap and the pressure vessel head B with nozzle are both just within the limits of shell length for reasonable rate of convergency.

There are ways of overcoming this disadvantage. One is to adopt the method of Kalnins Ref.(3-31) spliting the shell into a number of sections, each section of a length within the limit capable of being analysed by the step-by-step integration procedure. Independently, influence coefficients are obtained for each section, after which, these influence coefficients for all shell section are then analysed by matrix procedure to obtained solution for the complete shell. This however involves the development and writing of a new program. Another simple method is to use a computer that uses longer 'word-length'. The IBM 7090 & 7094 computers, used on all the above calculations, use floating-point values defined by 48 binary bits giving an accuracy for each variable of 7 to 8 significant decimal figures. Computers that use longer 'word-length' than 48 bits can store numerical values to a higher accuracy. This should increase the

limiting shell-length of the program in a ratio of the number of significant figures of a working variable.

The elastic program PVA1 is for most problems quite convenient to use. It is of course necessary to check that the branch length is within the limiting length. Also, at areas of stress discontinuity, like that caused by geometry change or by local loading, the integration interval length has to be reduced, but, in general, the allowable maximum for the number of intervals is more than sufficient. The program has a large number of error messages if the data is found to be wrong, and many diagnostic messages if the problem cannot converge. The two manuals explaining the program and its use are found by many to be convenient to use. The author, for example, knows of instances where engineers unfamiliar with the program have, with little or no help, used the program to analyse problems without great difficulty.

The elastic-plastic program PLINTH is in general less convenient to use than the elastic program. The development work on this program was terminated in a shorter time than expected, and there was, compared with PVA1, less tidying-up efforts, less provision for automatic check, diagnostic and error messages, and user's manual was less well prepared. Compared with elastic problems, the elastic-plastic problems are much more complex and have more factors influencing the convergency of the solution. In general each problem has to be tried a first time and sometimes a second time or more before a successful final run, giving satisfactory solution beyond collapse of the shell, can be obtained.

The computing time needed for a complete elastic-plastic calculation to collapse is many times more than a elastic calculation. This is due mainly to two reasons. The first one is due to the large number of iterations required. In the elastic-plastic calculation, solutions have to be obtained at a number of small increments of loading, and during each loading a number of iterations, each similar to a elastic calculation, have to be made to iterate for the correct plastic strains. Thus a complete elastic-plastic calculation is equivalent to a large number of simple elastic calculations. The second reason comes from the increased storage required on the computer. The elastic-plastic program requires many more parameters than the elastic program, and the former, in its final form, uses subsidiary store in the form of magnetic tapes or magnetic discs for storing the elastic-plastic stiffness coefficients. This use of subsidiary store increases very much the execution time of the calculation. The final result of these is that on the IBM 7094, where most of the computation was done, a typical elastic calculation uses about 0.5 to 1.0 minutes for execution while a typical elastic-plastic calculation takes 20 to 45 minutes.

13.2 Vessel Behaviour

From the test conducted and from the other test reported, it is not possible to get a simple rule to predict which vessel head may collapse with a sudden increase in strain and deformation, or may strain gradually until the deformation becomes very large. There appears to be a number of factors involved.

The Stoddart vessel head and the Kemper vessel head have similar shape and height-to-diameter ratio, but the latter vessel is thinner (see Table 8-1, p.98). However Stoddart observed a sharp increase of strain and deformation near collapse while this was not observed by Kemper. The cause of this difference in behaviour is thus very probably the large amount of strain hardening of the stainless steel in Kemper's vessel. As to the calculation, it was noticed that the theoretical solution for the Stoddart test did not show a similar sudden increase of strain and deformation at collapse. Since a perfectly plastic material is already assumed in the calculation, the evidence seems to point to inaccuracy in the solution. If one reviews in detail the tangent modulus method of elastic-plastic calculation by Marcal, it appears that by taking the tangent modulus over a finite load increment, any rapid change of strain would be smoothened over in the process. If this is true, there may be some application of the program where this inaccuracy may not be unimportant. Further confirmation of this finding is necessary and desirable.

The axial load tests conducted on the two mild steel nozzles showed a final physical collapse in the form of a sudden increase in the strain rate. This collapse was not observed in the calculations. The mild steel has negligable strain-hardening until the strain is very large. While this difference may again be due to the failure of the calculation to predict a sharp change of strain rate, there is an additional factor here in that the axial loading on the spherical shell was compressive i.e. inwards, and at large deformation the instability

load may be lowered because of the changed geometry. It is thus not possible to judge whether the results of the elastic-plastic calculation are at fault here.

Geometry change may also be the reason for the underestimation in the calculation of the pressure resistance of the stainless steel test vessel. The calculation predicted at high loads a much higher straining than that observed. The change of geometry of torispherical heads under internal pressure normally increases their pressure resistance.

In spite of these two possible errors of the elastic-plastic calculation at large deformation of vessels, the proposed method of tangent for obtaining collapse laads is found to work well for correlating the actual and predicted collapse loads, and the two errors do not seem to affect their agreement.

The test vessel was twice given repeated loading and unloading cycling during the tests. One of the observations was that these cyclings did not interrupt the general load-strain and load-deformation curves. One other observation can be made here from these repeated loadings. This comes from the fact that the strain and deformation increased during each load cycle, but the rate was found to decrease gradually with increasing number of cycles. If the increase of strain and deformation fell to zero, this would either be a shakedown or an alternating plasticity behaviour. In the plasticity theory of ideal materials, there is a cellar-cut difference between shakedown and alternating plasticity, but in actual metals the distinction is not so precise. The above repeated loading method can thus be used as an

experimental observation of the maximum shakedown load; this may be interpreted as the highest repeated load value where the maximum strain increment after a large number of cycles decreased sufficiently to zero and at the same time the hysteresis loop of maximum strain becomes sufficiently narrow.

13.3 Design Interest

The near future design interest on elastic-plastic calculations depends on what approach is used for pressure vessel design. The ASME boiler and pressure vessel codes require the determination of stress level at different parts of the vessel to be used as the major criterion of design. The stress has to be separated into different categories: membrane, primary and secondary. Different criterions are given to the maximum permissible stress levels for each type of stresses. These stress levels are of course elastic stress levels, although this is not to imply that elastic-plastic strains are not of interest. Investigations with elastic-plastic calculation could be used indirectly, say, to obtain better criteria for the stress levels, and to give additional limitations for different modes of failures and for different component.

The British Standards for pressure vessel design consider separately the design of different vessel components. It is here that investigations by elastic-plastic calculation of specific components, like the vessel heads and axisymmetric nozzles considered in this thesis, can get more direct application. Individual pressure vessel components can fail in a number of manners. Most of these failure modes involve plastic straining before

final failure occurs , and in such cases a better understanding of the failure can be achieved through the use of elastic-plastic calculations.

Plastic Collapse

Plastic collapse is a common but severe mode of failure for both pressure vessel heads and nozzles. Destructive testing is of course the best procedure for ensuring a safe design. Theoretical procedure for determining this plastic collapse load has been attempted by using the limit analysis method. At present the available limit solutions that can be applied to pressure vessel design are for axisymmetric nozzles of both the flush and protruding type, and on torispherical heads whose solutions are claimed to be similarly applicable to toriconical heads. However from the above investigations with elastic-plastic calculations, it can be seen that, the gap of knowledge of collapse load on other shell geometries and on non-typical geometries can immediately be filled by such calculations. Examples of other geometries, which must of course be axisymmetric, are flat heads, ellipsoidal heads, concial heads, different types of "shell-reducers", and toroidal expansion bellows.

Assumptions of non-work-hardening in collapse load calculation make the solution over-conservative in the case of annealed stainless steels and some non-ferrous metals with a large amount of strain hardening. One remedy is to assume a higher yield stress in the calculation, say, the one percent proof stress. Design of vessels of such materials, when the collapse load is the limiting criterion, can however be more realistic and accurate if

the strain-hardening could be taken into account. There is a large scope for the use of elastic-plastic calculation here. The effect of strain-hardening on collapse load has so far not been investigated.

Shakedown

Loadings on pressure vessels are never constant during their working life and very often is repetitive in nature. Shakedown considerations may be required when local yielding occurs many times during the life time of the component. When the yielded zone is well surrounded by material that remains elastic, Langer, Ref. 8-3, suggested that shakedown should occur under any repeated loading when the maximum load is less than twice that causing the maximum strained region to start yield. This is a convenient rule to apply and is used in the ASME Section III Code for nuclear vessels, to limit the level of secondary stress at the working load. The actual maximum shakedown load of course vary according to the geometry of the vessel component, with the factor 2.0 being the upper ceiling for the ratio to first yield load.

Theoretical analysis of pressure vessel nozzles, flush and protruding, was made by Leckie. In this case only the elastic solution is required to obtain the shakedown solution. This is because pressure vessel nozzles have in general a narrow zone of high stress with the location of this zone accurately known to be on the junction between vessel and nozzle. Pressure vessel heads have however a less concentrated region of high stress and this property makes it impossible for vessel

heads to be analysed for shakedown by the same method using elastic solutions. To obtain the shakedown pressure, a method used by Crisp [Ref. 8-1] makes use of solutions obtained by the method of elastic-plastic analysis. This is one of the immediate applications of the elastic-plastic analysis. From a survey of shakedown solution of a range of torispherical pressure vessel heads, he observed that the average shakedown pressure is about 1.66 of the pressure to cause first yield, and none of them, as expected, exceeded twice the first-yield pressure. This same procedure could equally well be applied to many other pressure vessel components, especially those without abrupt changes of geometry that give rise to narrow regions of stress concentration, Ellipsoidal heads and pipe-line toroidal expansion-bellows are examples of geometries that can be thus used to obtain shakedown solutions.

Low-Cycle Fatigue

Low-cycle fatigue (also called high-stain fatigue) is a mode of failure where plastic straihing plays an essential role. Strictly speaking, a vessel component, when designed so that it will shakedown, would only require elastic fatigue considerations. There are however many cases where designers, for good reasons, may be interested in low-cycle fatigue. First example occurs when one finds a range of standard design of vessel components that has in the past been used satisfactorily outside the shakedown load, and there is thus no justification to limit them in future to a lower load from shakedown consideration. Secondly, ~~there are~~ power station that may be started-up once a day would subject

its equipments, in a working life of say 20 or 25 years, to working-load cycles of less than 10,000. Thus in some such instances, reasonable saving can be obtained by designing equipments to this 10,000-cycle working life. Thirdly the designer may very often come across materials with a large amount of work-hardening, and shakedown design using the proportional limit to the stress-strain curve would not make good use of the reserve of work-hardening strength of the material. The alternate solution of using a higher proof-stress value is an acceptable compromise, but this has to be confirmed by actual testing since the shakedown theorem, in its present form, assumes non-workhardening behaviour. The better alternative in such a case may be to design to low-cycle fatigue.

The contribution to low-cycle-fatigue analysis, of methods of elastic-plastic analysis of shell components, lies in their ability to predict the elastic-plastic strain concentration at different loads. Assuming that the correlation between the fatigue life of specimen and pf actual structure is known, one can determine from specimens the strain-range and fatigue-life relations, and use elastic-plastic analysis to calculate the maximum strain in the actual shell component, and thus predict its fatigue life. The same procedure is of course used to predict high-cycle or elastic fatigue life of structures using elastic analysis instead of elastic-plastic analysis. One difficulty that arises is because the plastic straining in the actual structure is caused by cylic loading while the elastic-plastic analyses assume a steady increasing load. On this point, it has

been suggested that the use of a cyclic stess-strain curve in the method of analysis should give a true prediction of the strain concentration under cyclic loading. The cyclic stress-strain curve*, each to be defined for an infinite or a specific number of loading cycles, is a curve of the cyclic strain-range against the corresponding cyclic stress-range at the specified number of cycles, and this is usually obtained by cyclically testing small loading specimens of the material under constant strain-range, each specimen for a different strain-range. This procedure of predicting low-cycle fatigue life has been tried with success, but more confirmation of the validity of the procedure under different circumstances is required.

The strain-range of interest for this application is higher than that for the shakedown appliction, but both should be of similar of order of magnitude; hence the required plastic strain for both is thus of similar magnitude to the elastic strain. The load range for this application is again higher than that for shakedown, but here there is an upper ceiling since the low-cycle fatigue load cannot be greater than the collapse load.

---

* Blatherwick A.D. & Lazan B.J. The effect of changing cyclic modulus on bending fatigue strength. Proc. ASTM 56,1012,1956.

14. CONCLUSIONS

Literature Review

The following findings are revealed, helping to set the course of investigation in this thesis :

a) The elastic-plastic analysis of the stress and the behaviour of axisymmetric pressure vessel shells by numerical computation forms a useful and logical extension to the early, and current, theoretical study of thin-walled pressure vessels.

b) Such methods of analysis developed by Marcal, and by others, have not been sufficiently compared in detail against appropriate and accurate expeirments.

c) The possible applications into design of elastic-plastic solution have not been sufficiently investigated, and thus not well exploited.

d) Medium thick pressure vessel heads, commonly in the the shape of torispheres, can be analysed elastically. However, for some common modes of failure, it is inappropriate to design according to elastic analysis, and application into design by elastic-plastic theory may be of immediate interest.

e) On the possible design of pressure vessel nozzles, using these and other more accurate procedures, greater urgency is required to attain a ~~more~~ wide-spread adoption of better and consistant arrangement of nozzle reinforcements, to obtain a better prediction of the very local peak-stresses at nozzle junctions, and to achieve a better understanding of the role these peak stresses play in different modes of failures.

Design Interests of Elastic-Plastic Analysis

The possible design interests vary according to the modes of failure, and to a lesser degree, according to the vessel component.

f) Design against excessive deformation of nozzles requiring accurate alignment, requires the value of deformation. In many other cases, this excessive deformation failure may be a plastic collapse, where the collapse load is required as the ceiling of hydraulic proof-test pressure and any occassional over-load of vessels in service. For vessel heads under internal pressure, this load is about 1.5 - 2.2 of the first-yield load.

g) Failure under repeated loading can be prevented by designing for shakedown or against low-cycle fatigue. The load range of interest in shakedown design is less than that for design against collapse. A proposed method, where elastic-plastic analysis can usefully be applied, would require the values and the ratios of the peak stresses at small amount of plastic straining.

h) The load range of interest in design against low-cycle fatigue is ~~again~~ *also* smaller than that for design against collapse. At the failure load, the amount of plastic straining in the elastic-plastic calculation is of similar magnitude to that in the calculation needed to predict shakedown. These calculations would however be on strain-hardening material since the cyclic stress-strain curve would be used. What is required from these calculations would be the peak-

strain value, either the total strain, or its plastic component.

Elastic Behaviour of Nozzles and Heads

i) The elastic solutions from the computer programs, PVA1 and PLINTH, used in this investigation are found to be reliable and accurate for normal vessel shell calculations, with geometry and loading within the assumptions of the theory, and with no intersections of shells where the thickness and the direction of the shell-meridian change across the intersection.

j) Tests conducted to check the accuracy of the programs have to be carefully planned and executed to eliminate a number of other sources of disagreements. Especially important is getting an accurate shell geometry, since this is found to affect very much the resulting deflection and stress-distribution. The axial deflections, for example, of the two nozzle-on-spherical-cap specimens are found to depend very much on the precise shape and edge-restraint of the caps.

k) The programs have difficulty in converging to an accurate solution at the crown centre of some tori-spherical-head problems, including that of the stainless steel test-vessel head A. Other than this, however, the elastic solution gives good prediction of the maximum stresses and the stress distribution.

l) The programs cannot give similar accuracy for axisymmetric nozzle problems. It is known, and confirmed, that the normal shell-theory procedure to approximate a nozzle-on-vessel by intersecting shells

gives over-estimation of the peak junction stress, especially when nozzle and vessel have very different thicknesses. The two attmepts to improve on the results, one by the method of Smooth Representation, the other by modifying the program to approximate better to thick curved shells, both give substantial improvement for the three test nozzles, but are not sufficient to give good agreement with the maximum strain gauge readings. The Smooth Representaion applies only to flush nozzles with no partial penetration welds.

Vessel Behaviour and Elastic-Plastic Analysis

m) The accuracy of elastic-plastic predictions depends on a number of factors. During the vessel test, reasonable precautions were taken, based on earlier experience, to achieve a uniform yield-stress property together with an accurate mathematical reproduction of the actual stress-strain curve, and to obtain an accurate elastic-stress prediction. However nothing could be done about possible error caused by geometry change at large deformation of the shells. It was found difficult to allocate the share of each of the above factors causing the difference in the calculated and measured results, and equally difficult to judge how far the calculated results are in error, due to the program and the theory used.

At the crown centre of torispherical heads, where the elastic results are in error, the comparison of the vessel head A shows that the elastic-plastic

results are also wrong. Comparison of the Stoddart test results shows that the computation process does not converge sufficiently to the correct solution, when the strain-rate (i.e. change of strain per unit load increase) changes rapidly, and thus tend to smoothen out any sudden change of slope in the load-strain and load-deformation curves. This however needs further confirmation.

n) Whether or not any inaccuracy from the present program can be easily reduced, the present results look more favourable, however, when judged as to their possible design use. The two interests in this case are, the behaviour at small plastic straining, and the collapse load. Allowing for inaccuracies caused by the differences in the elastic results, the peak-strain and deflection results show good agreement at small amount of plasticity. The axial tests on the mild-steel nozzles are not suitable for comparing collapse because of the proximity of the vessel-base and the nozzle. For the vessel test, good agreement is obtained for the collapse load, as defined by the proposed method of intersection of tangent lines to the load-strain and load-deformation curves. Agreement is also obtained for this collapse load when the calculation is compared against the Stoddart vessel test.

o) The collapse values as defined by this method of tangents show not only good agreement, for the two vessel heads and one nozzle, between that from the

theoretical curves and the experimental curves, they also show reasonable agreement to the limit-analysis results using appropriate yield-stress values. The method gives values that are not very sensitive as to which peak strain curves are used, these peak strains must of course be near the collapse zones. Values from the overall deflection curves are also in reasonable agreement. The method is also not very sensitive to errors due to inaccurate stress-strain curve, or to geometrical change of the real vessel. It is less convenient to use than that based on a certain value of peak strain, but it deserves further investigation into its consistency and applications.

p) The test vessel continues to hold pressure many times the first yield pressure, and the design pressure of 360 lb/in^2. (Testing stopped at 1165 lb/in^2.) This comes from the large amount of ducitility of the annealled stainless steel used. Kemper and his co-worker observed the same phenomenon during their vessel tests.

q) Cycling the test vessel at 870 lb/in^2 and at 1070 lb/in^2 (2.6, 3.1 times respectively the observed first yield of the nozzle and 2.4, 3.0 times respectively the observed first yield of vessel head A) did not cause noticeable incremental straining at the 7th cycle. Any effect these cycling may cause to the overall load-strain and load-deflection curves is undetectable.

REFERENCES

2-1 THOMPSON,S.J.Boilers-past and present. Proc.I.Mech.E.148,4,p132,1942.

2-2 REEMAN,H.F.Notes on the development of the steam boiler. Proc.I.Mech.E.147,p72,1942.

2-3 BACH,C. Untersuchungen über die Formänderungen und die Anstrengun gewölbter Böden. (Investigations into the stresses and deformations of curved plates.) VDI 43, 51, 1585-1594,1613-1625,1899.

2-4 HOEHN,E. and HUGGENBERGER,A. Über die Festigkeit der gewölbten Böden und der zylinderschale. (Monograph),Springer,Berlin,1927.

2-5 ENGINEERING. The Strength of Dished Ends. Engineering,128,1-4,July 5,1929.

2-6 MEISSNER,E.Das Elastizitätsproblem für dünne Schalen von Ringflächen-, Kugel-oder Kegelform, (in German). Physik,14, 343pp. 1913. (Also TMB Translation 238, The elasticity problem for thin shells of toroidal, spherical,or conical shape. 1951.)

2-7 COATES,W.M. States of stresses in full heads of pressure vessels.Trans. ASME.,52,22,117-131,1930.

2-8 PRESSURE VESSEL RESEARCH COMMITTEE. Report on the design of pressure vessel heads,.Appendix 1, History of the design of heads for pressure vessels. Welding J.Res. Suppl.41S-48S,Jan.1953.

2-9 SIEBEL,E. and KÖRBER,F. Versuche über die Anstrengung und die Formänderugen gewolbter Kesselboden mit und ohne Mannloch bei der Beanspruchung durch inneren Druck. Mitt.K.W.Inst. Eisenforsch.,7,10,113-177,1926,and 8, 1,1-51,1926.

2-10 TAYLOR,J.H.and WATERS,E.O.Effect of openings in pressure vessels. Trans. ASME,56,3,119-140,1934.

2-11 EVERETT,F.L. and MCCUTCHAN,A. Investigation of stress conditions in a full-size welded branch connection. Trans. ASME,60,p.399,1938.

2-12 BESKIN,L.Strengthening of circular holes in plates under edge loads. Trans.ASME,66,p.A-140,1944.

2-13 INGLIS,C.E. Engineering 95,p.415,1913.

2-14 KOOISTRA,L.F.and BLASER,R.U. Experimental technique in pressure vessel testing. Trans.ASME

72,579-587,1950.

2-15 GROSS,N. Research on welded pressure vessels and pipelines. Brit. Weld. J.1,4,149-160,1954.

2-16 DRUCKER,D.C. Three-dimensional photoelasticity. Ch.17,part II of Hetenyi,M.(ed.) Handbook of Experimental Stress Analysis. New York,Wiley, 1950.

2-17 GLASGOW,ROYAL COLLEGE OF SCIENCE AND TECHNOLOGY. Nuclear Reactor Containment Buildings and Pressure Vessels. Proc.sym.organised by Dept.of Mech.,Civil, and Chem.Eng., Royal Coll. Sci.Tech.,Glasgow,17-20th May 1960. London,Butterworths,1960.

2-18 INSTITUTION OF MECHANICAL ENGINEERS. Proc.Sym. on Pressure Vessel Research Towards Better Design. 18th and 19th Jan.1961: arranged by I.Mech.E. and B.W.R.A.,London,Inst.Mech.Engrs.,1962.

3-6 REISSNER,E.A new derivation of the equations for the deformation of elastic shells. Amer. J.Math,63,177-184,1941.

3-7 TIMOSHENKO,S. and WOINOWSKY-KRIEGER,S. Theory of plates and Shells. McGraw-Hill,1959.

3-8 KRAUS,H. Thin Elastic Shells. London,Wiley,1967.

3-9 WATTS,G.W. and LANG,H.A. Stresses in a pressure vessel with a conical head. Trans. ASME,74,315-326,1952.

3-10 TAYLOR,C.E. and WENK,E.Jr. Analysis of stresses in the conical elements of shell structures. Proc.2nd.U.S.Nat.Cong.Appl.Mech.,ASME,323-331, 1955.

3-11 WATTS,G.W.and LANG,H.A. Stresses in a pressure vessel with a hemispherical head. Trans.ASME,75, 83-89,1953.

3-12 GALLETLY,G.D. Influence coefficients for hemispherical shells with small opening at the vertex, J.Appl.Mech.22,20-24,1955.

3-13 GALLETLY,G.D. Influence coefficients for open-crown hemispheres. Trans.ASME 82A,73-81,1960.

3-14 GECKELER,J.W. Über die Festigkeit achsen-symetrischer Schalen. Forschungsarb. Ingwes., Berlin,276,1-52,1926.

3-15 NAGHDI,P.M. and DESILVA,C.N. Deformation of elastic ellipsoidal shells of revolution. Proc 2nd U.S. National Cong.Appl.Mech.,ASME,333-343, 1955.

3-16 DESILVA,C.N. Deformation of elastic paraboloidal shells of revolution. J.Appl. Mech.24,397-404, 1957.

3-17 LECKIE,F.A. Localized loads applied to spherical shells. J.Mech.Eng.Sci.3,111-118,1961.

3-18 LECKIE,F.A. and PENNY,R.K. A critical study of the solutions for the axisymmetric bending of spherical shells. Weld. Res. Council Bull. No. 90,1963.

3-19 FLUGGE,W. Statik und Dynamik der Schalen. Berlin, Julius Springer Verlag,1934.

3-20 LUR'E,A.I. The general theory of thin elastic shells,Prikl. Mat. Mekh.4,7,1940.

3-21 HILDEBRAND,F.B.,REISSNER,E. and THOMAS,G.B.

Notes on the foundations of the theory of small displacements of orthortropic shells. NACA-TN-1833, March 1949.

3-22 NAGHDI,P.M. On the theory of thin elastic shells, Q.Appl. Math.14,369-380,1957.

3-23 KLOSNER,J.M. and LEVINE,H.S. Further comparison of elasticity and shell theory solutions. AIAA Journal 4,467-480,1966.

3-24 PENNY,R.K. Symmetric bending of the general shell of revolution by finite difference methods. J.Mech.Eng.Sci.3,369-377,1961.

3-25 SEPETOSKI,W.K.,PEARSON,C.E.,DINGWELL,I.W. and ADKINS,A.W. A digital computer program for the general axisymmetric thin shell problems. J.Appl. Mech.29,655-661,1962.

3-26 RADKOWSKI,P.P.,DAVIS,R.M. and BOLDUC,M.R. Numerical analysis of equations of thin shells of revolution. Amer. Rocket Soc. J.32,36-41,1962.

3-27 BUDIANSKY,B. and RADKOWSKI,P.P. Numerical analysis of unsymmetrical bending of shells of revolution. AIAA J.1,1833-1842,1963.

3-28 GALLETLY,G.D. Bending of open crown ellipsoidal shells. Weld. Res.Council Bull.54.1959.

3-29 GALLETLY,G.D. Edge influence coefficients for toroidal shells. Trans.ASME,82B,60-64,65-68,1960.

3-30 MIRABAL,J.A. and DIGHT,D.G. SOR-II, a program to perform stress analysis of shells of revolution. KAPL-M-EC-19,Knolls Atomic Power Lab., Schenectady,N.Y.,1962.

3-31 KALNINS,A. Analysis of shells of revolution subjected to symmetrical and non-symmetrical loads. J.Appl. Mech.31, 467-476,1964.

3-32 PILGRIM,W.R.,CHEUNG,J.S.T. and MARCAL,P.V. Computer program for elastic analysis of pressure vessels. RD-C-N-22, Central Elect. Generating Board,London,June,1965.

3-33 NATIONAL PHYSICAL LABORATORY Modern Computing Methods. London, Her Majesty's Stationery Office, 1961.

3-34 FOX,L.(ed) Numerical Solution of Ordinary and Partial Differential Equations. London,Pergamon,, 1962.

3-35 GRAFTON,P.E. and STROME,D.R. Analysis of axisymmetrical shells by the direct stiffness method. AIAA J.1,2342-2347,1963.

3-36 FRIEDRICH,C.M.SEAL-SHELL 2, a computer program for the stress analysis of a thick shell of revolution with axisymmetric pressure,temperatures and distributed loads. WAPD-TM-38, Bettis Atomic Power Lab., Pittsburgh,Pa.,1963.

3-37 KRAUS,H. A review and evaluation of computer programs for the analysis of stresses in pressure vessels. Weld. Res. Council Bull.108,11-28,1965.

3-38 PENNY,R.K. and PERRYMAN,K.R. VESSL. 1,IBM 7090 program for computing stresses in shells of revolution. Central Elect. Generating Board, Computing Dept., London,1962.

3-39 GALLETLY,G.D. Analysis of discontinuity stresses adjacent to a central circular opening in a hemispherical shell. Report 870,David Taylor Model Basin, Washington,D.C., May,1956.

3-40 ROSE,R.T. and THOMPSON,J.M.T. Calculated stress concentration factor for nozzles in spherical pressure vessels. Paper 1 of (3-5).

3-41 LECKIE,F.A. and PENNY,R.K. Solution for the stresses at nozzles in pressure vessels, Paper 2. Stress concentration factors for the stresses at nozzle intersections in pressure vessels, Paper 3. Welding Res. Council Bull.90, Sept.1963.

3-42 O'CONNELL,J.M. and CHUBB,E.J. An Improved method of calculating stresses at the intersection of a cylindrical nozzle and a spherical shell. Paper 5 Applied Mechanies Convention, Proc.I.Mech.E. 178,3J,224-230,1963-64.

3-43 DRUCKER,D.C. Limit analysis of cylindrical shells under axially-symmetric loading. Proc. 1st. Midw. Conf. Solid Mech.(Urbana,1953)158-163,1954.

3-44 ONAT,E.T. and PRAGER,W. Limit analysis of shells of revolution. Proc. Roy. Netherlands Acad.Sci. B57,534-548,1954.

3-45 HODGE,P.G.Jr. Yield conditions for rotationally symmetric shells under axisymmetric loading. J. Appl. Mech.27,323-331,1960.

3-46 HOPKINS,H.G. and PRAGER,W. The load carrying capacities of circular plates. J.Mech.Phys. Solids,2,1-13,1953.

3-47 HODGE,P.G.Jr. Yield point load of an annular plate. J.Appl.Mech.26,454-455,1959.

3-48 HODGE,P.G.Jr. Limit Analysis of Rotationally Symmetric Plates and Shells. Prentice-Hall,1963.

3-49 MARCAL,P.V. and PILGRIM,W.R. A stiffness method for elastic-plastic shells of revolution. J. Strain Analysis,1,4,339-350,1966.

3-50 SPERA,D.A. Analysis of elastic-plastic shells of revolution containing discontinuities. AIAA J.1,11,2583-2589,1963.

3-51 BIJLAARD,P.P. Stresses from radial loads in cylindrical pressure vessels. Weld. J.33,615S-623S,1954.

3-52 BIJLAARD,P.P. Stresses from radial loads and external moments in cylindrical pressure vessels. Weld.J.,34,608S-617S,1955.

3-53 WICHMAN,K.R.,HOPPER,A.G. and MERSHON,J.L. Local stresses in spherical and cylindrical shells due to external loadings. Weld.Res.Council Bull.107, 1965.

3-54 LUR'E,A.I. Concentration of stresses in the vicinity of an aperture in the surface of a circular cylinder (in Russian). Priki.Mat.Mek. 10,397-406,1946. Also, English Trans. IMM-NYU 280,New York University,Inst. of Math.Sciences, Nov.1960.

3-55 WITHUM,D. The circular cylindrical shell with circular section cut out under shear stress. (In German). Ing.Archiv.26,435-446,1958. Also, English translation,C.E. Trans. 2728,Central Elect. Generating Board,Central Tech. Information Service,London,S.E.1.

3-56 REIDELBACH,W. The state of stress at the perpendicular intersection of two right circular cylinders (in German). Ing. Archiv.30,5,1961. English trans. by M.M.Stanisic,General Tech. Copr., Tech. note 3-1,1962.

3-57 ERINGEN,A.C., NAGHDI,A.K. and THIEL,C.C. State

of stress in a circular cylindricial shell with a circular hole. Weld. Res. Council Bull.102, Jan.1965.

3-58 ERINGEN,A.C. and SUHUBI,E.S. Stress distribution at two normally intersecting cylindrical shells. Nuclear Struct. Engg.2,253-270,1965.

3-59 CLOUGH,R.W. and JOHNSON,C.P. A finite element approximation for the analysis of thin shells. Int. J. Solids Struct.4,1,p43,1968.

4-1 JONES,N. An appraisal of the stress-probing method. Engineer,218,5675,715-716,Oct.1964.

4-2 SWANSON,S.A.V. and FORD,H. Stresses in thick-walled plane pipe bends. J.Mech.Eng.Sci.1,2, 103-112,1959.

4-3 MANTLE,K.G. and PROCTER,E. Use of resistance strain gauges. Engineer,March 25,1960,527-528.

4-4 RILEY,W.F. Experimental determination of stress distributions in thin walled cylindrical and spherical pressure vessels with circular nozzles. NASA CR 53580,Dec.1963.

4-5 MORGAN,W.C. and BIZON,P.T. Experimental investigation of stress distributions near abrupt change in wall thickness in thin-walled pressurized cylinders. NASA TN-D-1200. June 1962.

4-6 WELLS,A.A.,LANE,P.H.R.,and ROSE,R.T. Stress analysis of nozzles in cylindrical pressure vessels. Paper 2,21 of (2-17).

4-7 KOOISTRA,L.F. and LEMCOE,M.M. Low cycle fatigue research on full-size pressure vessels. Weld. Res. Suppl. 41,p297S,July 1962.

4-8 KITCHING,R. and DUFFIELD,N.A. Stresses due to axial loads and internal pressure on forged nozzles in a spherical pressure vessel. Int. J.Mech.Sci. 6,77-103,1964.

4-9 ROSE,R.T. Stress analysis on nozzles in thin walled cylindrical pressure vessels. Brit. Welding J.12,2,80-89,1965.

4-10 DINNO,K.S. and GILL,S.S. An experimental investigation into the plastic behaviour of flush nozzles in spherical pressure vessel. Int. J.Mech.Sci.7, 817-839,1965.

4-11 PERRY,C.C. and LISSNER,H.R. The Strain Gage Primer,McGraw Hill,2nd ed., 1962.

4-12 BERMAN,J. and PAI,D.H. An experimental investigation of stresses in an HY-80 marine boiler drum. Welding Res. Supplement,p307-S,July,1962.

4-13 ANDERSON,B.R. Low-cost technique for stress-analysis of solid-rocket cases. Proc. Soc. Expt. Stress Analysis, 20,1,14-21,1963.

4-14 BOWDEN,A.T. and DRUMM,J.C. Design and testing of

large gas ducts. Proc. I.Mech.E.174,3,119-158, 1960.

4-15 CRANCH,E.T. An experimental investigation of stresses in the neighbourhood of attachments to a cylindrical shell. Weld.Res.Council Bull.No. 60,May 1960.

4-16 LANE,P.H.R. and ROSE,R.T.Comparative performance of pressure vessel nozzles under pulsating pressure. Paper 4 of (2-17).

4-17 MORGAN,W.C. and BIZON,P.T. Experimental evaluation of theoretical elastic stress distributions for cylinder-to-hemisphere and cone-to-sphere junctions in pressurized shell structures. NASA TN D-1565, Feb.1963.

4-18 FESSLER,H. and ROSE,R.T. Photoelastic determination of stresses in a cylindrical shell. Brit.J.Appl. Physics 4,3,76-79,1953.

4-19 FESSLER,H. and LEWIN,B.H. Stress distribution in a tee junction of thick pipe. Brit.J.Appl. Physics.7,p76,1956.

4-20 FESSLER,H. and LAKSHIMINARAYANA,C.N. Stresses in hemispherical drum heads. Paper 8 of (2-17).

4-21 FESSLER,H. and STANLEY,P. Stresses in torispherical drumheads-a photoelastic investigation. J. Strain Analysis 1,1,p69,1965.

4-22 LEVEN,M.M. Photelastic analysis of reinforced openings and transition sections in spherical and cylindrical vessels subjected to internal pressure. Westinghouse Res. Report 907-5900-R1, June 1961.

4-23 KENNY,B. Effect of Poisson's ratio on stress distribution. Engineer 218,5675,706-712, Oct.30,1964

4-24 DUNDURS,J. Dependence of stress on Poisson's ratio in plane elasticity. Int. J.Solids Struct. 3,1013-1021,1967.

4-25 FESSLER,H. and STANLEY,P. Stresses in torispherical drumheads,2: A critical evaluation. J. Strain Analysis.1,2,89-101,1966.

4-26 MacLAUGHLIN,T.F. Photoelastic stress analysis of thick-walled closed-end cylinders. Expt. Mech.5,129-134,1965.

4-27 MARGOLIS,A.I. (Original paper in Russian). Inst. Acad. Sci.40,3,35-37,1960.

4-28 MERSHON,J.L. PVRC Research on reinforcement of openings in pressure vessels. Weld. Res. Council Bull.77,May,1962.

4-29 LANGER,B.F. PVRC interpretive report of pressure vessel research, Section 1- Design considerations, Weld. Res. Council Bull.95, April,1964.

4-30 KITCHING,R. and JONES,N. Effect of bending moments on nozzles with forged transition pieces. Proc. I.Mech. E.178,3J,p211,1963-64.

4-31 KITCHING,R.and OLSEN,B.E. Further experiments with forged nozzles in pressure vessels. Proc. I. Mech. E.,179,1,29,907-930,1964-65.

4-32 KAUFMAN,A. and SPERA,D.A Investigation of the elastic-plastic stress state around a reinforced opening in a spherical shell. NASA TN-D- 2672, Feb.1965.

5-1 NEAL,B.G. The Plastic Methods of Structural Analysis. London,Chapman & Hall, 1st ed.1956.

5-2 HODGE,P.G.Jr. Plastic Analysis of Structures. McGraw-Hill,1959.

5-3 DRUCKER,D.C. and SHIELD,R.T. Limit analysis of symmetrical loaded thin shells of revolution. J. Appl. Mech.61-68, March 1959.

5-4 SHIELD,R.T. and DRUCKER,D.C. Limit strength of thin walled pressure vessel with an ASME standard torispherical head. Proc. 3rd U.S. Nat. Congress Appl. Mech.665-672,1958.

5-5 SHIELD,R.T. and DRUCKER,D.C. Design of thin - walled torispherical and toriconical pressure - vessel heads. J. Appl. Mech. 28, 292-297,June 1961.

5-6 GILL, S.S. The limit pressure for a flush cylindrical nozzle in a spherical pressure vessel. Int. J. Mech. Sci. 6, 105-115,1964.

5-7 DINNO,K.S. and GILL,S.S. The limit analysis of a pressure vessel consisting of the junction of a cylindrical and spherical shell. Int. J. Mech. Sci., 7, 21-42,1965.

5-8 CLOUD, R.L. The limit pressure of radial nozzles in spherical shells. Nuc. Struct. Engg. 1,4,403-413, April 1965.

5-9 COTTAM,W.J. and GILL,S.S. Experimental investigation of the behaviour beyond the elastic limit of flush nozzles in cylindrical pressure vessels. J. Mech. Eng. Sci. 8, 3, 330-350,1966.

5-10 CLOUD,R.L. and RODABAUGH,E.C. Approximate analysis of the plastic limit pressure of nozzles in cylindrical shells. J. Engg. Power, Trans. ASME, 67-WA/PVP-4.

5-11 STODDART,J.S. A study of the initial yield and ultimate collapse of torispherical pressure vessel heads. Ph.D. Thesis, Univ. Durham, May 1967.

5-12 KEMPER,M., MORLEY,J.I., McWILLIAM,J.A. and SLATER, D. Pressure vessels of high proof strength warm worked stainless steel. Proc. I. Mech. E. 181,1, 7,137-168,1966-67.

5-13 NEAL,B.G. and SYMONDS,P.S. A method for cal - culating the failure load for a framed structure

subjected to fluctuating loads. J. Inst.Civil. Engrs. 35, p186,1950.

5-14 SIMONDS,P.S. and PRAGER,W. Elastic-plastic analysis of structures subjected to loads varying arbitrarily between prescribed limits. J. App. Mech.17, p315,1950.

5-15 KOITER,W.T. A new general theorem on shake-down of elastic-plastic structures. Proc.k.Ned. Akad. Wet.(B),59,24,1956.

5-16 SYMONDS,P.S. Shakedown in continuous media. J. Appl. Mech. 85-89, March 1951.

5-17 LECKIE,F.A. Shakedown pressures for flush cylinder-sphere shell intersections. J. Mech. Eng.Sci. 7, 4, p367,1965.

5-18 LECKIE,F.A. & PENNY,R.K. Shakedown loads for radial nozzles in spherical pressure vessels. Int. J. Solid Struct. 3, 743-755,1967.

5-19 PARKES,E.W. Incremental collapse due to thermal stress. Aircraft Engg. 28, 395,1956.

5-20 EDMUNDS, H.G. and BEER,F.J. Notes on incremental collapse in pressure vessels. J. Mech. Eng. Sci. 3,3,187-199,1961.

6-1 PILGRIM,W.R. and MARCAL,P.V. Computer program for elastic analysis of pressure vessels, Users' manual. Report RD/C/N/36, Central Electricity Generating Board,Computing Branch, London Oct.1965.

6-2 TURNER,C.E. Study of the symmetrical elastic loading of some shells of revolution with special reference to toroidal elements. J.Mech. Eng.Sci. 1,2,1959.

6-3 TURNER,C.E. Introduction to Plate and Shell Theory. London,Longmans,1965.

6-4 FOX,L. The Numerical Solution of Two-point Boundary Problems in Ordinary Differential Equations. Oxford, Claradon Press, 1957.

6-5 FORD,H. and ALEXANDER,J.M. Advanced Mechanics of Materials. London,Longmans,1963.

6-6 YAMADA,Y., YOSHIMURA,N. and SAKURAI,T. Plastic stress-strain matrix and its application for the solution of elastic-plastic problems by the finite element method. Int. J.Mech.Sci. 10,5, 343-354, May 1968.

7-1 JOHNS,R.H. and ORANGE,T.W. Theoretical elastic stress distributions arising from discontinuities and edge loads in several shell-type structures. NASA TR-R-103,1961.

7-2 TURNER,C.E. and FORD,H. Stress and deflexion studies in pipe line expansion bellows. Proc. Inst. Mech. Engr. 171,15,526-544,1957.

7-3 TURNER,C.E. Stress and deflection studies of flat-plate and toroidal expansion bellows, subjected to axial, eccentric or internal pressure loading. J. Mech. Eng. Sci. 1,2,130-143,1959.

8-1 CRISP,R.J. A computer survey of the behaviour of torispherical drum heads under internal pressure loading,Part 11, The elastic-plastic analysis. To be published.

8-2 RODABAUGH,E.C. and CLOUD,R.L. Assessment of the plastic strength of pressure vessel nozzles. Trans. ASME, J. Engg. Industry,90,636-643,1968.

8-3 LANGER,B.F. Design of pressure vessels for low-cycle fatigue. Trans. ASME,J. Basic Engg. 84, 389,1962.

8-4 COFFIN,L.F. Jr. A study of the effects of cyclic thermal stresses in ductile metals. Trans.ASME, 76, 931-950,1954.

8-5 MARCAL,P.V. and TURNER,C.E. Limited life of shells of revolution subjected to severe local bending. J. Mech. Eng. Sci. 7,4,408-423,1965.

8-6 BLOMFIELD,J.A. and JACKSON,P.B.M. Fatigue tests on some cupro-nickel pipe bends and a comparison of some failure prediction methods. Accepted for Int. Conf. Pressure Vessel Tech., Delft, ASME-KIVI, 2, paper 38,1969.

8-7 LECKIE,F.A. and PAYNE,D.J. Some observations on the design of spherical pressure vessels with flush cylindrical nozzles. Proc. Inst. Mech. Eng. 180,1,20,497-512,1965-66.

8-8 FINDLAY,G.E. and SPENCE,J. Applying the shake-down concept to pressure vessel design. Engineer, 226,63,12th July 1968.

8-9 PROCTER,E. and FLINDERS,R.F. Shakedown investigations on partial penetration welded nozzles in a spherical shell. Nuc. Eng. Design. 8,1,171-185,1968.

8-10 STODDART, J.S. A study of the initial yield and ultimate collapse of torispherical pressure vessel heads. Ph.D. Thesis, Univ. Durham,May 1967.

8-11 HODGE,P.G. Limit Analysis of Rotationally Symmetric Plates and Shells.Ch.9. London,Prentic-Hall,1963.

8-12 McCRACKEN,D.D. & DORN,W.S. Numerical Methods and Fortran Programming. Ch.8. New York, Wiley.1954.

8-13 MARCAL,P.V. and TURNER,C.E. Elastic-plastic behaviour of flush nozzles in spherical pressure vessels. J. Mech. Eng.Sci.9,3,182-189,1967.

9-1 AMERICAN SOCIETY OF MECHANICAL ENGINEERS. Nuclear vessels, Boiler and Pressure Vessel Code, Sec.III, 1965.

9-2 MERSHON,J.L. PVRC research on reinforcement of openings in pressure vessels. Weld. Res. Council Bull. No.77,May 1962.

9-3 MERSHON,J.L. Preliminary evaluation of PVRC photo-elasticity data on reinforced openingsiin pressure vessels. Ibid. No.113, April,1966.

9-4 BRITISH STANDARDS INSTITUTION. Fusion Welded Pressure Vessels For Use In The Chemical, Petroleum And Allied Industries, Part 1, Carbon And Low Alloy Steel. BS 1500 Part 1,1958.

9-5 BRITISH STANDARDS INSTITUTION. Fusion Welded Pressure Vessels (Advanced Design And Construction) For Use In The Chemical, Petroleum And Allied Industries, Part 1, Carbon And Ferritic Alloy Steels. BS 1515, Part 1.1965.

9-6 BRITISH STANDARDS INSTITUTION. Carbon And Low Alloy Steel Pressure Vessels For Primary Circuits Of Nuclear Reactors. BS 3915,1965.

9-7 MORRISON,J.L.M. The yield of mild steel with particular reference to the effect of size of specimen. Proc. Inst. Mech. Eng. 142,193-223, 1939.

9-8 ALEXANDER,J.M. & BREWER,R.C. Mechanical Properties of Materials, Section 1.3.2. Van Nostrand,1963.

9-9 JOHNSON,W. and MELLOR,P.B. Plasticity for Mechanical Engineers,Section 6.6. Van Nostrand, 1962.

9-10 WATTS,A.B. and FORD,H. An experimental investigation of the yielding of strips between smooth dies. Proc. I. Mech. E., 1B,p.448,1952.

9-11 KOENIGSBERGER,F. Design for Welding in Mechanical Engineering, Ch.6. Longmans Green,1948.

10-1 BESKIN,L. Strengthening of circular holes in plates under edge loads. Trans.ASME 66,p.A-140, 1944.

10-2 GALLETLY,G.D. Analysis of discontinuity stresses adjacent to a central circular opening in a hemispherical shell. Report 870. David Taylor Model Basin, Washington, D.C.1956.

10-3 BIJLAARD, P.P. Local stresses in spherical shells from radial or moment loadings. Weld.J. Res. Supp. May 1957.

10-4 BIJLAARD,P.P. On the stresses from local loads on spherical pressure vessels and pressure vessel heads. Weld. Res. Council Bull. No.34. March 1957.

10-5 LECKIE,F.A. and PENNY,R.K. Solutions for the stresses at a nozzle in pressure vessels. Ibid. No.90. Sept.1963.

10-6 TAYLOR,C.E. and SCHWEIKER, J.W. A- 3-dimensional photoelastic investigation of the stresses near a reinforced opening in a reactor pressure vessel. Proc. Soc. Expt. Stress Analysis. 17, p.25,1959.

10-7 LEVEN,M.M. Photoelastic analysis of reinforced openings in cylindrical,spherical, and torispherical shells subjected to internal pressure. Res. Report 63-917-514-RI. Westinghouse Res. Lab., Pittsburgh, Penn. Feb.1963.

10-8 RILEY,W.F. Experimental determination of stress distribution in thin walled cylindrical and spherical pressure vessels with circular nozzles. NASA CR-53580. Dec.1963.

10-9 ZIENKIEWICZ,O.C. and CHEUNG,Y.K. The Finite Element Method in Structural and Continuum Mechanics. McGraw-Hill.1967.

10-10 FRIEDRICH,C.M. SEAL-SHELL-2 -A Computer program for the stress analysis of a thick shell of revolution with axisymmetric pressures, tem - peratures, and distributed loads. WAPD-TM-398. Bettis Atomic Power Lab., Pittsburgh,Pa.,Dec.1963.

10-11 PILGRIM,W.R.,CHEUNG,J.S.T. and MARCAL,P.V. Computer program for elastic analysis of pressure vessels. RD-C-N-22, Central Elect. Generating Board,London, June,1965.

A P P E N D I C E S

Appendix A

Item A-1 Flow diagram of elastic shell program 'PVA1'.

A-2 Flow diagrams for elastic-plastic shell program 'PLINTH', (a) Main program, (b) Main control routine 'MASTER'.

A-3 Errata and correction to Ref.(3-49) concerning description of elastic-plastic program.

FLOW DIAGRAM OF ELASTIC

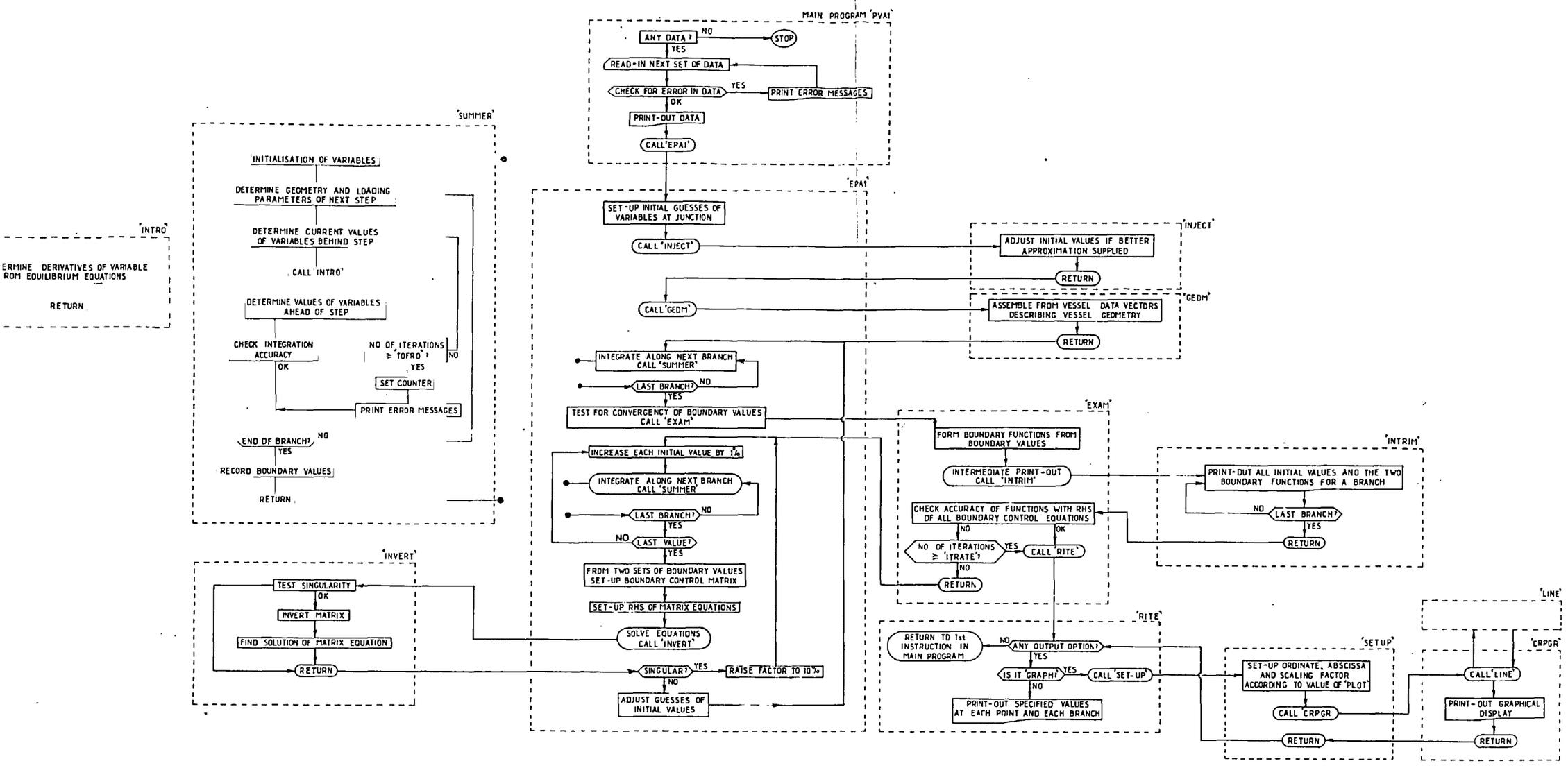

Other subroutines

'BLOCK' — A Block Data Subroutine
Initiates various program parameters and defines values of constants.

'MERGER' — Required when axial displacement is specified Superposition two solutions.

'RBAND' } — Required for 'O'Connell modification'
'BANDER' } — i e spreading load interaction at junction into a band of finite width

'BOUND' — A Function Subroutine Determines Boundary Function for any solution

This is a basic flow diagram, and does not include the following special cases:

1. Loading through fixed axial displacement
2. Loading at junction, Body force loading, Point loading
3. 'O'Connell modification' of load interaction at the junction

J.S T Cheung
Nov 1966

MAIN PROGRAM 'NOZLE'

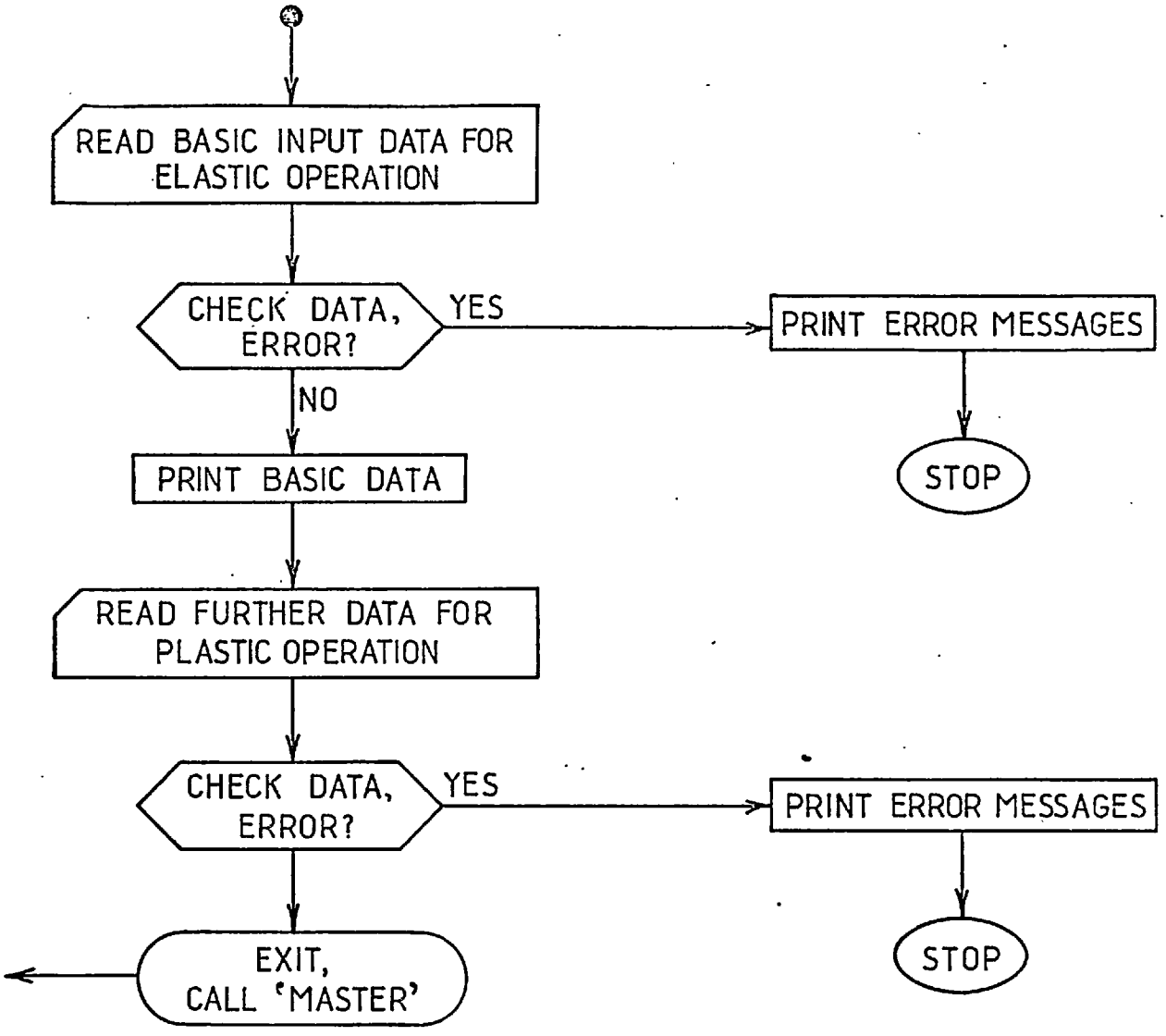

Subroutine MASTER

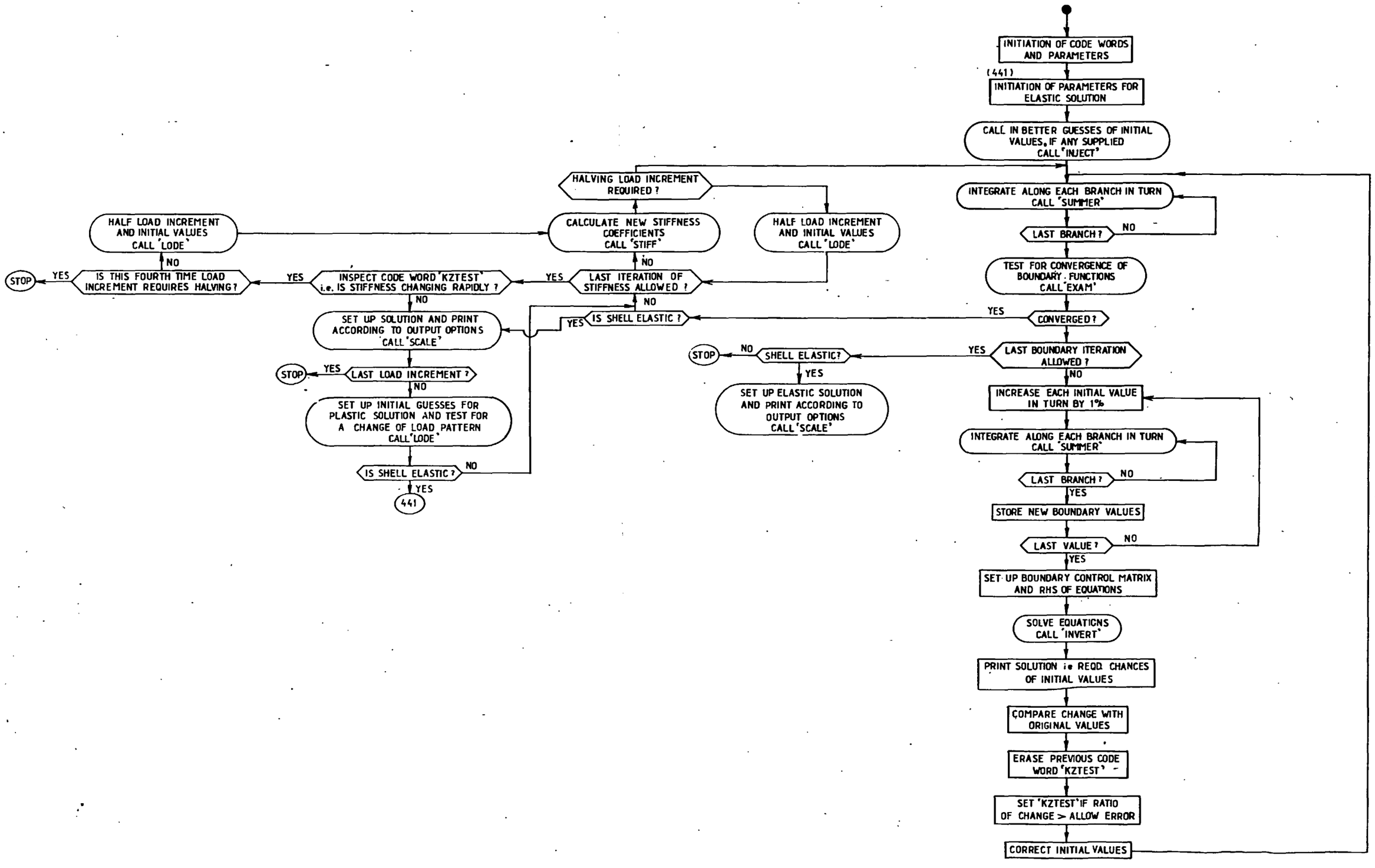

A-3 Errata and Correction to Ref.(3-49).

The following errata and corrections are necessary to Ref.(3-49) by Marcal and Pilgrim in the Journal of Strain Analysis,1966.

Page 341 Line 7 should read,"where m = additional strain required to cause yield/strain caused by".

Line 4, last paragraph of 'Generalized Stiffness Coefficients' should read, "divided into a maximum of ten equal intervals through the thickness and".

Page 347 Last line of page should read "branch j with starting values X^A_{ij}, i = 1 to 4."

Page 348 Last Line,paragraph 3, should read " ..... i.e. by $f_j\ (X^A_{ij}) = 0$,$g_j\ (X^A_{ij}) = 0$. "

Next paragraph,the two derivatives should read, " $\frac{\partial f_j}{\partial X^A_{ij}}$, $\frac{\partial g_j}{\partial X^A_{ij}}$ ".

Following lines,same paragraph,eq.(31a) and (31b) should read,

$$\sum_{i=1}^{4} \frac{\partial f_j}{\partial X^A_{ij}} \Delta X^A_{ij} = -f_j(X^A_{ij}) \qquad (31a)$$

$$\sum_{i=1}^{4} \frac{\partial g_j}{\partial X^A_{ij}} \Delta X^A_{ij} = -g_j(X^A_{ij}) \qquad (31b)$$

Next but one paragraph,lines (a) and (b) should read,

" (a) u is common for all branches, i.e. $X^A_{11} = X^A_{1j}$, j = 2 to M.

(b) ϕ is common for all branches, i.e. $X^A_{21} = X^A_{2j}$, j = 2 to M. "

Appendix B

Two Methods of Approximating Nozzle Junction Geometry With Thin-Walled Shell Elements, And A Comparison of Their Accuracy With Photoelasticity Results.

B.1 Simple and Smooth Representation of Nozzle Geometry

The thin-walled shell theory for shells of revolution, on which all the analysis with the computer programs are based, defines a shell according to the generating line of the shell mid-wall surface and the shell thickness, this being the perpendicular distance between the exterior and interior walls. A shell with two portions of different shapes is assumed to be joined at the intersection of these mid-wall lines. Because of this a pressure vessel nozzle is commonly represented as a cylinder intersecting a convex end, the latter being usually spherical. This we shall call the 'simple geometrical representation' of the junction, to distingusih from other refined representations. The shells are here assumed to end at the point of intersection of the mid-wall lines. From Fig.B-1, it can be seen that the corner of the actual junction is not represented while the location of the fillet is not clear. For these reasons it has always been difficult to give meaning to the stress calculated at the junction in terms of their actual loaction. This is a serious drawback of the simple representation since, in most cases, the stresses at the junction are the crital ones.

From calculations based on shell theories, it is known that stresses at a change of shell thickness are unrealistically high when an abrupt change is assumed. The stresses actually measured are very often found to be

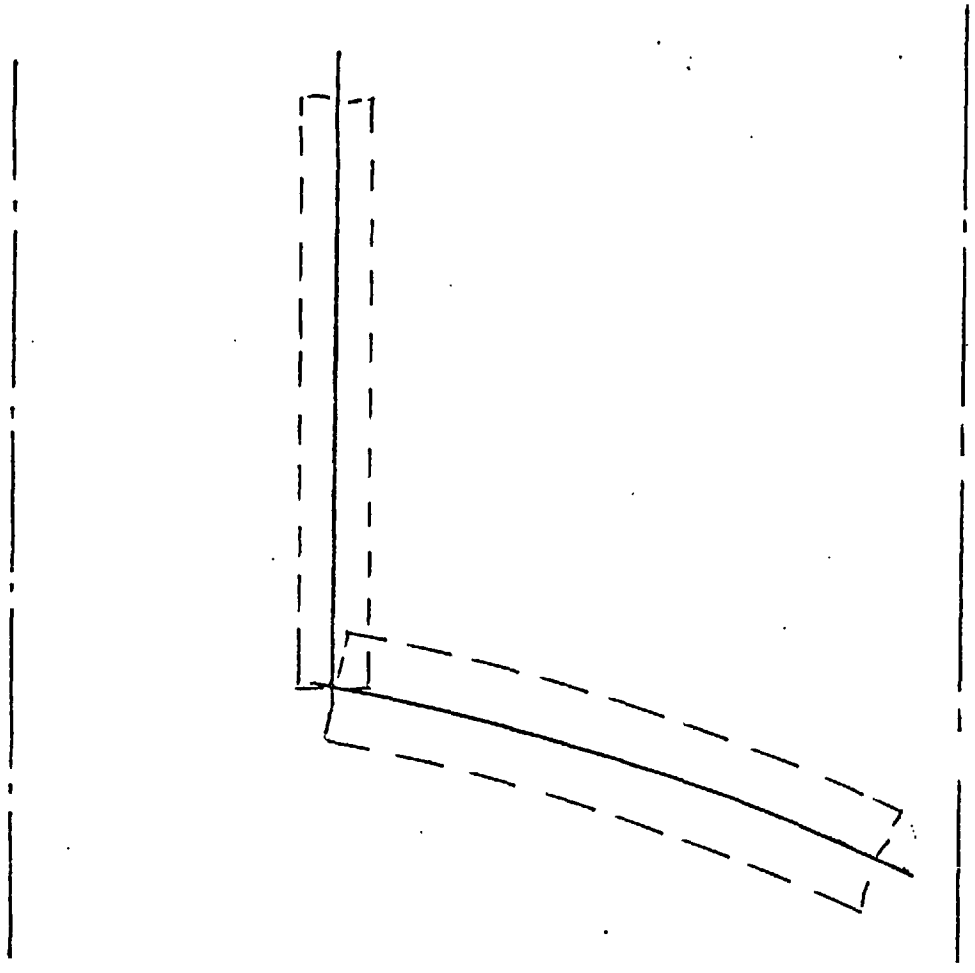

SIMPLE REPRESENTATION

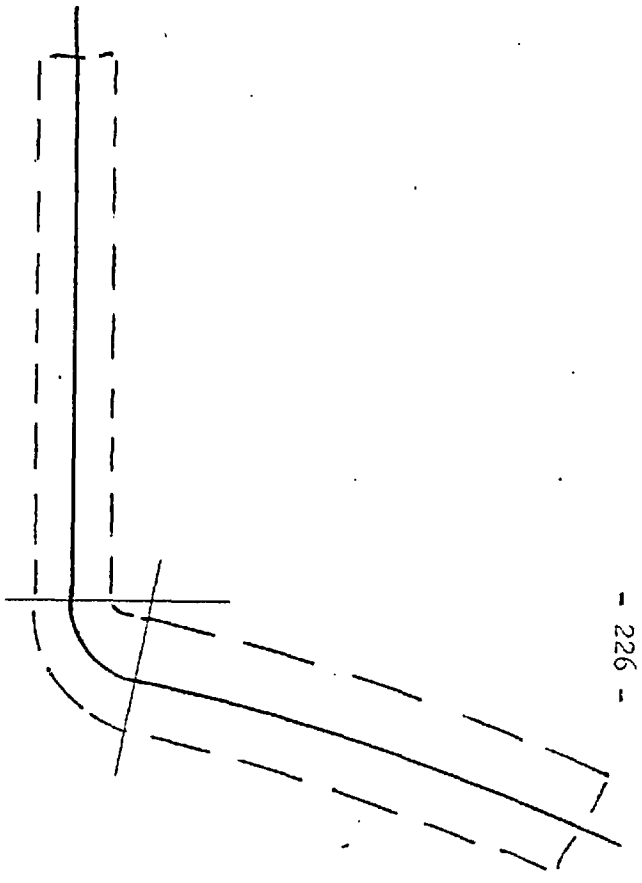

SMOOTH REPRESENTATION

FIG B-1 METHODS OF APPROXIMATING NOZZLE JUNCTION GEOMETRY

lower. A similar situation should exist between nozzle calculations and experimental measurements. The nozzle has in general a different thickness to that of the vessel. The simple representation for such cases will thus also have an abrupt change of thickness through the junction, while the actual junction may be left with a fillet weld or may be subsequently rounded or even may be constructed with a forged ring reinforcement. Thus it is not surprising that such calculations give higher values of stresses.

A small torus element of tapering thickness inserted between the cylinder and the sphere would remove both the thickness discontinuity and slope discontinuity of the meridian line,(see Fig.B-1). The nozzle thus represented in calculations is said to have a 'smooth junction representation'. No change to PVA1, the program being used, is necessary to specify this. Both a uniformly tapered element, and tori of positive as well as negative curvature, are allowed in the specification of geometrical data. There is however one difficulty in the representation. The actual junction in general can be rounded to different fillet and corner radii. Unless these radii have a special relations to each other, the smooth representation by the torus can only follow one of them. Mershon in interpretating a comprehensive series of experimental results carried out at the United States has noted that the stresses in the corner zone are almost independent of the fillet and corner radii. For this reason the fillet radius of the actual vessel is used to define the curvature of the torus. Although this is still not a perfect approximation, but any

further attempts at a better fit would be impractical. Point by point matching would have to be used, and the method will definitely be too cumbersome for normal design investigations.

When nozzles are designed against fatigue failures, both elastic or more often low-cycle fatigue actions, it is very desirable that nozzles be attached by full penetration welds and with corner and fillet rounded to adequate radii. In the 1965 British Standard 1515, they are left to the discretion of the designers. However in the 1963 A S M E Nuclear Vessel Code, these are laid down as necessary requirements for nozzle attachments. Except for minor attachments with no piping reactions and under small thermal stresses, full penetration welds are to be used in all cases. A radius not less than $\frac{1}{4}$ of the vessel thickness is required at the corner of flush nozzles. Fillet welds are to be ground to a smooth surface with transition radius not less than $\frac{1}{4}$ of the thickness of the thinner part being joined. For flush nozzles thus designed, the above mentioned method of representation can be used with ease, and should give satisfactory approximation of the true shape.

B.2 Comparison with Photoelasticity Results

Program PVA1 is based on thin-wall shell theory according to Turner. A comprehensive test of its reliability and accuracy has been conducted and reported in Ref.3-32 and Ch.7. It was concluded that the program was reliable and accurate to within the assumptions of the shell theory, and the accuracy of the shell geometrical representation and loading specification.

The ultimate test of any method of theoretical stress analysis must be made against actual measurements. Hence to establish this method of calculating nozzle stresses, the method must be checked against stress measurements of actual pressure vessel nozzles. For obtsining the latter, both strain gauge analysis and three dimensional photoelasticity can be used. It is however found that many published experimental results of pressure vessel nozzles are not suitable for this purpose. The peak stresses of interest are usually concentrated over small areas and many experiments were not conducted to measure accurately these stresses. Many of the other available results are not accurate enough for fine comparisons.

The Pressure Vessel Research Committee of the United States sponsored a series of programs of photoelastic tests on nozzles. Although many of these tests were on thick-wall vessels not accurately covered by the thin-wall theory on which PAV1 was based, a sufficient number of the rest remains to enable a good selection of a variety of shapes and dimensional parametric ratios. Nozzles WN-10D, WS-1LB, S-2AZ, N4-E and N4-A (labelled here nozzles 1,2,3,4 and 5) all tested photoelastically under internal pressure were chosen and compared against computations using the two representations.

Fig.B-2 shows the cross-sectional shapes of the five nozzle models. They are not drawn to the same scale, but are proportioned to have the same inside diameter of the spherical vessel. The dimensional ratios of these nozzles are given, Table B-1 below. D_i, d_i are the inside

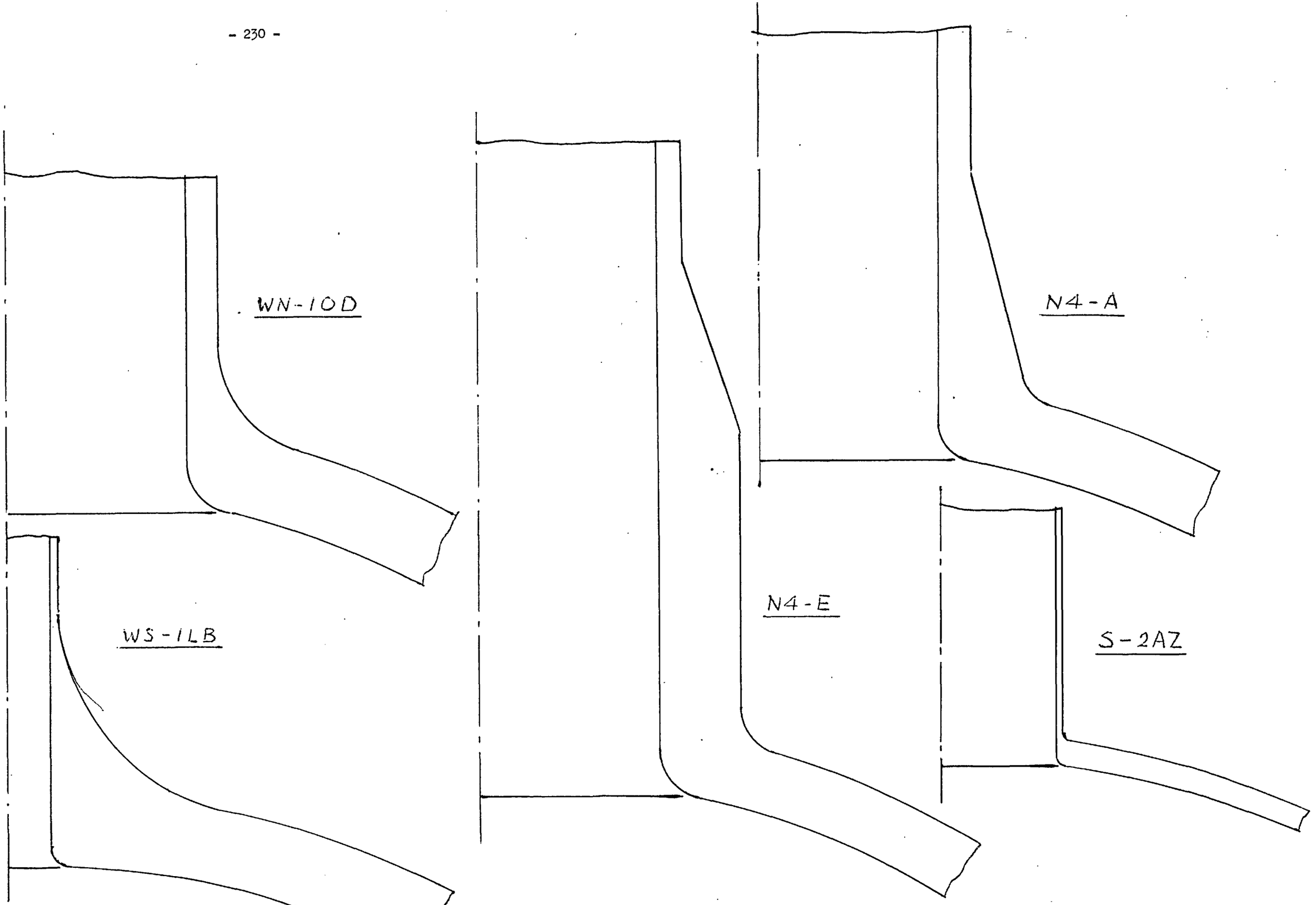

FIG B-2 GEOMETRY OF PHOTOELASTIC MODELS

Nozzle	Code No.	$\frac{D_i}{T}$	$\frac{d_i}{t}$	$\frac{d_i}{D_i}$	$\frac{t}{T}$	$\frac{r_o}{T}$	$\frac{r_i}{T}$
1	WN-10D	24.1	11.7	0.20	0.41	1.56	0.56
2	WS-1LB	24.2	11.5	0.05	0.105	2.95	0.25
3	S-2AZ	72.0	35.4	0.129	0.261	0.25	0.25
4	N4-E	27.0	4.4 14.0	0.20	1.23 0.39	0.77	0.77
5	N4-A	24.8	11.5	0.20	0.43	0.58	0.58

Table B-1 Dimension Ratios for Axisymmetric Nozzles

diameters of the vessel and nozzle respectively; T, t are their respective thicknesses. r_o and r_i are the (outside) fillet radius and the (inside) corner radius of the junction. Nozzles, 1,2 and 3 have normal rounded corner and fillet. Among them the latter two have the same r_o and r_i, but the former two have larger fillet radius r_o than r_i. Nozzles 4 and 5 have each a different type of local reinforcement. Here because of the additional reinforcements the contribution of the fillet to the reinforcing effect is negligible small, although it still has a definite radius. Nozzles 1,2,4 and 5 have similar diameter/thickness ratio to each other. They are reasonably thick walled (with nozzle di/t ratio between 11 and 12) and lie in the transitional zone where the thin-wall theory may begin to lose accuracy. Nevertheless there is no reason to assume that this probable loss of accuracy may alter, to different degrees, the accuracy of results of the two different junction representations. Thus comparisons can still be made between the two representations. Nozzles 3 has thinner walls than the others.

Table B-2 gives the results of the calculations tested alongside the experimental results. The stresses are expressed as stress concentration factors. The membrane circumferential stress of the sphere is used as unit stress. The maximum stress peaks and minimum stress troughs for the whole shell are tabulated for the external and internal surfaces, and in the meridional and circumferential directions. Spaces are left blank when such peaks or troughs do not exist, or when the peaks do not exceed the membrane value. The maximum values for nozzle and

Table B-2 Axisymmetric Nozzles Under Internal Pressure:

Stress concentration factor obtained from different methods of analysis

Nozzle No.	Nozzle Code	Method of Analysis	External Surface Circ. Max.	External Surface Circ. Min.	External Surface Merid. Max.	External Surface Merid. Min.	Internal Surface Circ. Max.	Internal Surface Circ. Min.	Internal Surface Merid. Max.	Internal Surface Merid. Min.	Error (%)	Ref.
1	WN-10D	Photoelastic	1.68	0.80	1.15	0.20	1.91	0.98	---	-.033		B-1
		PVAl,simple	4.53	0.81	4.66	-0.12	1.98	0.97	---	-3.64	+140	
		PVAl,smooth	2.43	0.87	1.61	0.06	1.88	0.99	---	-0.33	+ 27	
2	WS-1LB	Photoelastic	1.07	0.13	1.13	-0.14	2.03	0.21	---	-0.17		B-1
		PVAl,simple	3.49	0.82	3.12	-0.61	1.78	0.87	---	-2.13	+ 70	
		PVAl,smooth	1.77	0.04	1.49	-0.55	1.78	0.43	---	-0.04	- 12	
3	S-2AZ	Photoelastic	4.75	NA	3.00	NA	2.50	NA	NA	-2.50		B-2
		PVAl,simple	6.26	0.71	7.07	-0.39	2.37	-0.31	1.41	-6.07	+ 50	
		PVAl,smooth	5.11	0.71	4.40	-0.40	2.39	-0.94	1.40	-3.40	+ 8	
4	N4-E	Photoelastic	1.73	0.14	1.68	-0.20	1.68	0.53	---	-0.12		B-3
		PVAl,simple	2.15	0.15	1.88	-0.36	1.21	0.46	---	-0.82	+ 24	
		PVAl,smooth	2.06	0.13	1.71	-0.43	1.48	0.48	---	-0.38	+ 19	
5	N4-A	Photoelastic	1.79	0.23	1.74	-0.23	1.77	---	---	-0.09		B-4
		SEAL-SHELL 2	1.66	0.39	1.50	-0.23	1.80	---	---	-0.03	+ 1	B-5
		PVAl,simple	2.21	0.39	1.62	-0.25	1.26	---	---	-0.18	+ 23	
		PVAl,smooth	1.92	0.12	1.65	-0.37	1.40	---	---	-0.27	+ 7	

vessel are underlined. The difference between this maximum value and the corresponding experimental value is expressed as a percentage error shown on the column on the right-hand side.

The two methods of representation were both calculated with program BVA1. In the simple representation a discontinuity of the shell wall direction was allowed at the junction as in Fig. B-1. When necessary, shell walls with tapered thickness were used as in nozzle 4 and 5. The smooth representation calculations differ only by the geometrical specification at the junction.

The results show in general that calculations with simple representation give a maximum stress at the junction higher than that actually found. This is especially so for nozzles 1, 2, and 3 where the different calculated stresses are very much different from the actual stresses. Prediction errors of 140%, 70% and 50% respectively occur for the maximum tensile stresses. The calculations also show high compressive stresses in the meridional direction at the inner wall, but no such stress concentrations are found at the actual vessels. All these erroneously high stress peaks lie at the common discontinuity point between the nozzle and vessel, locating more often on the vessel side. It is further noticed that the three nozzles with very bad predicted results have, adjascent to the junction, a greater change of shell thickness than the others. All these evidence seem to show that the sudden change of shell thickness necessary in using the simple representation will give unrealistic stress peaks.

The calculations with smooth junctions show a marked

improvement. The greatest error is 22% for nozzle 1 whereas the simple representation gives a 140% error for the same case. The calculations all predect a stress slightly above that found by experiment. The only exception is nozzle 2; this nozzle is unusually proportioned with the fillet radius very much greater than the corner radius, and thus the method of representation cannot approximate closely to the shape with a tapered torus. Since the representation follows the value of the fillet radius, this results in an over-rounded corner and a low prediction of stresses. Nevertheless the calculation for this nozzle is only out by 12%. This shows that the method of representation can safely be used for a wide range of junction geometry.

B.3 References

B-1 LEVEN,M.M. Photoelastic analysis of reinforced openings in cylindrical,spherical, and toro-spherical shells subjected to internal pressure. Westinghouse Res.Lab. Report 63-917-514-R1,N63-23497, Feb.1963.

B-2 MERSHON,J.L. PVRC research on reinforcement of openings in pressure vessels. Weld. Res.Council Bull.77, May 1962.

B-3 TAYLOR,C.E. and SCHWEIKER,J.W. A three-dimensional photoelastic investigation of the stresses near a reinforced opening in a reactor pressure vessel. Proc. Soc. Expt. Stress Analysis,17,1,25-36,1960.

B-4 TAYLOR,C.E.,LIND,N.C. and SCHWEIKER,J.W. A three-dimensional photoelastic study of stress around reinforced outlets in pressure vessels. Weld. Res. Council Bull.51, June,1959.

B-5 FRIEDRICH,C.M. SEAL-SHELL-2. A computer program for the stress analysis of a thick shell of revolution with axisymmetric pressures, temperatures, and distributed loads. Bettis Atomic Power Lab., Pittsburgh. WAPD-TM-398, Dec.1963.

Appendix C
Modifications to Elastic-Plastic Program PLINTH to Accept for a Better Approximation Solution Shells With Large Meridional Curvature.

C.1 Basic Difference of Better Approximation Theory

The linear thin-walled shell equations by Turner (6-3) used in the pressure vessel programs assumed not only that the wall thickness 2h is small compared with the circumferential radius of rotation r , but also that 2h is small compared with the two radii of curvature. The derivation of the equations are given in Ref.6-3, and with minor modifications to the notations and sign conventions, these equations are repeated in Refs.3-32 and 3-49 in the forms as used in the two programs. The following discussions considers the modifications necessary to the basic sets of equations to give a better approximation solution when the meridional curvature radius b is not large compared with thickness 2h.

Equilibrium Equations

Turner's shell element, see Fig.6-1, is straight sided in the meridional direction. In general the shell equations express the conditions of equilibrium between the generalised interal forces S (i.e. direct force, shear force and bending moment) and the external and body loading L on the element. Three equations are necessary, two giving the equilibrium conditions of the two possible translatory movements, and the third for possible rotational movement, all along a radial plane through the shell central axis.

$$f_1 \ (S \ , L \ ) = 0$$

$$f_2 \ (S, \ L \ ) = 0$$

$$f_3 \ (S, \ L \ ) = 0$$

The equations should contain terms governed by the shape of this assumed infinitesimal shell element, since the element shape and its alignment govern the direction of actionof these generalised internal forces S.

The basic linear theory assumes, Fig.6-1, that the element is straight along the meridian and curved along the circumference, with lengths dl and $rd\psi$ respectively. When an element is flat and has all sides straight, as that used in plate theory, the direct force on the sides would not contribute to the resistance against pressure or outward-directed body force, and the full resistance against them would be taken by the transverse shear. With the curved circumferential edge, the shell element here allows the circumferential direct force N_ψ to contribute to this resistance, while the straight meridional edge means that the contribution of the meridional direct force N_θ is neglected in companison with the action of transverse shear. To a first order of accuracy, this being a linear first order theory, this is true. In applying this theory, inaccuracy should not arise for non-shallow shells, where the transverse pressure and body forces do not give rise to large stretching forces and for shells with straight or near-straight meridian - i.e. those approximating to a cylinder, cone or disc.*

* An important observation from these discussion, although not of immediate interest here, is that the crown regions of torispherical and elliptical vessel heads do not come under these two categories, and the basic theory may not be adequate for accurate solution unless special shallow shell equations are used. This possible inaccuracy affects of course the solution near to this region and not otherwise.

There are two alternatives open to the proposed modified theory. The more accurate alternative is to allow of a non-linear stress distribution across the shell thickness and at the same time use a shell element with curved meridional edge. The simplier alternative allows of a non-linear stress distribution, but the element remains the same shape. After preliminary investigation into both, it was found that the first one requires a completely new derivation of the shell equations. Also, the second alternative is found to have the same limitation as the basic theory, that good accuracy would be obtained only for non-shallow or straight sided shells, but a good accuracy of solution for a small curvature radius b should be attained if, in the numerical calculation, dl is small compared with b.

The second alternative is thus used in this investigation, because of the much smaller amount of work involved in the alternation. The same shell element is used, with modifications to the internal stress distribution. For this element, the basic expressions for the equilibrium equation should be the same as before. This is because the shell equations, as observed, depend on the shape and alignment of the elements and on the arrangement of the generalised forces and loadings, and not on how the internal stress is distributed to give the generalised forces.

Geometry of Deformation

(a) Mid-wall Strains

In the basic theory, the mid-wall strains $\bar{e}_\psi$ and $\bar{e}_\theta$ are related to the displacements u , v and rotation ϕ , see

Fig. 6-1, by the expressions

$$\bar{e}_\psi = u / r$$

$$du/dl = -\phi \cos\theta + \bar{e}_\theta \sin\theta$$

Under the new assumptions, the expression for circumferential strain $\bar{e}_\psi$ would not be affected, since this is independent of the curvature of the shell element. The mid-wall circumfernetial circle increases in length during straining, from $2\pi r$ to $2\pi (r + u)$, and causes a strain of

$$\bar{e}_\psi = \frac{2\pi(r+u) - 2\pi r}{2\pi r} = \frac{u}{r}$$

The expression for mid-wall meridional strain $\bar{e}_\theta$ is obtained by equating the change of radial displacement du to the components caused by meridional straining and rotational straining. Consider what happens if, for accuracy, one takes a curved meridional edged element Fig. C-2, with a change of inclination from θ at the bottom edge to $\theta + d\theta$ at the top edge, giving $d\theta = - dl/b$. After straining, the displacements at the bottom edge are u and v, while that at the top edge are u + du and v + dv. As in the derivation of $\bar{e}_\theta$ in the basic theory, du and dv consist of a combination of meridional straining, $\bar{e}_\theta$ dl in the direction $\theta + d\theta$ of the top edge, and of rotational movement, ϕ dl in the perpendicular direction. Resolving components in the radial direction,

$$du = -\phi \cos(\theta + d\theta) dl + \bar{e}_\theta \sin(\theta + d\theta) dl$$

The effect of $d\theta$ is of second order and can be neglected, leaving

$$du/dl = -\phi \cos\theta + \bar{e}_\theta \sin\theta$$

which is the same expression as the basic theory.

(b) Strains at a General Shell Fibre.

At a general shell fibre, Fig. C-1, at distance z perpendicular to the shell element mid-surface, the basic theory relates the general strains e_ψ and e_θ at this fibre to $\bar{e}_\psi$ and $\bar{e}_\theta$ by

$$e_\psi = \bar{e}_\psi + z \frac{\sin\theta}{r} \phi$$

$$e_\theta = \bar{e}_\theta + z \frac{d\phi}{dl}$$

It can be seen that here the meridional strain e varies linearly across the shell wall, since

$$e_\theta - \bar{e}_\theta \propto z$$

This is not necessarily so when the meridional curvature is not large relative to the thickness, b not $\gg$ 2h.

In a better first approximation to such a case, only the more basic assumption is made, that the cross-sectional planes at the top and bottom edges of the shell element remain plane during deformation. Consider temporarily again the initially curved element, Fig. C-2, with curvature radius b, b being positive when the centre is inside the shell of revolution.

A general fibre at distance z from mid-surface has a meridional length $(b + z)\ (dl/b) = (1 + z/b)\ dl$. Under strain, the mid-surface fibre extends by $\bar{e}_\theta\ dl$. In addition, the element suffers a rotation of ϕ at the bottom edge and $\phi + d\phi$ at the top edge, causing an extension at the general fibre of $z d\phi$. The total charge in length of this general fibre is

$$\bar{e}_\theta\ dl + z d\phi$$

The corresponding strain is thus

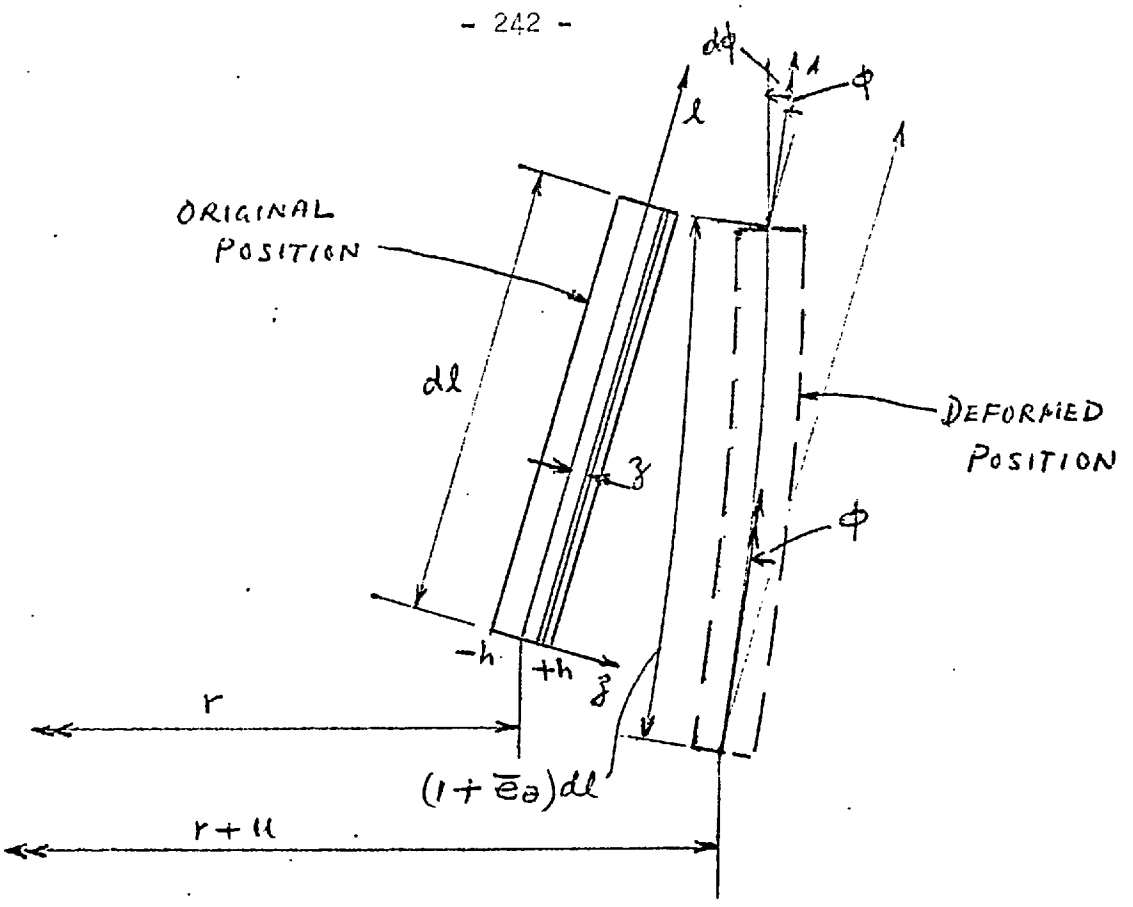

FIG C-1 GEOMETRY OF DEFORMATION OF STRAIGHT SIDED ELEMENT

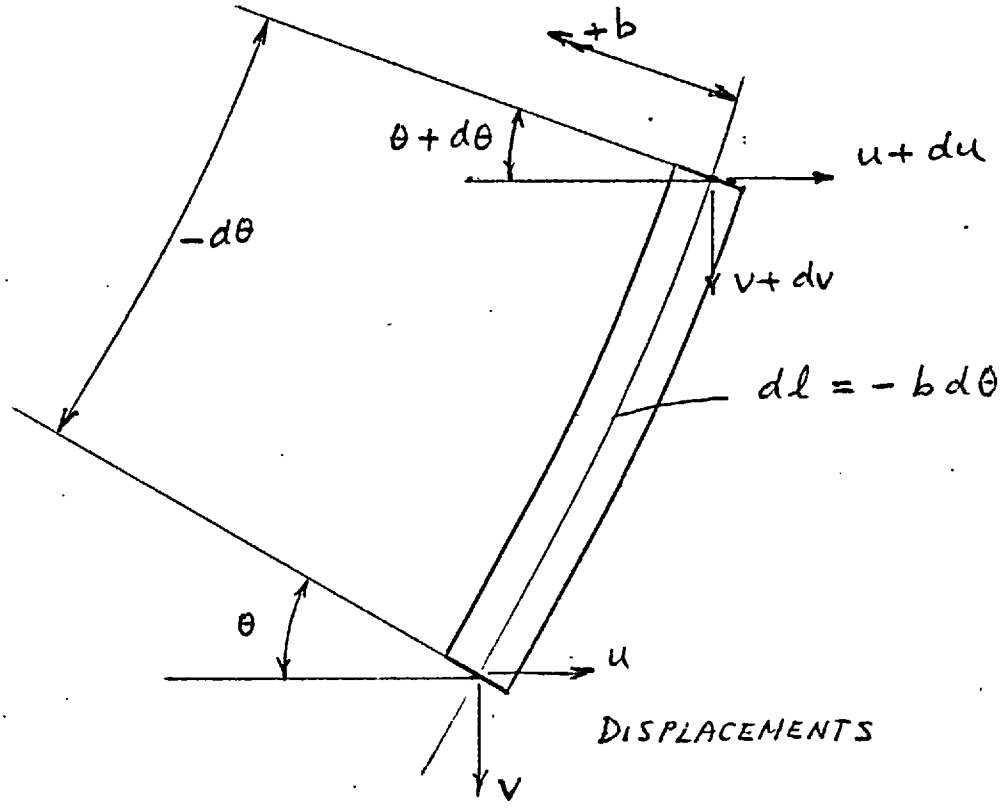

FIG C-2 CURVED SIDED ELEMENT

$$e_\theta = \frac{\bar{e}_\theta dl + z d\phi}{(1 + z/b)\, dl}$$

$$= (\bar{e}_\theta + z \frac{d\phi}{dl}) / (1 + z/b)$$

This is different to the basic expression by the factor $(1 + z/b)$.

The circumferential strain e can be obtained by determining the radial displacement of the general fibre. The mid-surface fibre has a radial displacement given by u . Due to a rotation ϕ , the additional displacement at the general fibre is $z\phi \sin\theta$, giving a total displacement $u + z\phi \sin\theta$.

Original length of a circumferential circle through point z is $2\pi (r + z \cos\theta)$.
Under straining, this length is $2\pi (r + z \cos\theta + u + z\phi \sin\theta)$. The circumferential strain is thus

$$\bar{e}_\psi = \frac{2\pi(r + z\cos\theta + u + z\phi\sin\theta)}{2\pi(r + z\cos\theta)} - 1$$

$$= (u + z\phi\sin\theta) / (r + z\cos\theta)$$

i.e. $$e_\psi = (\bar{e}_\psi + z \frac{\sin\theta}{r} \phi) / (1 + \frac{z}{r}\cos\theta)$$

In the basic theory, it is taken that $\frac{h}{r} \ll 1$, and since the better approximation considered here only deals with cases h/b not $\ll 1$ and not other cases, thus the term $\frac{z}{r}\cos\theta$ is here neglected in the denominator*, leaving

* The neglect of this term is not justified when either h/r not $\ll 1$, or θ not aproaching 90°. This happens at the apex of a closed shell when the closure is in the form of a cone whose semi-included-angle is not near to 90°.

$$e_\psi = \bar{e}_\psi + z\,(\sin\theta/r)\,\phi$$

which is the same as that of the basic theory.

Stress-strain Relations

The stress-strain relations, elastic or elastic-plastic, are for the condition at a local fibre and the expressions are unrelated to the shape and geometry of the shell element. They should thus be the same in the modified theory.

Conclusions

To accommodate a better approximation for the case of shells with large meridional curvatures, only one expression has to be altered among the set of basic equations of equilibrium , of compatibility at the mid-wall, of compatibility at a general fibre, and of the stess-strain relations. The new expression defines the meridional strain e_θ at a general fibre, and is in the form

$$e_\theta = (\bar{e}_\theta + z\,d\phi/d\ell) / (1 + z/b) \qquad (-h \leq z \leq h)$$

which reverts back to the basic form when $h/b \ll 1$.

C.2 Modifications to the Tangent Modulus Method for Elastic-Plastic Shells of Revolution.

The tangent modulus method as used in the elastic-plastic shell program has been reported by Marcal and Pilgrim, Ref.3-49. In an elastic-plastic analysis, numerical calculations are performed on small increments of loading, each giving the corresponding incremental stress, strain, force, moment and displacements. The relations between

these latter parameters are not straight forward expressions. For the convenience of numerical mainpulation, these relations are expressed in matrix form and the coefficients are called stiffness coefficients and generalised stiffness coefficients. For example, the stress-strain relations for a shell fibre can be written as

$$\begin{bmatrix} \delta\sigma_\theta \\ \delta\sigma_\psi \end{bmatrix} = \begin{bmatrix} \alpha_{11} & \alpha_{12} \\ \alpha_{21} & \alpha_{22} \end{bmatrix} \begin{bmatrix} \delta e_\theta \\ \delta e_\psi \end{bmatrix}$$

where the α coefficients are called the stiffness coefficients. Also, for the stress state at a shell element, the force and moment system consists of N_θ, N_ψ, M_θ, M_ψ. The strain state of the same element can be defined completely by four parameters $\bar{e}_\theta$, $\bar{e}_\psi$, ϕ', ϕ. Again using the increment of these parameters, then relations can be written as

$$\begin{bmatrix} \delta N_\theta \\ \delta N_\psi \\ \delta M_\theta \\ \delta M_\psi \end{bmatrix} = \begin{bmatrix} A_{11} & A_{12} & \cdots & A_{14} \\ A_{21} & & & \vdots \\ \vdots & & & \vdots \\ A_{41} & \cdots & & A_{44} \end{bmatrix} \begin{bmatrix} \delta\bar{e}_\theta \\ \delta\bar{e}_\psi \\ \delta\phi' \\ \delta\phi \end{bmatrix}$$

The A's are called the generalised stiffness coefficients.

As mentioned above in C-1, the stress-strain relations, are not changed in the modified method, thus the α's would remain the same. The expression for $\bar{e}_\theta$ is however changed and this results in a different set of relations defining the generalised stiffness coefficients (G S C). The following discussions give the derivation of these G S C under the modified method.

The δN's and δM's are forces and moments at the edges of a shell element, and can be calculated by integrating

the direct stresses $\delta\sigma_\theta$, $\delta\sigma_\psi$ through the thickness.

$$\delta N_\theta = \int_{-h}^{h} \delta\sigma_\theta \, dz = \int_{-h}^{h} (\alpha_{11} \delta e_\theta + \alpha_{12} \delta e_\psi) \, dz$$

$$\delta N_\psi = \int_{-h}^{h} \delta\sigma_\psi \, dz = \int_{-h}^{h} (\alpha_{21} \delta e_\theta + \alpha_{22} \delta e_\psi) \, dz$$

$$\delta M_\theta = \int_{-h}^{h} \delta\sigma_\theta \, z \, dz = \int_{-h}^{h} (\alpha_{11} \delta e_\theta + \alpha_{12} \delta e_\psi) \, z \, dz$$

$$\delta M_\psi = \int_{-h}^{h} \delta\sigma_\psi \, z \, dz = \int_{-h}^{h} (\alpha_{21} \delta e_\theta + \alpha_{22} \delta e_\psi) \, z \, dz$$

In the basic theory

$$\delta e_\theta = \delta \bar{e}_\theta + z \, \delta\phi'$$

$$\delta e_\psi = \delta \bar{e}_\psi + z \, \frac{\sin\theta}{r} \, \delta\phi$$

However in the modified theory,

$$\delta e_\theta = (\delta \bar{e}_\theta + z \, \delta\phi') / (1 + 3/b)$$

while δe_ψ remains the same.

These result in the relations, (dropping the incremental notation δ, for convenience)

$$N_\theta = \bar{e}_\theta \int \frac{\alpha_{11} \, dz}{(1 + z/b)} + \bar{e}_\psi \int \alpha_{12} \, dz + \phi' \int \frac{\alpha_{11} \, z \, dz}{(1 + z/b)} + \frac{\sin\theta}{r} \phi \int \alpha_{12} \, z \, dz$$

$$N_\psi = \bar{e}_\theta \int \frac{\alpha_{21} \, dz}{(1 + z/b)} + \bar{e}_\psi \int \alpha_{22} \, dz + \phi' \int \frac{\alpha_{21} \, z \, dz}{(1 + z/b)} + \frac{\sin\theta}{r} \phi \int \alpha_{22} \, z \, dz$$

$$M_\theta = \bar{e}_\theta \int \frac{\alpha_{11} \, z \, dz}{(1 + z/b)} + \bar{e}_\psi \int \alpha_{12} \, z \, dz + \phi' \int \frac{\alpha_{11} \, z^2 dz}{(1 + z/b)} + \frac{\sin\theta}{r} \phi \int \alpha_{12} \, z^2 dz$$

$$M_\psi = \bar{e}_\theta \int \frac{\alpha_{21} \, z \, dz}{(1 + z/b)} + \bar{e}_\psi \int \alpha_{22} \, z \, dz + \phi' \int \frac{\alpha_{21} \, z^2 dz}{(1 + z/b)} + \frac{\sin\theta}{r} \phi \int \alpha_{22} \, z^2 dz$$

The program considers separately the cases when the element is at an elastic state and at a elastic-plastic state. The stiffness coefficients at an elastic state

can all be calculated directly as is shown below.

The elastic stress-strain relations for a plane stress system can be written as

$$\sigma_\theta = \frac{E}{1-\nu^2} e_\theta + \frac{\nu E}{1-\nu^2} e_\psi$$

$$\sigma_\psi = \frac{\nu E}{1-\nu^2} e_\theta + \frac{E}{1-\nu^2} e_\psi$$

which give directly, $\alpha_{11} = \alpha_{22} = \frac{E}{1-\nu^2}$

$$\alpha_{12} = \alpha_{21} = \frac{\nu E}{1-\nu^2}$$

Listing the G S C's, we have

$$A_{11} = \frac{E}{1-\nu^2} \int \frac{dz}{1+z/b}, \quad A_{21} = \nu \frac{E}{1-\nu^2} \int \frac{dz}{1+z/b}$$

$$A_{12} = \frac{\nu E}{1-\nu^2} \int dz, \quad A_{22} = \frac{E}{1-\nu^2} \int dz$$

$$A_{13} = \frac{E}{1-\nu^2} \int \frac{z\,dz}{1+z/b}, \quad A_{23} = \frac{\nu E}{1-\nu^2} \int \frac{z\,dz}{1+z/b}$$

$$A_{14} = \frac{\nu E}{1-\nu^2} \frac{\sin\theta}{r} \int z\,dz, \quad A_{24} = \frac{E}{1-\nu^2} \frac{\sin\theta}{r} \int z\,dz$$

$$A_{31} = \frac{E}{1-\nu^2} \int \frac{z\,dz}{1+z/b}, \quad A_{41} = \frac{\nu E}{1-\nu^2} \int \frac{z\,dz}{1+z/b}$$

$$A_{32} = \frac{\nu E}{1-\nu^2} \int z\,dz, \quad A_{42} = \frac{E}{1-\nu^2} \int z\,dz$$

$$A_{33} = \frac{E}{1-\nu^2} \int \frac{z^2 dz}{1+z/b}, \quad A_{43} = \frac{\nu E}{1-\nu^2} \int \frac{z^2 dz}{1+z/b}$$

$$A_{34} = \frac{\nu E}{1-\nu^2} \frac{\sin\theta}{r} \int z^2 dz, \quad A_{44} = \frac{E}{1-\nu^2} \frac{\sin\theta}{r} \int z^2 dz$$

The integrations are all from z = - h to z = h. They can be evaluated directly, some in series form.

$$\int_{-h}^{h} dz = 2h$$

$$\int_{-h}^{h} z\,dz = 0$$

$$\int_{-h}^{h} z^2 dz = \tfrac{2}{3} h^3$$

$$\int_{-h}^{h} \frac{dz}{1+z/b} = 2h\left[1 + \frac{1}{3}\left(\frac{h}{b}\right)^2 + \frac{1}{5}\left(\frac{h}{b}\right)^4 + \cdots\right]$$

$$\int_{-h}^{h} \frac{z\,dz}{1+z/b} = 2hb\left[-\frac{1}{3}\left(\frac{h}{b}\right)^2 - \frac{1}{5}\left(\frac{h}{b}\right)^4 - \cdots\right]$$

$$\int_{-h}^{h} \frac{z^2 dz}{1+z/b} = 2hb^2\left[\frac{1}{3}\left(\frac{h}{b}\right)^2 + \frac{1}{5}\left(\frac{h}{b}\right)^4 + \cdots\right]$$

when $(h/b)^2 < 1$

This leaves A_{14} , A_{24} , A_{33} , A_{43} zero, while in the basic theory A_{13} , A_{23} , A_{31} , A_{41} are also zero. Thus additional terms have to be kept in all expressions making use of these G S C's.

For the elastic-plastic element, the coefficients cannot be expressed in simple formulas since the α's giving the stress strain relations vary from fibre to fibre through the element thickness, depending on the stress state. A numerical integration is made in this case for each individual element, and the procedure for this is the same in the modified method as in the original method.

Appendix D

Accuracy Tests of The C Program

The C Program as described in Section 10.2 is a modified version of the elastic-plastic program PLINTH. When a shell to be analysed by the program has a meridional radius of curvature which is not large compared with the shell thickness, by an approximation, the program takes into account the resulting non-linear distribution of stress across the shell wall. To check for accuracy of such a modification a few problems were analysed.

Three simple problems were used to check the program. The first problem, shown in Fig.D-1, is that of a thick-walled toroidal ring with a complete slit in the plane of the ring, at the position either of maximum distance or of minimum distance from the ring central-axis. Load is applied to the sides of the slit to open the ring. The similar problem of a split cylindrical, rather than toroidal, ring can be easily solved analytically by the Winkler procedure; the two solutions can thus be compared. The diameter /thickness ratio, 2b/2h, is fixed at a value of 2.0 while radius a is varied for different calculations. It is found that the circumferential stresses and strains of the shell, i.e. those perpendicular to the sectional plane in Fig. D-1, decrease as radius a is increased. Thus by increasing radius a sufficiently, the condition of the meridional stress and strain distribution on this sectional plane approaches that of a plane-stress condition, which is that of a cylindrical ring. The sense of the circumferential strains follows that of the radial displacement. They are compressive for the outside slitted ring, and tensile for the inside slitted one.

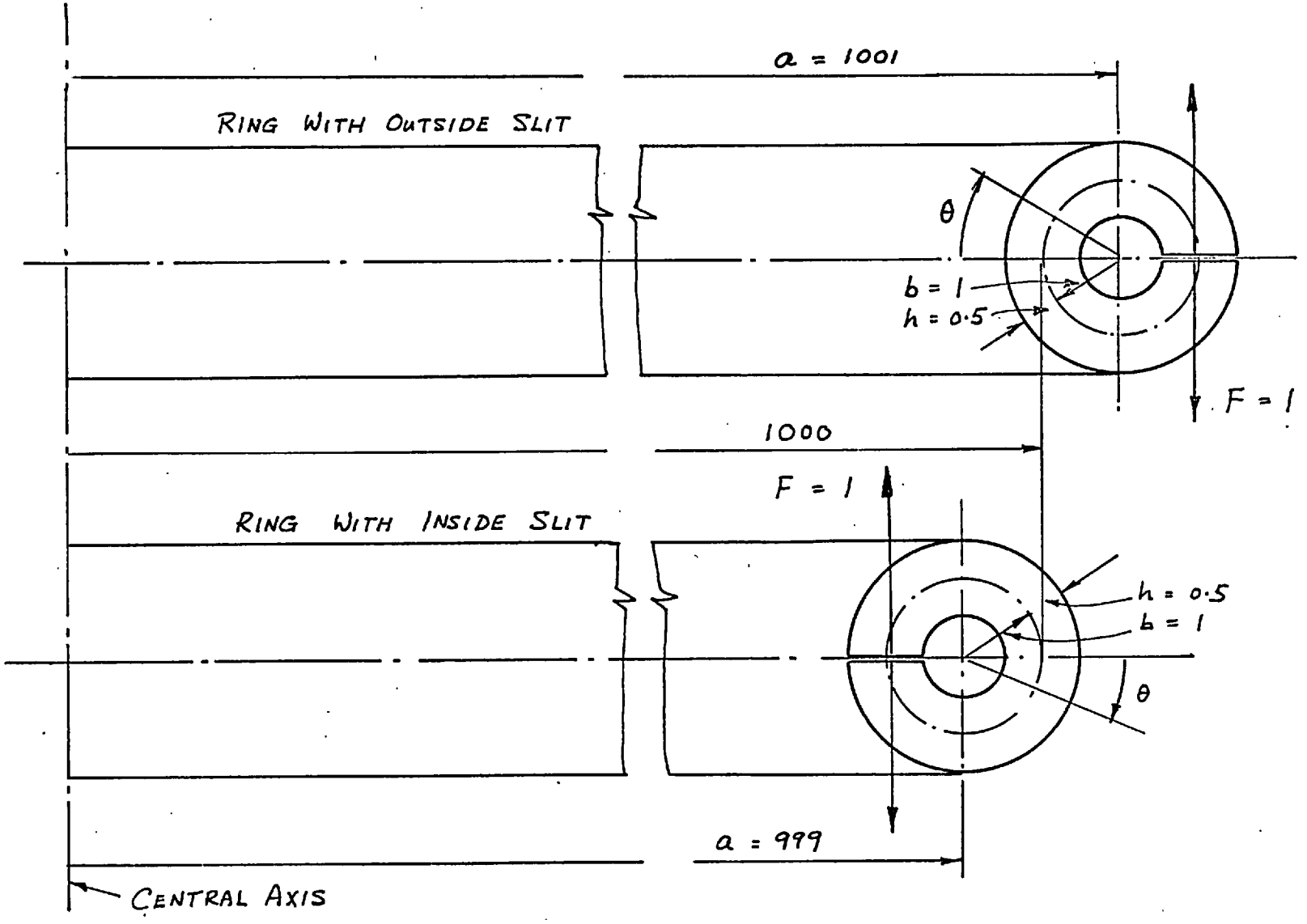

FIGURE D-1 THICK-WALLED TOROIDAL RING

It is expected that their influence on the meridional strains are opposite in sense, and, comparing results from both cases, an estimate can be made of the magnitude of this circumferential strain effect.

The different solutions to this problem are tabulated below, Table D-1. Strains values at two positions of the ring are compared, one at the cross-section diametrically opposite the slit, corresponding to $\theta = 0$, and the other at $\theta = 1.0$ radian.

	Winkler's Solution	C Program		Original Program	
		Inside Split	Outside Split		
Outer Surface	-6.97	-7.36	-7.37	-11.0	
Mid-wall	-0.82	-0.91	-0.91	1.0	θ=0 radian
Inner Surface	17.64	18.80	18.45	13.0	
Outer Surface	-5.60	-5.82	-5.82	-8.7	
Mid-wall	-0.86	-0.91	-0.91	-0.54	θ=1.0 radian
Inner Surface	13.35	13.80	13.80	9.8	

Table D-1 Relative values of strain at thick split under direct opening load.

The results of the modified program are very close although not exactly the same as the analytical Winkler solution for cylindrical ring. The computer solution using the original unmodified version is out by a large amount. The above values are of course elastic results. It is not possible here to check on the plastic results.

The other two problems used to check the program contain no toroidal elements, nor spherical elements, since this is a special case of a toroidal one. They are designed to check whether the modified program would give the same results as the original one to ensure that no error has crept in unnoticed from the many alterations necessary to the program subroutines and instructions. Both the elastic solution and the plastic solution are compared. The first vessel is a uniform circular cylinder with fixed ends under internal pressure load. The C Program solution is found to be exactly symmetrical about the mid position, and the elastic as well as the plastic solutions are found to be exactly the same as that of the original program. The second vessel consists of a 45^{o} conical pressure vessel head with reinforcements at the vessel side of the corner in the shape of a taper where the thickness increases towards the corner. The taper is being used here so that the terms connected with changes in thicknesses can be checked. Again in the final form of the modified program the solutions agree exactly.

LIST OF ILLUSTRATIONS

Figures

1-1 Torispherical Pressure Vessel Head.
6-1 Axisymmetric Thin-Walled Shell Element.
6-2 Force and Stress System of Shell Element.
7-1 Stress Distribution, Cylinder Under Internal Pressure.
7-2 Stress Distribution, Toriconical Head Under Internal Pressure.
7-3 a) Circumferential Stresses, Flat Plate Bellows.
b) Meridional Stresses, Flat Plate Bellows.
7-4 Circumferential Strains, Bellows C.
8-1 Mild Steel Torispherical Head, Stoddart.
8-2 Stainless Steel Vessels, Kemper, Theoretical Elastic Strains.
8-3 Stainless Steel Vessels, Kemper, Theoretical Plastic Strains.
8-4 Strain Gauge Readings of Low Proof Vessel, Kemper.
9-1 Nominal Dimensions of Thick Cap and Thin Cap.
9-2 Welding and Machining Details of Nozzles.
9-3 a) Tensile Tests, Load-Crosshead Movement, Specimen 1.
b) Tensile Tests, Load-Crosshead Movement, Specimen 2.
9-4 Plane Strain Compression Tests, Hoop Specimen 1 & 2.
9-5 Plane Strain Compression Tests, Hoop Specimen 3.
9-6 Plane Strain Compression Tests, Axial Specimen 1 & 2.
9-7 Basic Bridge Circuit of Recorder.
9-8 Meridional Strains at Nozzle of Thin Cap.
9-9 Circumferential Strain at Nozzle of Thin Cap.
9-10 Plastic Behaviour of Thin Cap, Strain Gauge Readings.
9-11 Collapse Behaviour of Thin Cap.
9-12 Meridional Strains at Nozzle of Thick Cap.
9-13 Circumferential Strains at Nozzle of Thick Cap.
9-14 Plastic Behaviour of Thick Cap, Strain Gauge Readings.
9-15 Collapse Behaviour of Thick Cap.
10-1 'Smooth' Representation of Nozzle Junction.
10-2 Equivalent Stress Intensity at Nozzle of Thin Cap.
10-3 Equivalent Stress Intensity at Nozzle of Thick Cap.
10-4 Constant Strain-Rate Loading of Thin Cap.

11-1 Test Vessel Nominal Dimensions.
11-2 Details of Test Nozzle.
11-3 Position of Strain Gauges on Test Vessel.
11-4 Position of Dial Gauges on Test Vessel.
11-5 Pressure Circuit.
12-1 Elastic Circumferential Strain Distribution on Test Vessel Heads.
12-2 Elastic Meridional Strain Distribution on Test Vessel Heads.
12-3 Elastic Circumferential Strain, Nozzle End of Test Vessel (Head B).
12-4 Elastic Meridional Strain, Nozzle End of Test Vessel (Head B).
12-5 Axial Deflection at End Nozzle Junction.
12-6 Circumferential Strain At End Nozzle Junction.
12-7 Pressure-Volume Curve.
12-8 Circumferential Strain Around Kunckle of Closed Dished End (Head A).
12-9 Meridional Strains Around Kunckle of Closed Dished End (Head A).
12-10 Circumferential Strains Around Kunckle of Dished End with Nozzle (Head B).
12-11 Meridional Strains Around Kunckle of Dished End with Nozzle (Head B).
12-12 Circumferential Strains at Junction of End Nozzle.
12-13 Meridional Strains at Junction of End Nozzle.
12-14 Axial Deflections Relative to Mid-Vessel.
12-15 a) Strains Near Crown Centre of Closed Dished End (Head A).
b) External Circumferential Strains at Vessel Body.
12-16 Equivalent Stress-Strain Curves for Test Vessel.
12-17 Equivalent Stress-Strain Curves for End Nozzle.

Plates

9-1 Multi-Channel Strain Recorder.
9-2 Test Arrangement.

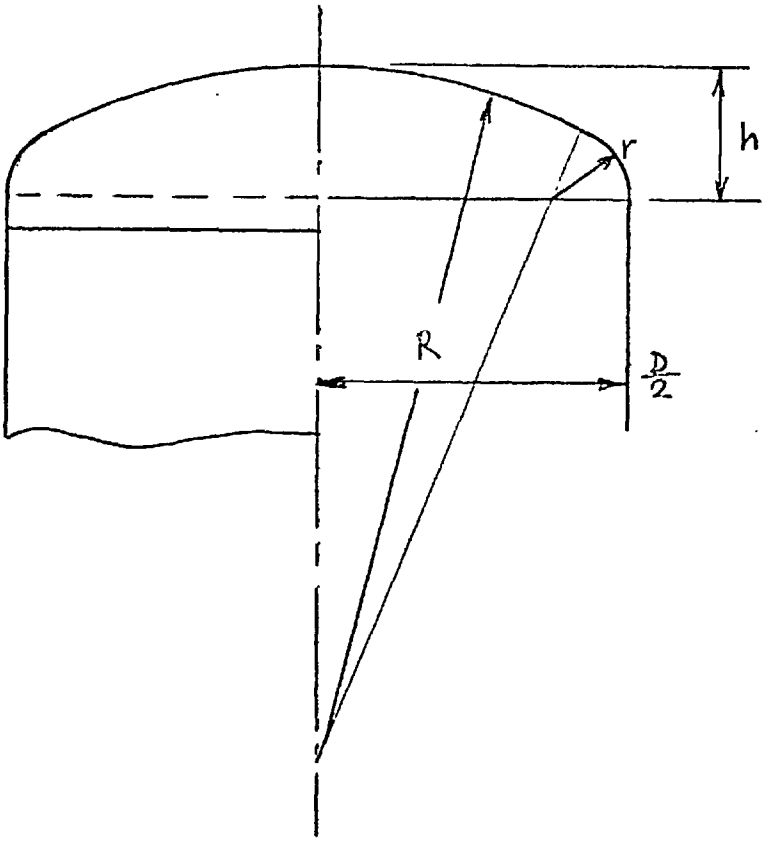

FIG 1-1 TORISPHERICAL PRESSURE VESSEL HEAD

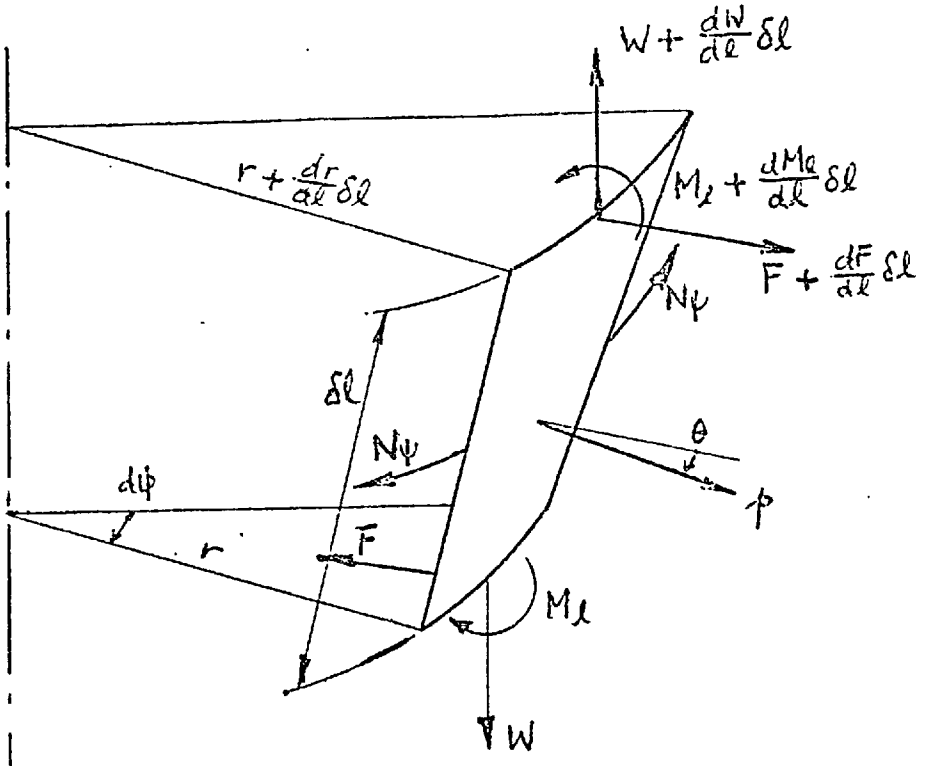

FORCE DIAGRAM

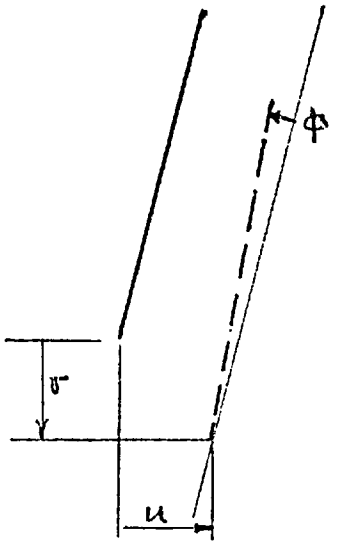

DISPLACEMENT DIAGRAM

FIG 6-1 AXISYMMETRIC THIN-WALLED SHELL ELEMENT

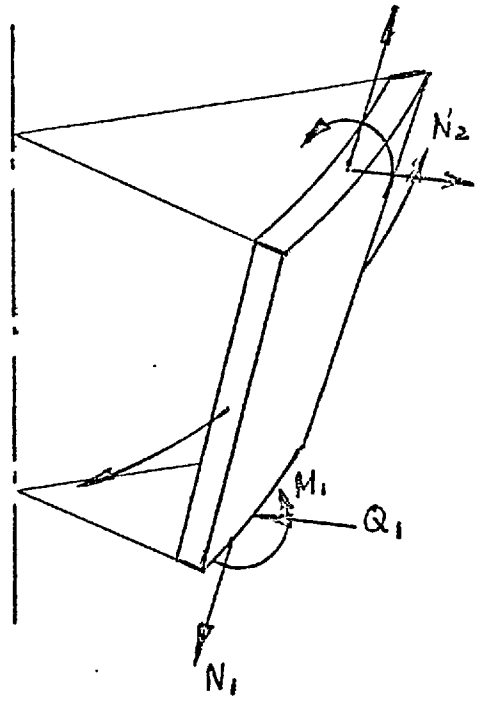

(a)

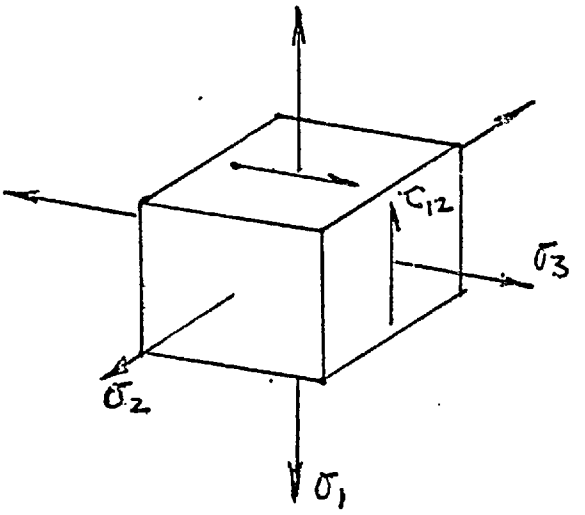

(b)

FIG 6-2 FORCE AND STRESS SYSTEM OF SHELL ELEMENT

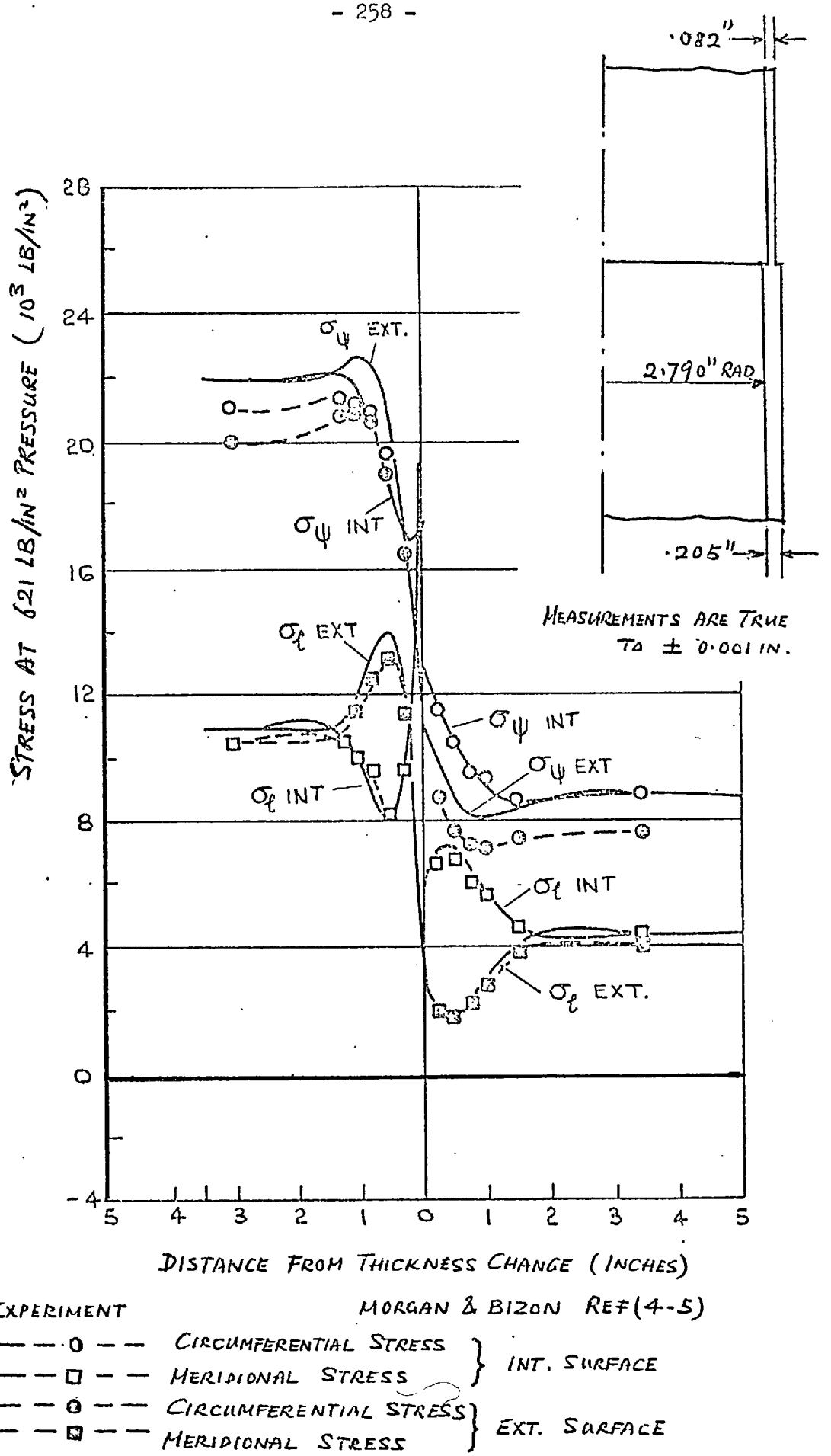

FIG. 7-1 STRESS DISTRIBUTION
CYLINDER UNDER INTERNAL PRESSURE

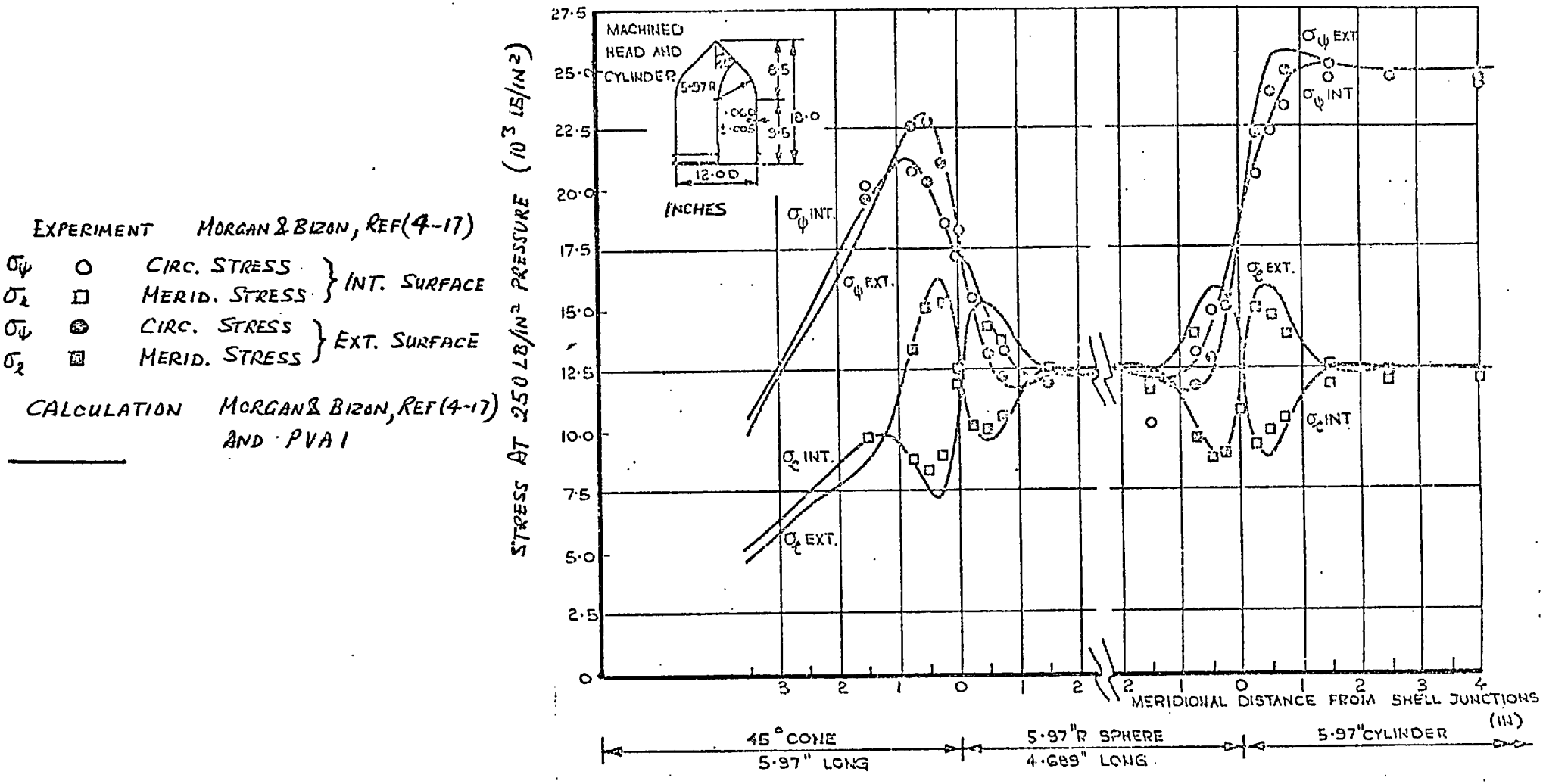

FIG 7-2 STRESS DISTRIBUTION, TORICONICAL HEAD UNDER INTERNAL PRESSURE

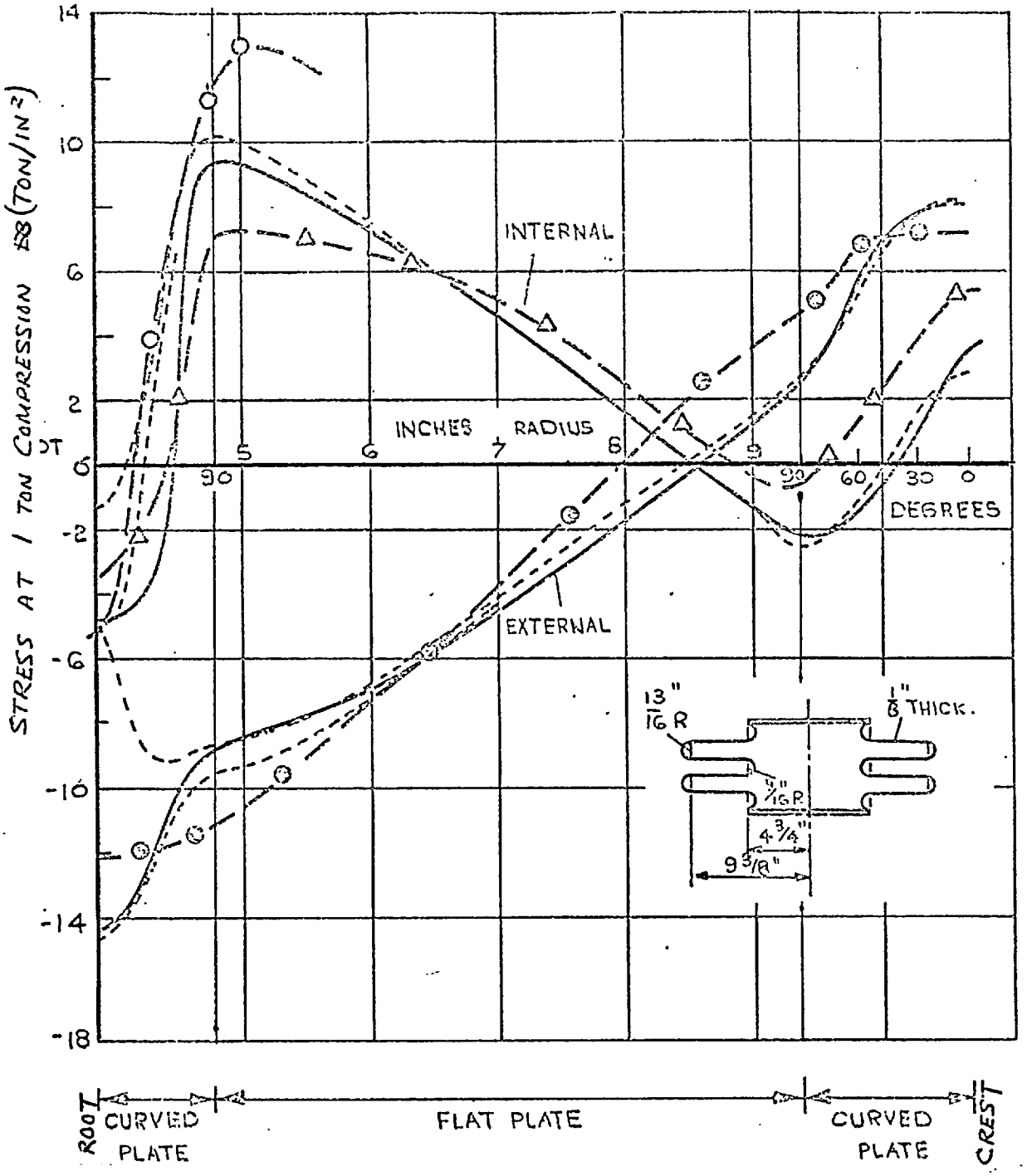

EXPERIMENT — TURNER & FORD, REF (7-2)

— ● — EXTERNAL STRESS } END 1/4 CONVOLUTION
— △ — INTERNAL STRESS }

— ○ — INTERNAL STRESS MIDDLE 1/4 CONVOLUTION

CALCULATION

——— TURNER, REF (6-2)

— — — — PVA1

FIG 7-3 (a) CIRCUMFERENTIAL STRESS, FLAT PLATE BELLOWS.

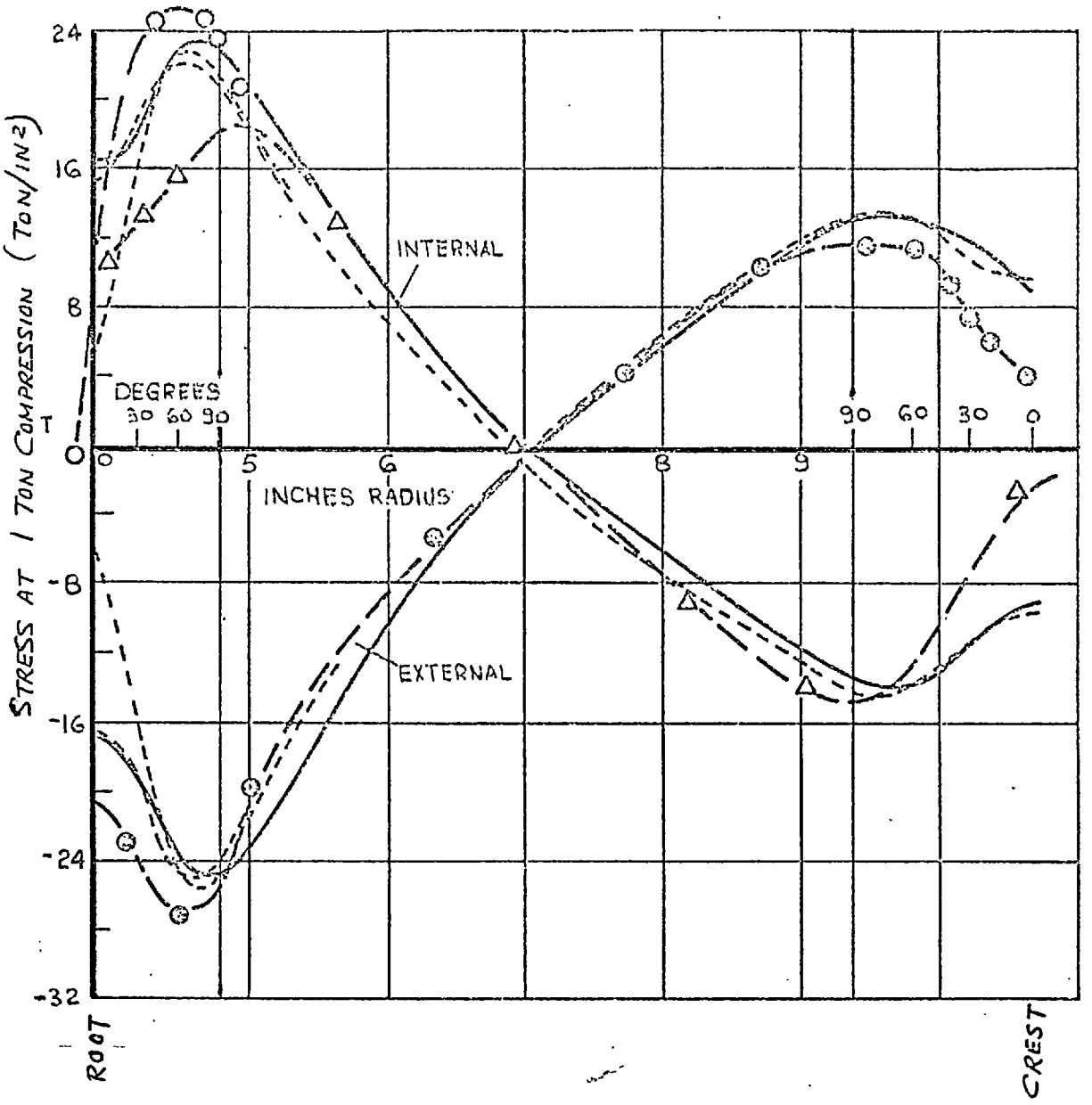

FIG 7-3(b) MERIDIONAL STRESSES, FLAT PLATE BELLOWS

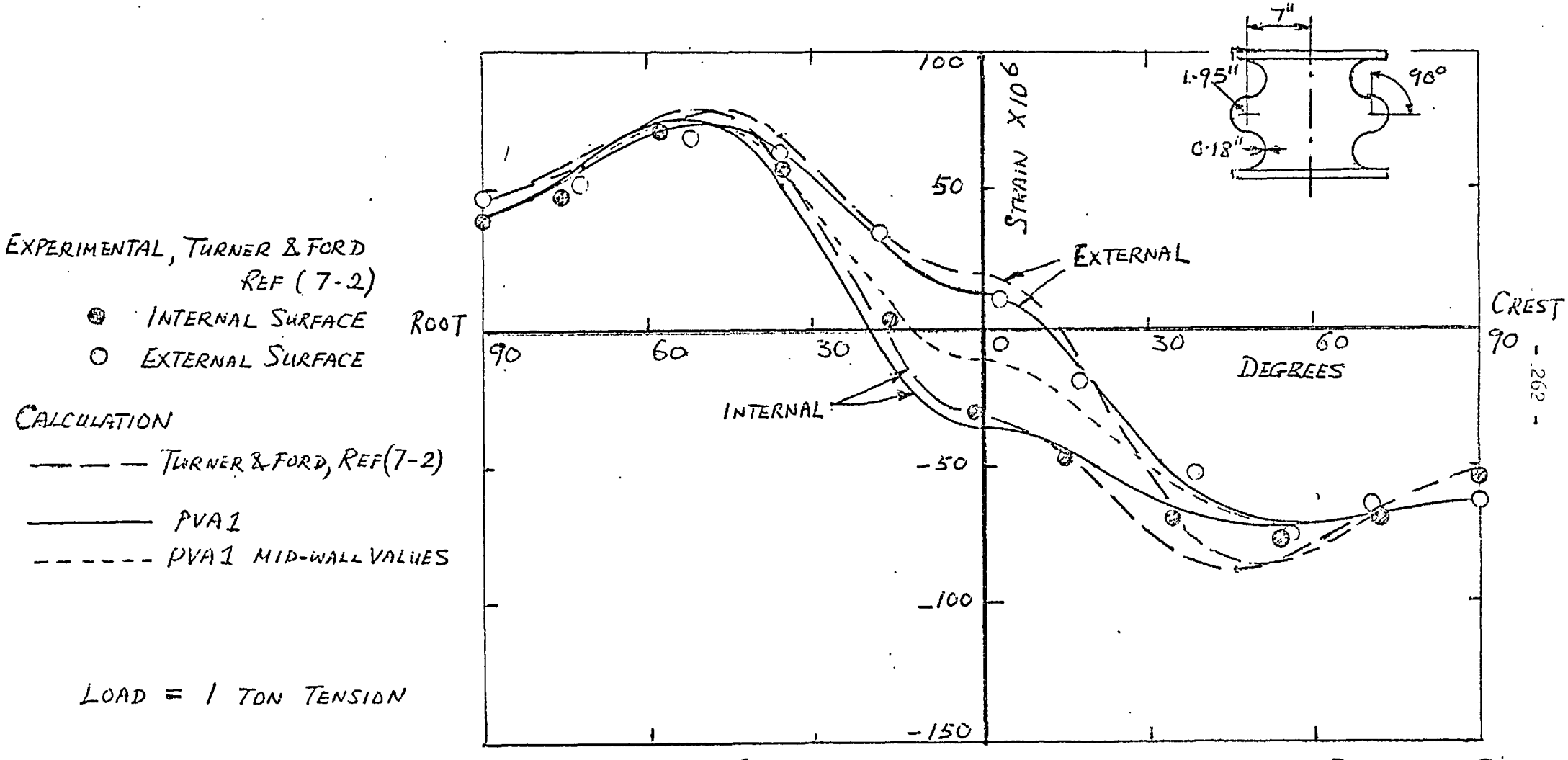

FIG 7-4 CIRCUMFERENTIAL STRAINS, BELLOWS C

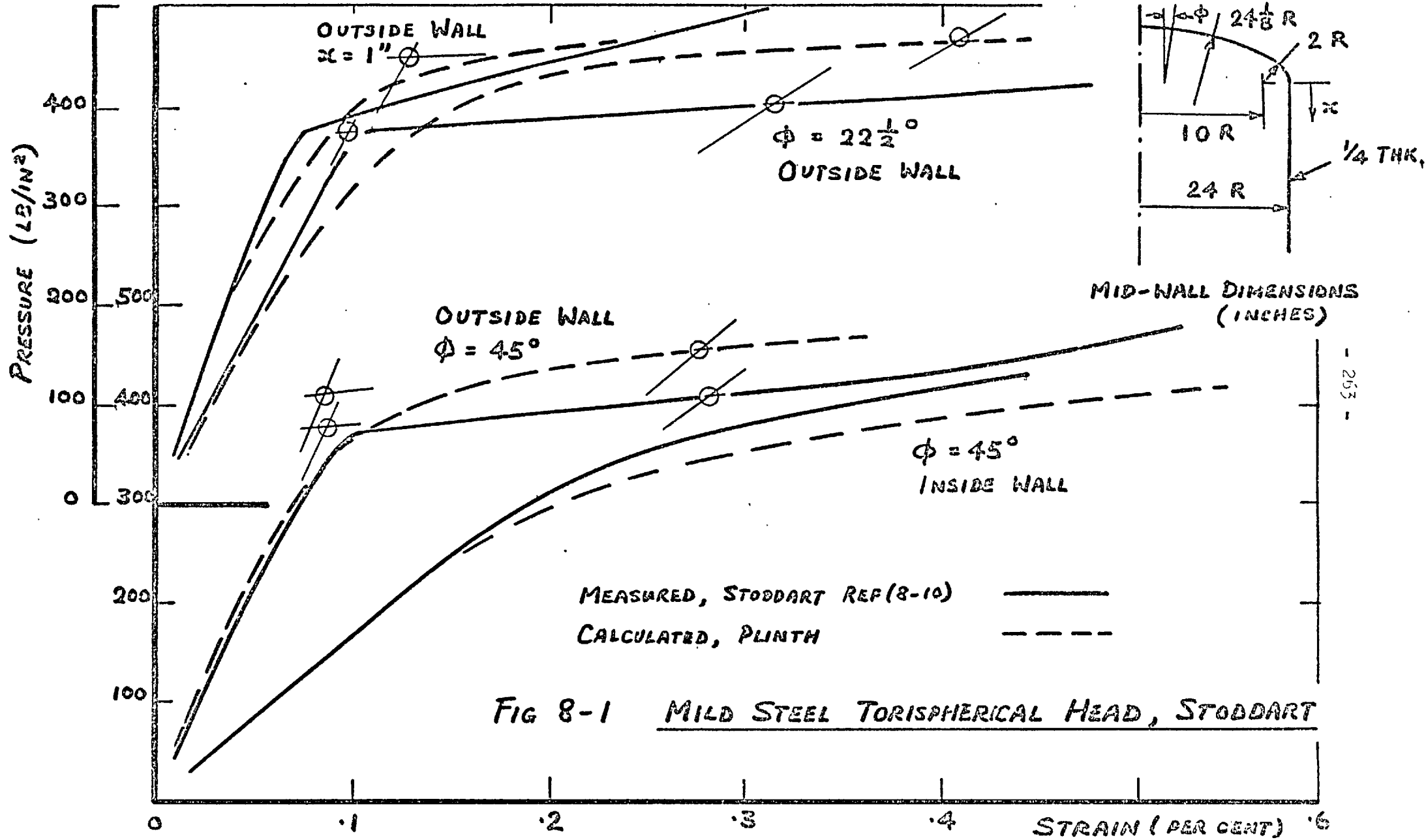

FIG 8-1 MILD STEEL TORISPHERICAL HEAD, STODDART

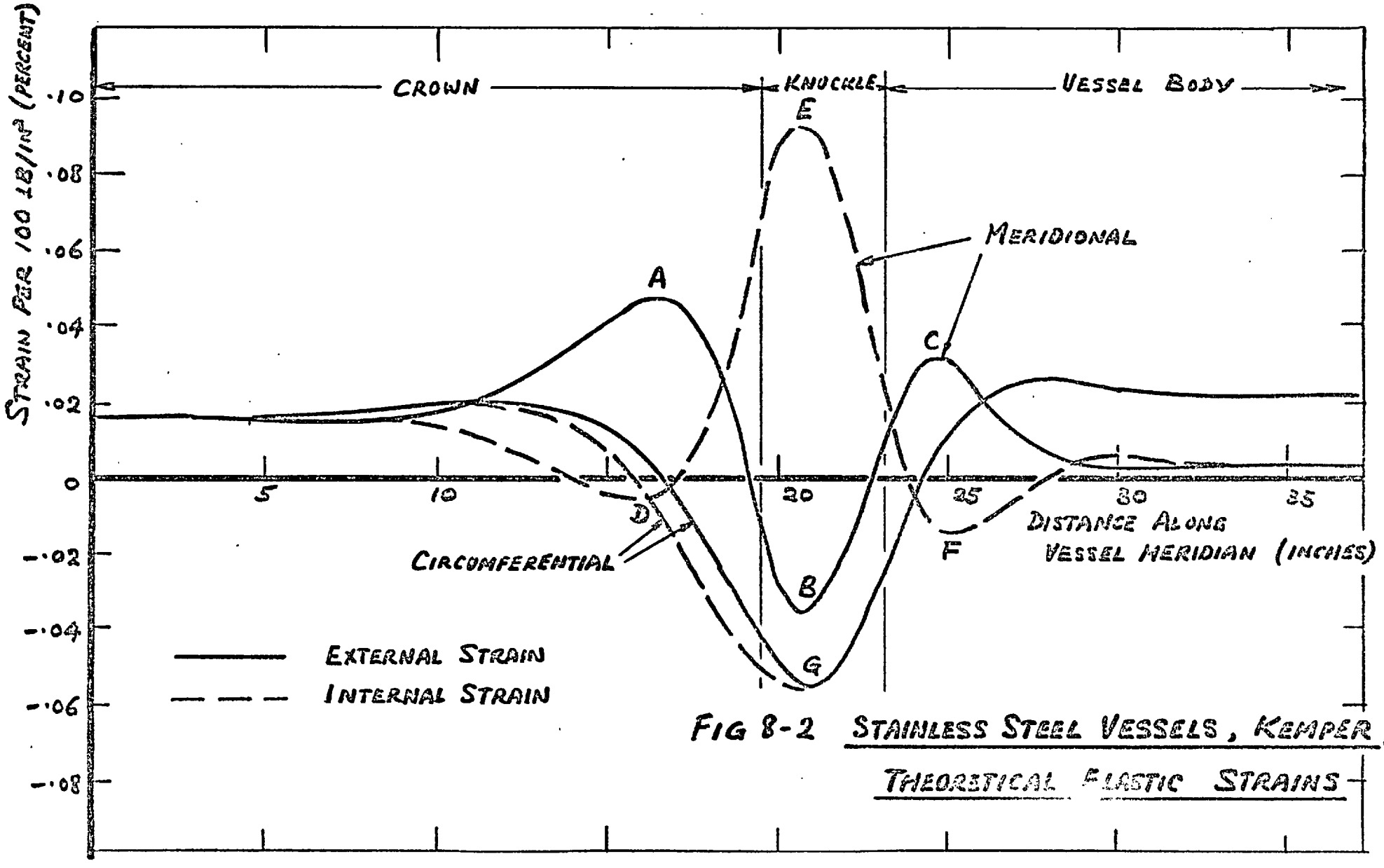

FIG 8-2 STAINLESS STEEL VESSELS, KEMPER, THEORETICAL ELASTIC STRAINS

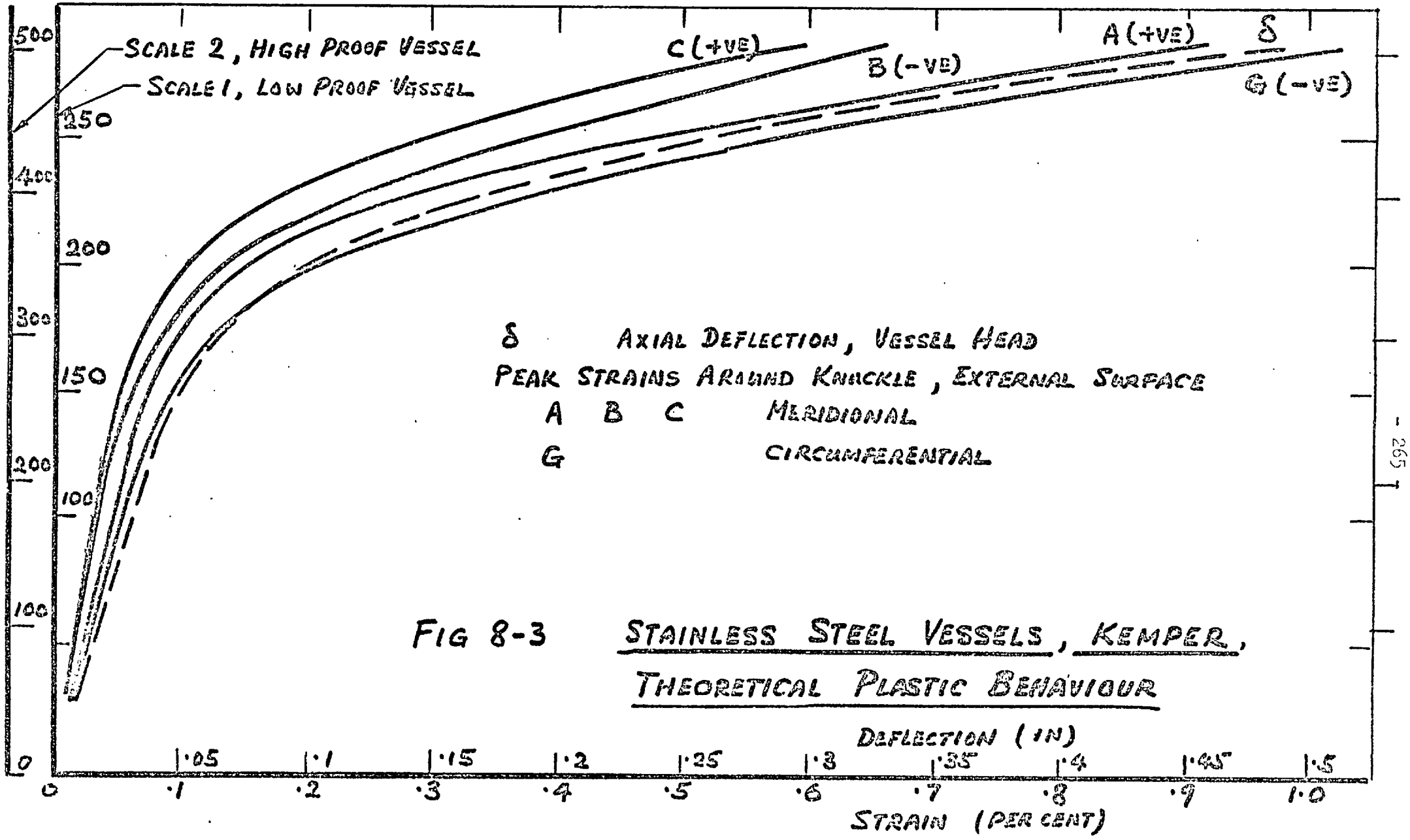

FIG 8-3 STAINLESS STEEL VESSELS, KEMPER, THEORETICAL PLASTIC BEHAVIOUR

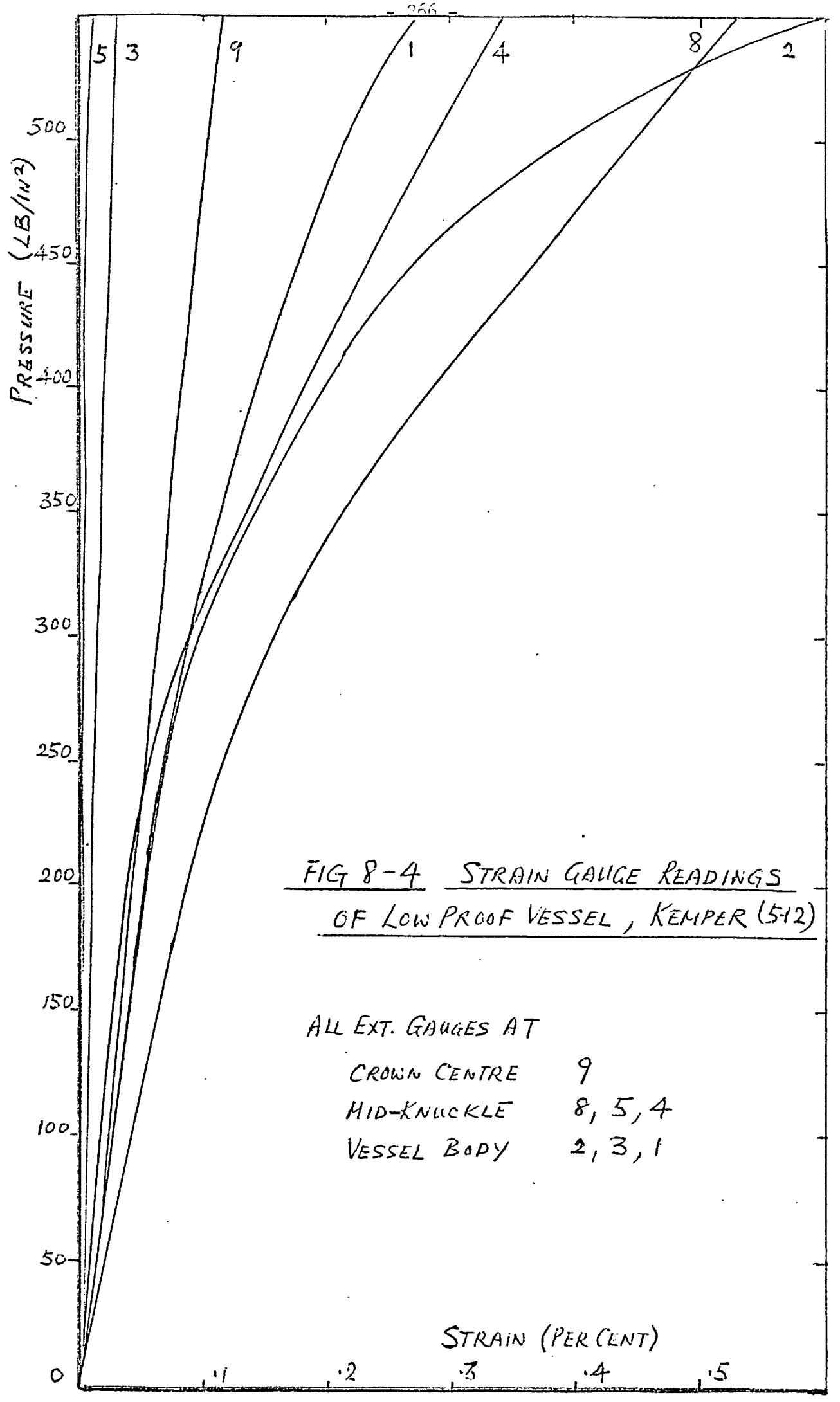

FIG 8-4 STRAIN GAUGE READINGS OF LOW PROOF VESSEL, KEMPER (5-12)

ALL EXT. GAUGES AT

CROWN CENTRE	9
MID-KNUCKLE	8, 5, 4
VESSEL BODY	2, 3, 1

FIG. 9-1 NOMINAL DIMENSION OF THICK CAP AND THIN CAP

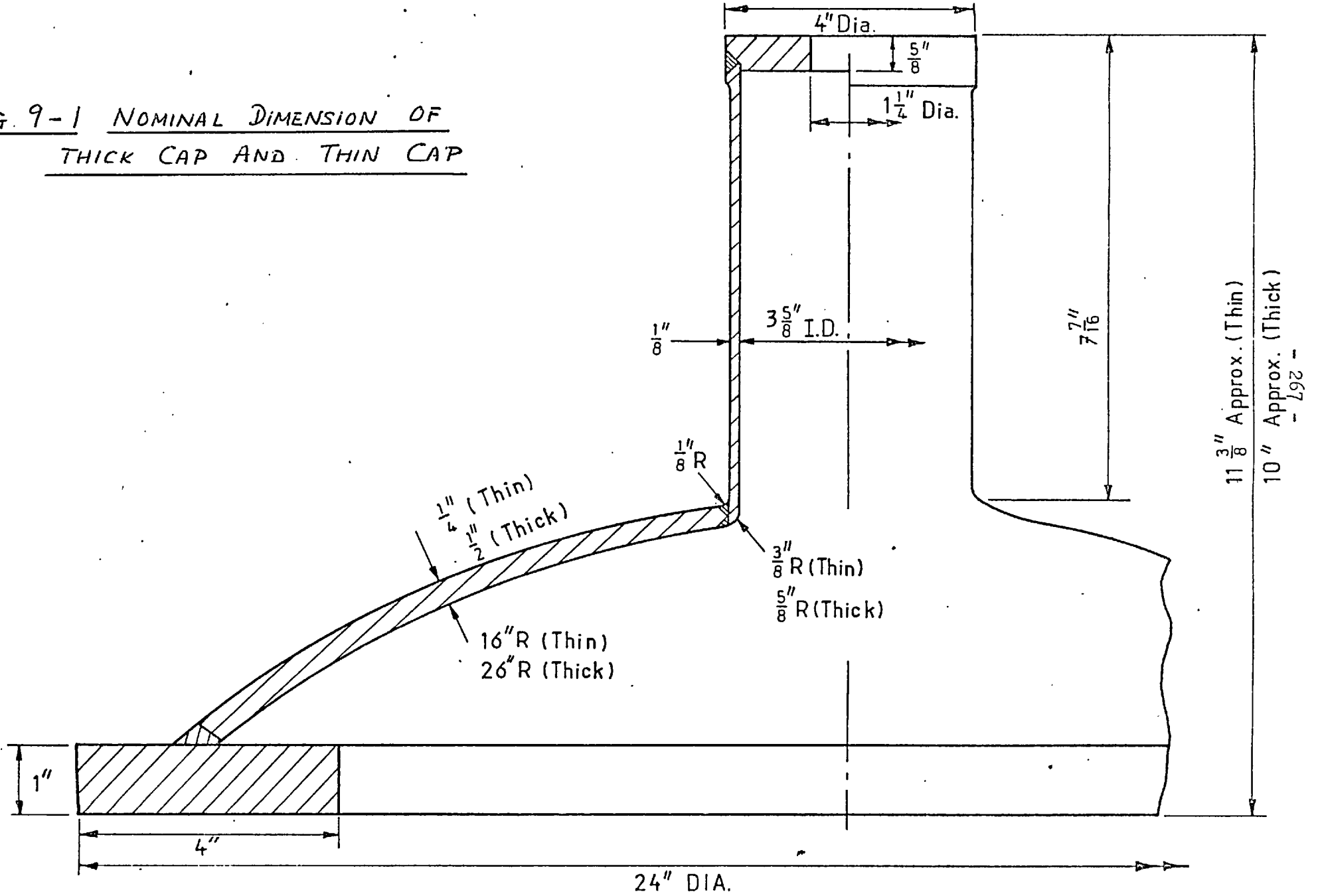

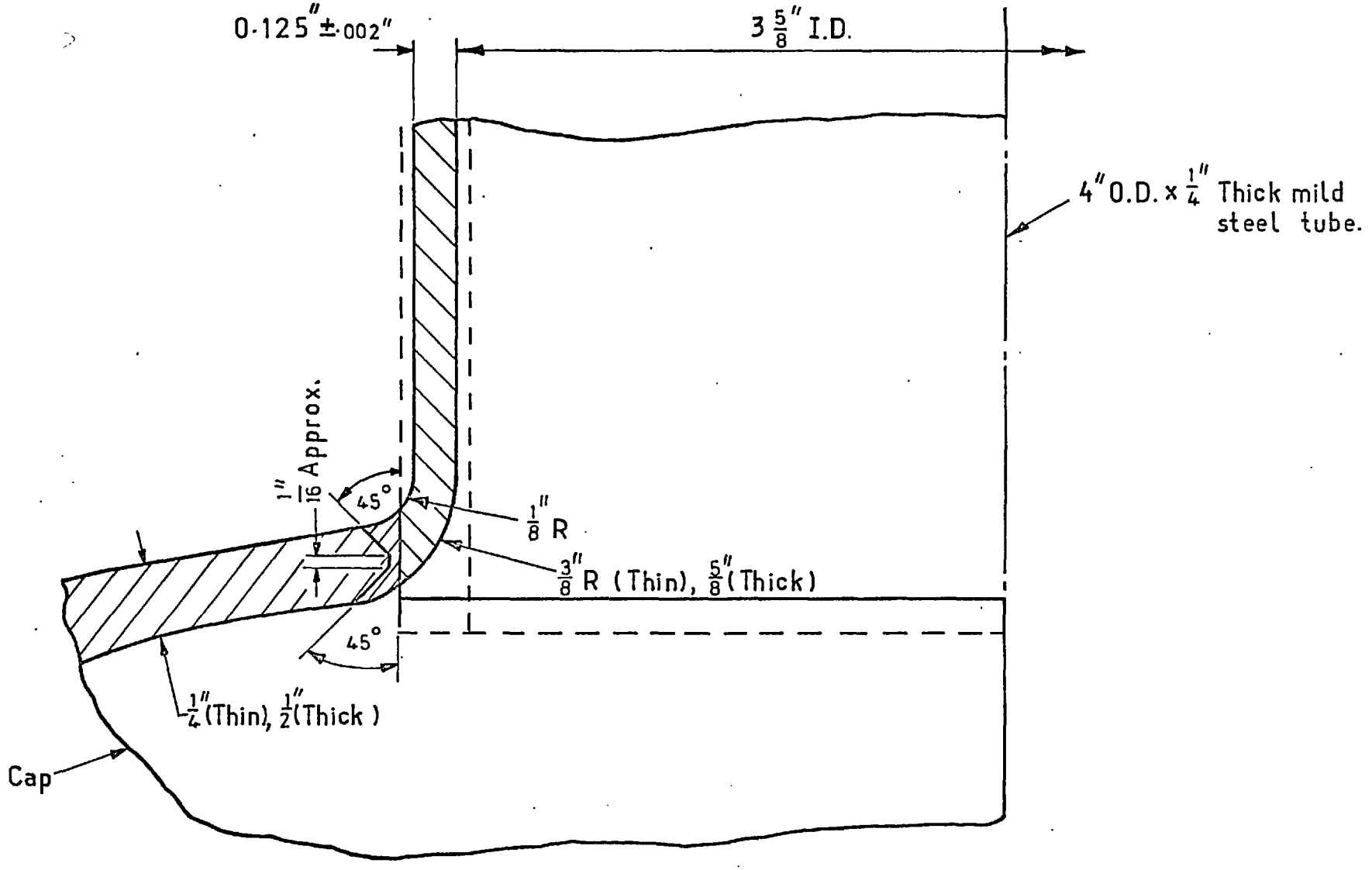

FIG.9-2 WELDING AND MACHINING DETAILS OF NOZZLES.

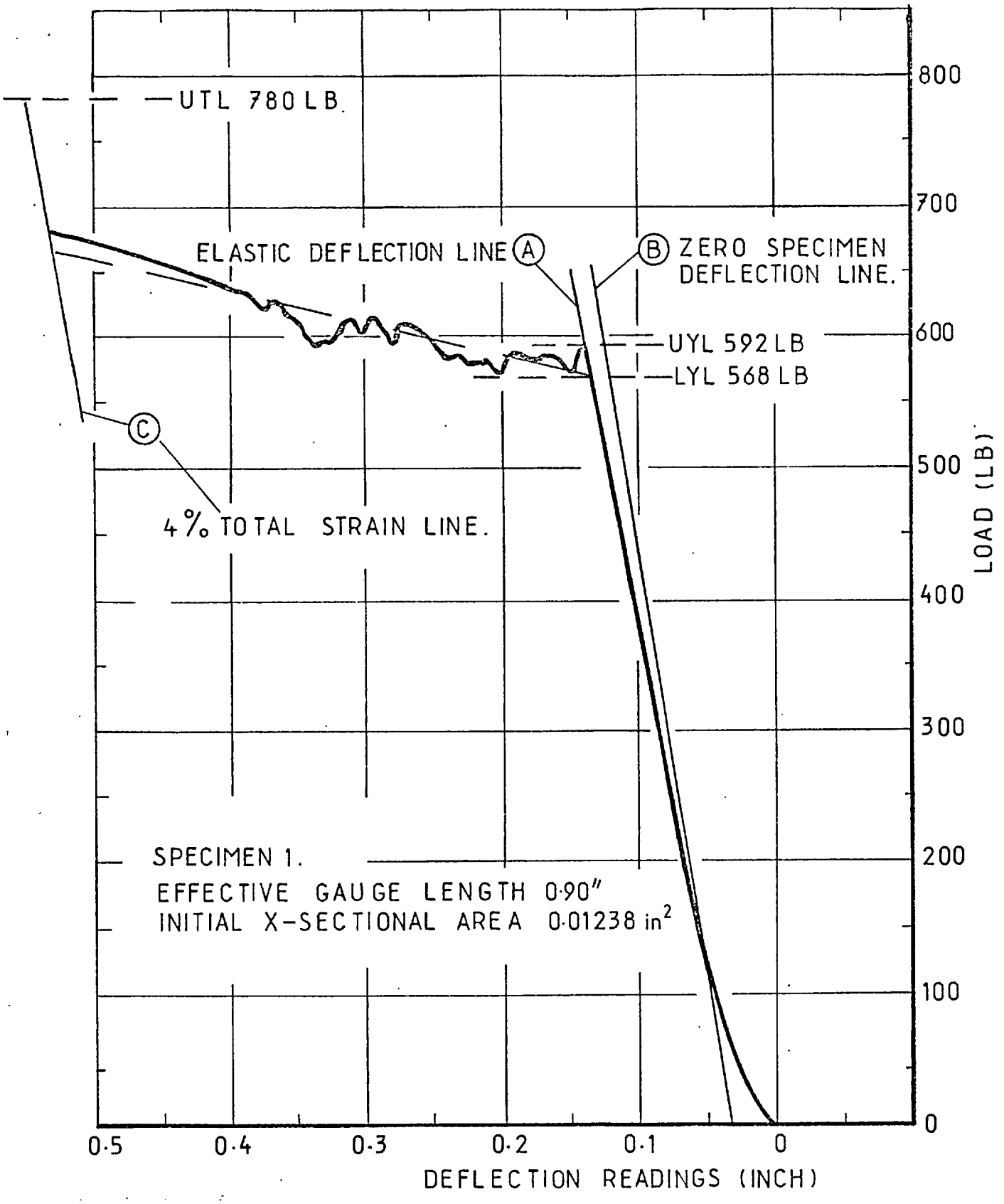

FIG 9-3A TENSILE TESTS, LOAD ~ CROSSHEAD MOVEMENT.

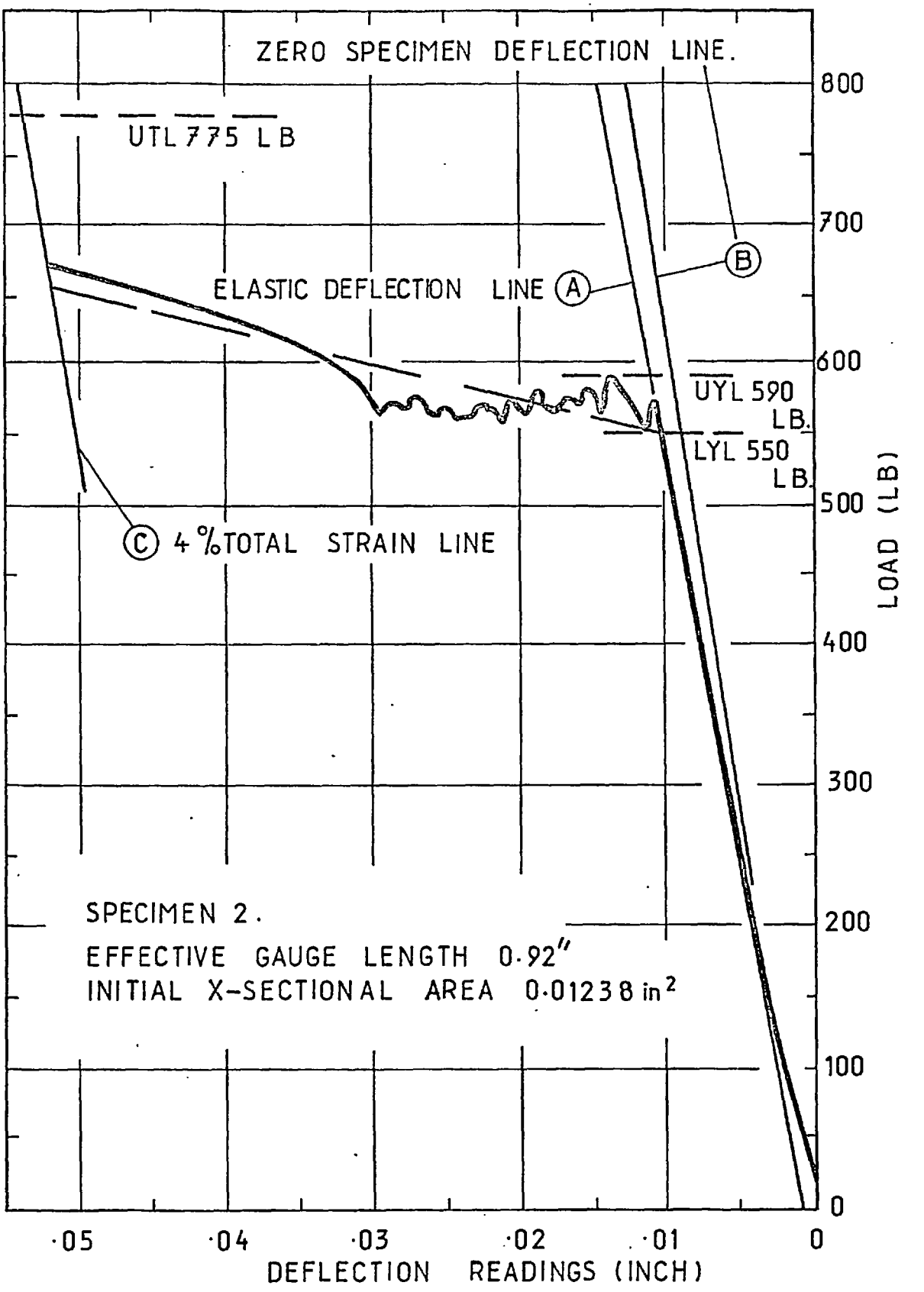

FIG. 9-3B TENSILE TESTS, LOAD ~ CROSSHEAD MOVEMENT.

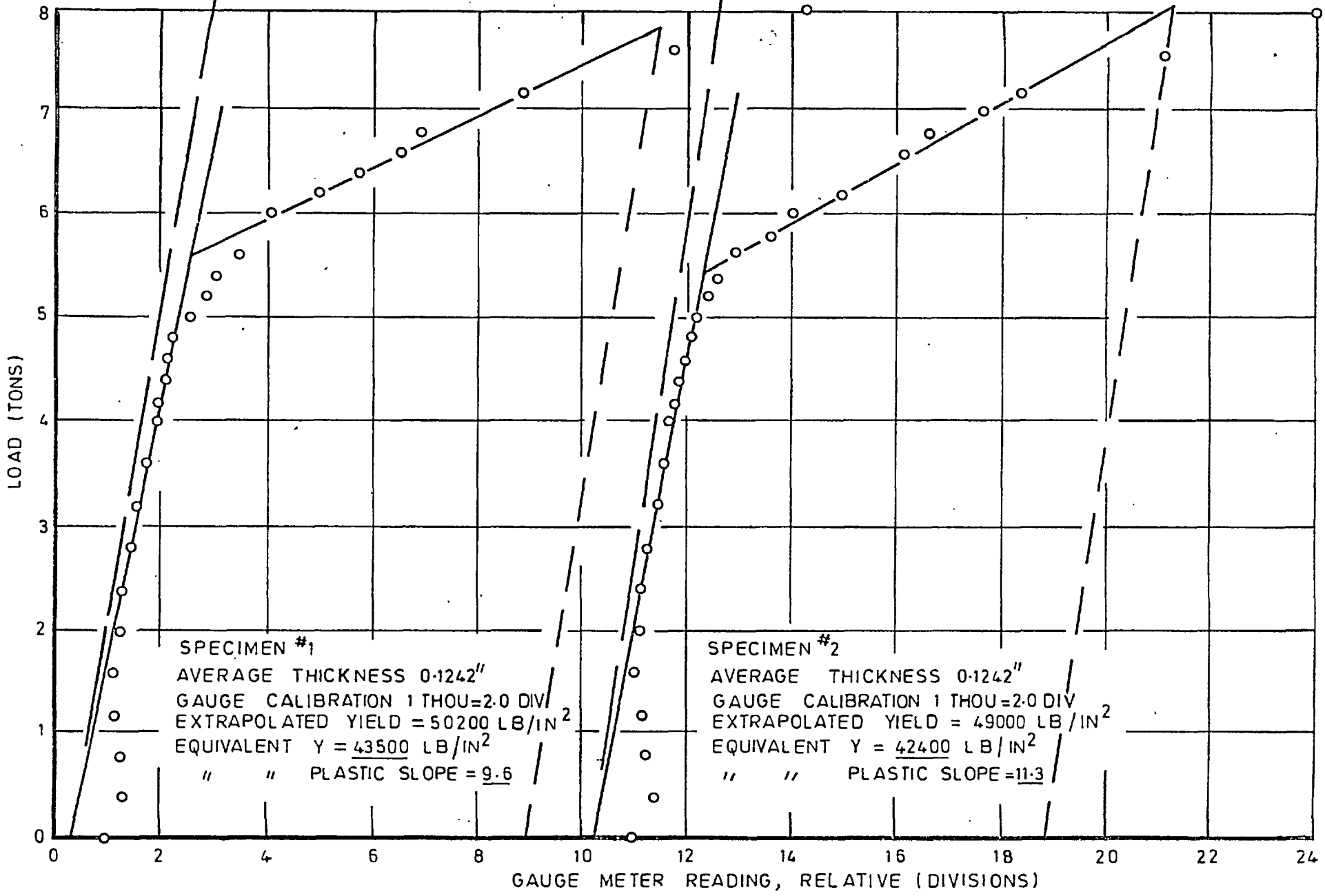

FIG 9-4 PLANE STRAIN COMPRESSION TESTS, HOOP SPECIMEN #1, 2.

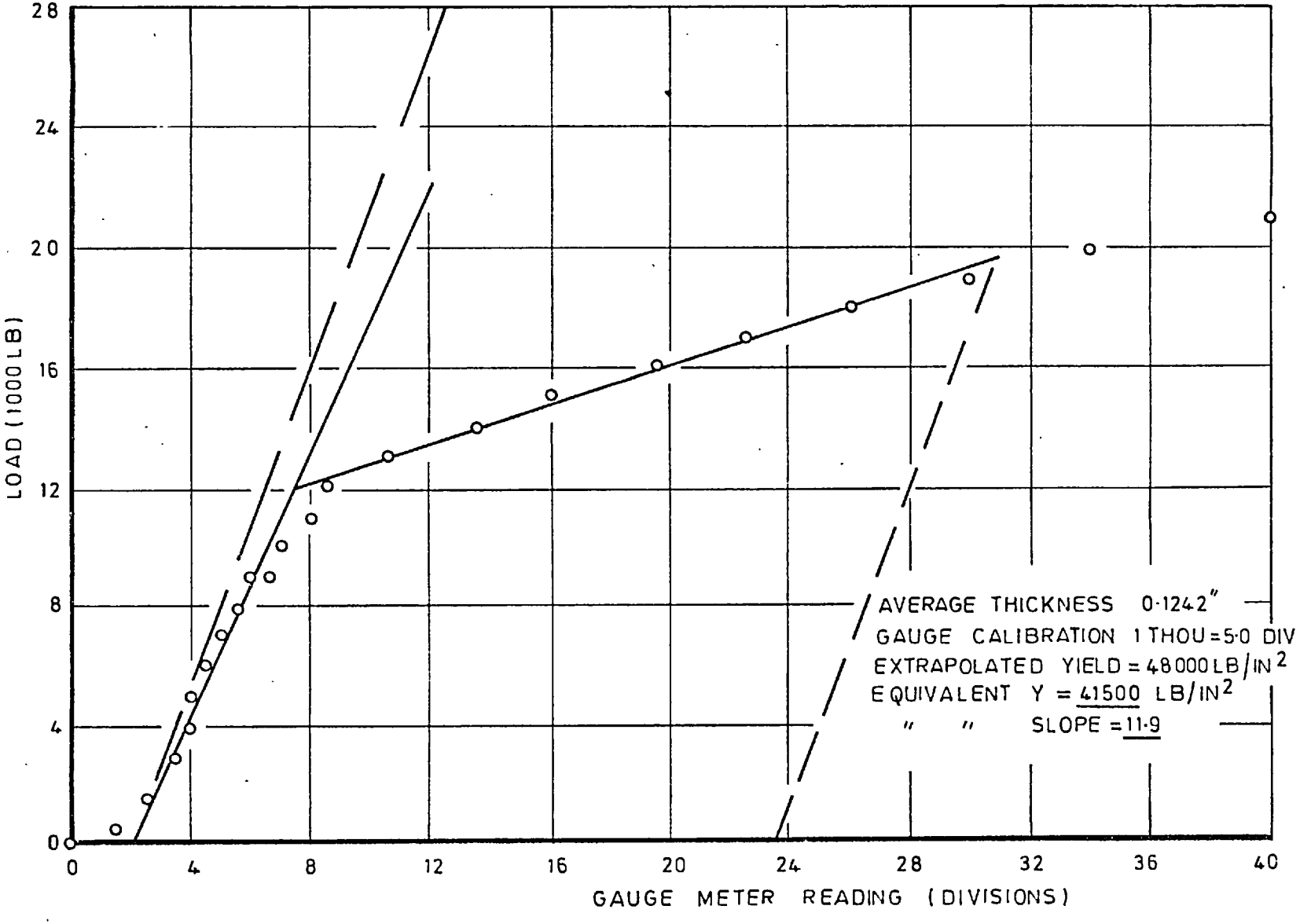

FIG. 9-5 PLANE STRAIN COMPRESSION TEST, HOOP SPECIMEN #3.

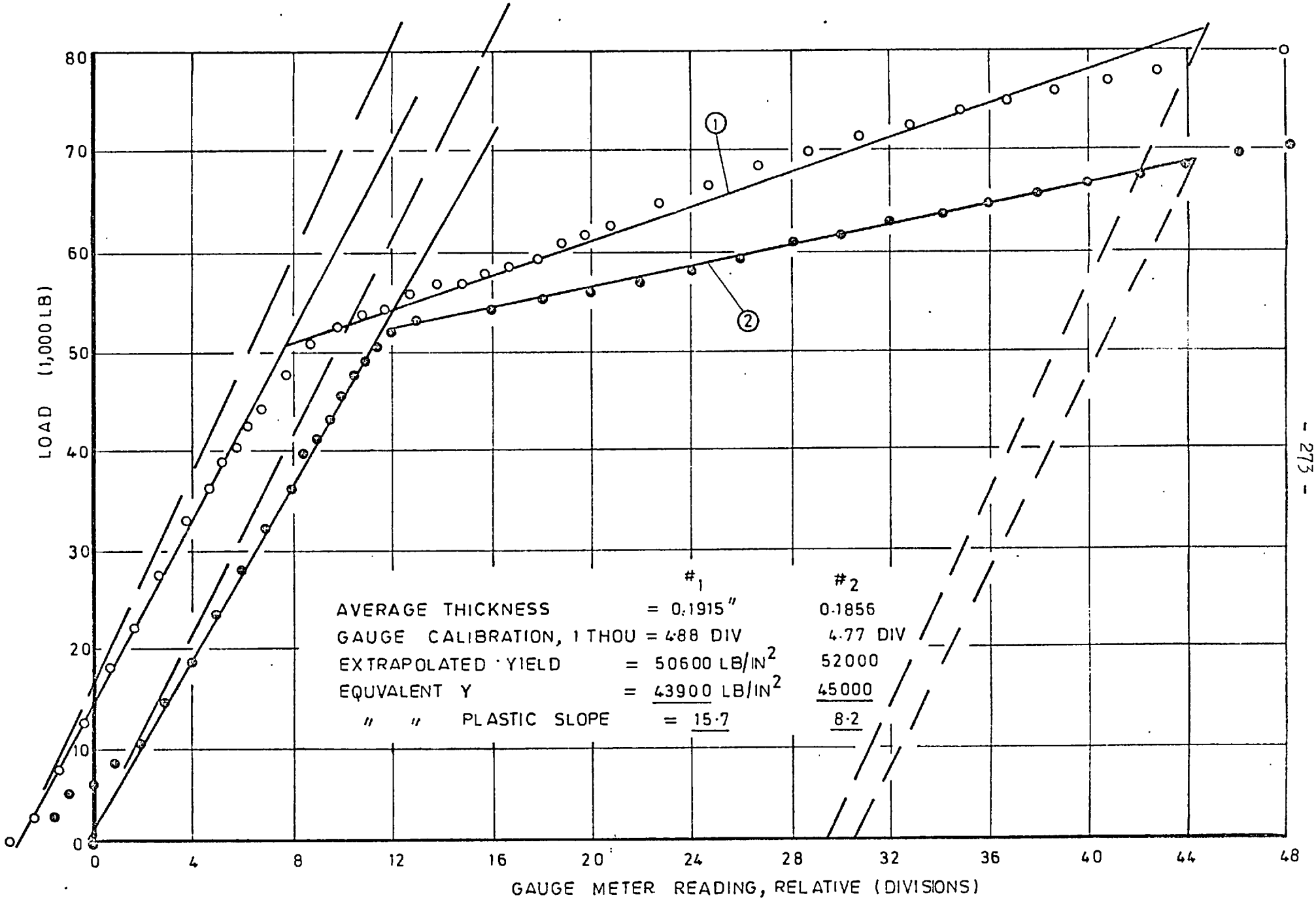

FIG 9-6 PLANE STRAIN COMPRESSION TEST, AXIAL SPECIMEN #1 & 2.

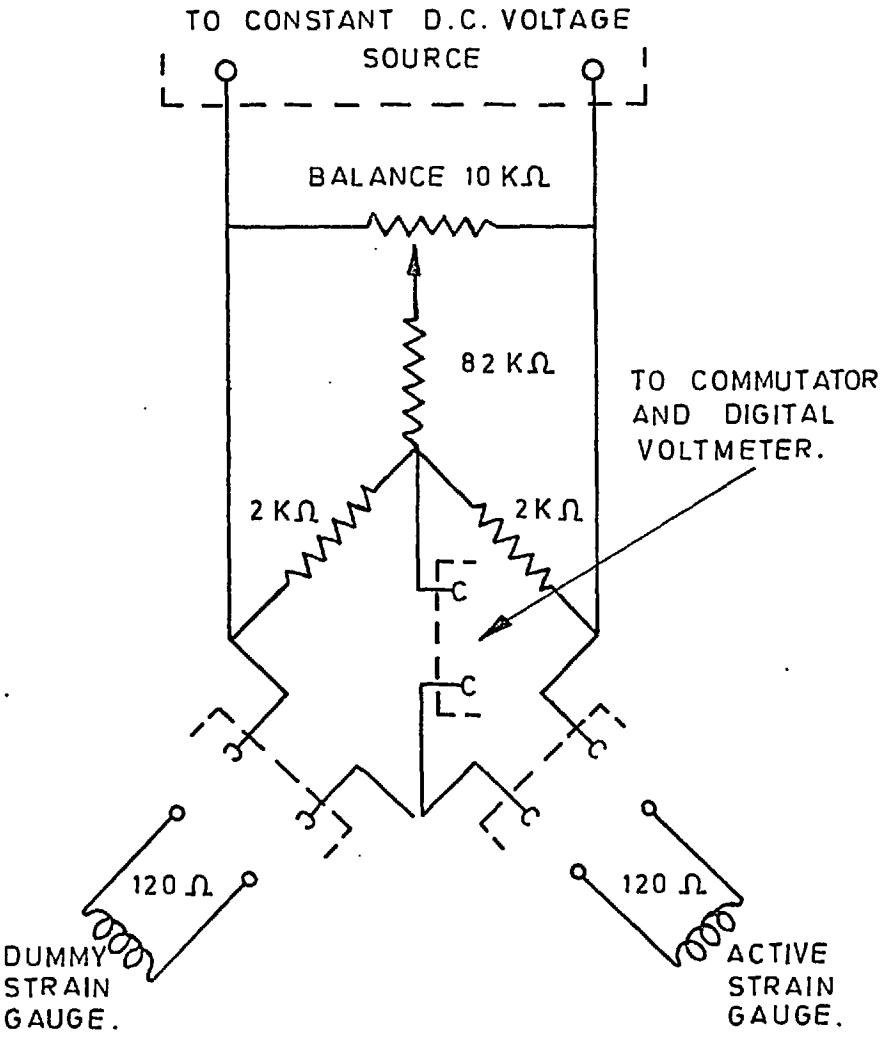

FIG 9.7 BASIC BRIDGE CIRCUIT OF STRAIN RECORDER.

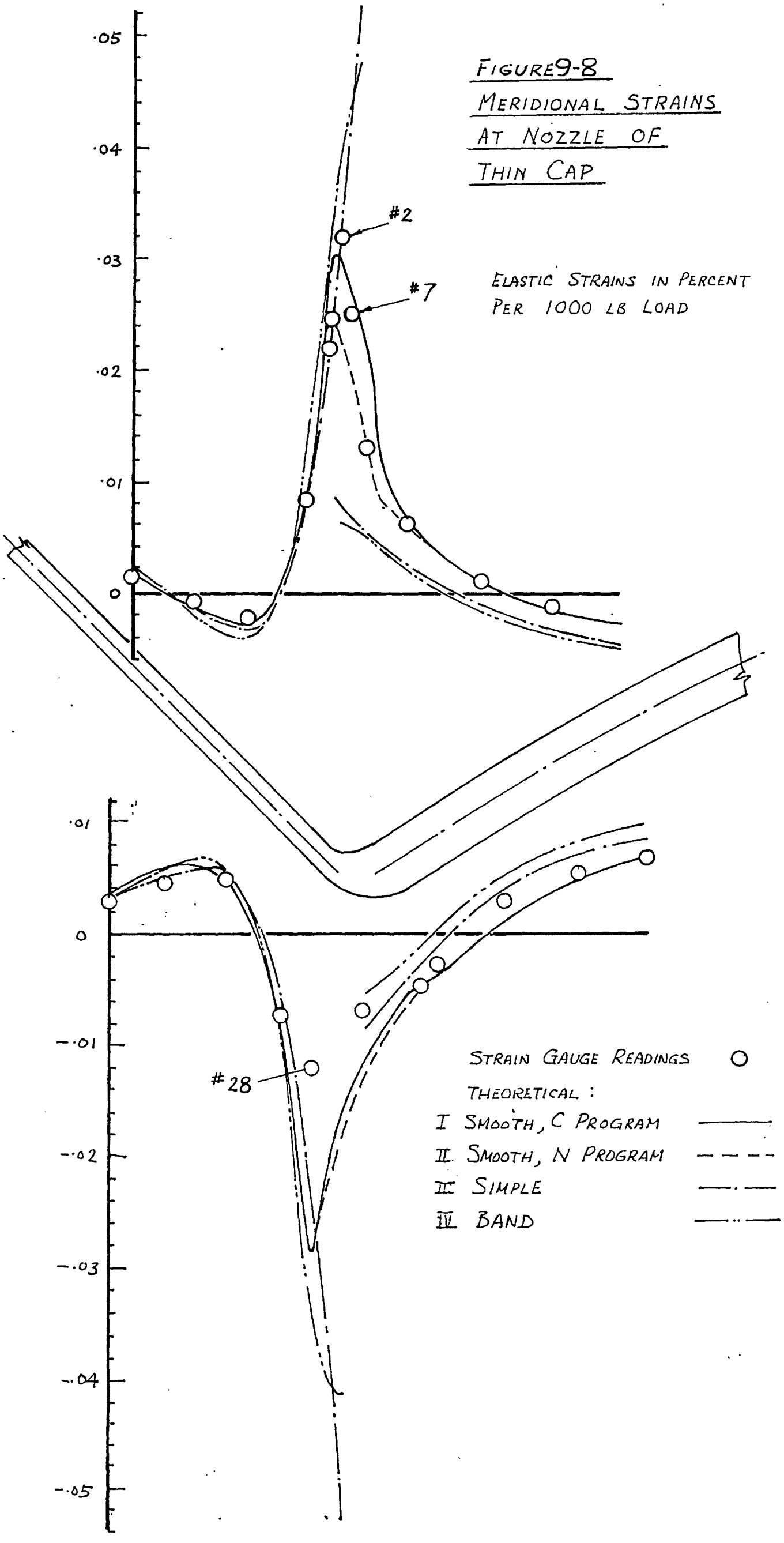

FIGURE 9-8
MERIDIONAL STRAINS
AT NOZZLE OF
THIN CAP

ELASTIC STRAINS IN PERCENT
PER 1000 LB LOAD

FIGURE 9-9

CIRCUMFERENTIAL STRAINS AT NOZZLE OF THIN CAP

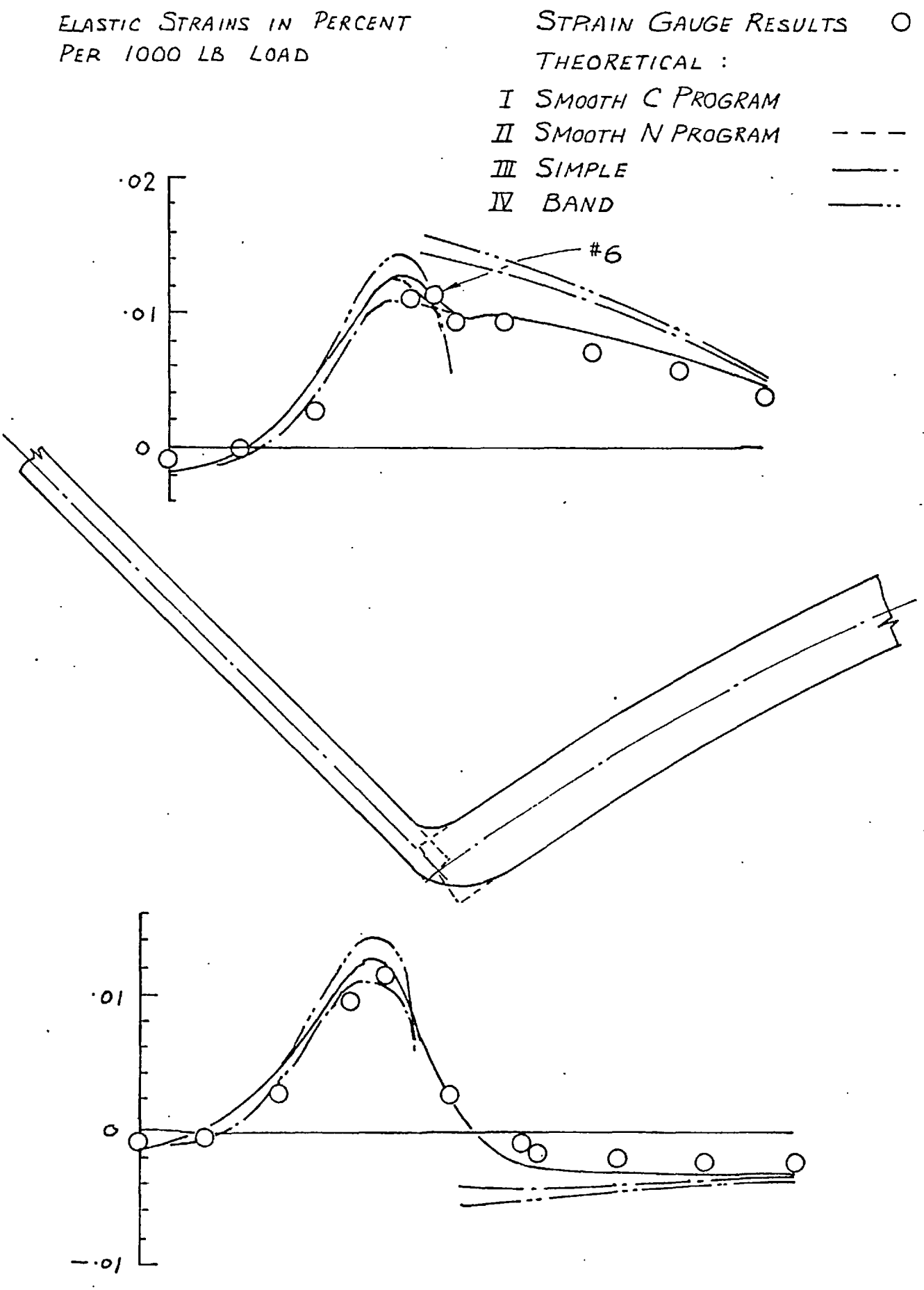

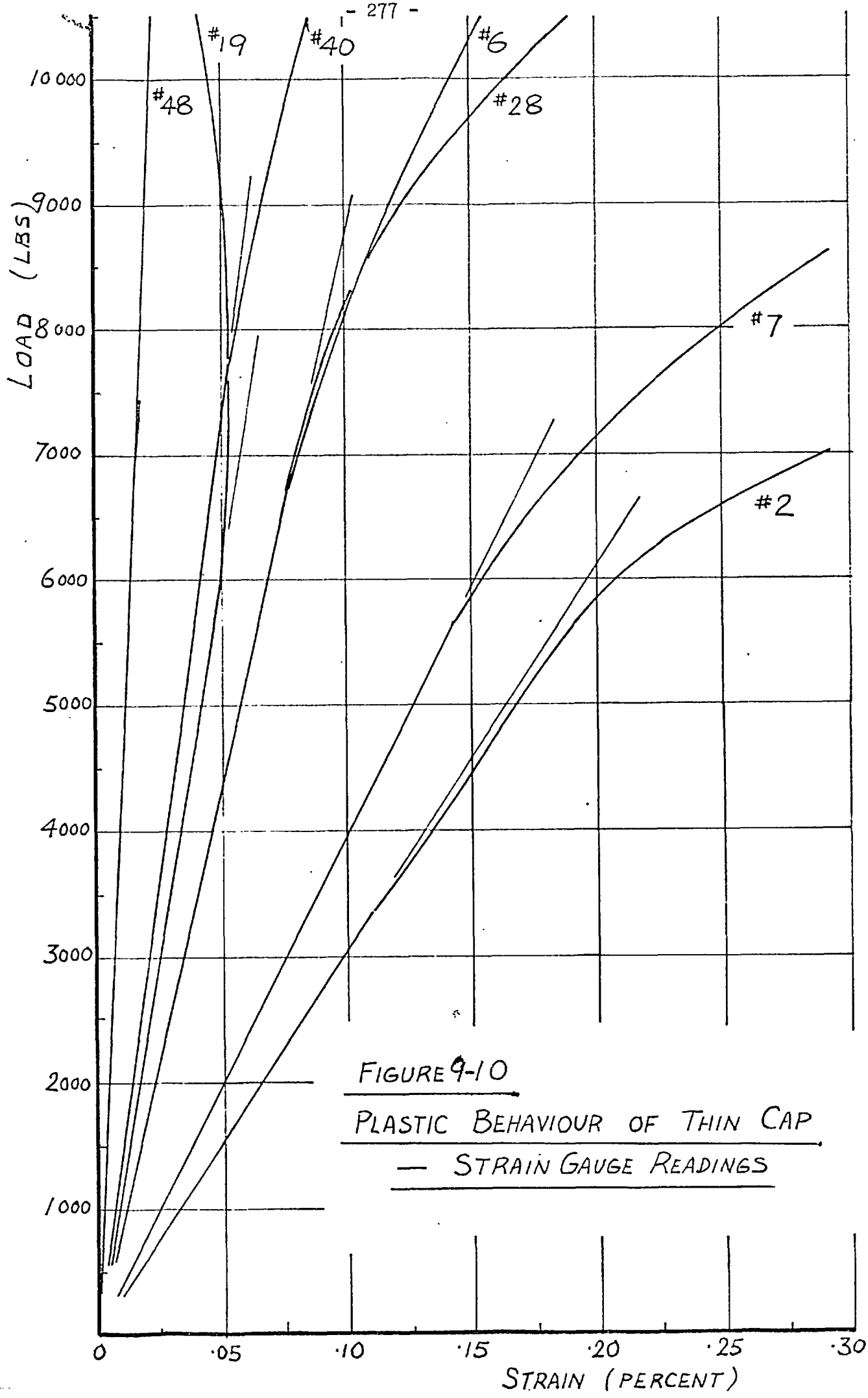

FIGURE 9-10

PLASTIC BEHAVIOUR OF THIN CAP

— STRAIN GAUGE READINGS

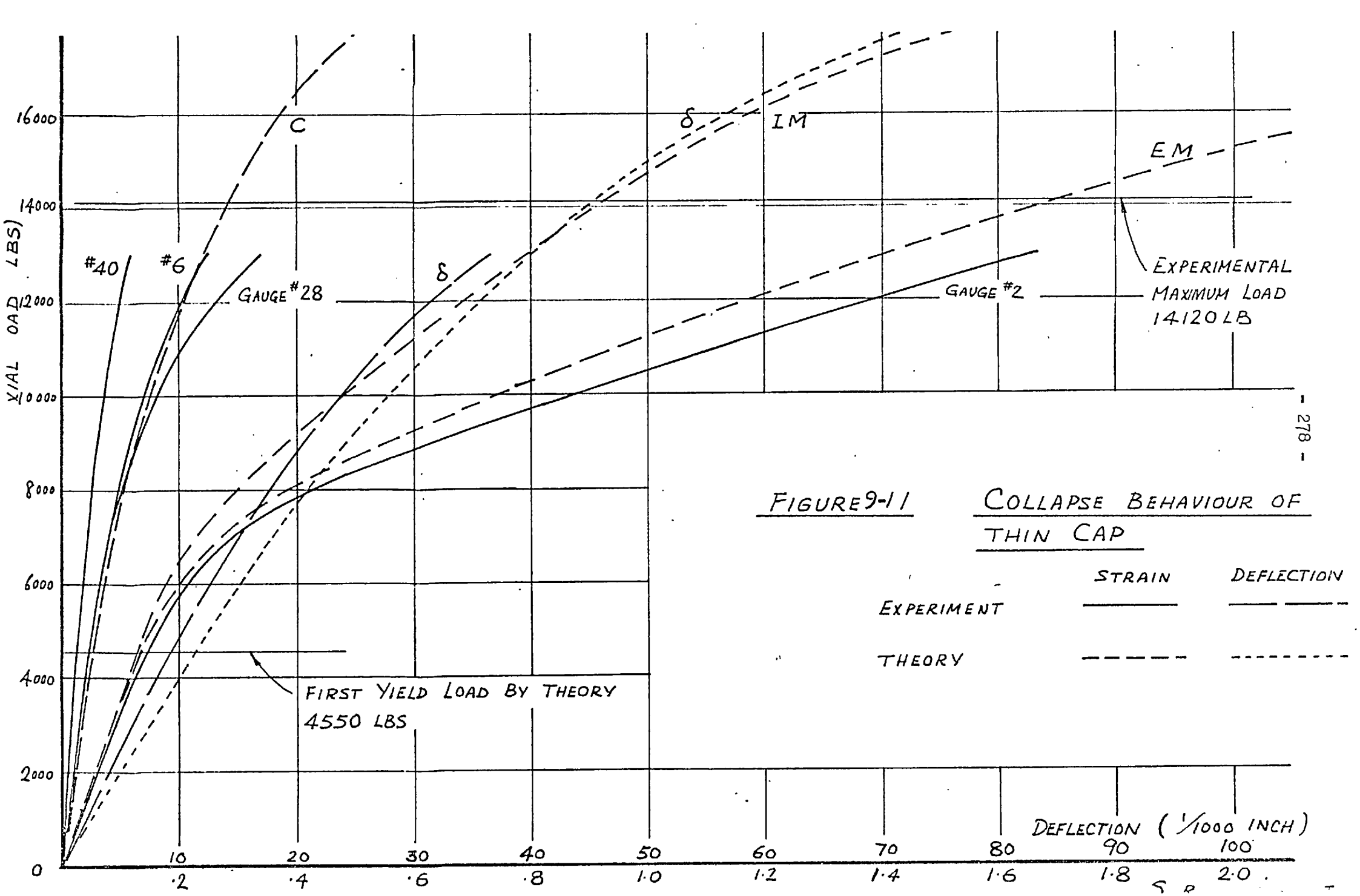

FIGURE 9-11 COLLAPSE BEHAVIOUR OF THIN CAP

FIG. 9-12

MERIDIONAL STRAINS AT NOZZLE OF THICK CAP

ELASTIC STRAINS IN PERCENT PER 1000 LB LOAD

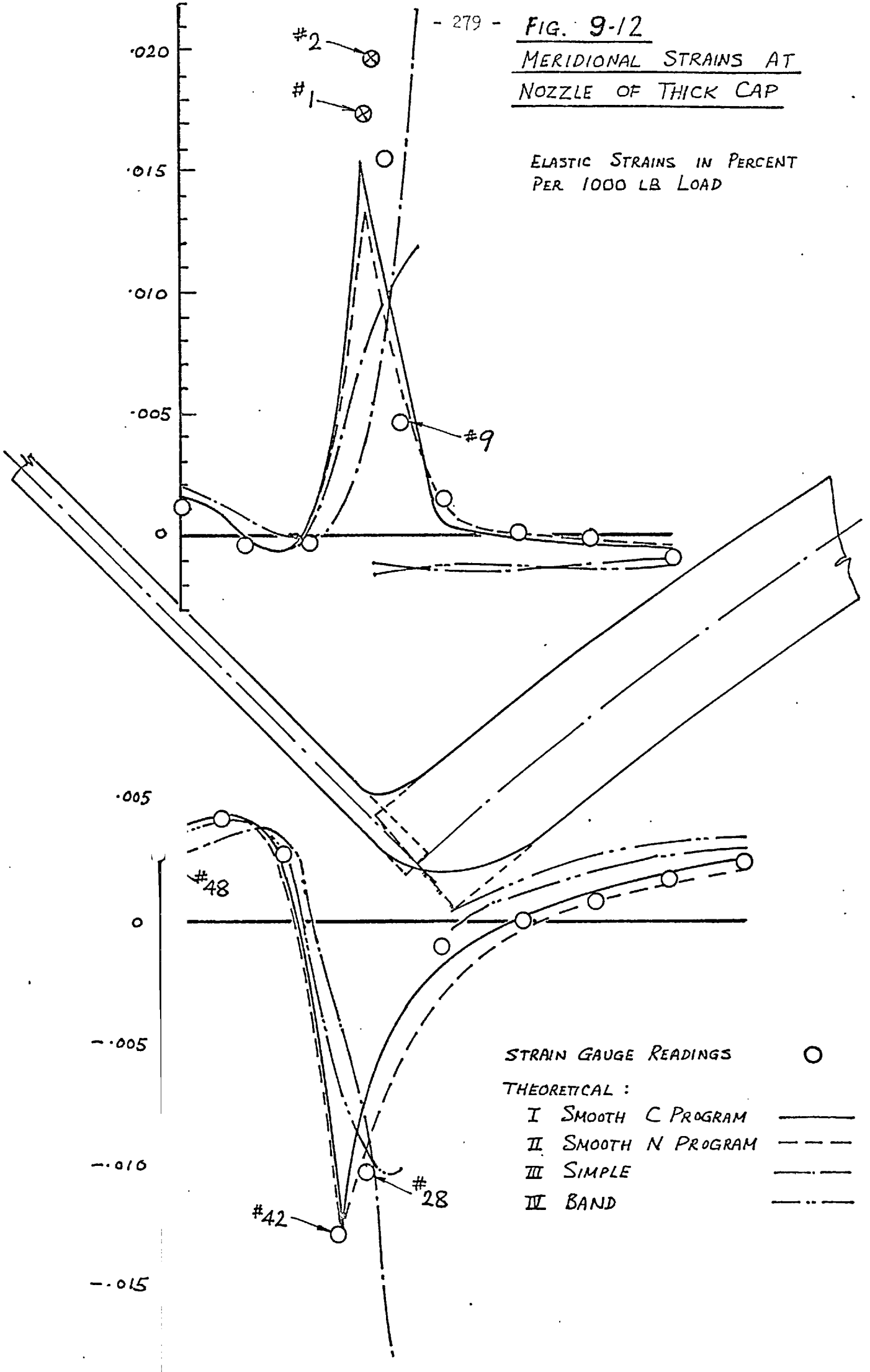

FIGURE 913

CIRCUMFERENTIAL STRAINS AT NOZZLE OF THICK CAP

ELASTIC STRAINS IN PERCENT PER 1000 LB LOAD

STRAIN GAUGE READINGS O

THEORETICAL :

I SMOOTH C PROGRAM ——————

II SMOOTH N PROGRAM — — — —

III SIMPLE ——·——

IV BAND ——··——

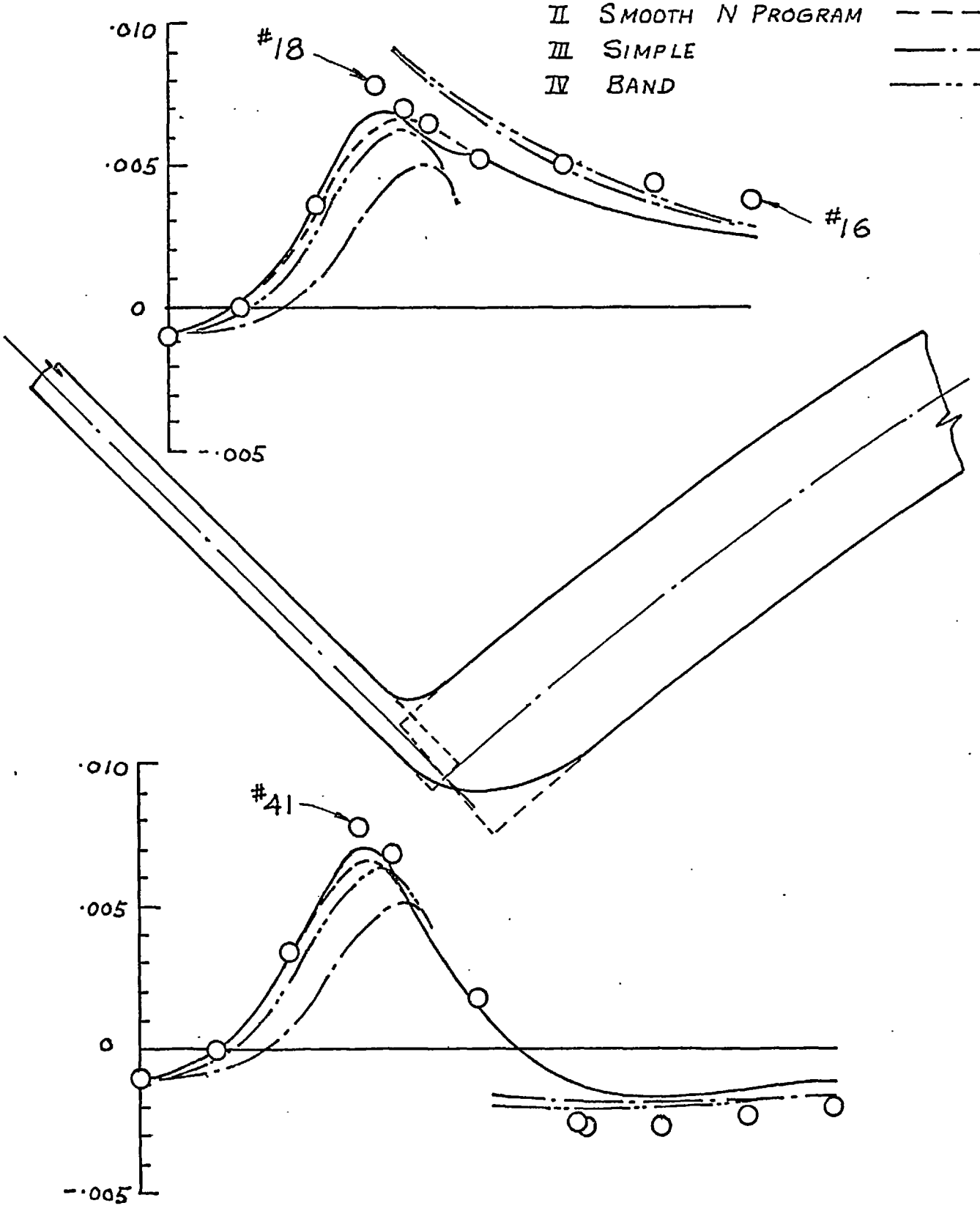

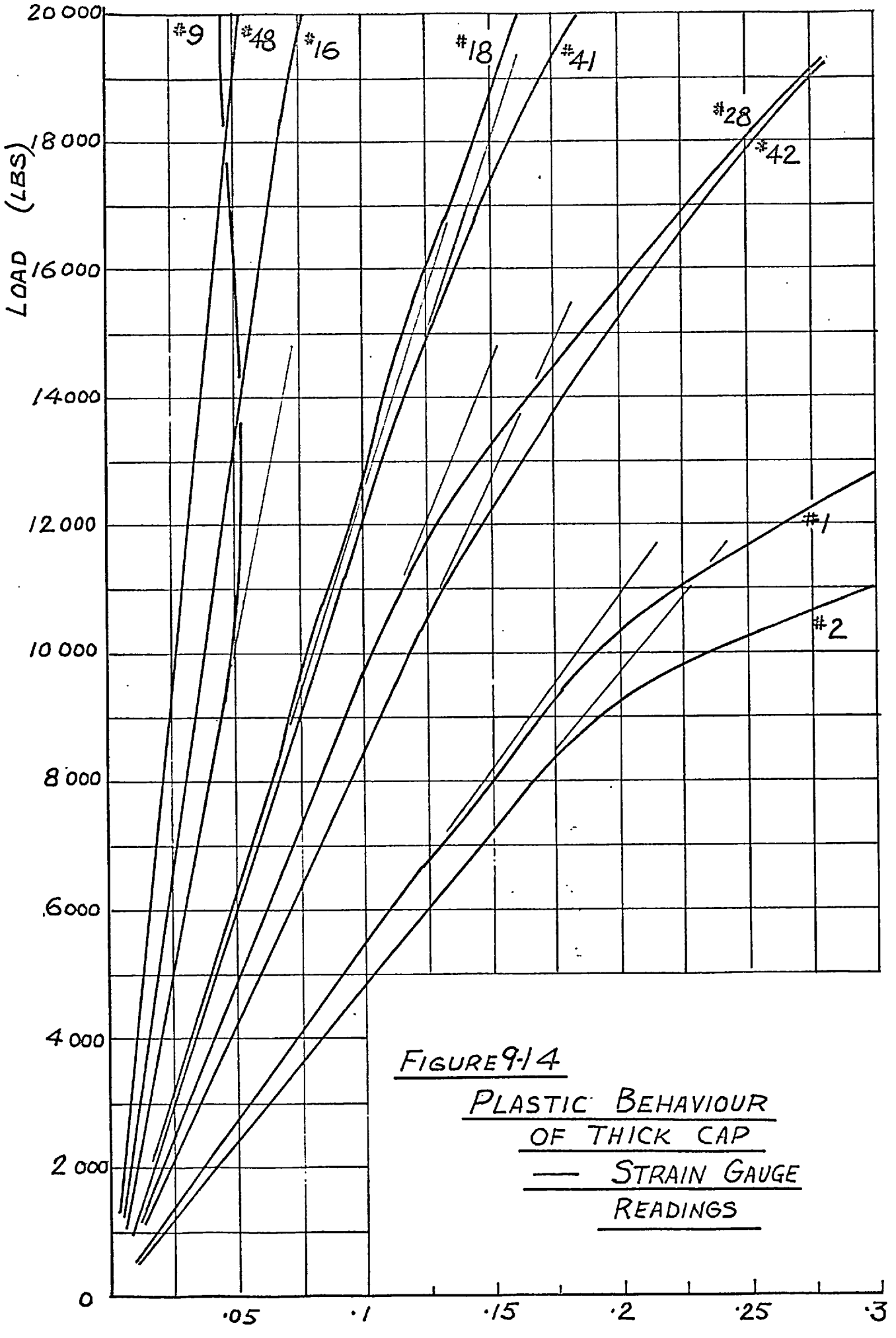

FIGURE 9-14

PLASTIC BEHAVIOUR OF THICK CAP — STRAIN GAUGE READINGS

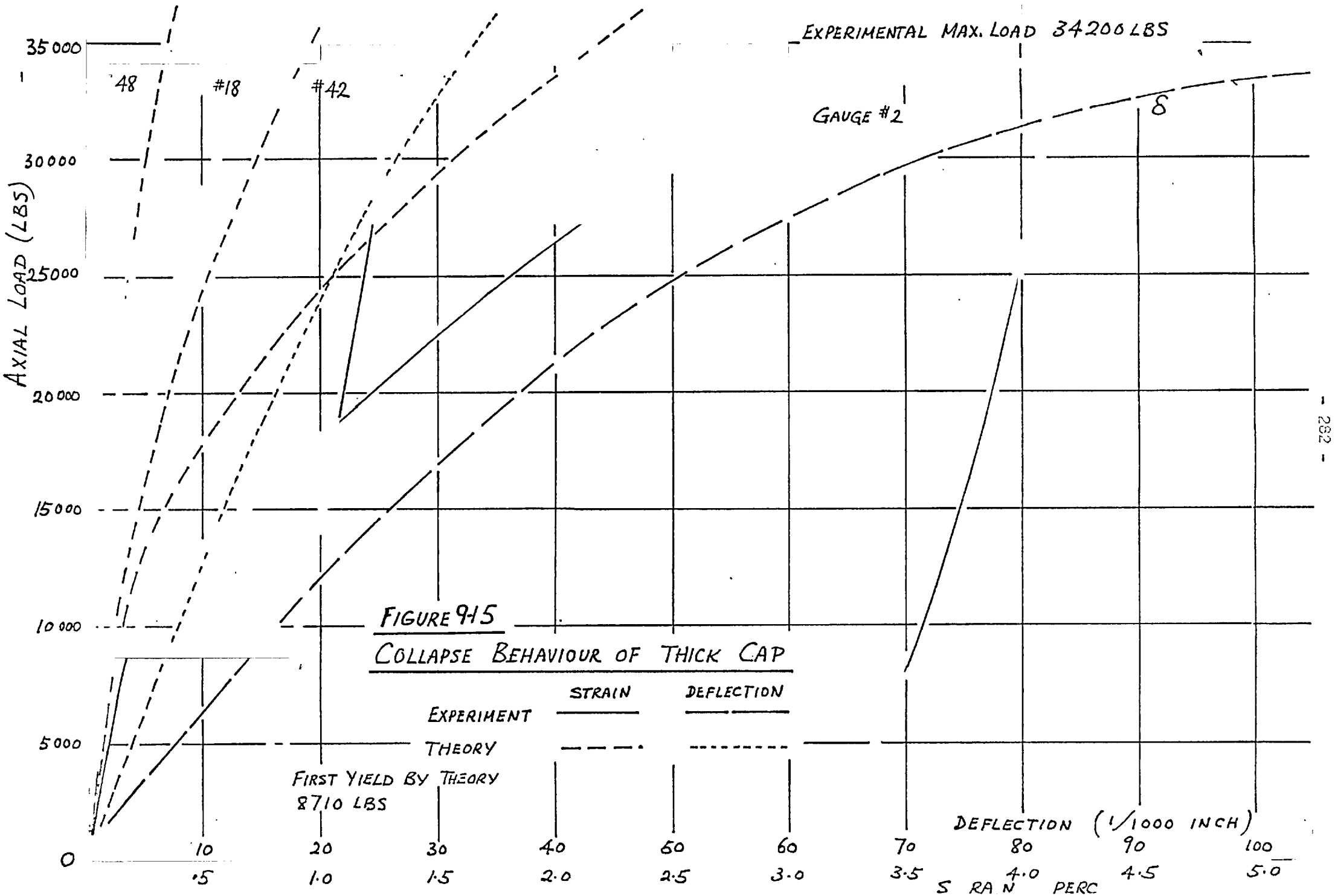
EXPERIMENTAL MAX. LOAD 34200 LBS
48
#18
#42
GAUGE #2
δ
AXIAL LOAD (LBS)
35000
30000
25000
20000
15000
10000
5000
0
FIGURE 9-15
COLLAPSE BEHAVIOUR OF THICK CAP
STRAIN
DEFLECTION
EXPERIMENT
THEORY
FIRST YIELD BY THEORY
8710 LBS
DEFLECTION (1/1000 INCH)
10
20
30
40
50
60
70
80
90
100
·5
1·0
1·5
2·0
2·5
3·0
3·5
4·0
4·5
5·0
STRAIN PERC

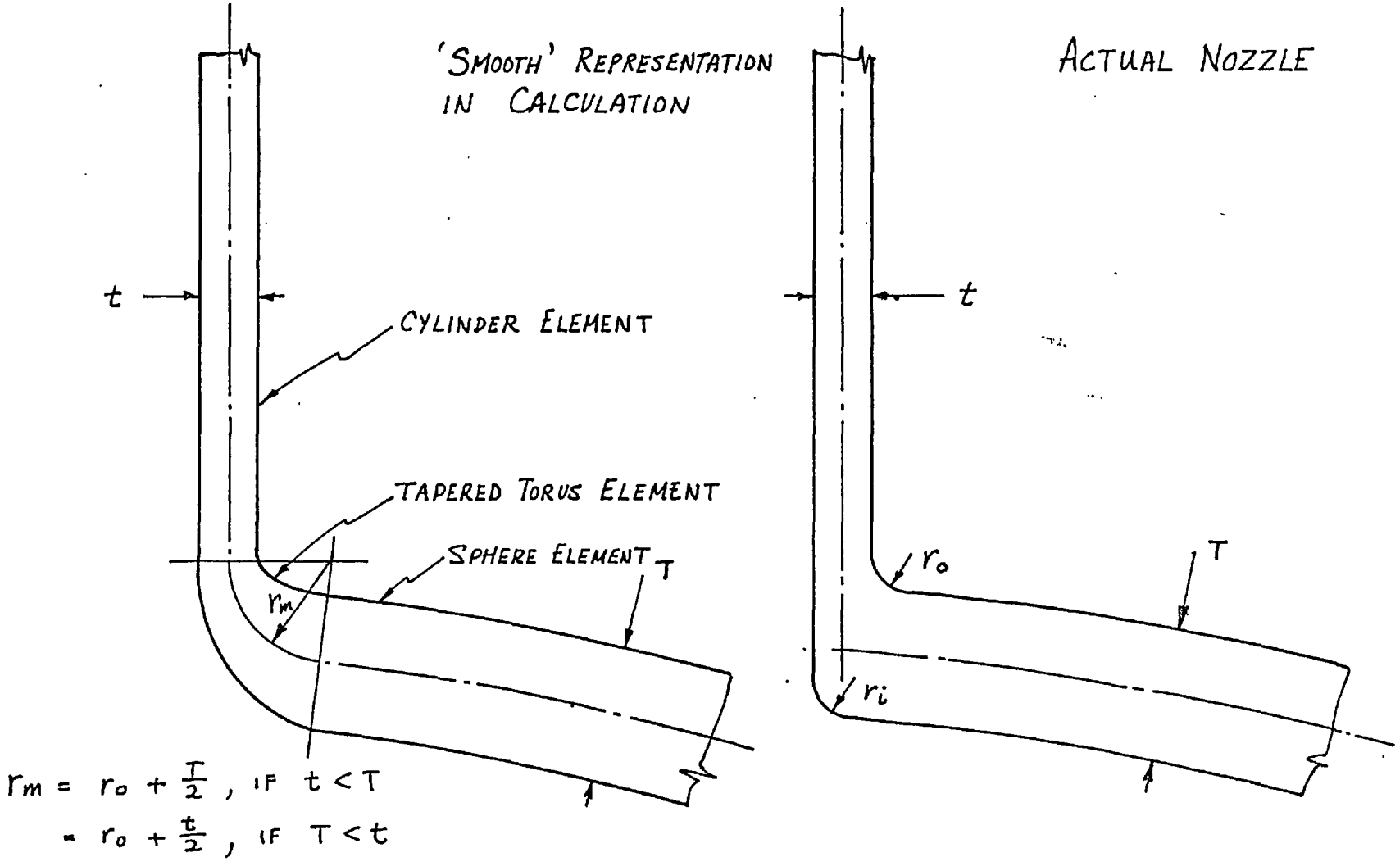

FIGURE 10-1 'SMOOTH' REPRESENTATION OF NOZZLE JUNCTION

FIGURE 10-2

EQUIVALENT STRESS INTENSITY AT NOZZLE OF THIN CAP

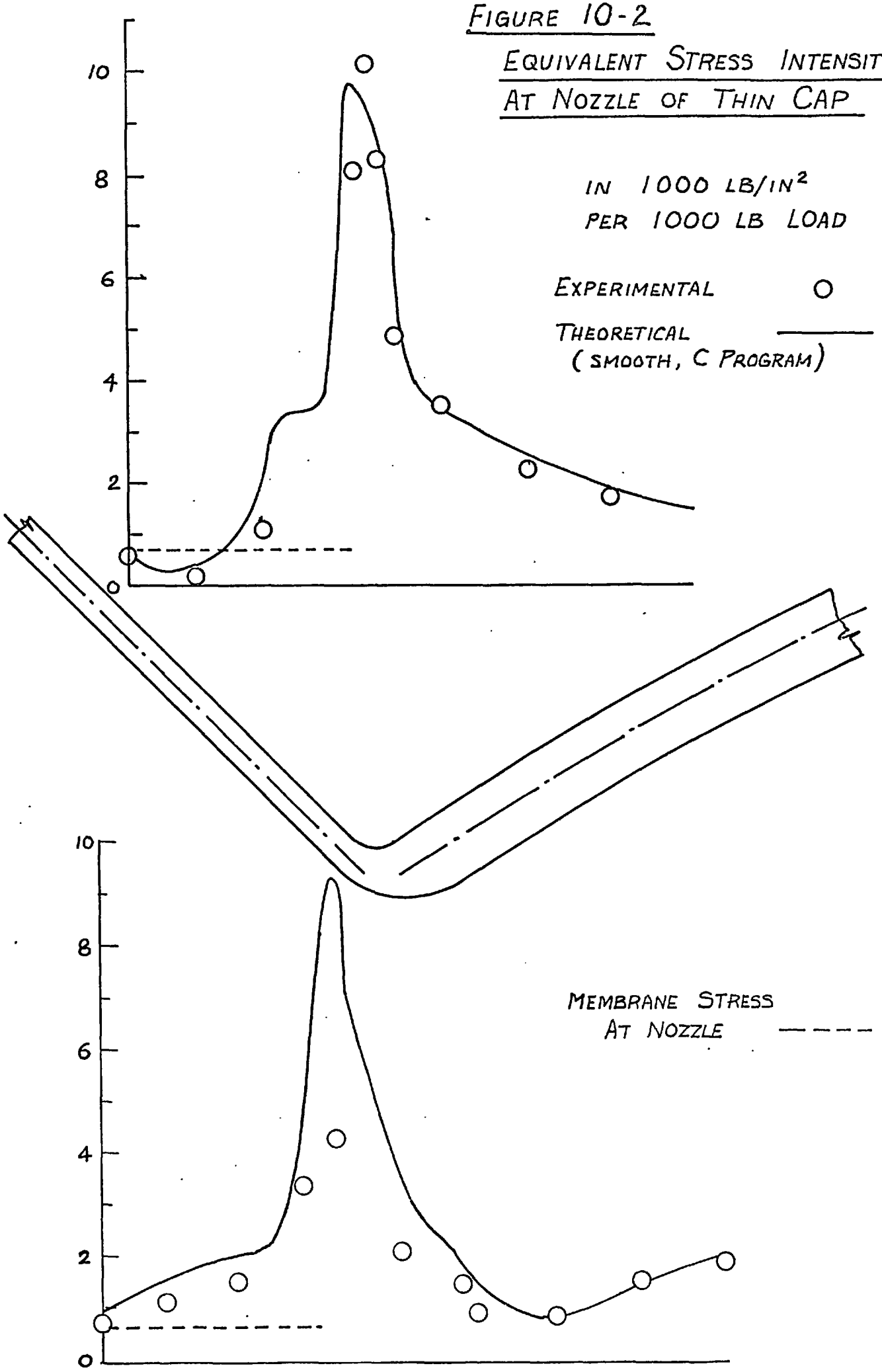

FIGURE 10-3

EQUIVALENT STRESS INTENSITY

AT NOZZLE OF THICK CAP

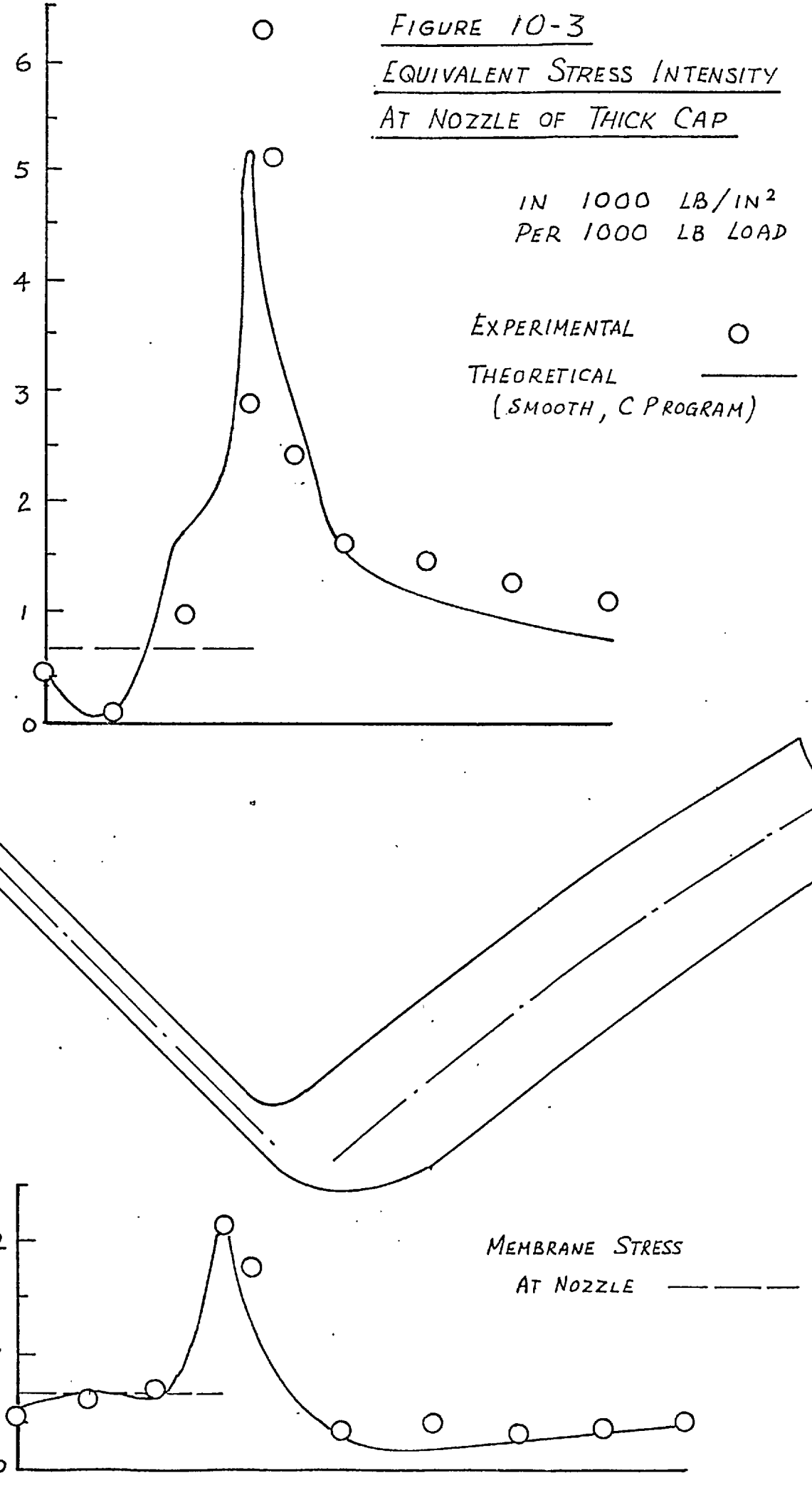

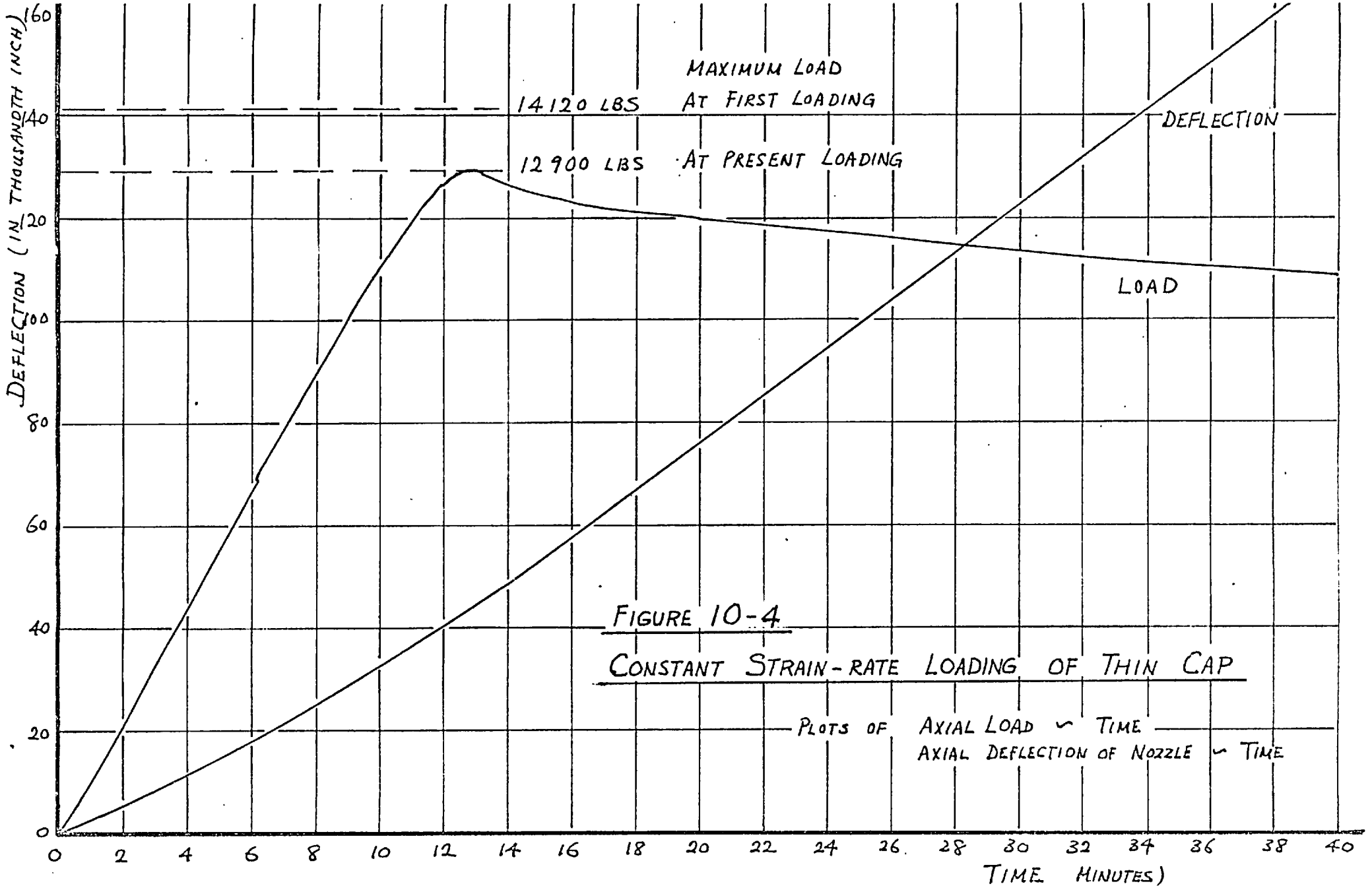

FIGURE 10-4

CONSTANT STRAIN-RATE LOADING OF THIN CAP

PLOTS OF AXIAL LOAD ~ TIME
AXIAL DEFLECTION OF NOZZLE ~ TIME

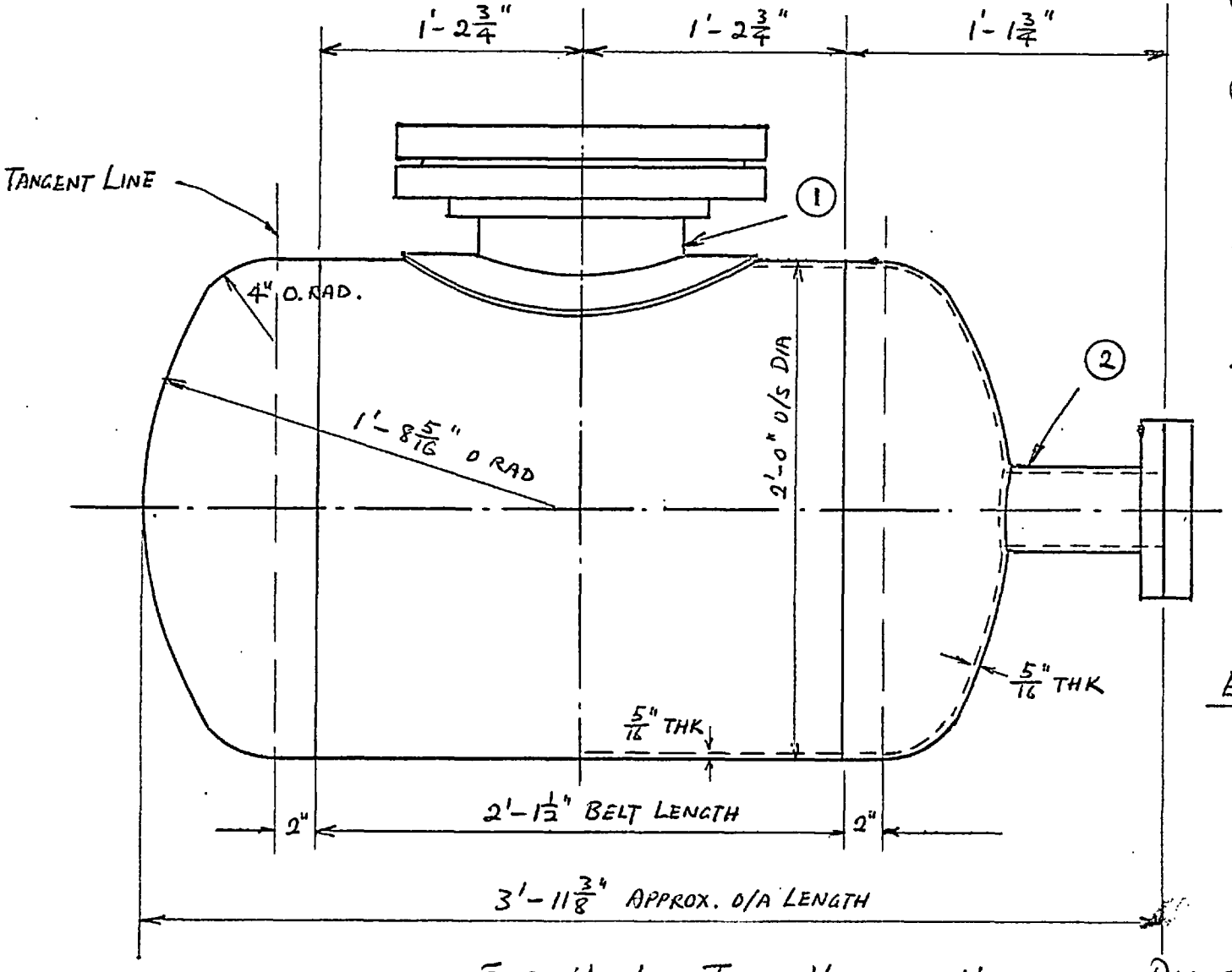

(1) ACCESS NOZZLE
NOM. SIZE 10"

(2) TEST NOZZLE
FOR DETAILS SEE FIG 11-2

MATERIAL
18/8/Ti STAINLESS STEEL

DESIGN PRESSURE 360 LB/IN²

ELEVATION

FIG 11-1 TEST VESSEL NOMINAL DIMENSIONS

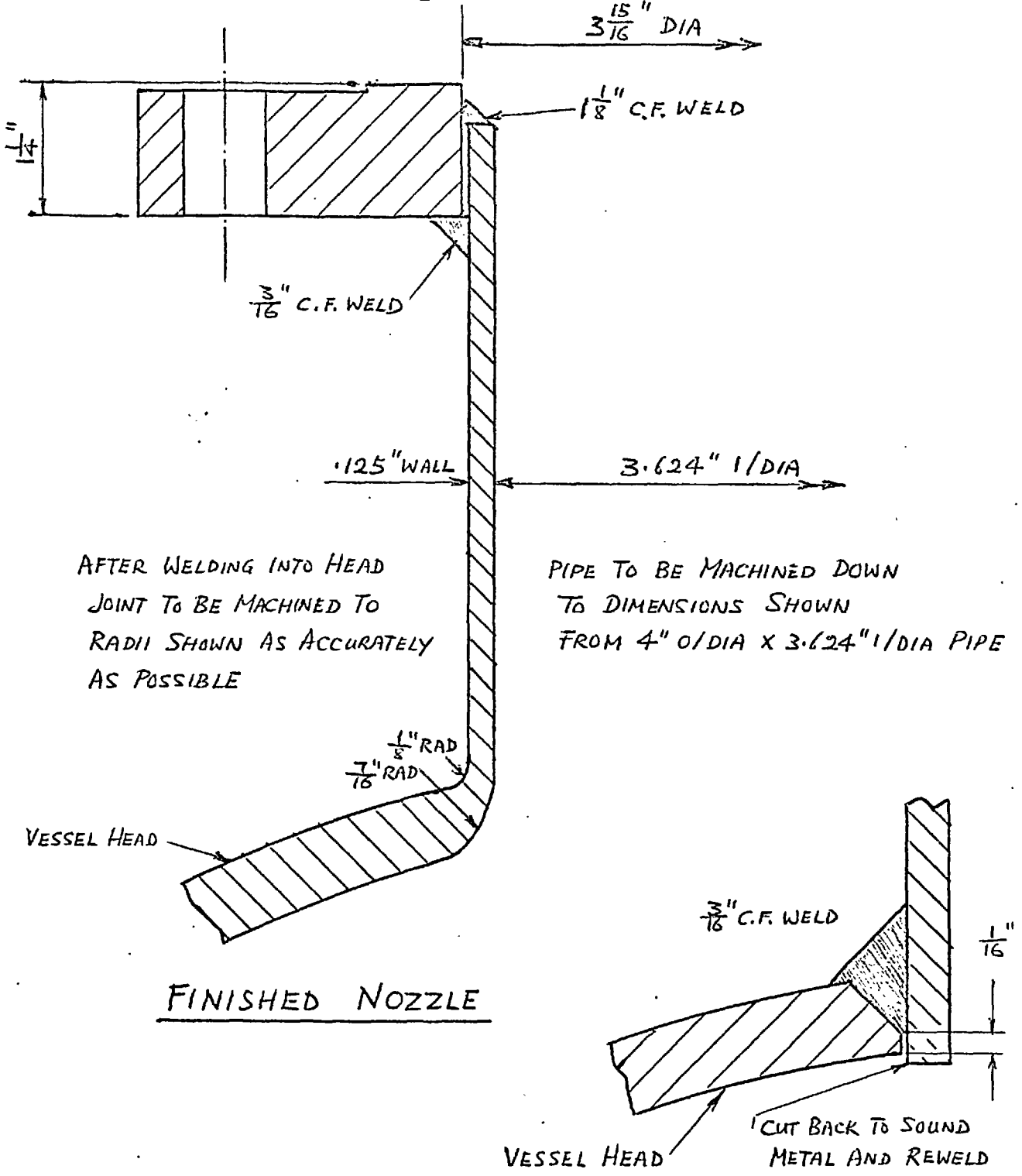

FIG 11-2 DETAILS OF TEST NOZZLE

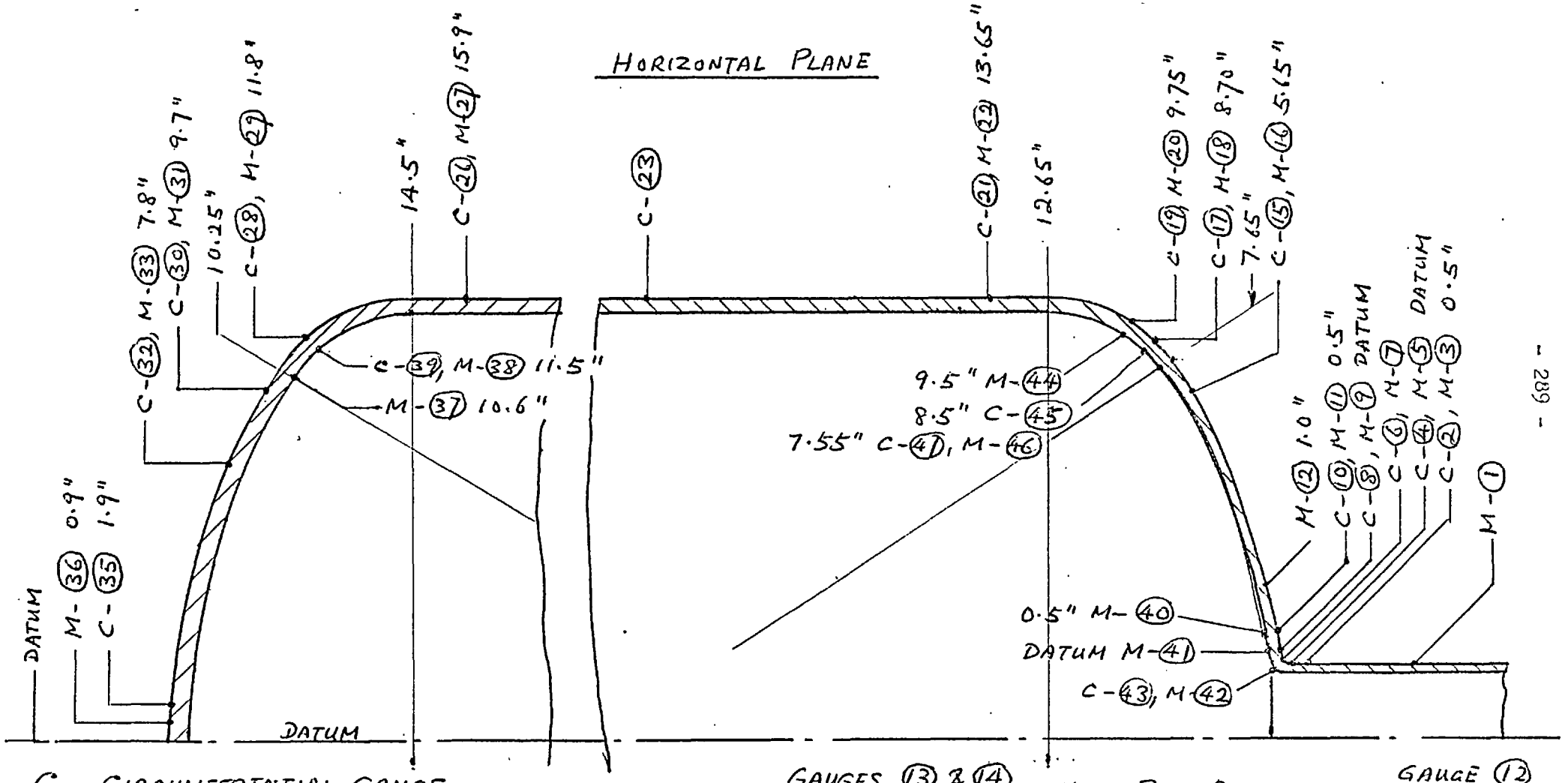

C - CIRCUMFERENTIAL GAUGE

M - MERIDIONAL GAUGE

ALSO SHOWN ARE DISTANCES ALONG SHELL SURFACE FROM DATUM POSITIONS

GAUGES (13) & (14) HAVE SAME POSITION AS GAUGE (12)
GAUGES (24) & (25) BUT IN PLANES 90° APART GAUGE (23)

FIG. 11-3 POSITION OF STRAIN GAUGES ON TEST VESSEL

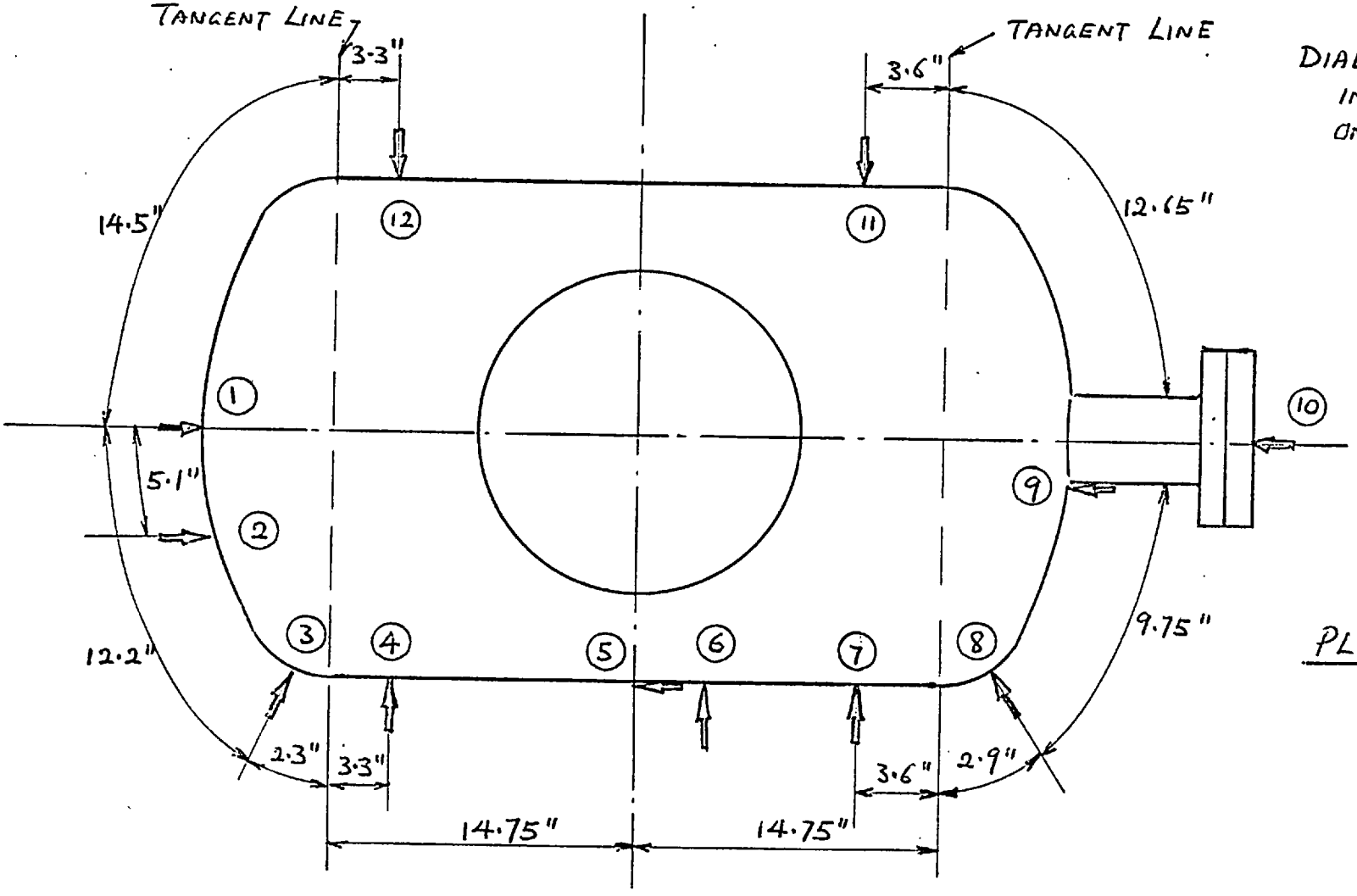

FIG 11-4 POSITION OF DIAL GAUGES ON TEST VESSEL

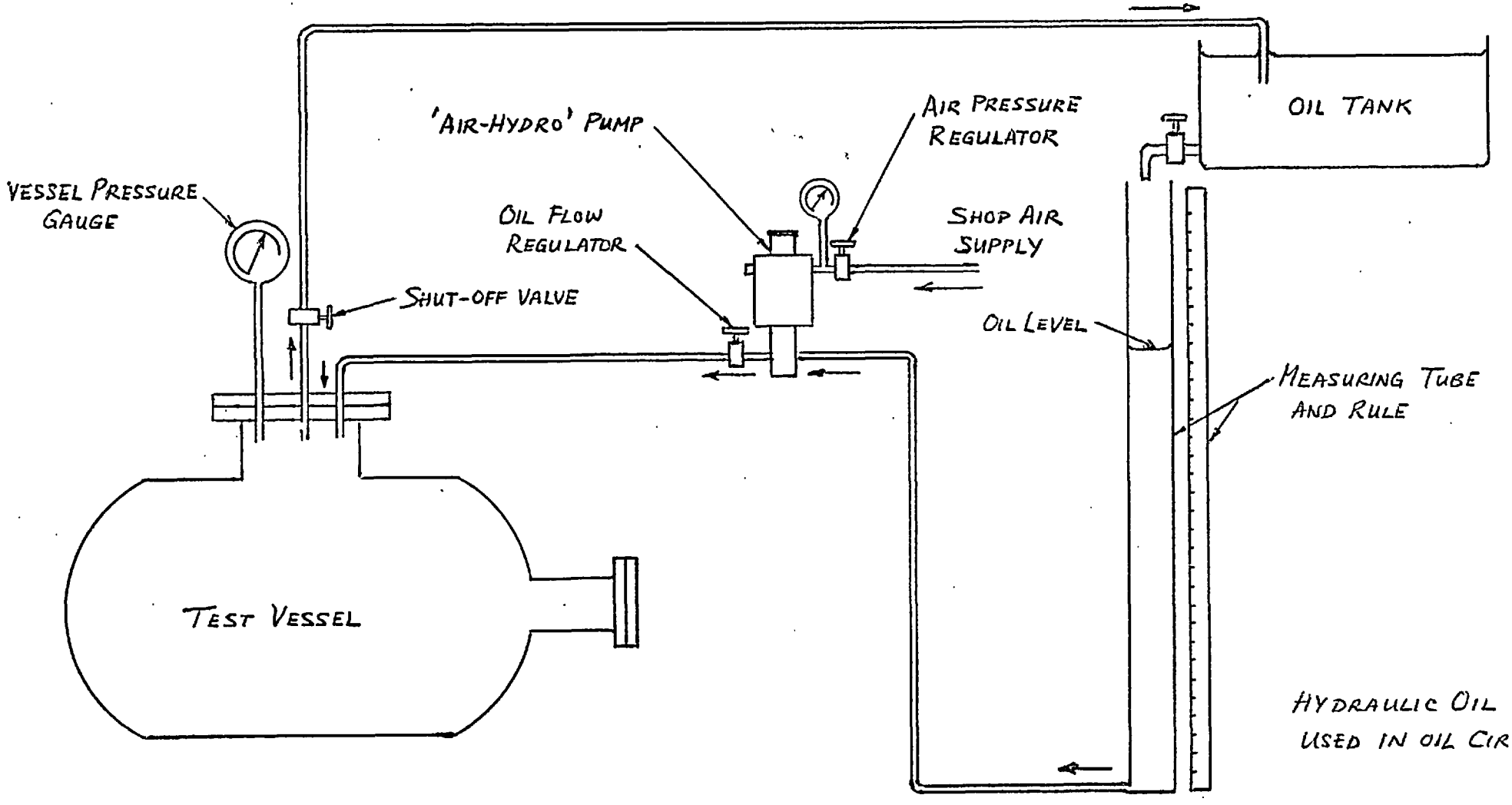

FIG 11-5 PRESSURE CIRCUIT

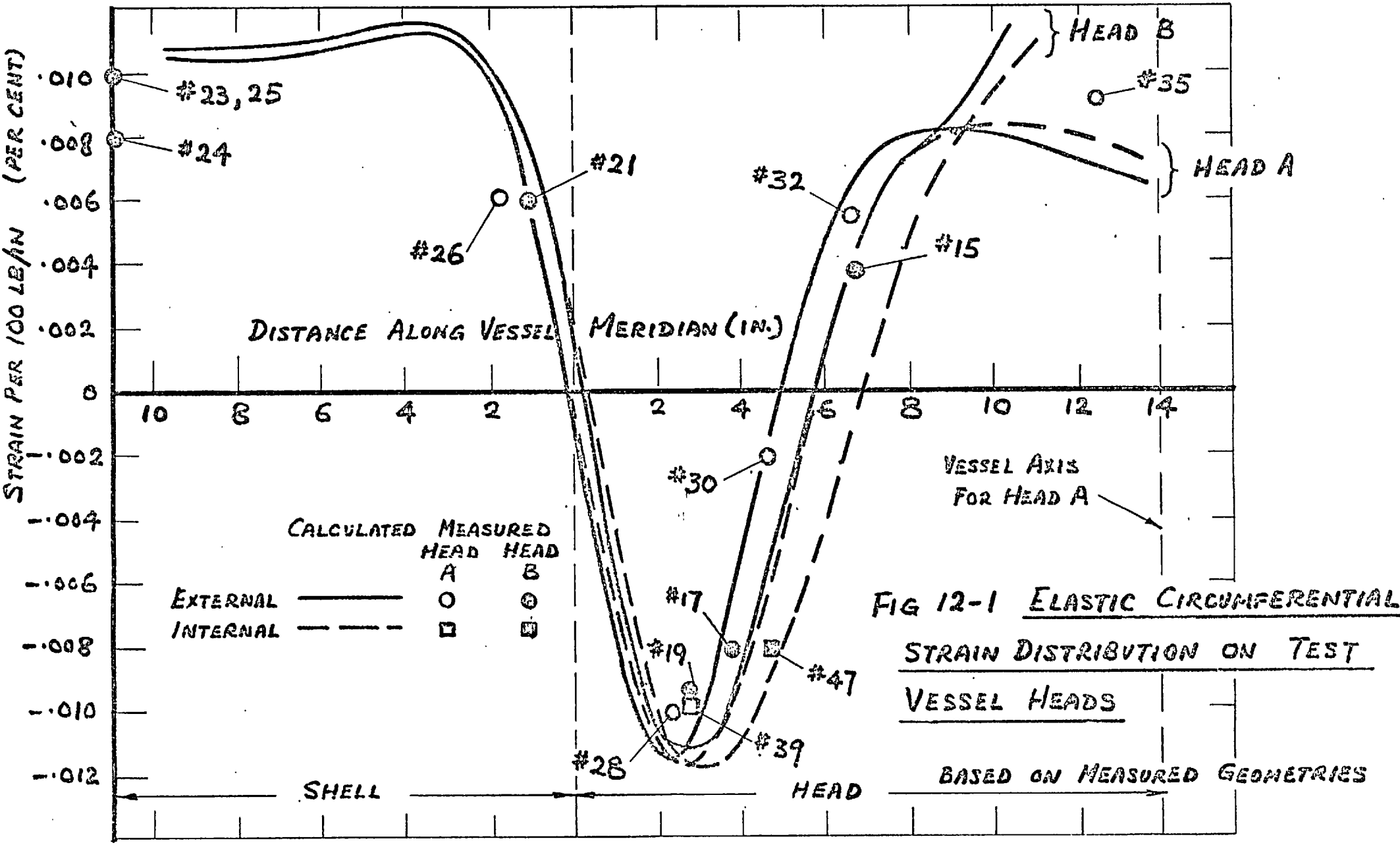

FIG 12-1 ELASTIC CIRCUMFERENTIAL STRAIN DISTRIBUTION ON TEST VESSEL HEADS

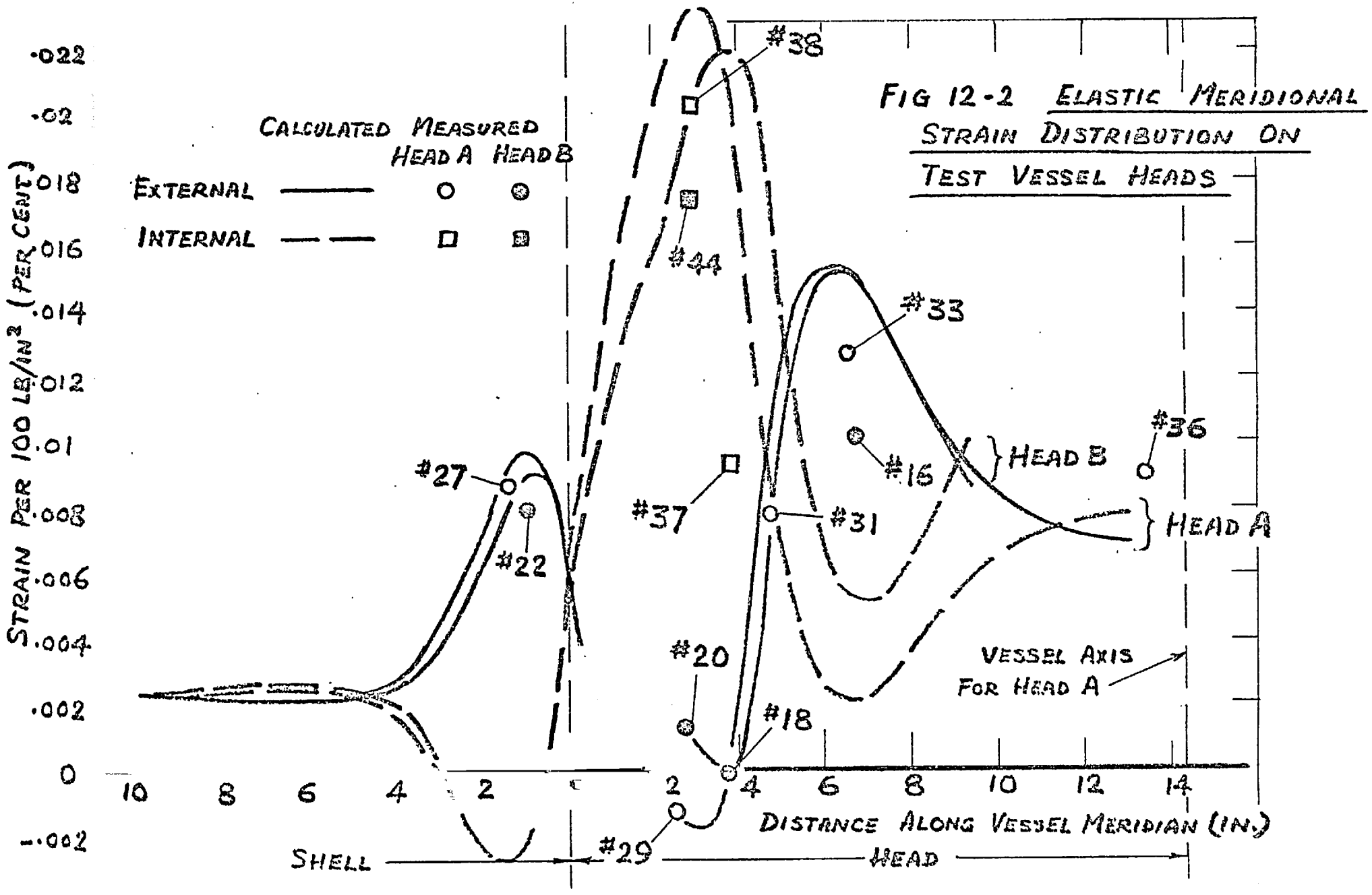
FIG 12-2 ELASTIC MERIDIONAL STRAIN DISTRIBUTION ON TEST VESSEL HEADS
CALCULATED MEASURED
HEAD A HEAD B
EXTERNAL
INTERNAL
STRAIN PER 100 LB/IN² (PER CENT)
.022
.02
.018
.016
.014
.012
.01
.008
.006
.004
.002
0
-.002
#38
#44
#33
#36
#16
HEAD B
#27
#37
#31
HEAD A
#22
#20
#18
VESSEL AXIS FOR HEAD A
10 8 6 4 2 2 4 6 8 10 12 14
DISTANCE ALONG VESSEL MERIDIAN (IN.)
SHELL
#29
HEAD

FIG 12-3 ELASTIC CIRCUMFERENTIAL STRAIN

NOZZLE END OF TEST VESSEL (HEAD B)

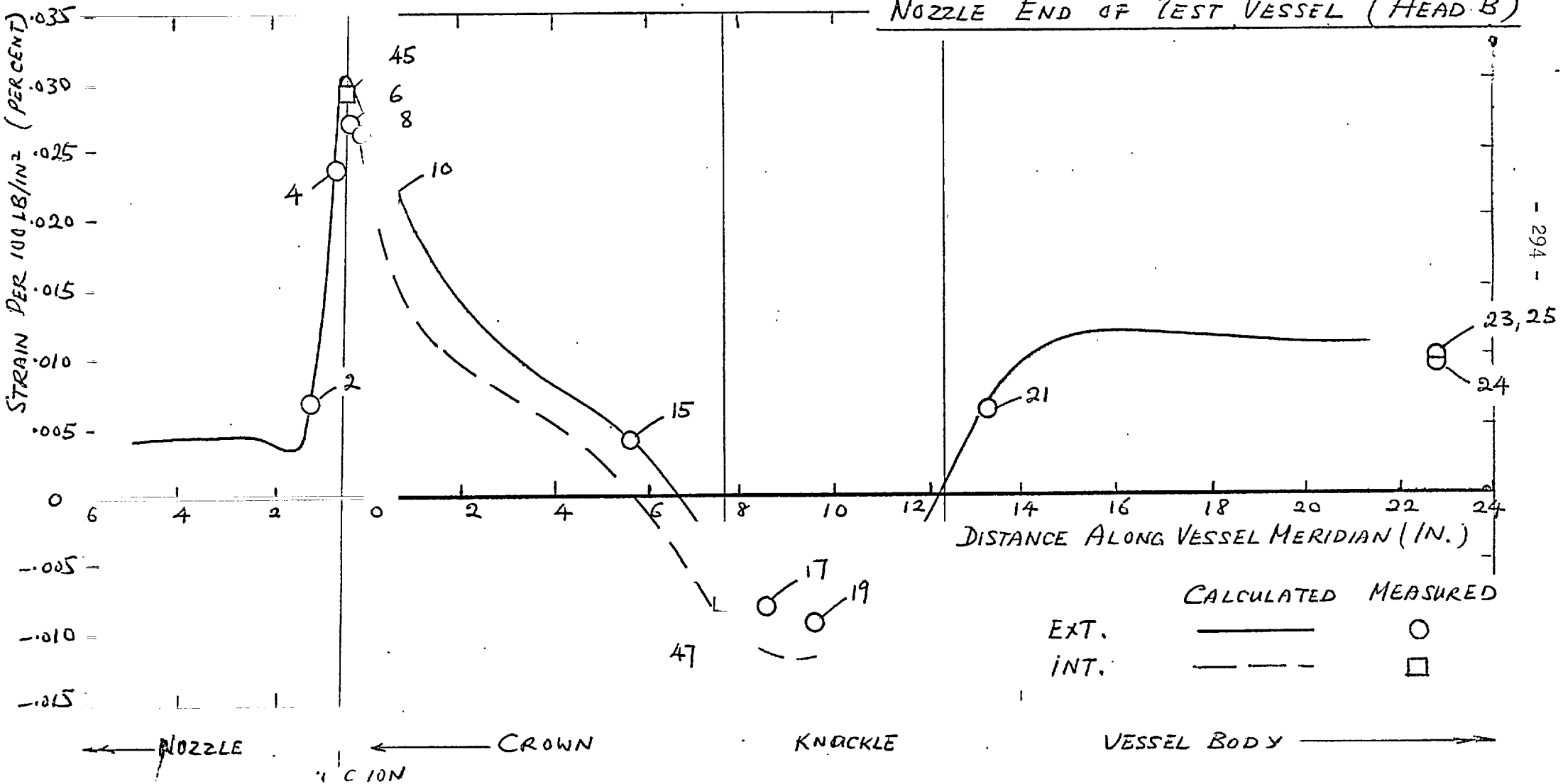

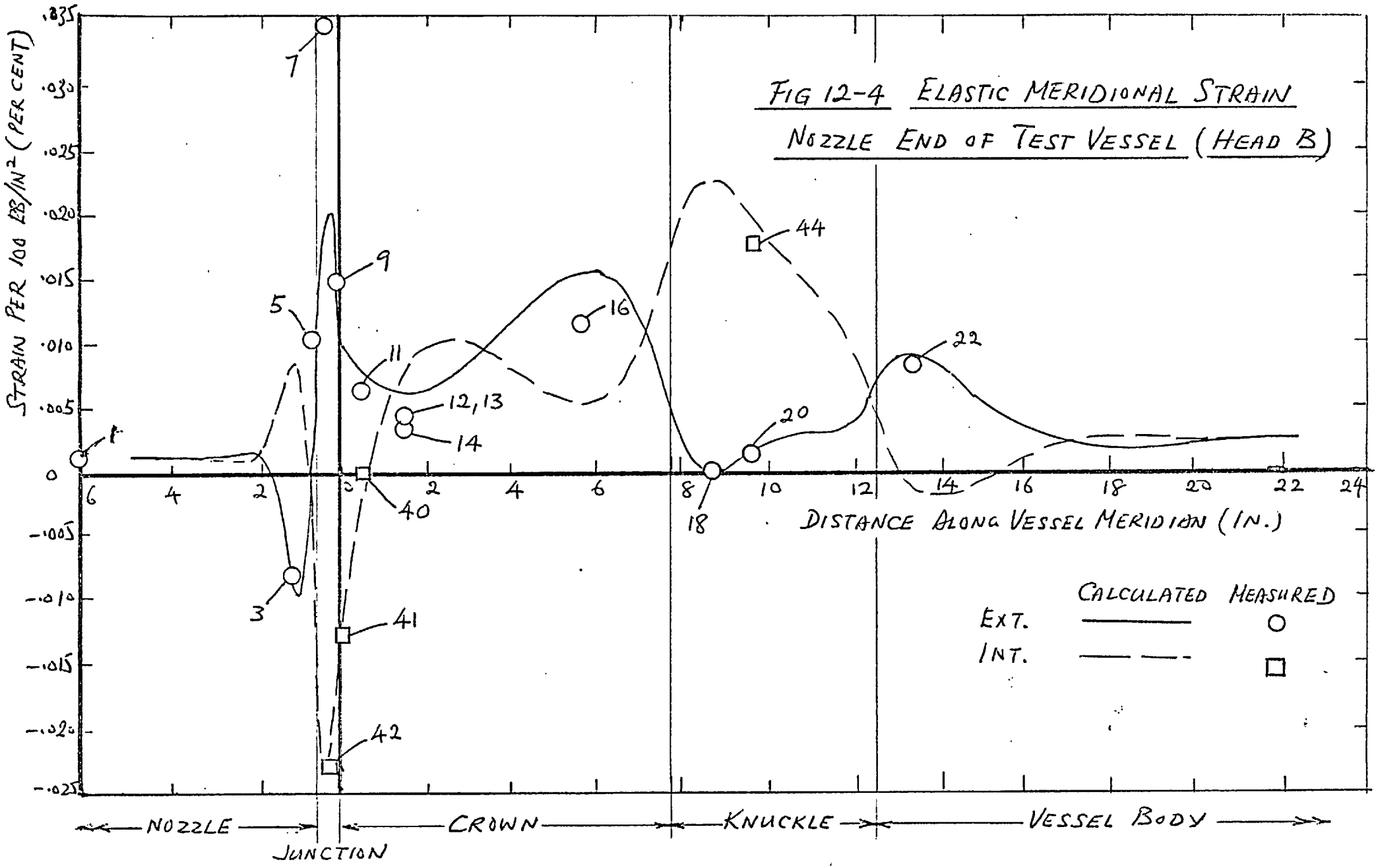
FIG 12-4 ELASTIC MERIDIONAL STRAIN
NOZZLE END OF TEST VESSEL (HEAD B)
STRAIN PER 100 LBS/IN² (PER CENT)
.035
.030
.025
.020
.015
.010
.005
0
-.005
-.010
-.015
-.020
-.025
6 4 2 0 2 4 6 8 10 12 14 16 18 20 22 24
DISTANCE ALONG VESSEL MERIDION (IN.)
1
3
5
7
9
11
12,13
14
16
18
20
22
40
41
42
44
CALCULATED MEASURED
EXT.
INT.
NOZZLE
JUNCTION
CROWN
KNUCKLE
VESSEL BODY

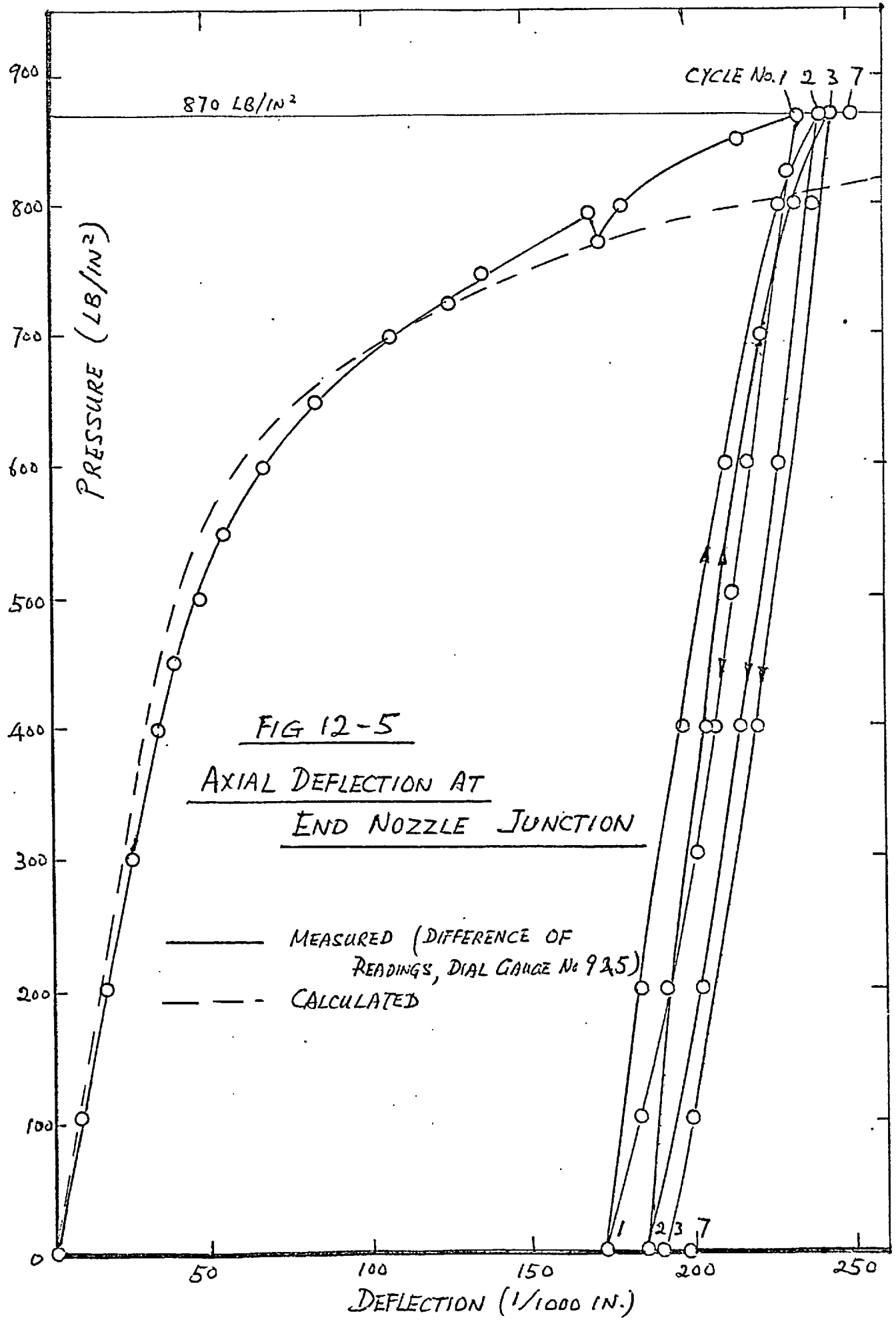

FIG 12-5

AXIAL DEFLECTION AT END NOZZLE JUNCTION

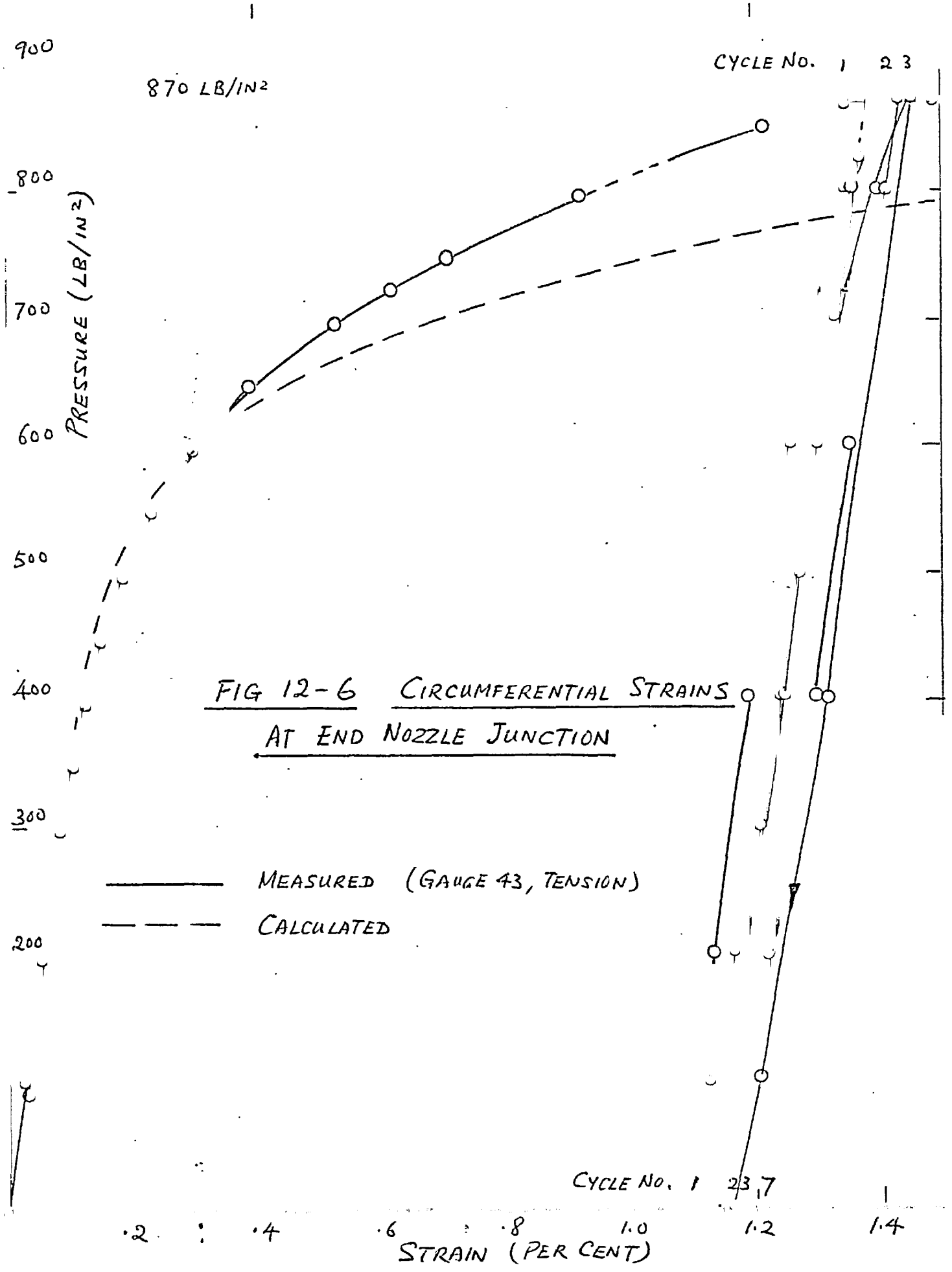

FIG 12-6 CIRCUMFERENTIAL STRAINS AT END NOZZLE JUNCTION

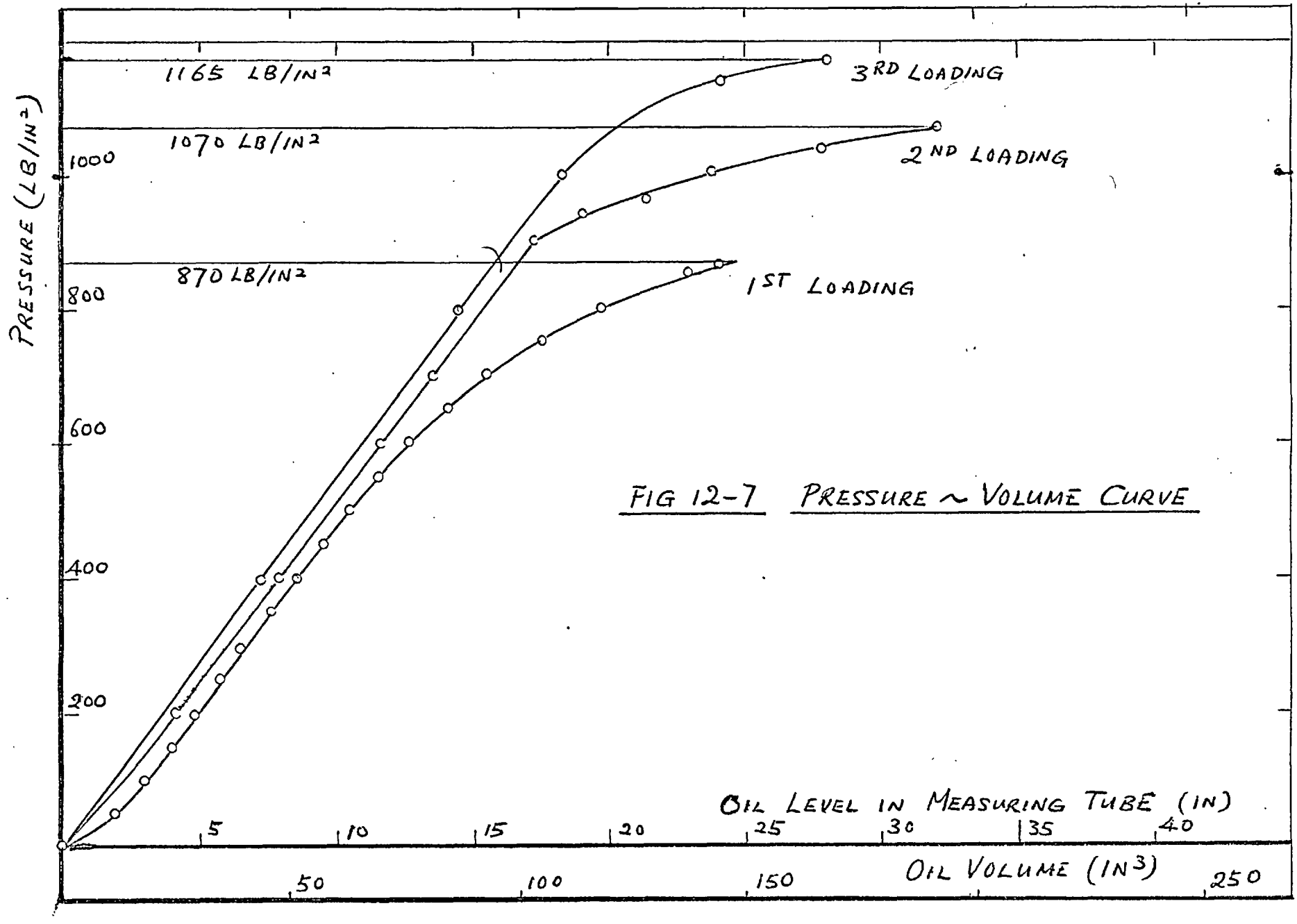

FIG 12-7 PRESSURE ~ VOLUME CURVE

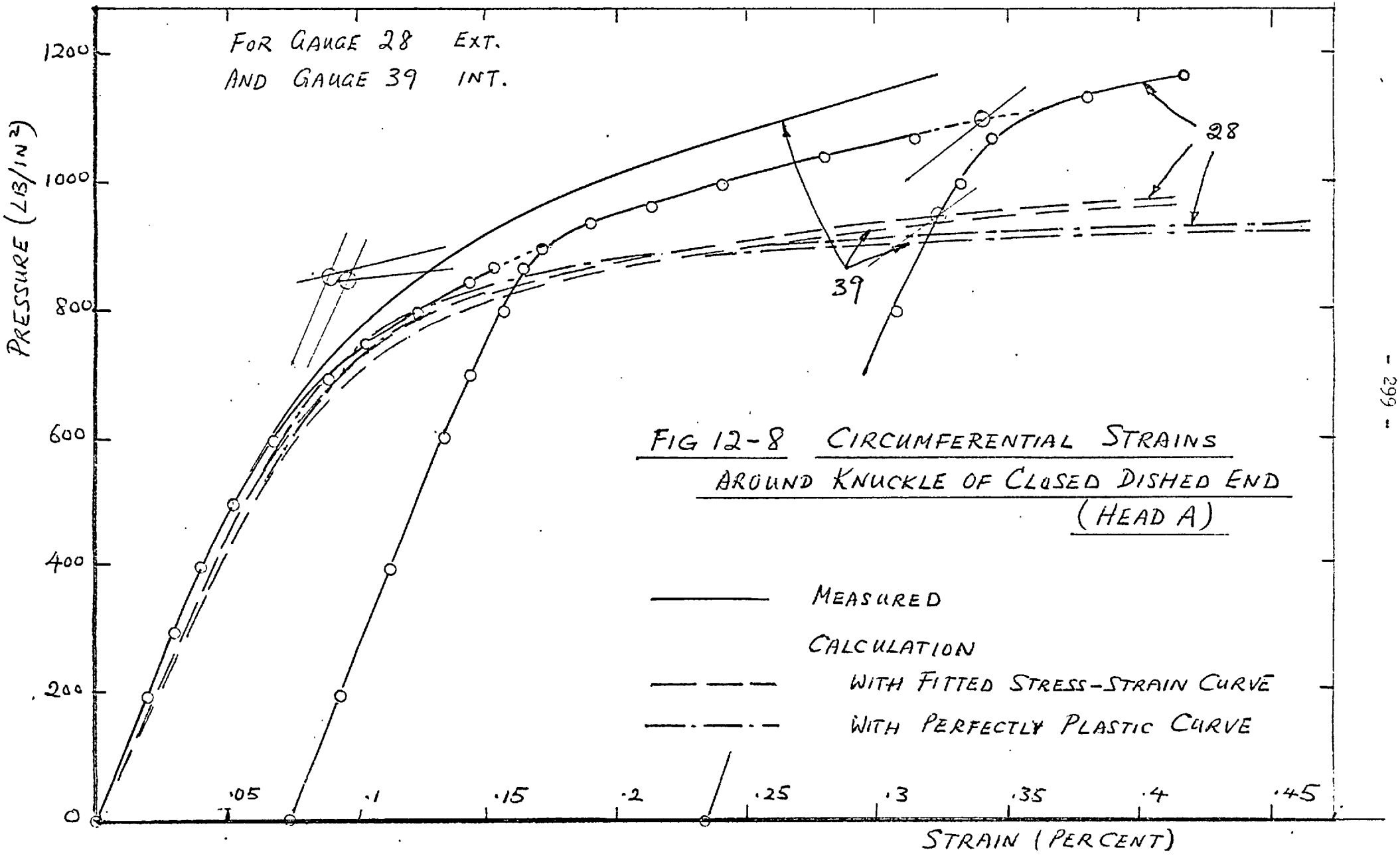

FIG 12-8 CIRCUMFERENTIAL STRAINS AROUND KNUCKLE OF CLOSED DISHED END (HEAD A)

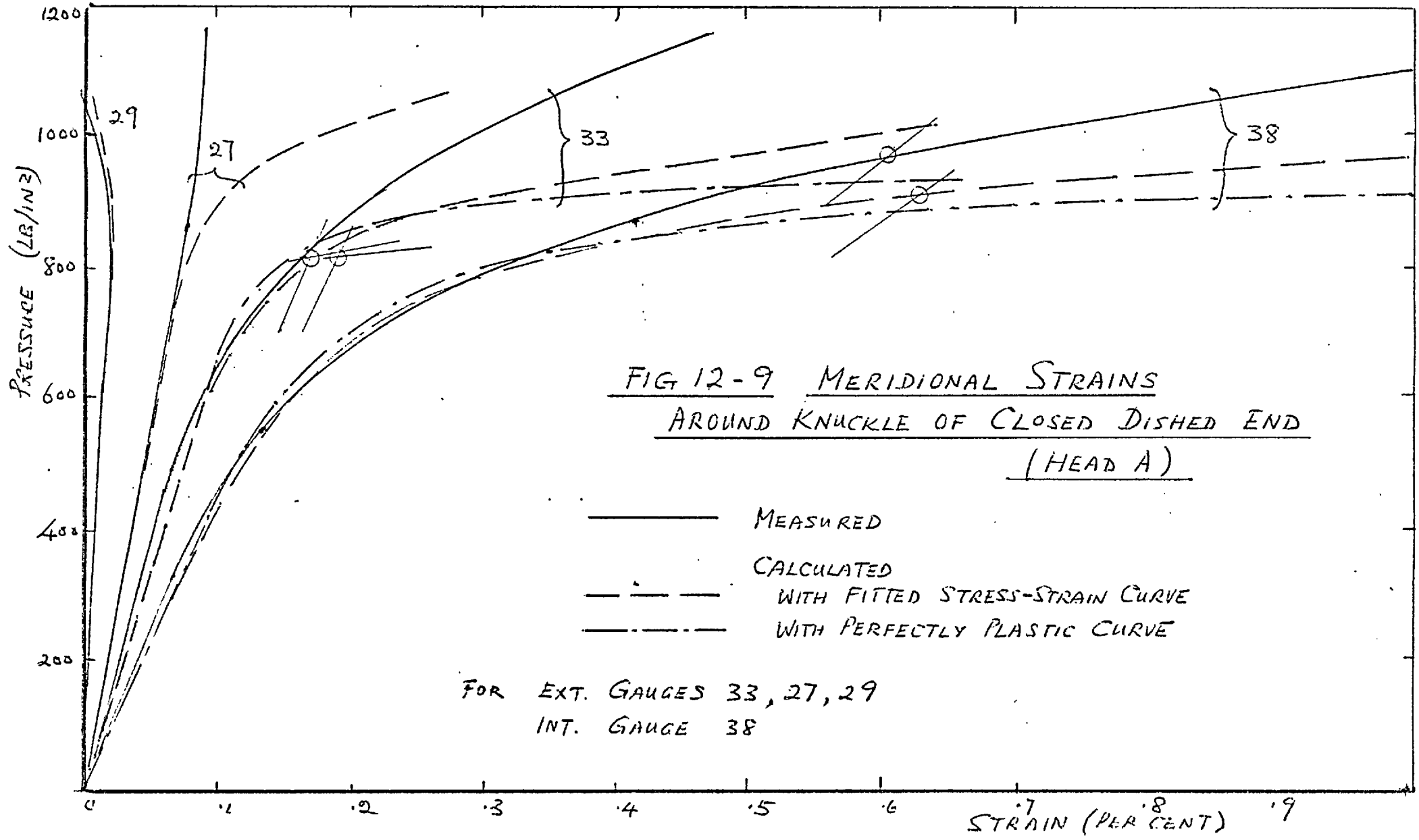

FIG 12-9 MERIDIONAL STRAINS AROUND KNUCKLE OF CLOSED DISHED END (HEAD A)

MEASURED

CALCULATED
WITH FITTED STRESS-STRAIN CURVE
WITH PERFECTLY PLASTIC CURVE

FOR EXT. GAUGES 33, 27, 29
INT. GAUGE 38

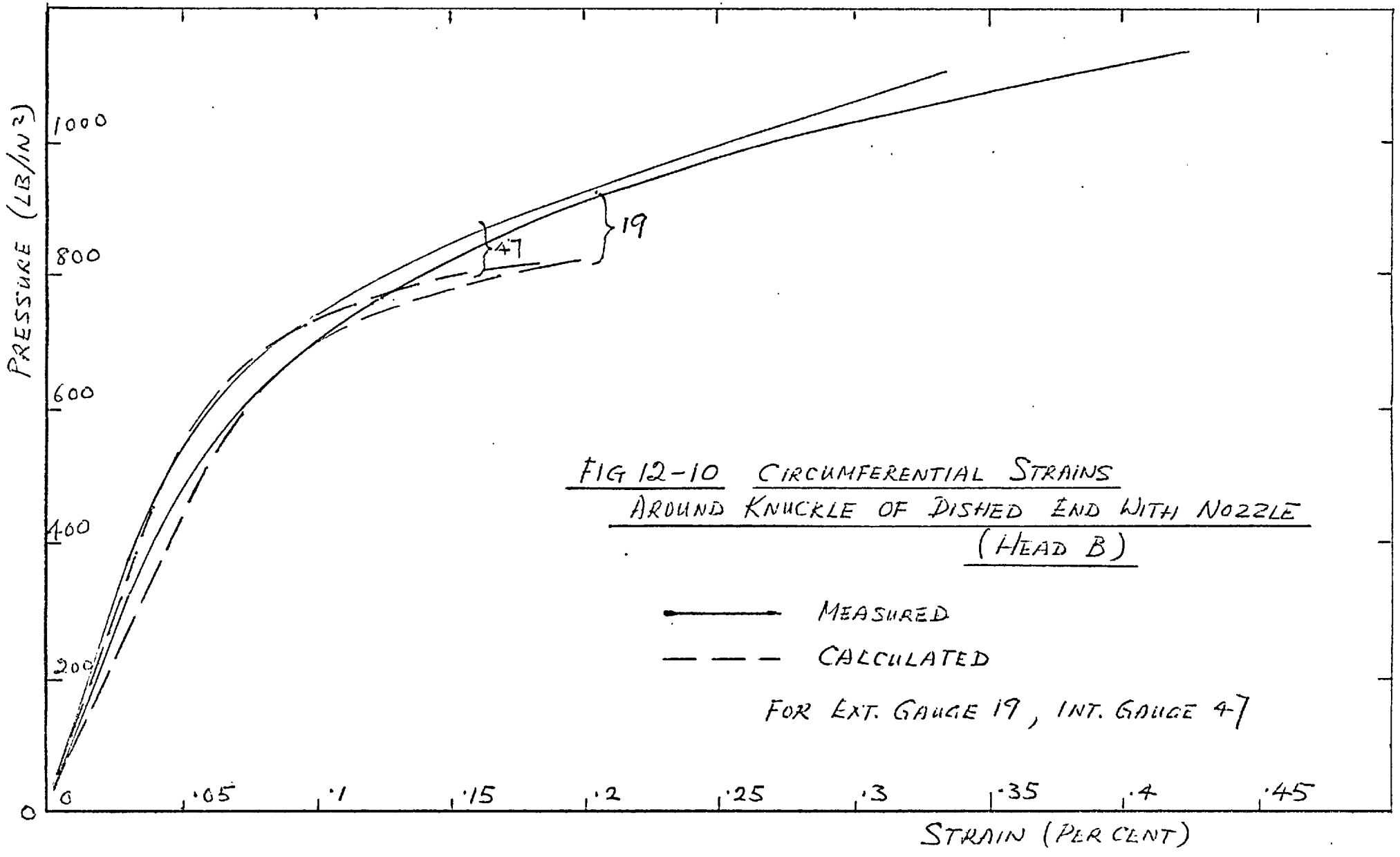

FIG 12-10 CIRCUMFERENTIAL STRAINS AROUND KNUCKLE OF DISHED END WITH NOZZLE (HEAD B)

——— MEASURED

— — — CALCULATED

FOR EXT. GAUGE 19, INT. GAUGE 47

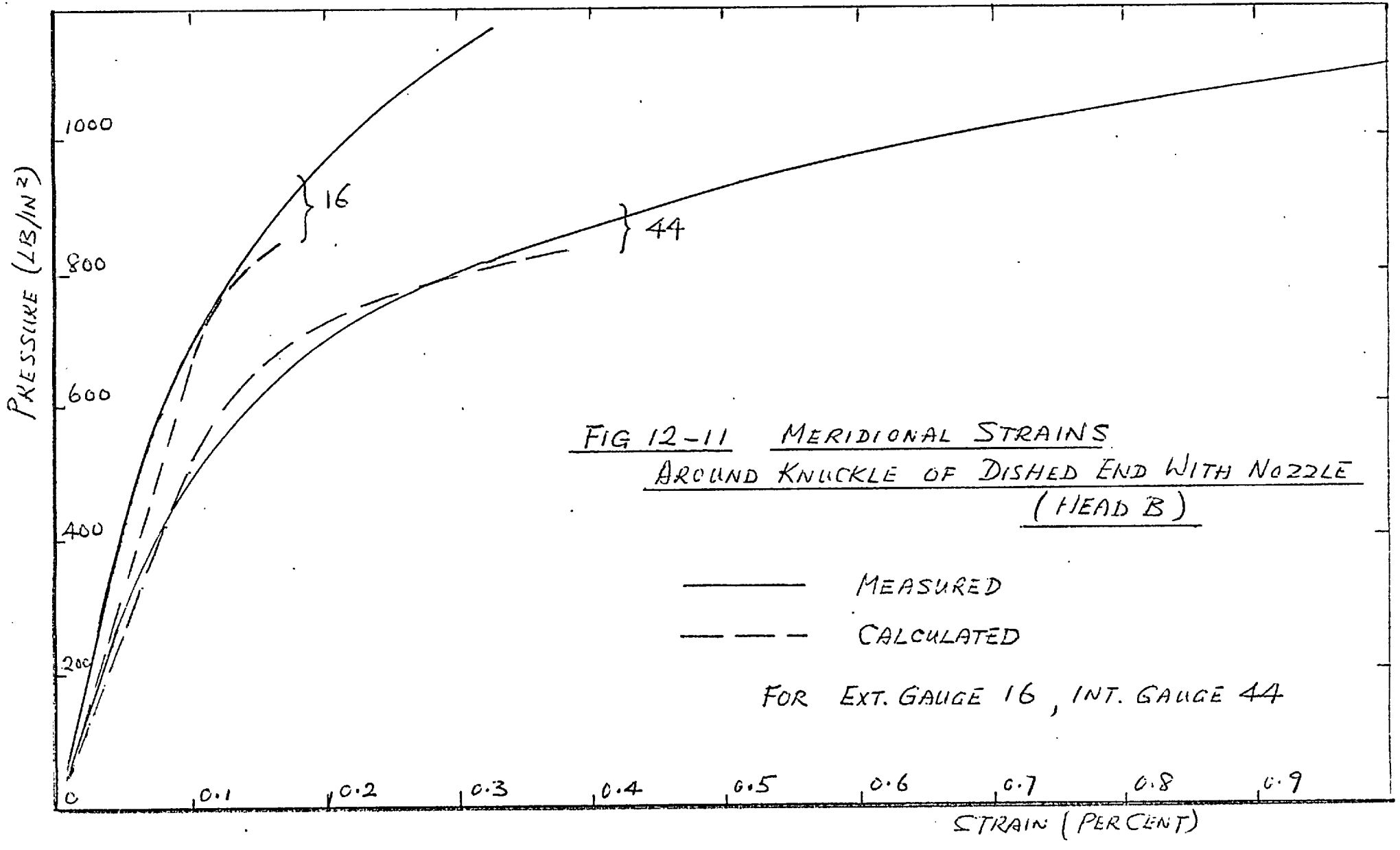

FIG 12-11 MERIDIONAL STRAINS AROUND KNUCKLE OF DISHED END WITH NOZZLE (HEAD B)

——— MEASURED

— — — CALCULATED

FOR EXT. GAUGE 16, INT. GAUGE 44

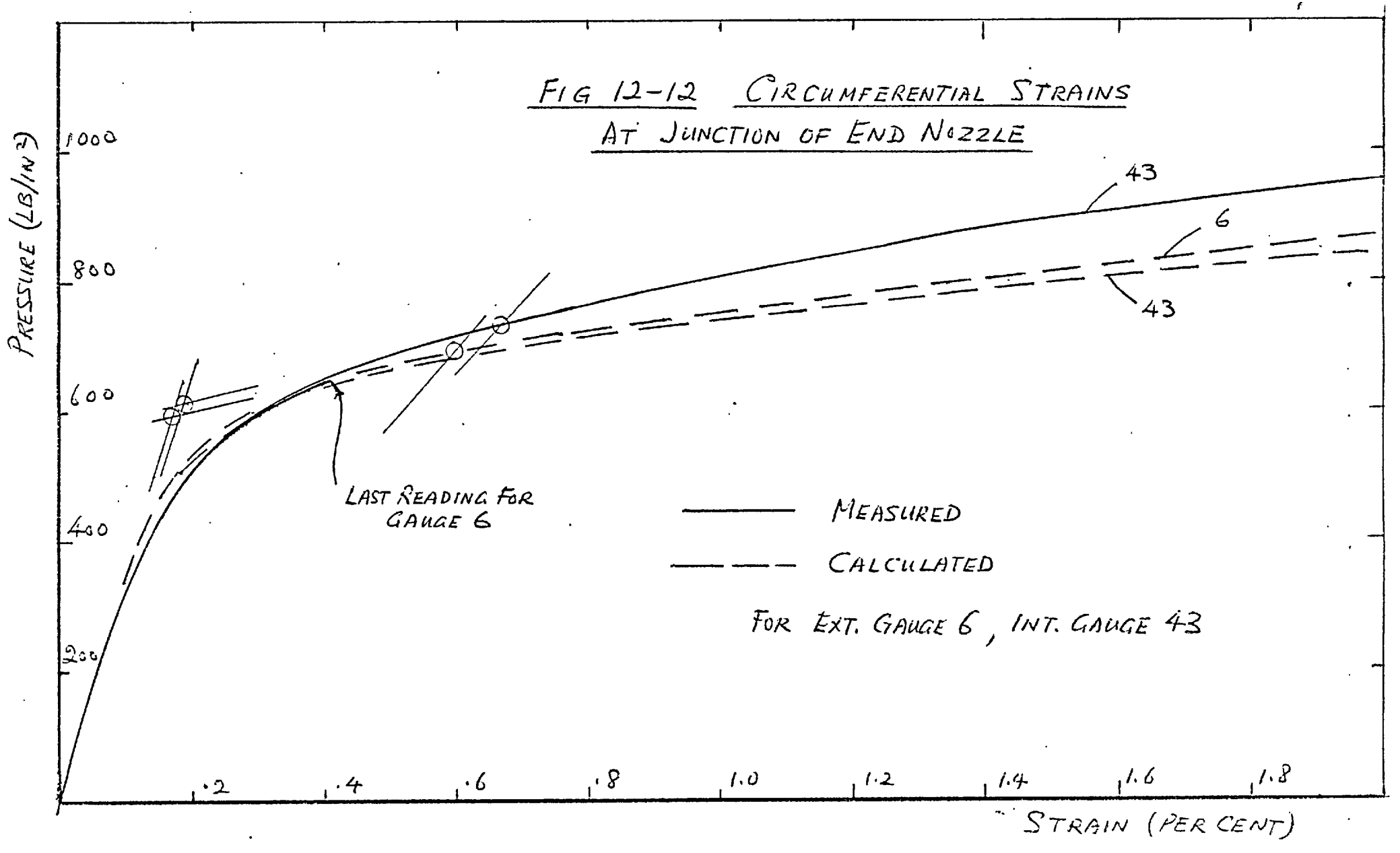
FIG 12-12 CIRCUMFERENTIAL STRAINS
AT JUNCTION OF END NOZZLE
PRESSURE (LB/IN²)
1000
800
600
400
200
43
6
43
LAST READING FOR GAUGE 6
MEASURED
CALCULATED
FOR EXT. GAUGE 6, INT. GAUGE 43
.2
.4
.6
.8
1.0
1.2
1.4
1.6
1.8
STRAIN (PER CENT)

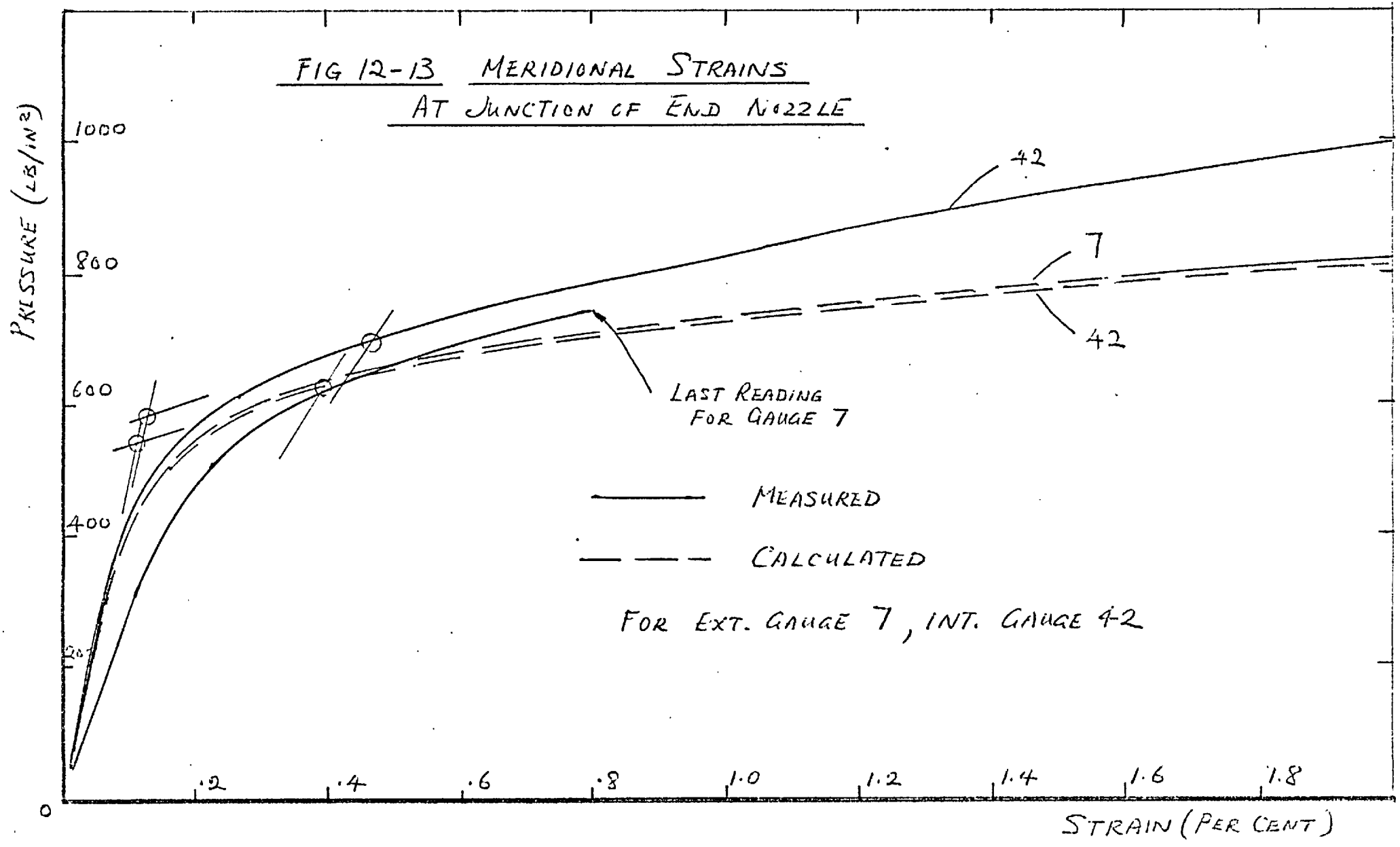
FIG 12-13 MERIDIONAL STRAINS
AT JUNCTION OF END NOZZLE
PRESSURE (LBS/IN²)
1000
800
600
400
200
0
42
7
42
LAST READING
FOR GAUGE 7
MEASURED
CALCULATED
FOR EXT. GAUGE 7, INT. GAUGE 42
.2
.4
.6
.8
1.0
1.2
1.4
1.6
1.8
STRAIN (PER CENT)

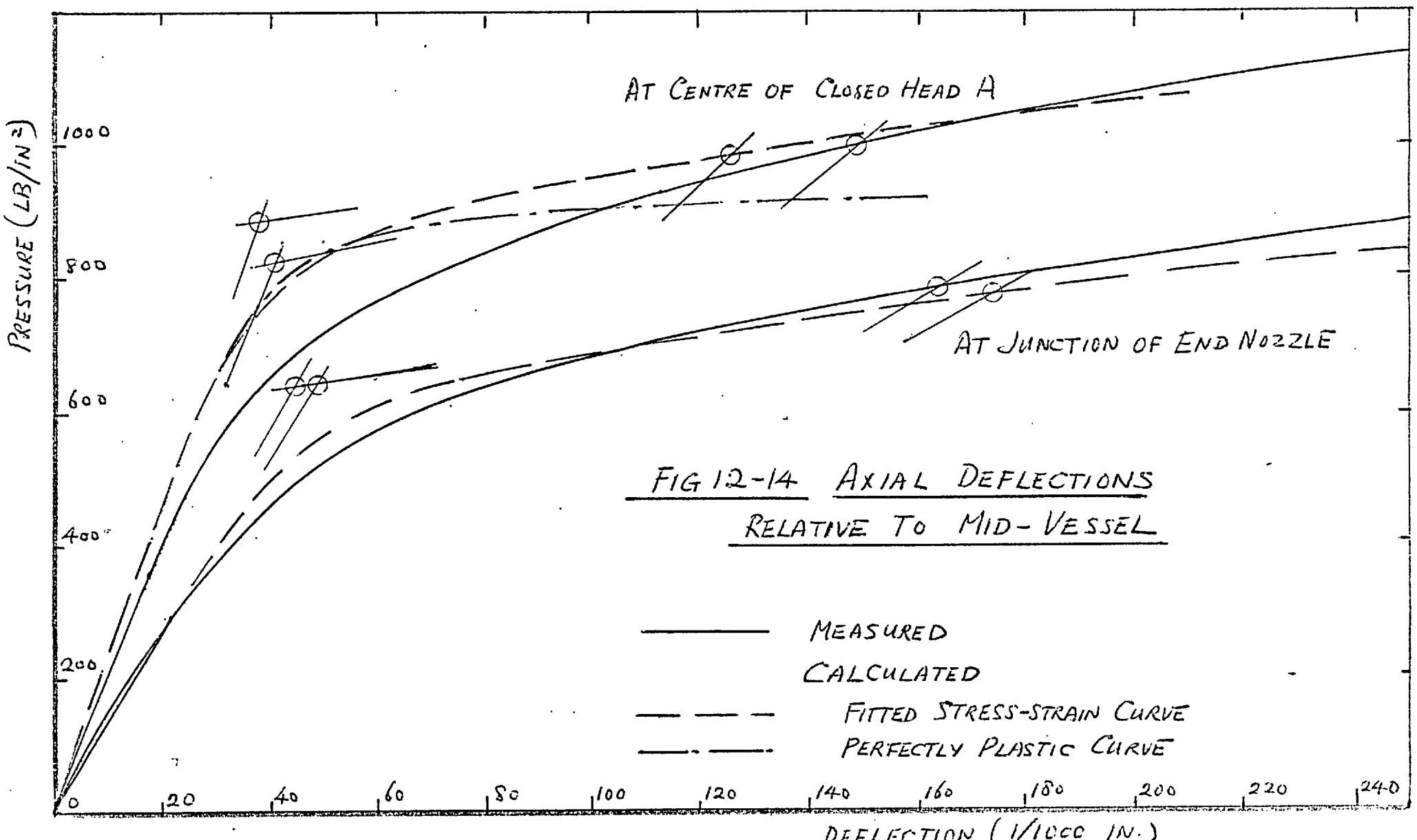

FIG 12-14 AXIAL DEFLECTIONS RELATIVE TO MID-VESSEL

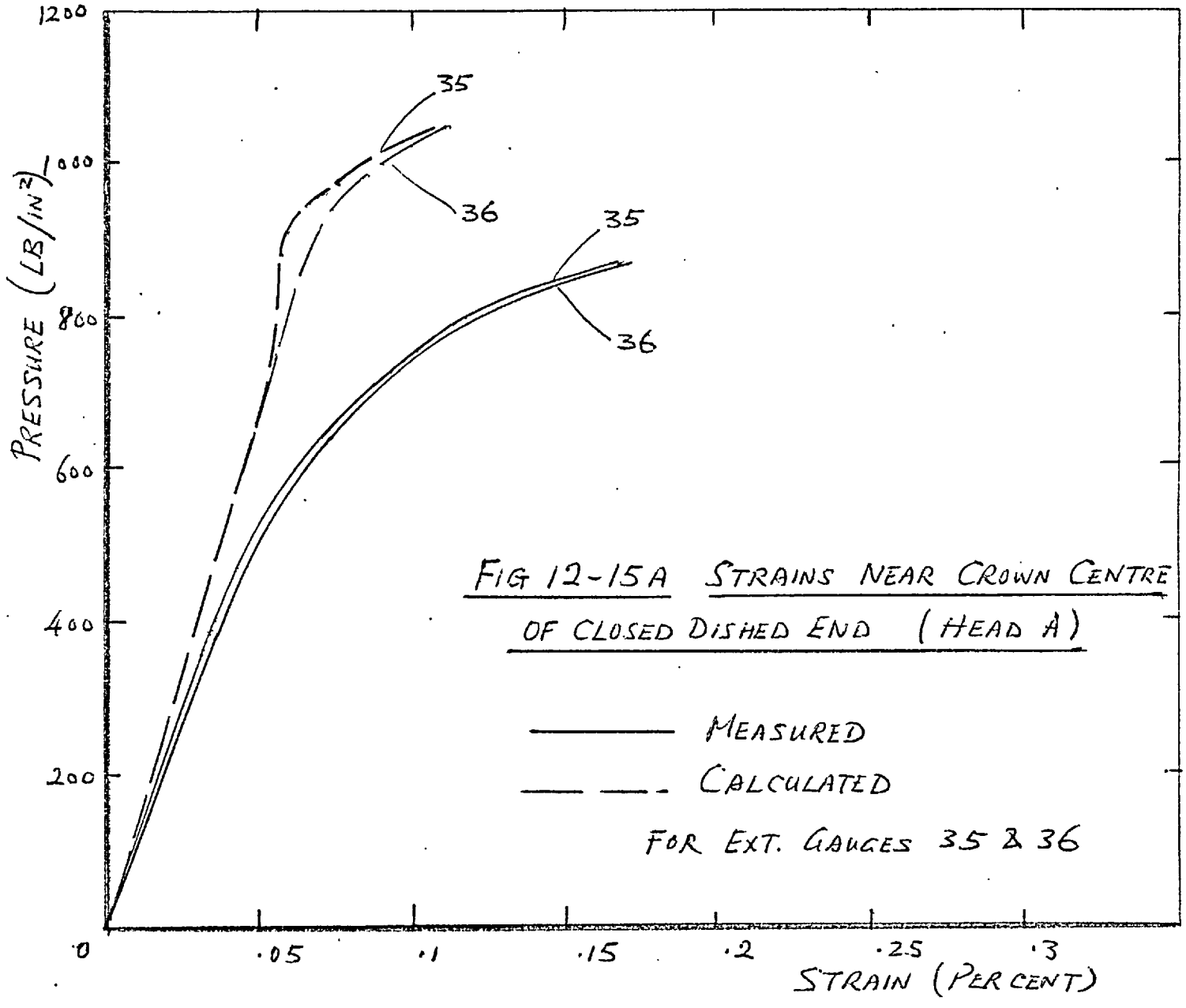

FIG 12-15A STRAINS NEAR CROWN CENTRE OF CLOSED DISHED END (HEAD A)

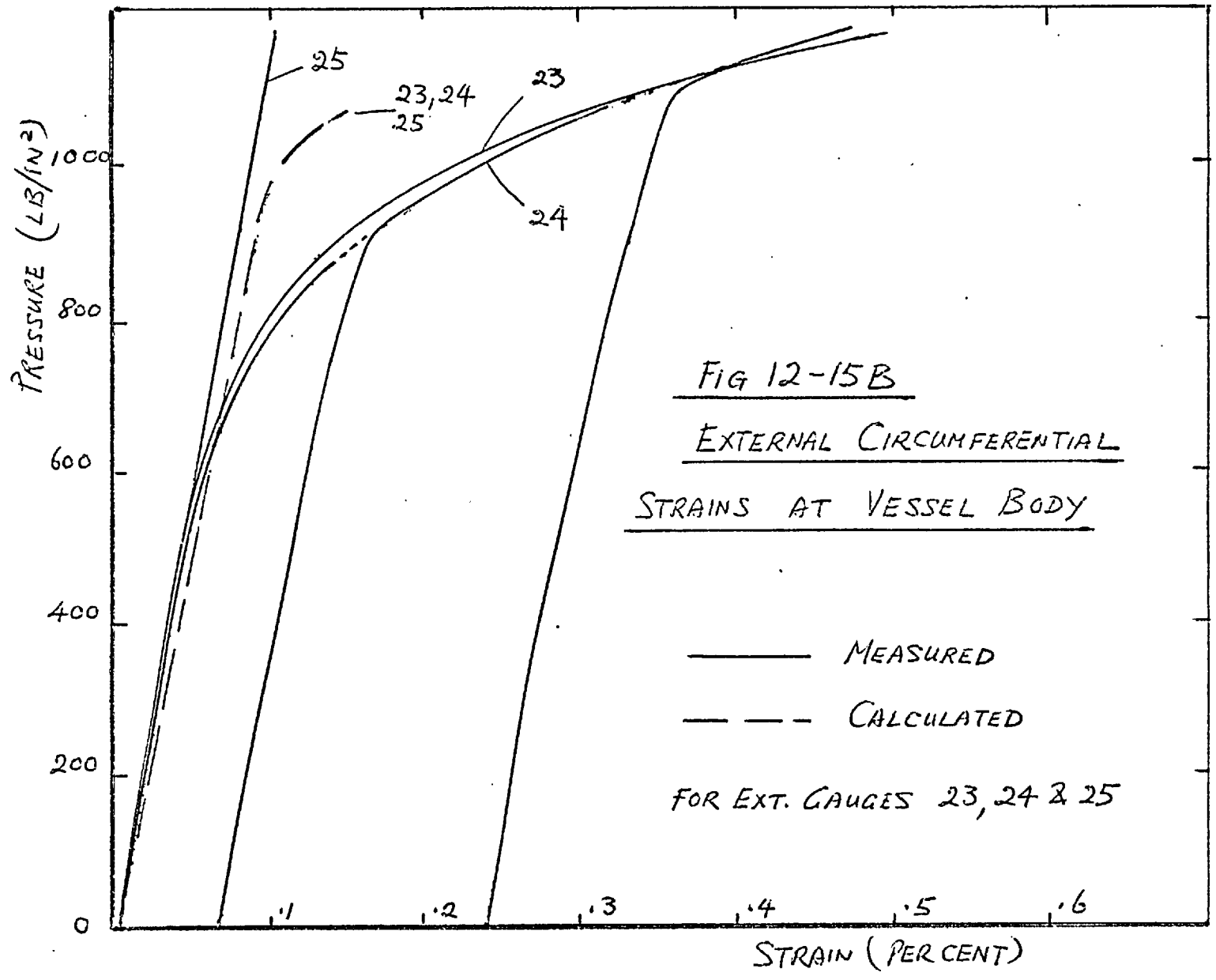

FIG 12-15B

EXTERNAL CIRCUMFERENTIAL STRAINS AT VESSEL BODY

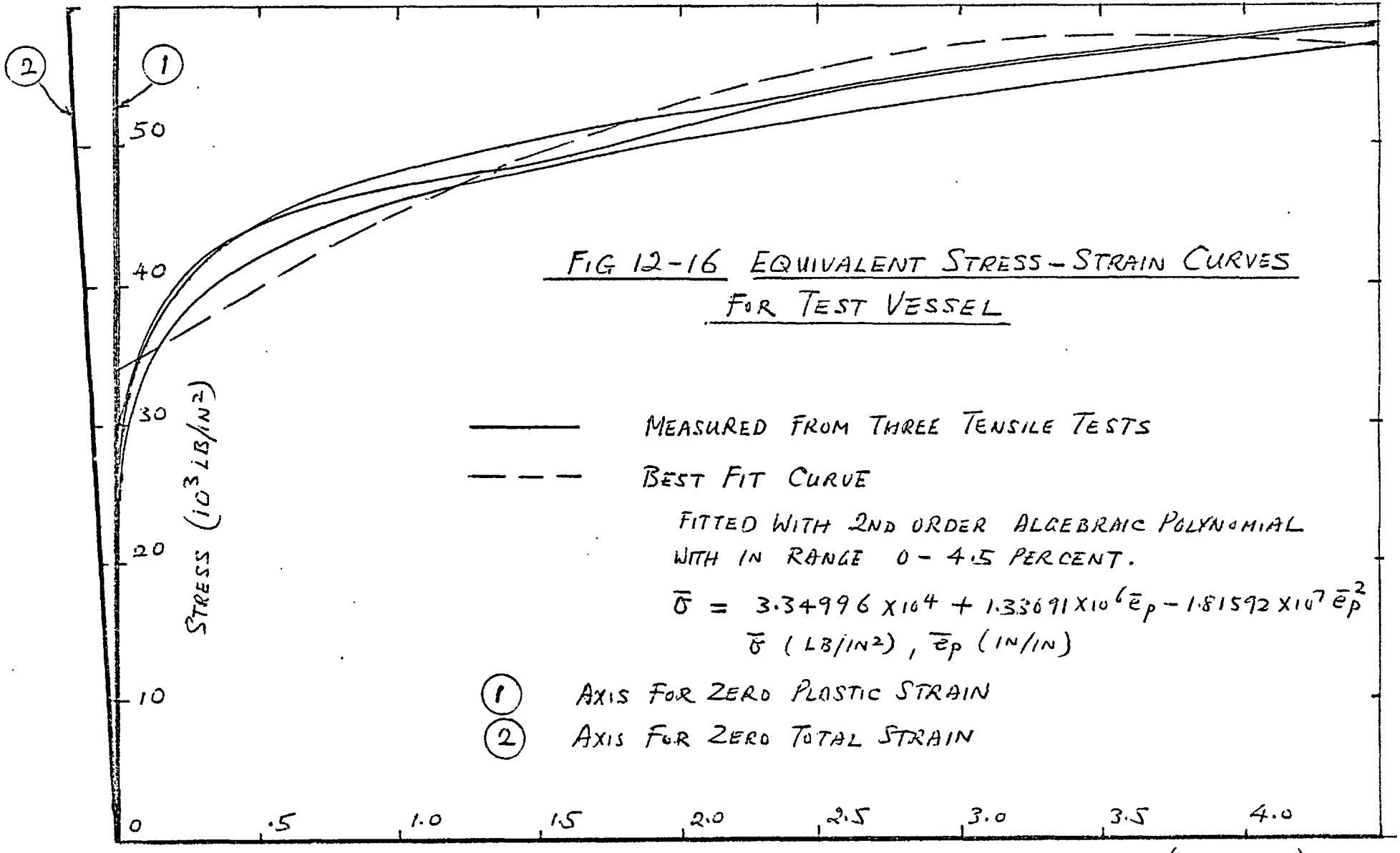

FIG 12-16 EQUIVALENT STRESS-STRAIN CURVES FOR TEST VESSEL

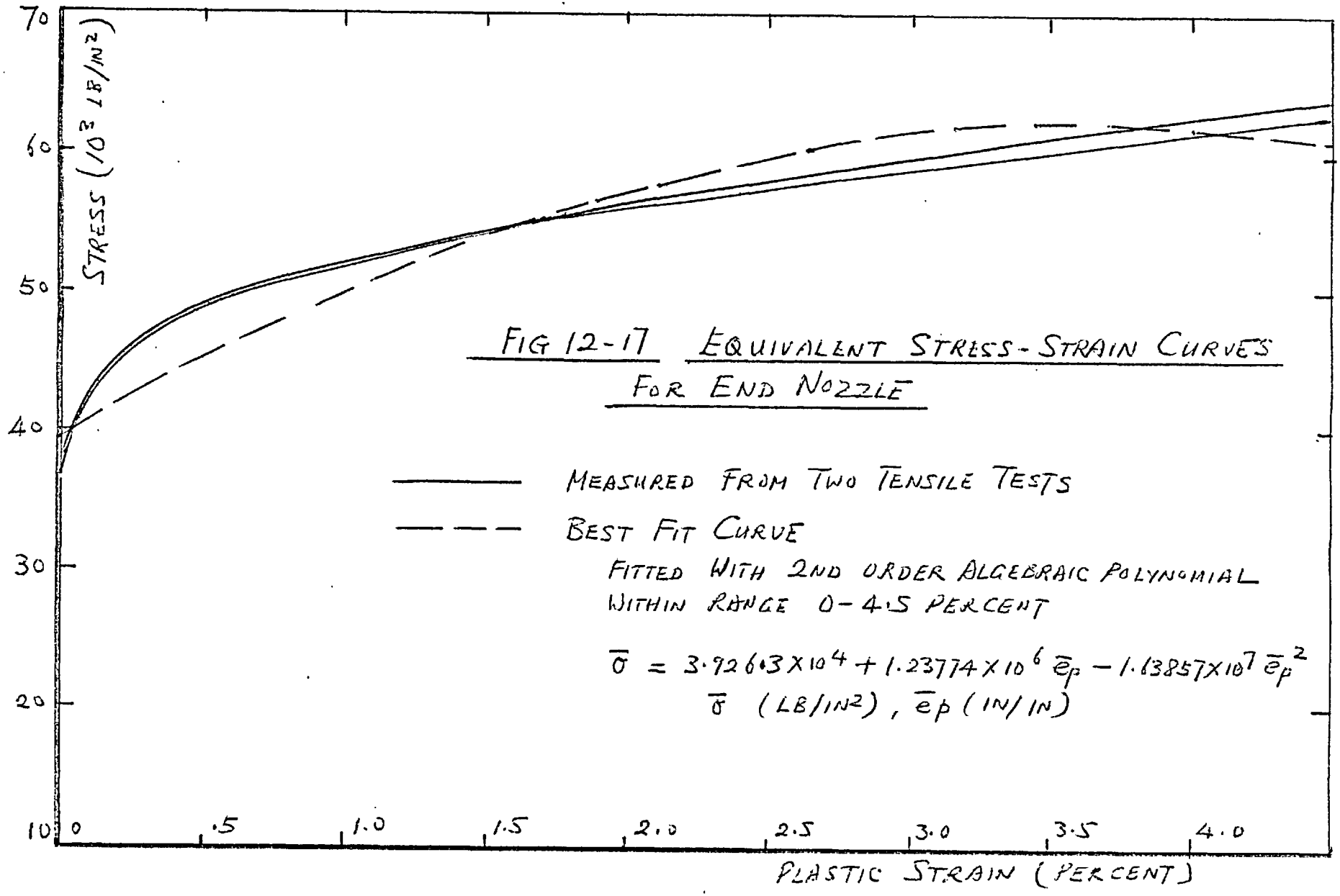

FIG 12-17 EQUIVALENT STRESS-STRAIN CURVES FOR END NOZZLE

——— MEASURED FROM TWO TENSILE TESTS

— — — BEST FIT CURVE

FITTED WITH 2ND ORDER ALGEBRAIC POLYNOMIAL WITHIN RANGE 0-4.5 PERCENT

$$\bar{\sigma} = 3.92603 \times 10^4 + 1.23774 \times 10^6 \bar{e}_p - 1.63857 \times 10^7 \bar{e}_p^2$$

$\bar{\sigma}$ (LB/IN^2), $\bar{e}_p$ (IN/IN)

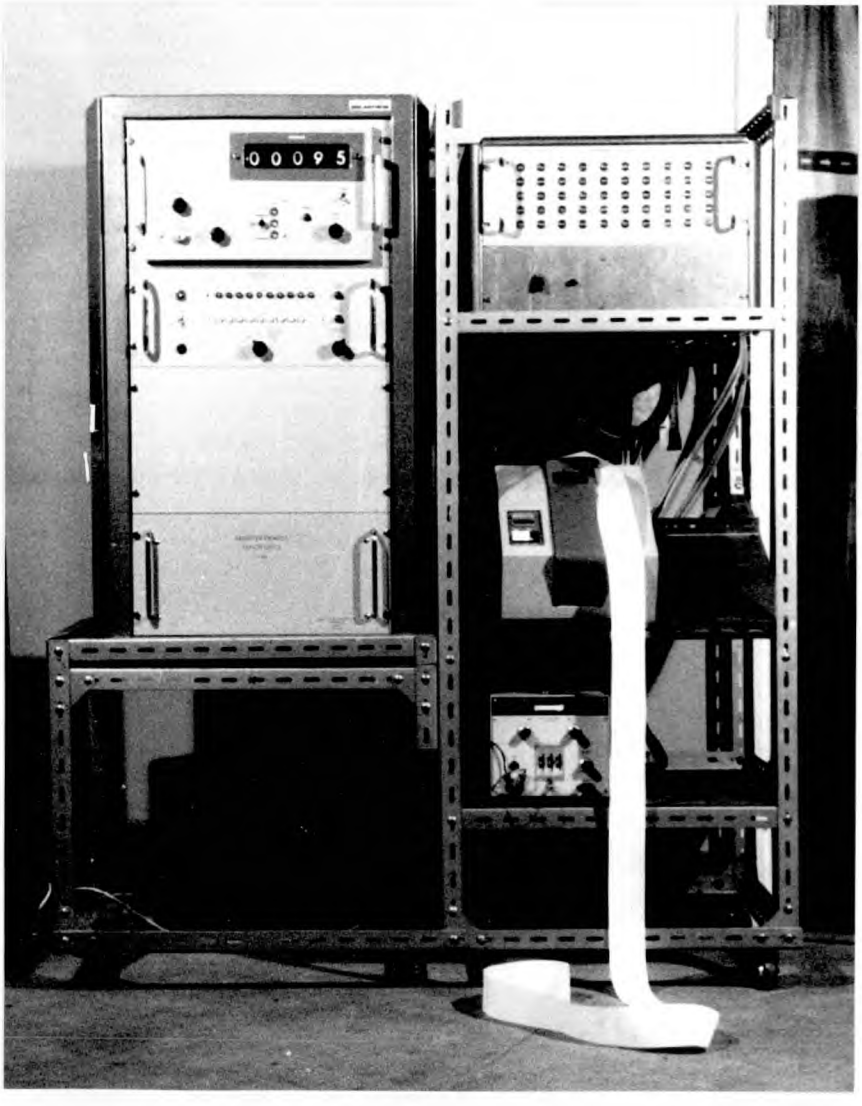

Plate 1 Multi-channel Strain Recorder

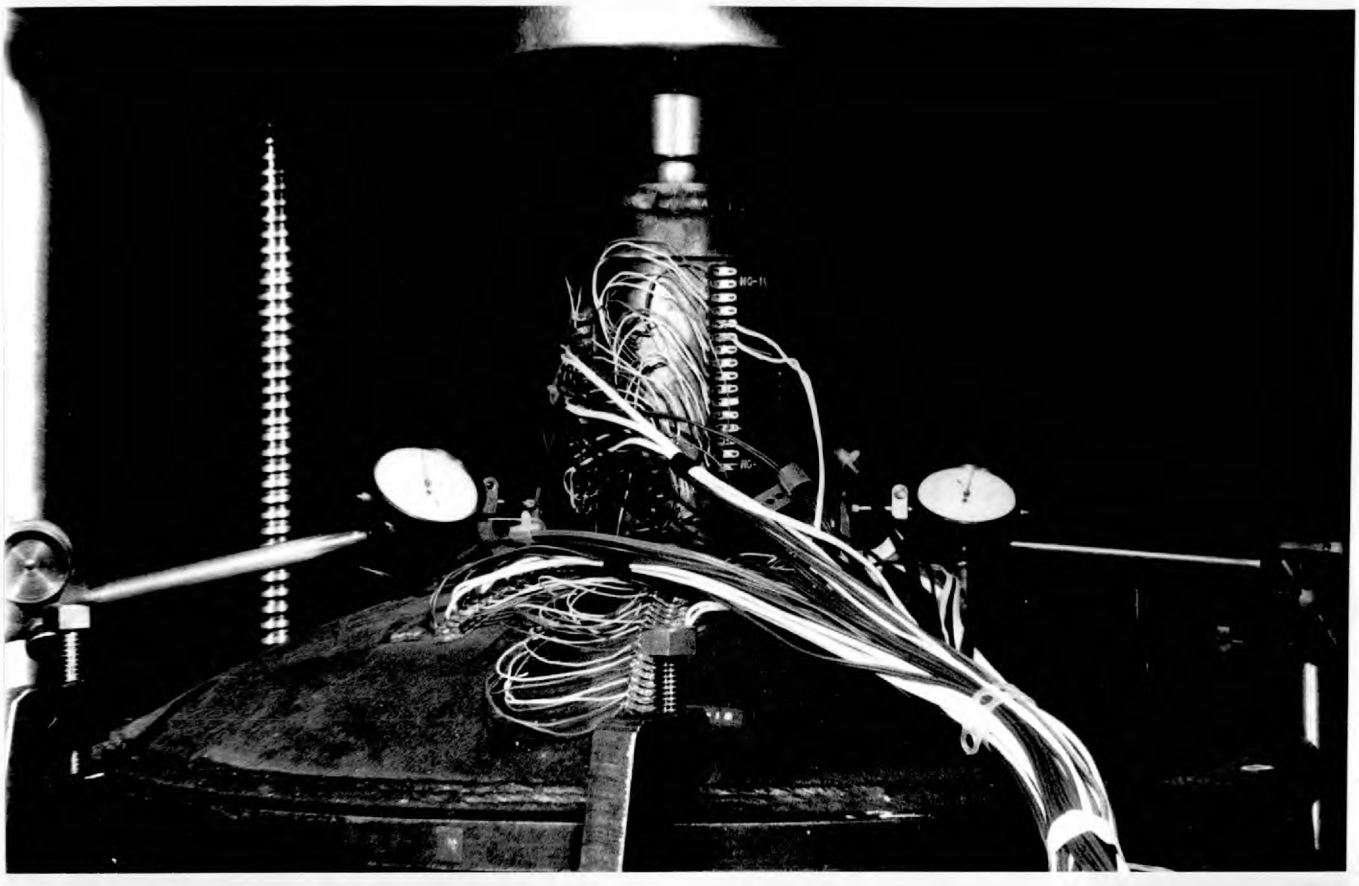

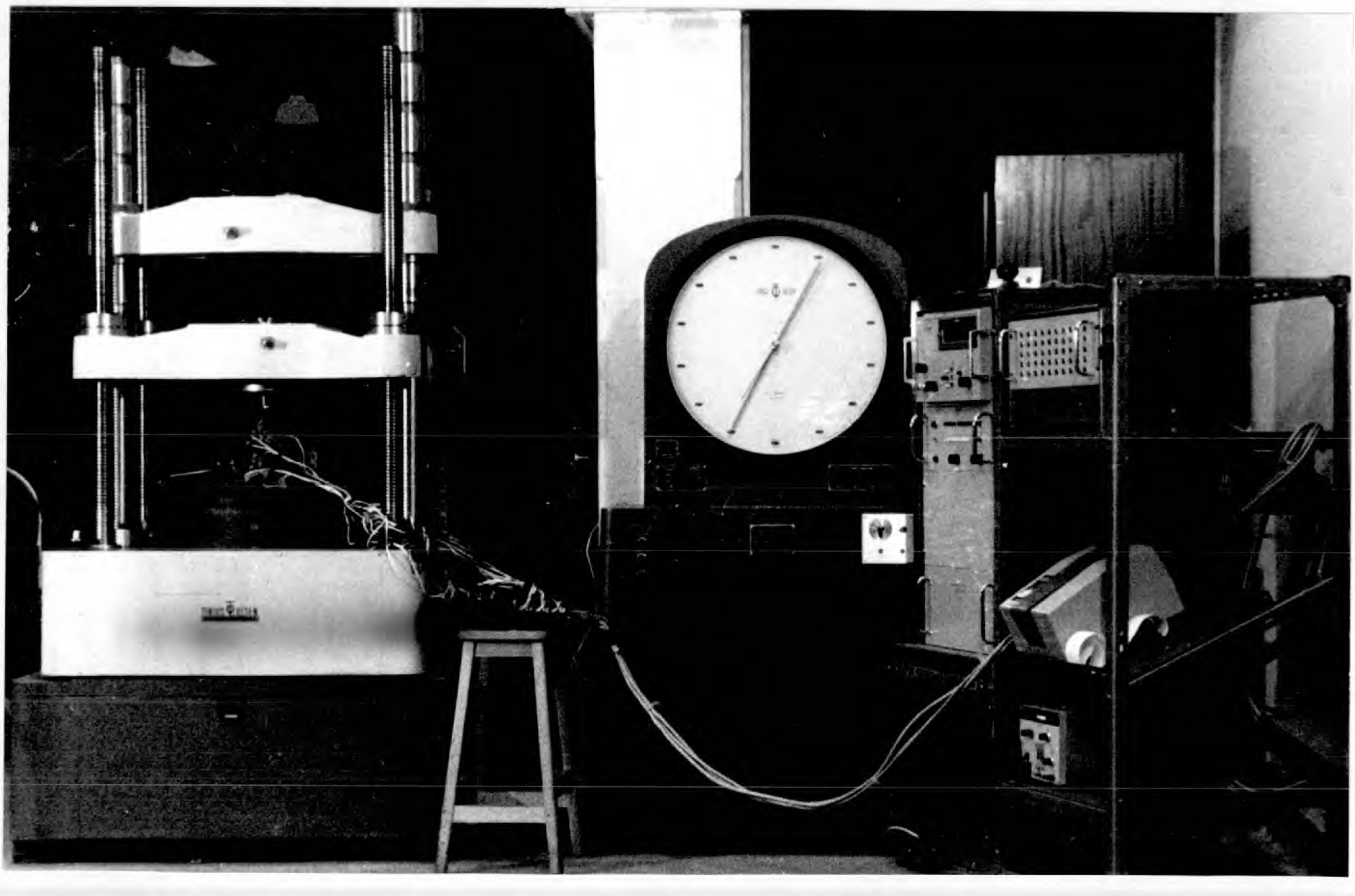

Plate 2 Arrangement for Axial Tests